

INFORMATION TO USERS

This manuscript has been reproduced from the microfilm master. UMI films the text directly from the original or copy submitted. Thus, some thesis and dissertation copies are in typewriter face, while others may be from any type of computer printer.

The quality of this reproduction is dependent upon the quality of the copy submitted. Broken or indistinct print, colored or poor quality illustrations and photographs, print bleedthrough, substandard margins, and improper alignment can adversely affect reproduction.

In the unlikely event that the author did not send UMI a complete manuscript and there are missing pages, these will be noted. Also, if unauthorized copyright material had to be removed, a note will indicate the deletion.

Oversize materials (e.g., maps, drawings, charts) are reproduced by sectioning the original, beginning at the upper left-hand corner and continuing from left to right in equal sections with small overlaps.

Photographs included in the original manuscript have been reproduced xerographically in this copy. Higher quality 6" x 9" black and white photographic prints are available for any photographs or illustrations appearing in this copy for an additional charge. Contact UMI directly to order.

ProQuest Information and Learning
300 North Zeeb Road, Ann Arbor, MI 48106-1346 USA
800-521-0600

UMI[®]

MODELING THE INFLUENCES OF CLIMATE CHANGE, PERMAFROST
DYNAMICS, AND FIRE DISTURBANCE ON CARBON DYNAMICS OF
HIGH LATITUDE ECOSYSTEMS

A

THESIS

Presented to the Faculty
of the University of Alaska Fairbanks
in Partial Fulfillment of the Requirements

For the Degree of

DOCTOR OF PHILOSOPHY

By

Qianlai Zhuang, M.S.

Fairbanks, Alaska

December 2001

UMI Number: 3029826

UMI[®]

UMI Microform 3029826

Copyright 2002 by Bell & Howell Information and Learning Company.

All rights reserved. This microform edition is protected against
unauthorized copying under Title 17, United States Code.

Bell & Howell Information and Learning Company

300 North Zeeb Road

P.O. Box 1346

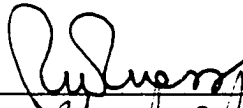
Ann Arbor, MI 48106-1346


MODELING THE INFLUENCES OF CLIMATE CHANGE, PERMAFROST
DYNAMICS, AND FIRE DISTURBANCE ON CARBON DYNAMICS OF
HIGH LATITUDE ECOSYSTEMS


By

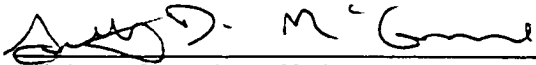
Qianlai Zhuang

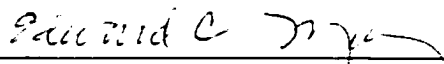
RECOMMENDED:





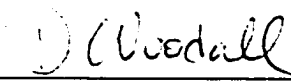


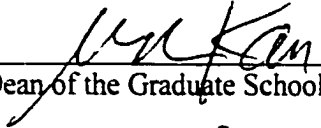


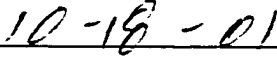
Advisory Committee Chair


Department Head of Biology and Wildlife

APPROVED:



Dean, College of Science, Engineering and Mathematics


Dean of the Graduate School


Date

ABSTRACT

A Soil Thermal Model (STM) with the capability to operate with a 0.5-day internal time step and to be driven with monthly input data was developed for applications with large-scale ecosystem models. The use of monthly climate inputs to drive the STM resulted in an error of less than 1° C in the upper organic soil layer and in an accurate simulation of seasonal active layer dynamics. Uncertainty analyses identified that soil temperature estimates of the upper organic layer were most sensitive to variability in parameters that described snow thermal conductivity, moss thickness, and moss thermal conductivity. The STM was coupled to the Terrestrial Ecosystem Model (TEM), and the performance of the STM-TEM was verified for the simulation of soil temperatures in applications to black spruce, white spruce, aspen, and tundra sites. A 1° C error in the temperature of the upper organic soil layer had little influence on the carbon dynamics simulated for a black spruce site. Application of the model across the range of black spruce ecosystems in North America demonstrated that the STM-TEM has the capability to operate over temporal and spatial domains that consider substantial variations in surface climate. To consider how fire disturbance interacts with climate change and permafrost dynamics, the STM was updated to more fully evaluate how these factors influence ecosystem dynamics during stand development. The ability of the model to simulate seasonal patterns of soil temperature, gross primary production, and ecosystem respiration, and the age-dependent pattern of above-ground vegetation carbon storage was verified. The model was applied to a post-fire chronosequence in interior Alaska and was validated with estimates of soil temperature, soil respiration, and soil carbon storage

that were based on measurements of these variables in 1997. Sensitivity analyses indicate that the growth of moss, changes in the depth of the organic layer, and nitrogen fixation should be represented in models that simulate the effects of fire disturbance in boreal forests. Furthermore, the sensitivity analyses revealed that soil drainage and fire severity should be considered in spatial application of these models to simulate carbon dynamics at landscape to regional scales.

TABLE OF CONTENTS

Abstract	III
List of Figures	IX
List of Tables	XIII
Acknowledgements	XV
CHAPTER 1. Overview: Influences of climate change, permafrost dynamics, and fire disturbance on carbon dynamics of high latitude ecosystems	1
References.....	8
CHAPTER 2. Incorporation of a permafrost model into a large-scale ecosystem model: evaluation of temporal and spatial scaling issues in simulating soil thermal dynamics...	17
Abstract.....	17
1. Introduction.....	18
2. Methods.....	21
2.1. Overview.....	21
2.2. Model Development	22
2.3. Evaluation of STM Performance	24
2.3.1. Parameterization	24
2.3.2. Model Simulations.....	25
2.4. Uncertainty Analyses	27
2.5. Evaluation of STM-TEM Performance for Different Ecosystem Types.....	28
2.6. Evaluation of Carbon Fluxes for a Black Spruce Forest.....	30

2.7. Application to the Range of Black Spruce Ecosystems across North America.....	31
3. Results.....	31
3.1. Evaluation of STM Performance.....	31
3.1.1. Simulated Daily Soil Temperature.....	31
3.1.2. Simulated Monthly Soil Temperature and Active Layer Depth.....	33
3.2. Uncertainty Analyses.....	35
3.3. Applications to Different Ecosystem Types.....	36
3.4. Evaluation of Carbon Fluxes Simulated for a Black Spruce Forest.....	37
3.5. Application to the Range of Black Spruce Ecosystems across North America.....	38
4. Discussion.....	39
4.1. Temporal Scaling Issues.....	40
4.2. Spatial Scaling Issues.....	41
4.3. Additional Issues and Future Directions.....	43
Acknowledgements	45
References.....	46
CHAPTER 3. Modeling soil thermal and carbon dynamics of a fire chronosequence in Interior Alaska.....	81
Abstract.....	81
1. Introduction	83
2. Methods.....	86

2.1. Overview.....	86
2.2. Alaska Chronosequence.....	87
2.3. Model Development.....	89
2.4. Model Parameterization and Verification.....	94
2.5. Model Application to the Fire Chronosequence	98
2.6. Sensitivity Analyses.....	102
3. Results.....	103
3.1. Soil Thermal Dynamics.....	103
3.2. Soil Respiration Dynamics.....	105
3.3. Soil Carbon Dynamics.....	106
3.4. Sensitivity Analyses.....	109
3.4.1. Sensitivity to Moss Growth.....	109
3.4.2. Sensitivity to Moisture Conditions.....	111
3.4.3. Sensitivity to Fire Severity.....	113
4. Discussion.....	115
4.1. Evaluation of Soil Thermal Dynamics.....	116
4.2. Evaluation of Carbon Dynamics.....	117
4.3. Additional Issues and Future Directions.....	122
Acknowledgements.....	126
Appendix A: The Hydrological Model (HM).....	127
References.....	143

CHAPTER 4. Future opportunities	190
1. Implications of Freeze-Thaw Dynamics for the Global Carbon Cycle.....	190
2. Issues to Address in Future Model Development and Application.....	193
2.1. Moss and Organic Layer Dynamics during Succession.....	194
2.2. Soil Drainage and Other Issues Associated with Soil Moisture.....	195
2.3. Allocation of Vegetation Tissue to Leaves, Wood, and Roots.....	198
2.4. Variability of Below-Ground Carbon Dynamics with Depth in the Soil Profile.....	200
2.5. Nitrogen Cycle Issues.....	201
2.6. Development of Spatial Data Sets.....	203
References.....	205

LIST OF FIGURES

CHAPTER 2

2.1. (a) Structure of the soil thermal model (STM) in the study. (b) Flow of data in the coupled model (STM-TEM)	67
2.2. Research design for evaluating performance of the STM with respect to the temporal resolutions of internal time step and climate inputs.	68
2.3. (a) Air temperature and (b) snow depth for the black spruce ecosystem at Bonanza Creek Experimental Forest from May 1996 to April 1997.....	69
2.4. Observed and simulated daily soil temperatures for (a) the surface of the soil and (b) the upper organic soil layer.....	70
2.5. Observed and simulated monthly soil temperatures for (a) the surface of the soil and (b) the upper organic soil layer.....	71
2.6. Proportion of variation in simulated soil temperature of the upper organic layer explained by variability in parameters in the uncertainty analyses conducted in this study.....	72
2.7. Proportion of variation in simulated soil temperature of the upper organic layer to variation in snow thermal conductivity in uncertainty analyses conducted for nine different climate scenarios	73
2.8. Proportion of variation in simulated soil temperature of the upper organic layer to variation in moss thickness in uncertainty analyses conducted for nine different climate scenarios	74

2.9. Monthly observed and simulated soil temperatures for an old black spruce ecosystem in northern Manitoba, Canada, from 1994 to 1996.....	75
2.10. Monthly observed and simulated soil temperatures for a white spruce ecosystem in Alaska from 1994 to 1997.....	76
2.11. Monthly observed and simulated soil temperatures for an aspen ecosystem in Alaska from 1994 to 1997.....	77
2.12. Monthly observed and simulated soil temperatures for a tundra ecosystem in Alaska from 1995 to 1997.....	78
2.13. Field-based and simulated estimates of (a) monthly gross primary production (GPP) and (b) ecosystem respiration (RESP) for an old black spruce ecosystem in northern Manitoba, Canada from 1994 to 1997	79
2.14. Spatial distribution of mean annual soil temperature for the upper soil organic layer simulated by the application of the STM-TEM across the range of black spruce ecosystems in North America north of 50°N during four decades separated by 50 years during the simulation period (1900 -2100).....	80

CHAPTER 3

3.1. Flow diagram for the research design in this study	174
3.2. (a) Overview of the model used in this study, which required coupling a hydrological model (HM) with a soil thermal model (STM) and a terrestrial ecosystem model (TEM), and (b) The structure of the hydrological model (HM).....	175

3.3. Dependence of the scalar function $f(\text{FOLIAGE})$ in the GPP formulation of TEM on vegetation carbon (C_V) simulated by TEM.....176

3.4. Comparison of monthly carbon fluxes between simulated and field-based estimates for an old black spruce forest in the northern study area of the boreal ecosystem atmosphere study (BOREAS).....177

3.5. Comparison of monthly evapotranspiration and monthly volumetric soil moisture between simulated and field-based estimates for two old black spruce forests of the boreal ecosystem atmosphere study (BOREAS), one in the northern study area (NSA-OBS) and one in the southern study area (SSA-OBS).....178

3.6. Comparison of simulated above-ground vegetation carbon with forest inventory estimates for black spruce forests in interior Alaska.....179

3.7. Overview of the simulation of net carbon exchange (NCE) between boreal forest ecosystems and the atmosphere by the Terrestrial Ecosystem Model (TEM) to investigate the effects of fire disturbance on carbon dynamics in boreal forest ecosystems.....180

3.8. Flow diagram for the derivation of carbon and nitrogen pools in simulating ecosystem dynamics of the control and recently burned stands of the fire chronosequence in interior Alaska181

3.9. Comparison of monthly soil temperature estimates at 10 cm depth during the growing season in 1997 between simulated and field-based estimates during the growing season for control and burned stands of the fire chronosequence in interior Alaska.....182

3.10. Comparison of regressions of monthly soil temperature estimates at 10 cm depth during the growing season in 1997 between simulated and field-based estimates with the 1:1 lines.....	183
3.11. Comparison of monthly soil respiration during the growing season in 1997 between simulated and field-based estimates for control and burned stands of the fire chronosequence in interior Alaska	184
3.12. Comparison of regressions of monthly soil respiration estimates during the growing season in 1997 between simulated and field-based estimates with the 1:1 lines.....	185
3.13. Simulated soil carbon dynamics for control stands (last burned in 1825, 1855, and 1915) and recently burned stands (burned in 1987, 1990, 1994, and 1996) of the fire chronosequence in interior Alaska	186
3.14. The dynamics of soil temperature, soil moisture, nitrogen cycling, carbon fluxes, and carbon stocks in the sensitivity analysis for moss growth.....	187
3.15. The dynamics of soil moisture, soil temperature, nitrogen cycling, carbon fluxes, and carbon stocks in the sensitivity analysis for soil moisture	188
3.16. The dynamics of soil temperature, soil moisture, nitrogen cycling, carbon fluxes, and carbon stocks in the sensitivity analysis for fire severity	189

LIST OF TABLES

CHAPTER 2

2.1. Parameters Used for Simulations of the Soil Thermal Model (STM) for a Black Spruce Stand at the Bonanza Creek Experimental Forest (BNZ) Near Fairbanks, Alaska and the Coupling of the STM with the Terrestrial Ecosystem Model (STM-TEM) for a Black Spruce Stand in Canada (NSA-OBS), and White Spruce (WS), Aspen (AS), and Tussock Tundra (TT) sites in Alaska.....	56
2.2. Combinations of Different Air Temperature and Snow Depth Scenarios for the Study of the Uncertainty Analyses for Simulations of Soil Temperature by the Soil Thermal Model (STM) for the Black Spruce Ecosystem at Bonanza Creek Experimental Forest near Fairbanks, Alaska.....	59
2.3. Applications of the Coupled Model (STM-TEM) in Which the Soil Thermal Model (STM) Was Coupled to the Terrestrial Ecosystem Model (TEM), to Simulate Soil Temperature for Four Different Representative Ecosystem Types in High-Latitude Regions of North America.....	60
2.4. Slope, Intercept, and Proportion of Variation (R^2) Explained by Linear Regressions Between Field-Based and Simulated Daily and Monthly Soil Temperatures at Various Depths and Active Layer Depths for Simulations I, II, III, and IV of the Black Spruce Stand at Bonanza Creek Experimental Forest from May 1996 to April 1997.....	61

2.5. Root Mean Square (RMS) Deviations of Simulated Daily and Monthly Soil Temperature Between Pairwise Combinations of Simulations I, II, III, and IV of Soil Temperature and Active Layer Depths for the Black Spruce Stand at Bonanza Creek Experimental Forest from May 1996 to April 1997.....	64
2.6. Slope, Intercept, and Proportion of Variation Explained by Regression Analyses Between Observed and Simulated Soil Temperature at Various Depths in the Soil Profile for an Old Black Spruce Forest in Canada, a White Spruce Forest in Alaska, an Aspen Forest in Alaska, and a Tussock Tundra Site in Alaska.....	65

CHAPTER 3

3.1. Location, Site Characteristics, and History of Burning for Stands of the Fire Chronosequence in Interior Alaska.....	163
3.2. Comparison of Monthly Climate among Tok Junction from 1954 to 1999, Big Delta from 1937 to 1999, and Tok Junction in 1997. Reported Values Represent the Mean +/- Standard Deviation.	164
3.3. Values and Sources of Parameters for the Hydrologic Model Used in This Study..	167
3.4. Values and Sources for Estimated Pools and Fluxes Used to Parameterize the Model for a Black Spruce Forest at Bonanza Creek, Alaska.....	171
3.5. Comparison between Simulated and Field-based Growing Season (May - September) Estimates in 1997 for Soil Temperature at 10 cm, Soil Temperature at 20 cm, Soil Respiration, and Soil Carbon for Stands of the Fire Chronosequence in Interior Alaska.....	172

ACKNOWLEDGEMENTS

First, I would like to sincerely thank my major advisor Dr. A. David McGuire. With his expertise in ecosystem modeling and analysis, he not only guided me in my dissertation research, but also trained me to be a disciplined scientist. He showed me how to use modeling as a tool to address scientific questions, how to write for scientific publication, and how to deliver scientific presentations. I highly appreciate his mentorship in exposing me to a scientific ideology and methodology that was different from my experience prior to coming to the University of Alaska. Through numerous drafts for each manuscript I learned many lessons on how to clearly and accurately to present research findings. Through seemingly tedious rehearsals for each oral presentation I gained more and more skills to efficiently communicate with an audience of scientists. Also, I would like to thank him for his friendship and kindness throughout my graduate education. With his kind care and help, my family has not been intimidated by the long, cold, and dark winter in Fairbanks. I believe that my academic pursuits will benefit from his mentorship throughout the rest of my career.

I would also like to acknowledge my graduate committee, which provided excellent advice on the interdisciplinary questions that I addressed during my dissertation research. Their research was valuable as I needed to use mathematics and computer science to represent the complexity of interactions among soil thermal, hydrological, and ecosystem processes in models of ecosystem dynamics. Dr. F. Stuart Chapin, III, with his broad and profound expertise in ecosystem science often offered me insightful ideas and suggestions. His interactions with me occurred not only in the formal committee

meetings, courses, and seminars, but also in different informal social functions. His broad perspectives on ecosystem science and research paradigms have inspired me in my research. I believe his influences on the nature of my academic pursuits will be tremendous throughout my career. Dr. Roger W. Ruess, with his thorough understanding of ecosystem processes, provided me with insight into plant ecology. He also provided me with numerous suggestions on my dissertation proposal and manuscripts. Dr. Vladimir E. Romanovsky, who is an expert in the soil thermal dynamics of permafrost, provided me with invaluable professional guidance to develop a soil thermal model that was appropriate for incorporation into the Terrestrial Ecosystem Model (TEM). Without his direction and help, the development and application of STM-TEM would have been extremely difficult. Also, I am in debt to advisors outside of my committee. Dr. Larry D. Hinzman provided me with advice on hydrological dynamics of high latitude ecosystems. Through numerous discussions with him, I obtained invaluable insight and suggestions. I also learned much from Dr. David L. Verbyla on the use of GIS and remote sensing technology and the ways to address issues of spatial scale.

I will also never forget the help and friendship of my co-authors. Dr. Jennifer Harden, with her passion and talents for soil physics, soil biology, and soil processes, provided me with state-of-the-art advice concerning soil biogeochemical processes in boreal forests. Her enthusiasm and creativeness always encouraged me, in particular during the research for the third chapter of my dissertation. I hope that her advice, encouragement, and friendship will continue. Dr. Katherine P. O'Neill generously shared her field and experimental data with me so that I could develop and apply models to

investigate interactions between fire disturbance and ecosystem processes. Her expertise and profound understanding of these interactions was extremely helpful to research represented in the third chapter of my dissertation. In addition to his participation in the study represented by the third chapter of my dissertation, Dr. John Yarie also provided advice on my dissertation research proposal.

I would like to thank people in the Spatial Ecology Lab for their help on various aspects of my research. In particular, I thank Rose Meier, Joy Clein, Jim Long, and Gregg Christopher. I also acknowledge help from Cherie Silapaswan, Catharine Copass, Jack McFarland, Richard Brenner, and other top-notch graduate students. I would also like to acknowledge assistance that I received from staff of the Department of Biology and Wildlife, the Alaska Cooperative Fish and Wildlife Research Unit, and the Institute of Arctic Biology. In particular, I thank Kathy Pearse, Judy Romans, Laura Morisky, and Marta Conner.

Last, but not at least, I would like to thank my wife Shaomin Hu. Shaomin has been responsible for diligently taking care of almost every tedious aspect of work for daily life at home, and has shouldered the responsibility for my son's schooling and after-school activities. I also want to share credit with Shaomin because of the assistance she provided to me through her expertise in computer science. Her sacrifices and assistance helped my dissertation research go very smoothly.

CHAPTER ONE

OVERVIEW: INFLUENCES OF CLIMATE CHANGE, PERMAFROST DYNAMICS, AND FIRE DISTURBANCE ON CARBON DYNAMICS OF HIGH LATITUDE ECOSYSTEMS

The Intergovernmental Panel on Climate Change (IPCC) predicts that global mean temperature will increase 1.4 to 5.8° C by 2100 as a result of growing greenhouse gas (GHG) concentrations in the atmosphere if current trends in fossil fuel use continue to the future [IPCC, 2001]. This rate of warming is without precedent in the last 10,000 years [IPCC, 2001]. The predicted rate of warming is dramatic when one considers that the difference between average global temperatures today and during the last Ice Age is about 4° C [Houghton *et al.*, 1990]. In particular, there is evidence that warming is occurring in some high-latitude areas [Beltrami and Mareschal, 1991; Chapman and Walsh, 1993; Osterkamp and Romanovsky, 1999; Serreze *et al.*, 2000], although some regions are experiencing cooling and interannual variability in climate is substantial throughout high latitudes [Everett and Fitzharris, 1998]. Ground temperature records for North America reconstructed from borehole temperature logs support the notion that large-scale warming has been occurring since the 19th century [Lachenbruch *et al.*, 1982; Lachenbruch and Marshall, 1986]. For example, annual surface temperatures in Alaskan boreal and arctic regions have increased 2° to 4° C during the last century [Lachenbruch and Marshall, 1986] and 1° to 2° C in recent decades [Osterkamp and Romanovsky,

1999]. The warming being experienced in Alaska during recent decades is part of a warming trend that is occurring throughout northwestern North America [Beltrami and Mareschal, 1994; Oechel and Vourlitis, 1994; Serreze et al., 2000]. The soil thermal regime and the distribution of permafrost in regions with discontinuous permafrost are especially sensitive to climate changes [Osterkamp and Romanovsky, 1999; Brown, 1960; Halsey et al., 1995]. Over the last few hundred years, permafrost conditions in the Arctic have changed and are likely to continue changing [Overpeck et al., 1997]. For instance, a recent study shows that the warming may have pronounced effects on permafrost dynamics in Alaska [Osterkamp and Romanovsky, 1999]. In the western boreal forest of Canada, permafrost has responded dynamically to climatic changes that have been occurring since the little Ice Age [Vitt et al., 2000].

In addition to the impact of climate on permafrost dynamics, the cycles of permafrost degradation (thermokarst) and aggradation [Thie, 1974] have in some cases occurred in association with fire [Zoltai, 1993], which is a major disturbance in boreal forests [Kasischke et al., 2000]. Fire disturbance in North America's boreal forests was higher in the 1980's than in any previous decade on record [Murphy et al. 1999], and the area of western Canadian boreal forest burned annually has doubled in the last 20 years [Kasischke et al., 2000]. Some studies have indicated that wildfire activity may be related to the warming trend in North America. For example, fire regimes are sensitive to climate in both Alaska [Hess et al., 2001] and Canada [Stocks et al., 2000]. In addition, warming has been identified by Kurz et al. [1995] as a possible factor in the increasing fire frequency observed in Canada since 1970 [Kurz and Apps, 1995]. Analyses that have

used simulations of changes in climate associated with doubled atmospheric CO₂ suggest that the boreal forest region could experience a 40% increase in the annual amount of area burned [Flannigan and Van Wagner, 1991]. Moreover, the prospect of summer drought, indicated by recent trends in Alaska [Wotton and Flannigan, 1993; Barber et al., 2000] threatens to increase the occurrence of fire.

High latitude ecosystems occupy a large proportion (22%) of the terrestrial surface and contain approximately 40% of the world's soil carbon inventory that is potentially reactive in near-term climate change [McGuire et al. 1995; Melillo et al., 1995; McGuire and Hobbie, 1997]. Among the world's biomes, boreal forests contain the largest soil carbon pools in the world [Chapin and Mathews, 1993; Post et al., 1982; Gorham, 1991]. Much of the boreal forest is underlain by permafrost. Several studies have indicated that permafrost dynamics may substantially influence carbon storage [Vitt et al., 2000] and carbon dynamics [Hillman, 1992; Waelbroeck et al., 1997; Goulden et al., 1998] of high-latitude ecosystems. Goulden et al. [1998] suggested that the stability of the soil carbon pool at a black spruce site in Canada appears sensitive to the depth and duration of thaw, and climatic changes that promote thaw are likely to cause a net efflux of carbon dioxide from the site. Furthermore the thawing of permafrost after fire has the potential to change the thermal and moisture properties of the soil that have led to substantial soil carbon storage in boreal forest ecosystems.

Fire influences the structure of boreal forest ecosystems through influences on population and vegetation dynamics [Zackrisson, 1977; Schimmel and Granstrom, 1996; De Grandpre et al., 1993; Lynham, et al., 1998; Luc and Luc, 1998]. These structural

changes have profound influences on the dynamics of permafrost, soil moisture, and soil nutrient cycles in boreal forests [Viereck, 1972, 1973; Dyrness *et al.*, 1989; Wardle *et al.*, 1998; Driscoll *et al.*, 1999; Grogan *et al.*, 2000; Smith *et al.*, 2000; Brais *et al.*, 2000; Yoshikawa *et al.*, in press]. Changes in the fire regime of boreal forests may have consequences for the global carbon budget. For example, some studies suggest that disturbance and growth patterns after disturbance at high latitudes may have contributed substantially to the approximately 15% increase in the amplitude of the seasonal cycle measured at some high latitude CO₂ monitoring stations since the 1960s [Zimov *et al.*, 1999; Randerson *et al.* 1997]. Kurz and Apps [1999] also indicated that the fire disturbance is one of most important factors affecting the interaction of carbon and permafrost dynamics in North America. Furthermore, some studies have indicated that boreal forests may be a net source of CO₂ if warming greatly increases fire frequency or decomposition [Kasischke *et al.*, 1995; Kurz and Apps, 1995]. On the other hand, warming may not always lead to C losses [Shaver *et al.*, 1992; McGuire *et al.*, 1992, 2000a, 2001; Oechel *et al.*, 2000; Clein *et al.*, 2000, in press]. It is not clear if high-latitude ecosystems are presently storing or releasing carbon or if there is interannual variability in the source-sink activity of high latitudes [Chapin *et al.*, 2000].

The structure and functioning of high-latitude ecosystems are expected to be influenced by spatial and temporal variability in climate, responses of permafrost dynamics, and change in fire disturbance [McGuire and Hobbie, 1997; Epstein *et al.*, 2000; McGuire *et al.*, 2000a]. The response of carbon dynamics in high-latitude ecosystems to these changes is of concern, because this response has the potential to

influence CO₂ concentrations in the atmosphere [Oechel *et al.*, 1993; McGuire and Hobbie, 1997; McGuire *et al.*, 2000a]. Large-scale ecosystem models have been developed to simulate the carbon dynamics of the terrestrial biosphere [McGuire *et al.*, 2001]. Although it has been demonstrated that representing the insulative effects of snowpack on the soil thermal regime improves the ability of large-scale ecosystem models to reproduce seasonal features of atmospheric CO₂ concentrations at high-latitude monitoring stations [McGuire *et al.*, 2000b], these models have been slow to integrate a consideration of permafrost into their dynamics. Also large-scale models have been slow to integrate interactions between fire disturbance and ecosystem dynamics because of the long time scales over which these disturbance effects persist and the lack of long-term studies to monitor these changes. In this dissertation, I focused on making progress in representing how interactions among climate, permafrost dynamics, and fire disturbance influence ecosystem processes in large-scale ecosystem models.

Large-scale ecosystem models are often driven by monthly climate data when they are applied over substantial spatial and temporal domains because of both computational and data limitations [e.g., see McGuire *et al.*, 2001]. In contrast, models of permafrost dynamics are generally driven by daily or sub-daily climate data and operate with an internal time step of less than one hour. In the second chapter of this dissertation, I examine whether a model of permafrost dynamics with a coarse resolution internal time step (0.5 days) that is driven by monthly climate inputs, referred to as the soil thermal model (STM), is adequate for representing soil thermal dynamics in large-scale ecosystem models that are driven by monthly climate inputs. In this study I

evaluated temporal scaling issues for the STM, conducted extensive uncertainty analyses for the STM, coupled the STM to the Terrestrial Ecosystem Model, and conducted applications of the coupled model at both fine and coarse temporal and spatial scales at high latitudes. These studies result in a new version of terrestrial ecosystem model, the STM-TEM that can be applied to evaluate how interactions between climate change and soil thermal dynamics influence the carbon dynamics of high latitude ecosystems.

In the third chapter of this dissertation, my goal is to modify the STM-TEM so it can be used to evaluate how interactions among climate change, permafrost dynamics, and fire disturbance influence carbon dynamics of high latitude ecosystems. In this study, I first update the STM-TEM to represent interactions among soil thermal, hydrologic, and biogeochemical dynamics during stand development. Second, I evaluate performance of the updated model in simulating the short-term and long-term effects of fire disturbance on soil thermal and carbon dynamics of a fire chronosequence in interior Alaska. Third, I conduct sensitivity analyses to evaluate the effects of different scenarios of moss growth after fire, soil moisture conditions, and fire severity on post-fire carbon dynamics to gain additional insight for the large-scale applications of the model in high latitudes. The results of the study indicate that the updated model is a powerful tool that can be used to evaluate how interactions among climate change, permafrost dynamics, and fire disturbance influence carbon dynamics of high latitude ecosystems. In addition, the sensitivity analyses indicate that the growth of moss, changes in the depth of the organic layer, and nitrogen fixation should be represented in models that simulate the effects of fire disturbance in boreal forests. Furthermore, the sensitivity analyses

revealed that soil drainage and fire severity should be considered in spatial application of the model to simulate carbon dynamics at landscape to regional scales.

In the fourth and final chapter of this dissertation, I identify some future opportunities for application and further development of the models described in Chapters 2 and 3 for simulating carbon dynamics of high latitude ecosystems at landscape to global scales.

References

- Barber, V. A., G. P. Juday, and B. P. Finney, Reduced growth of Alaska white spruce in the twentieth century from temperature-induced drought stress. *Nature*. 405. 668-673. 2000.
- Beltrami, H., and J. C. Mareschal. Recent warming in eastern Canada inferred from geothermal measurements. *Geophys. Res. Lett.*, 18. 605-608. 1991.
- Beltrami, H. J., and C. Mareschal. Ground temperature changes in eastern Canada: borehole temperature evidence compared with proxy data. *Terra Nova*. 5. 21-28. 1994.
- Brais, S., P. David, and R. Ouimet. Impacts of wild fire severity and salvage harvesting on the nutrient balance of jack pine and black spruce boreal stands. *Forest Ecology and Management*. 137. 231-243. 2000.
- Brown, R. J. E.. The distribution of permafrost and its reaction to air temperature in Canada and the U.S.S.R. *Arctic*. 13. 163-177. 1960.
- Chapin, F. S., III, and E. Mathews. Boreal carbon pools: approaches and constraints in global extrapolations. In: *Carbon cycling in boreal forests and sub-arctic ecosystems* (eds Vinson, TS, Kolchugina, TP), pp. 9-20. U. S. Dept. Commerce, Nat. Tech. Information Service, Washington DC, 1993.
- Chapin, F. S., III, et al.. Feedbacks from arctic and boreal ecosystems to climate. *Global Change Biol.*, 6. 211-223, 2000.
- Chapman, W. L., and J. E. Walsh. Recent variations of sea ice and air temperatures in high latitudes. *Bull. Am. Meteorol. Soc.*, 74. 33-47. 1993.

- Clein, J. S., B. L. Kwiatkowski, A. D. McGuire, J. E. Hobbie, E. B. Rastetter, J. M. Melillo, and D. W. Kicklighter. Modeling carbon responses of tundra ecosystems to historical and projected climate: A comparison of a fine- and coarse-scale ecosystem model for identification of process-based uncertainties. *Global Change Biology*, 6 (Suppl. 1), 127-140, 2000.
- Clein, J. S., A. D. McGuire, X. Zhang, D. W. Kicklighter, J. M. Melillo, S. C. Wofsy, and P. G. Jarvis. The role of nitrogen dynamics in modeling historical and projected carbon balance of mature black spruce ecosystems across North America: Comparisons with CO₂ fluxes measured in the Boreal Ecosystem Atmosphere Study (BOREAS). *Plant and Soil*, *in press*.
- De Grandpre, L., L. Gagnon, and Y. Bergeron. Changes in the understorey of Canadian southern boreal forest after fire. *J. Veg. Sci.*, 4, 803-810, 1993.
- Driscoll, K. G., J. M. Arocena, and H. B. Massicotte. Post-fire soil nitrogen content and vegetation composition in Sub-boreal spruce forests of British Columbia's central interior, Canada. *Forest Ecology and Management*, 121, 227-237, 1999.
- Dyrness, C. T., K. Van Cleve, and J. D. Levison. The effect of wildfire on soil chemistry in four forest types in interior Alaska. *Can. J. For. Res.*, 19, 1389-1396, 1989.
- Epstein, H. E., M. D. Walker, F. S. Chapin III, and A. M. Starfield. A transient, nutrient-based model of arctic plant community response to climate warming. *Ecol. Appl.*, 10, 3, 2000, 824-841, 2000.
- Everett, J. T., and B. B. Fitzharris. The Arctic and the Antarctic, in *The Regional Impacts of Climate Change: An Assessment of Vulnerability*, edited by R. T. Watson, M.

- C. Zinyowera, R. H. Moss, and D. J. Dokken, pp. 85-103. Cambridge Univ. Press. New York, 1998.
- Flannigan, M. D. F., and C. E. Van Wagner, Climate change and wildfire in Canada. *Canadian Journal of Forest Research*, 21, 66-72, 1991.
- Gorham, E., Northern Peatlands, Role in the Carbon Cycle and Probable Responses to Climatic Warming, *Ecological Applications*, 1, 182-195, 1991.
- Goulden, M. L., S. C. Wofsy, J. W. Harden, S. E. Trumbore, P. M. Crill, S. T. Gower, T. Fries, B. C. Daube, S.-M. Fan, D. J. Sutton, A. Bazzaz, and J. W. Munger. Sensitivity of boreal forest carbon balance to soil thaw. *Science*, 279, 210-217, 1998.
- Grogan, P., T. D. Bruns, and F. S. Chapin, III. Fire effects on ecosystem nitrogen cycling in a California bishop pine forest. *Oecologia*, 122, 537-544, 2000.
- Halsey, L. A., D. H. Vitt, and S. C. Zoltai. Disequilibrium response of permafrost in boreal continental western Canada to climatic change. *Clim. Change*, 30, 57-73, 1995.
- Hess, J. C., C. A. Scott, G. L. Hufford, and M. D. Fleming, El Nino and its impact on fire weather conditions in Alaska. *International Journal of Wildland Fire*, 10, 1-13, 2001.
- Hillman, G. R., Some hydrological effects of peatland drainage in Alberta's boreal forest. *Can. J. For. Res.*, 22, 1588-1596, 1992.
- Houghton, R. A., J. L. Hackler, and K. T. Lawrence. The U.S. carbon budget: contributions from land-use change. *Science*, 285, 74-78, 1999.

- IPCC. Summary for Policemakers. Climate Change 2001: Impacts, Adaptation, and Vulnerability, A Report of Group II of the Intergovernmental Panel on Climate Change, also see <http://www.ipcc.ch/pub/wg2SPMfinal.pdf>. 2001.
- Kasischke, E. S., N. L. Christensen, and B. J. Stocks. Fire, global warming, and the carbon balance of boreal forests. *Ecological Applications*, 5, 437-451, 1995.
- Kasischke, E. S., K. P. O'Neill, N. H. F. French, and L. L. Borgeau-Chavez. Controls on patterns of biomass burning in Alaskan boreal forests, in *Fire, Climate Change, and Carbon Cycling in the North American Boreal Forest*, edited by E. S. Kasischke and B. J. Stocks, pp.148-163. Ecological Studies Series, Springer-Verlag, 2000.
- Kurz, W. A., M. J. Apps, B. J. Stocks, and W. J. A. Volney. Global climate change: disturbance regions and tropospheric feedbacks of temperate and boreal forests. *In Biotic Feedbacks in the Global Climate System*. Eds. G. M. Woodwell and F. T. Makenzie. Oxford University Press, New York, 1995.
- Kurz, W. A., and M. J. Apps. Retrospective assessment of carbon flows in Canadian boreal forests. *In Forest Ecosystems, Forest Management and the Global Carbon Cycle*. Eds. M. J. Apps and D. T. Price. Springer-Verlag, NATO Advanced Science Institute Series, 1995.
- Kurz, W. A., and M. J. Apps. A 70-year retrospective analysis of carbon fluxes in the Canadian forest sector, *Ecological Applications*, 9, 56-547, 1999.

- Lachenbruch, A. H., J. H. Sass, B. V. Marshall, and T. H. Moses Jr., Permafrost, heat flow, and the geothermal regime at Prudoe Bay, Alaska. *J. Geophys. Res.*, 87, 9301-9316, 1982.
- Lachenbruch, A. H., and B. V. Marshall, Changing climate: Geothermal evidence from permafrost in the Alaskan Arctic. *Science*, 234, 689-697, 1986.
- Luc, L., and S. Luc, Vegetation changes caused by recent fires in the northern boreal forest of eastern Canada. *J. of Vegetation Science*, 9, 483-492, 1998.
- Lynham, T. J., G. M. Wickware, and J. A. Mason, Soil Chemical changes and plant succession following experimental burning in immature jack pine. *Can. J. Soil Sci.*, 78, 93-104, 1998.
- McGuire, A. D., J. M. Melillo, L. A. Joyce, D. W. Kicklighter, A. L. Grace, B. Moore III, and C. J. Vorosmarty, Interactions between carbon and nitrogen dynamics in estimating net primary productivity for potential vegetation in North America. *Global Biogeochem. Cycles*, 6, 101-124, 1992.
- McGuire, A. D., J. M. Melillo, D. W. Kicklighter, and L. A. Joyce, Equilibrium responses of soil carbon to climate change: Empirical and process-based estimates. *Journal of Biogeography*, 22, 785-796, 1995.
- McGuire, A. D., et al., Carbon balance of the terrestrial biosphere in the twentieth century: Analyses of CO₂, climate and land-use effects with four process-based ecosystem models. *Global Biogeochemical Cycles*, 15, 1, 183-206, 2001.
- McGuire, A. D., J. M. Melillo, J. T. Randerson, W. J. Parton, M. Heimann, R. A. Meier, J. S. Clein, D. W. Kicklighter, and W. Sauf, Modeling the effects of snowpack on

heterotrophic respiration across northern temperate and high latitude regions: Comparison with measurements of atmospheric carbon dioxide in high latitudes. *Biogeochemistry*, 48, 91-114, 2000a.

McGuire, A. D., J. Clein, J. M. Melillo, D. W. Kicklighter, R. A. Meier, C. J. Vorosmarty, and M. C. Serreze. Modeling carbon responses of tundra ecosystems to historical and projected climate: The sensitivity of pan-arctic carbon storage to temporal and spatial variation in climate. *Global Change Biology*, 6, 141-159, 2000b.

McGuire, A. D., and J. E. Hobbie. Global climate change and the equilibrium responses of carbon storage in arctic and subarctic regions. In *Modeling the Arctic System: A Workshop Report on the State of Modeling in the Arctic System Science Program*. pp. 53-54. The Arctic Research Consortium of the United States, Fairbanks, Alaska, 1997.

Melillo, J. M., D. W. Kicklighter, A. D. McGuire, W. T. Peterjohn, and K. M. Newkirk. Global change and its effects on soil organic carbon stocks. In *Role of Nonliving Organic Matter in the Earth's Carbon Cycle*, ed. R. G. Zepp and C. Sonntag, pp. 175-189. John Wiley & Sons, New York, 1995.

Murphy, P. J., B. J. Stocks, E. S. Kasischke, D. Barry, M. E. Alexander, N. H. F. French, and J. P. Mudd. Historical fire records in the North American boreal forest. In: *Fire, Climate Change and Carbon Cycling in North American Boreal Forests*. Eds. E. S. Kasischk and B. J. Stocks, pp 274-288. Ecological Studies Series Springer-Verlag, New York, 1999.

- Oechel, W. C., S. J. Hastings, G. L. Vourlitis, M. Jenkins, G. Reichers, and N. Grulke. Recent change of arctic tundra ecosystems from a net carbon dioxide sink to a source. *Nature*, 361, 520-523. 1993.
- Oechel, W. C., and G. L. Vourlitis. The effects of climate change on land-atmosphere feedbacks in arctic tundra regions. *Trends in Ecology and Evolution*, 9, 324-329. 1994.
- Oechel, W. C., G. L. Vourlitis, S. J. Hastings, R. C. Zulueta, L. Hinzman, and D. Kane. Acclimation of ecosystem CO₂ exchange in the Alaskan Arctic in response to decadal climate warming. *Nature*, 406, 978-981. 2000.
- Osterkamp, T. E., and V. E. Romanovsky. Evidence for warming and thawing of discontinuous permafrost in Alaska. *Permafrost Periglacial process.*, 10, 17-37. 1999.
- Overpeck, J., et al., Arctic environmental change of the last four centuries. *Science*, 278, 1251-1256. 1997.
- Post, W. M., W. R. Emanuel, P. J. Zinke, and A. G. Stangenberger. Carbon pools and world life zones. *Nature*, 298, 156-159. 1982.
- Randerson, J. T., M. V. Thompson, T. J. Conway, I. Y., Fung, and C. B. Field. The contribution of terrestrial sources and sinks to trends in the seasonal cycle of atmospheric carbon dioxide. *Global Biogeochemistry and Cycles*, 11, 535-560. 1997.

- Shaver, G. R., W. D. Billings, F. S. Chapin III, A. E. Giblin, K. J. Nadelhoffer, W. C. Oechel, and E. B. Rastetter, Global change and the carbon balance of arctic ecosystems, *BioScience*, 42, 433-441, 1992.
- Schimmel, J., and A. Granstrom, Fire severity and vegetation response in the boreal Swedish forest, *Ecology*, 77, 1436-1450, 1996.
- Serreze, M. C., J. E. Walsh, F. S. Chapin III, T. Osterkamp, M. Dyurgerov, V. E. Romanovsky, W. C. Oechel, J. Morison, T. Zhang, and R. G. Barry, Observational evidence of recent change in the northern high-latitude environment, *Clim. Change*, 46, 159-207, 2000.
- Smith, C. K., M. R. Coyea, and A. D. Munson, Soil carbon, nitrogen, and phosphorus stocks and dynamics under disturbed black spruce forests, *Ecological Applications*, 10, 3, 775-788, 2000.
- Stocks, B. J., M. A. Fosberg, M. B. Wotton, T. J. Lynham, and K. C. Ryan, Climate change and forest fire activity in North American boreal forests, in *Fire, Climate Change, and Carbon Cycling in the North American Boreal Forest*, edited by E. S. Kasischke and B. J. Stocks, pp. 312-319, Springer-Verlag, New York, 2000.
- Thie, J., Distribution and thawing of permafrost in the southern part of the discontinuous permafrost zone in Manitoba, *Arctic*, 27, 189-200, 1974.
- Viereck, L. A., Wildfire in the taiga of Alaska, *Quaternary Research*, 3, 465-495, 1973.
- Viereck, L. A., Ecological effects of river flooding and forest fires on permafrost in the taiga of Alaska, *permafrost: North America Contribution to 2nd International Conference*, 60-67, 1972.

- Vitt, H. D., L. A. Halsey, and S. C. Zoltai. The changing landscape of Canada's western boreal forest: The current dynamics of permafrost. *Can. J. For. Res.*, 30, 283-287. 2000.
- Waelbroeck, C., P. Monfray, W. C. Oechel, S. Hastings, and G. Vourlitis. The impact of permafrost thawing on the carbon dynamics of tundra. *Geophys. Res. Lett.*, 24, 3, 229-232, 1997.
- Wardle, D. A., O. Zackrisson, and M. -C. Nilsson. the charcoal effect in Boreal forests: mechanisms and ecological consequences. *Oecologia*, 115, 419-426, 1998.
- Wotton, B. M., and M. D. Flannigan. Length of the fire season in a changing climate. *Forest Chronicle*, 69, 187-192, 1993.
- Yoshikawa, K., W. R. Bolton, V. E. Romanovsky, M. Fukuda, and L. D. Hinzman. Impacts of wildfire on the permafrost in the boreal forests of interior Alaska. *Journal of Geophysical Research - Atmospheres*, in press.
- Zackrisson, O., Influence of forest fires on the North Swedish boreal forest. *Oikos*, 29, 22-32, 1977.
- Zimov, S. A., S. P. Davidov, G. M. Zimova, A. I. Davidova, F. S. Chapin III, M. C. Chapin, and J. F. Reynolds. Contribution of disturbance to increasing seasonal amplitude of atmospheric CO₂. *Science*, 284, 1973-1976, 1999.
- Zoltai, S. C., Cyclic development of permafrost in the peatlands of northwestern Alberta, Canada. *Arctic Alpine Research*, 25, 240-246, 1993.

CHAPTER TWO

INCORPORATION OF A PERMAFROST MODEL INTO A LARGE-SCALE ECOSYSTEM MODEL: EVALUATION OF TEMPORAL AND SPATIAL SCALING ISSUES IN SIMULATING SOIL THERMAL DYNAMICS¹

Abstract. This study evaluated whether a model of permafrost dynamics with a 0.5-day resolution internal time step that is driven by monthly climate inputs is adequate for representing the soil thermal dynamics in a large-scale ecosystem model. An extant version of the Goodrich model was modified to develop a soil thermal model (STM) with the capability to operate with either 0.5-hour or 0.5-day internal time steps and to be driven with either daily or monthly input data. The choice of internal time step had little effect on the simulation of soil thermal dynamics of a black spruce site in Alaska. The use of monthly climate inputs to drive the model resulted in an error of less than 1°C in the upper organic soil layer and in an accurate simulation of seasonal active layer dynamics. Uncertainty analyses of the STM driven with monthly climate inputs showed that soil temperature estimates of the upper organic layer were most sensitive to

¹In press at *Journal of Geophysical Research – Atmospheres*. Zhuang, Q., V. E. Romanovsky, and A. D. McGuire, Incorporation of a permafrost model into a large-scale ecosystem model: Evaluation of temporal and spatial scaling issues in simulating soil thermal dynamics.

variability in parameters that described snow thermal conductivity, moss thickness, and moss thermal conductivity. The STM was coupled to the Terrestrial Ecosystem Model (TEM), and the performance of the coupled model was verified for the simulation of soil temperatures in applications to a black spruce site in Canada and to white spruce, aspen, and tundra sites in Alaska. A 1°C error in the temperature of the upper organic soil layer had little influence on the carbon dynamics simulated for the black spruce site in Canada. Application of the model across the range of black spruce ecosystems in North America demonstrated that the STM-TEM has the capability to operate over temporal and spatial domains that consider substantial variation in surface climate given that spatial variability in key structural characteristics and physical properties of the soil thermal regime are described.

1. Introduction

There is evidence that warming is occurring in some high-latitude areas [*Beltrami and Mareschal*, 1991; *Chapman and Walsh*, 1993; *Osterkamp and Romanovsky*, 1999; *Serreze et al.*, 2000]. Ground temperature records for North America reconstructed from borehole temperature logs support the notion that large-scale warming has been occurring since the 19th century [*Lachenbruch et al.*, 1982; *Lachenbruch and Marshall*, 1986]. Over the last few hundred years, permafrost conditions in the Arctic have changed and are likely to continue changing [*Overpeck et al.*, 1997]. In the western boreal forest of Canada, permafrost has responded dynamically to climatic changes that have been

occurring since the little Ice Age [Vitt *et al.*, 2000]. The soil thermal regime and the distribution of permafrost in regions with discontinuous permafrost are especially sensitive to climate changes [Osterkamp and Romanovsky, 1999; Brown, 1960; Halsey *et al.*, 1995].

Although warming is occurring in high latitudes, some high-latitude regions are warming, other regions are cooling, and there is substantial interannual variability in climate across high latitudes [Everett and Fitzharris, 1998]. Projections of climate trends for high-latitude regions exhibit substantial temporal and spatial heterogeneity [McGuire *et al.*, 2000a], and this variability is expected to influence the structure and function of high-latitude ecosystems [McGuire and Hobbie, 1997; Epstein *et al.*, 2000; McGuire *et al.*, 2000a]. The response of carbon dynamics in high-latitude ecosystems, which contain approximately 40% of the reactive soil carbon in the terrestrial biosphere [McGuire *et al.*, 1995], to spatial and temporal variability in climate is of concern because the response has the potential to influence CO₂ concentrations in the atmosphere [Oechel *et al.*, 1993; McGuire and Hobbie, 1997; McGuire *et al.*, 2000a].

A number of studies have indicated that permafrost dynamics may substantially influence carbon storage [Vitt *et al.*, 2000] and carbon dynamics [Hillman, 1992; Waelbroeck *et al.*, 1997; Goulden *et al.*, 1998] of high-latitude ecosystems. Goulden *et al.* [1998] suggested that the stability of the soil carbon pool at a black spruce site in Canada appears sensitive to the depth and duration of thaw, and climatic changes that promote thaw are likely to cause a net efflux of carbon dioxide from the site. On the other hand, warming may not always lead to C losses [Shaver *et al.*, 1992; McGuire *et al.*,

1992, 2000a, 2001; *Oechel et al.*, 2000; *Clein et al.*, 2000, in press], and it is not clear if high-latitude ecosystems are presently storing or releasing carbon or if there is interannual variability in the source-sink activity of high latitudes [*Chapin et al.*, 2000].

Large-scale ecosystem models have been developed to simulate the carbon dynamics of the terrestrial biosphere [*McGuire et al.*, 2001]. Given that permafrost dynamics are currently changing in high latitudes and are likely to continue changing as the climate warms, it is important for these models to consider how changes in the soil thermal regime influence ecosystem structure and function. Although it has been demonstrated that representing the insulative effects of snowpack on the soil thermal regime improves the ability of large-scale ecosystem models to reproduce seasonal features of atmospheric CO₂ concentrations at high-latitude monitoring stations [*McGuire et al.*, 2000b], these models have been slow to integrate a consideration of permafrost into their dynamics.

Site-specific models of permafrost dynamics often simulate soil thermal dynamics based on a two-dimensional finite element or finite difference formulation [*Osterkamp and Gosink*, 1991; *Guymon and Hromadka*, 1977; *Guymon et al.*, 1984; *Romanovsky et al.*, 1991a, 1991b; *Garagulya et al.*, 1995]. These models typically use a fine-resolution internal time step (e.g., 0.5 hours) and fine resolution depth steps in the soil (e.g., 1 cm to 5 cm resolution depending on depth), and are driven by daily or subdaily resolution climate data. In contrast, large-scale ecosystem models are generally driven by monthly climate inputs [*Heimann et al.*, 1998; *Cramer et al.*, 1999; *Kicklighter et al.*, 1999; *McGuire et al.*, 2000a, 2000b, 2001]. Although a permafrost model with a fine internal

time step driven by fine resolution climate data has obvious numerical advantages in comparison to a model with coarser resolution. It imposes a substantial computational time cost on the coupled model.

In this study we address the question whether a model of permafrost dynamics with a coarse resolution internal time step (0.5 days) that is driven by monthly climate inputs is adequate for representing soil thermal dynamics in large-scale ecosystem models that are driven by monthly climate inputs.

2. Methods

2.1. Overview

In this study we modified an extant version of the Goodrich model [Goodrich, 1976, 1978a, 1978b] for Alaskan ecosystems [Romanovsky *et al.*, 1997] to develop a soil thermal model (STM) with the capability to operate with either 0.5-hour or 0.5-day internal time steps and to be driven by either daily or monthly input data. On the basis of empirical data, calibration, and review of the scientific literature, we specified parameters of the model for a black spruce forest stand located in the Bonanza Creek Experimental Forest near Fairbanks, Alaska, where soil and air temperatures were measured from May 1996 to April 1997. We applied the model in a factorial fashion to this site with respect to the temporal resolutions of internal time step (0.5 hours and 0.5 days) and input data (daily and monthly). To provide monthly inputs to the model, we aggregated air temperature and snow depth to monthly resolution. We evaluated the performance of the factorial applications of the model by comparing simulated daily and monthly soil

temperature to measurements of soil temperature at different depths. To evaluate issues of temporal scaling, we also analyzed differences among the factorial applications to determine the relative importance of internal time step and climate inputs to the differences. To evaluate spatial scaling issues, we conducted uncertainty analyses that allowed us to determine which parameters need to be described in a spatially explicit fashion for spatial application of the model. For application of the model to larger spatial scales, we coupled the STM with the Terrestrial Ecosystem Model (TEM) [*Xiao et al.*, 1998; *Tian et al.*, 1998, 1999, 2000; *Kicklighter et al.*, 1999; *Schimel et al.*, 2000; *McGuire et al.*, 2000a, 2000b, 2001; *Clein et al.*, 2000, in press; *Amthor et al.*, this issue], which provides the STM with monthly estimates of snowpack dynamics. To evaluate the performance of the coupled model for different vegetation types in high latitudes, we verified simulations of soil temperature by the model for white spruce, aspen, and tundra sites in Alaska in addition to a black spruce site in Canada. To determine whether it is appropriate to use simulated soil temperatures to drive ecosystem processes, we compared field-based and simulated estimates of carbon fluxes for the black spruce site in Canada. Finally, to evaluate the ability of the model to operate across a substantial spatial and temporal domain, we applied the black spruce parameterization of the coupled STM-TEM model to the range of black spruce forest ecosystems across North America.

2.2. Model Development

The Goodrich model is a one-dimensional finite difference model of heat flow in soils which considers phase changes between water and ice and includes the thermal effects of changes in snow depth and snow characteristics during the winter [*Goodrich*

1976, 1978a, 1978b]. The model simulates the thermal dynamics of a system that includes snow cover, thawed soil, and frozen soil in which the upper and lower boundaries of the system are specified. Soil thermal dynamics of the system are determined through finite difference calculations between specified depth steps within each of the major layers of the system.

In our modification of the Goodrich model, which we refer to as the soil thermal model (STM) in this study, the vertical profile is divided into snow cover, moss, upper organic soil, lower organic soil, and mineral soil layers (Figure 1a). Application of the model for a site requires specification of the thickness of each layer and simulation depth steps within each layer. The thermal properties of each layer also need to be prescribed. In addition, the dynamics of phase changes in the soils depend on the phase temperature, which we set to 0°C for applications of the model in this study. Specification of the upper boundary condition includes the temperature at the top of the moss layer during the summer and at the surface of snow during the winter. In this study we prescribed the depth, density, and thermal properties of snow cover. For the lower boundary condition we assumed a constant heat flux. Alternatively, the lower boundary condition can be specified as a temporally varying function of temperature or heat flux. Application of the model requires the prescription of initial conditions, which include specifying the initial soil temperatures of the system and the presence or absence of permafrost.

To drive the model with daily inputs, the model linearly interpolates to 0.5-hour or 0.5-day resolution with three sequential days of data on daily air temperature and snow depth for the current day, the previous day, and the next day. Similarly, to drive the

model with monthly inputs, the model linearly interpolates data on monthly air temperature and snow depth for the current month, the previous month, and the next month. For example, to determine air temperature data for the model's internal 0.5-day time step in November, approximately 60 points are linearly interpolated between mean monthly October and November air temperature to determine the 30 points for the first half of November, and approximately 60 points are interpolated between mean monthly November and December air temperature to determine the 30 points for the second half of November.

2.3. Evaluation of STM Performance

2.3.1. Parameterization. We specified the parameters of the STM for a black spruce stand in the Bonanza Creek Experimental Forest near Fairbanks, Alaska, based on empirical data, calibration, and review of the scientific literature. The ground layer of this stand is covered by a nearly continuous layer of feather moss (*Hylocomium Splendens* and *Pleurozium Shreberi*). The distribution of permafrost and the active layer thickness is consistently uniform across the stand. Observed data for the stand include measurements of daily air temperature and daily soil temperatures at different depths (0, 23, 32, 42, and 52 cm, where 0 cm is the top of the moss layer) from May 1996 to April 1997.

In the STM we set the lower-boundary condition for this stand to a constant geothermal heat flux of 0.05 W m^{-2} [Osterkamp and Romanovsky, 1999]. Within each layer, we calculated the soil thermal dynamics for 10 depth steps within the snow layer, for 3.5 cm depth steps within the 12 cm of living and dead moss layer, for 2.5 cm depth steps within the 28 cm of upper organic soil layer, for 2 cm depth steps within the 64 cm

of the lower organic soil layer, for 10 cm depth steps within the first 40 cm of the mineral soil layer, and for 50 cm depth steps down to the lower boundary of the mineral soil layer, which in our simulations was located at the 10 m depth from the top of the moss layer. We set the snow thermal conductivity to $0.2 \text{ W m}^{-1} \text{ K}^{-1}$. The thawed soil thermal conductivity, frozen soil thermal conductivity, and water content and heat capacity for the moss, organic soil, and mineral soil layers are documented in Table 1.

2.3.2. Model Simulations. To evaluate the performance of the STM with either 0.5-hour or 0.5-day internal time steps and with either daily or monthly climate inputs, we conducted simulations of the soil thermal regime for the black spruce stand at Bonanza Creek between May 1996 and April 1997 in a two-factor design that considered different combinations for the temporal resolutions of internal time step and input data (Figure 2): Simulation (I) 0.5-hour internal time step and daily inputs; (II) 0.5-day internal time step and daily inputs; (III) 0.5-hour internal time step and monthly inputs; and (IV) 0.5-day internal time step and monthly inputs. The inputs of daily air temperature (Figure 3a) and snow depth (Figure 3b) for simulations I and II were obtained from measurements made at the Fairbanks International Airport weather station. To provide monthly inputs for simulations III and IV, we calculated monthly means from the daily air temperature and snow depth data used in simulations I and II. Soil temperatures can be output by the STM at the resolution of the internal time step. For each of the simulations we calculated mean daily and mean monthly soil temperature at several depths in the system profile (0, 23, 32, 42, and 52 cm, where 0 cm is the top of the moss layer) for comparison with

observed mean daily and monthly soil temperature at corresponding depths in the correlation and regression analyses. In addition to evaluating performance at various depths of the system, we also evaluated the performance of the model to simulate the aggregated temperature within the upper organic layer, which is an important region for biological activity in the soil. The soil temperature in the upper organic layer ($T_{LO}^{(m)}$) at time m is obtained by linearly aggregating soil temperatures simulated at 2.5 cm depth steps throughout the 28 cm of the upper organic layer:

$$T_{LO}^{(m)} = \frac{\sum_{j=0}^{j=k} (T(m,j) * X(j))}{\sum_{j=0}^{j=k} X(j)} \quad (1)$$

Where $T(m,j)$ is the soil temperature at time m and node j , $X(n)$ is soil depth at node n , and k is the number of nodes within the upper organic layer with the zero node located at the boundary between the moss and the upper organic layer and the k node located at the boundary between the upper and the lower organic layers. We also calculated the root-mean-square deviation (D_{RMS}) of each soil depth and for the upper organic layer as well as active layer depths between each combination of the four simulations so that we could assess whether simulated soil temperature and active layer depth were more influenced by changing the resolution of the internal time step or by changing the resolution of the input data. We calculated D_{RMS} as

$$D_{\text{RMS}} = \sqrt{\frac{\sum_{i=1}^{i=n} (T_i - TT_i)^2}{n}} \quad (2)$$

Where T_i and TT_i are daily or monthly soil temperatures for each pair of simulations. i is simulation day or month, and n is number of days or months.

2.4. Uncertainty Analyses

Uncertainty analysis relates the variability in model predictions to uncertainty in the parameters of the model [Turner *et al.*, 1994]. In this study we conducted uncertainty analyses for the version of the model that used 0.5-day internal time step and monthly inputs to identify which parameters need to be specified for spatial application of the model. Our analysis focused on evaluating the parameter uncertainty of the simulated mean monthly temperatures aggregated for the upper organic layer between May 1996 and April 1997. Simple Pearson correlation coefficients (R) were calculated between each of the parameters and the model predictions. We used the squared Pearson correlation coefficient (R^2), which is the percentage of the total variance in an output variable of the model that was explained by variability in a particular parameter, as our index of uncertainty. If the parameters considered in the uncertainty analysis are independent of each other, then the squared Pearson correlation coefficient can be used as a sensitivity measure [Rose *et al.*, 1991]. The sum of the sensitivity measures quantifies the proportion of the total variance of the model prediction that relates linearly to variation in the parameter [Bartell *et al.*, 1988].

To examine how the uncertainty relationships between output variables and parameters potentially depend on climate, we evaluated another eight climate scenarios in addition to the normal climate scenario defined by the observed air temperature and snow depth at the site (Table 2). For scenarios that considered higher or lower air temperature and which considered shallower and deeper snow depths, we manipulated air temperature and snow depth by increasing or decreasing by 20% the monthly mean air temperature and snow depth derived from the data measured at Fairbanks International Airport between May 1996 and April 1997. For each uncertainty analysis we obtained the 100 values of each parameter for the analysis by randomly drawing from a uniform random distribution over the possible range for each parameter (see Table 1). In the uncertainty analyses we considered all parameters in Table 1 except for the parameters that defined the water content of the lower organic and mineral soil layers because we were interested in evaluating the sensitivity to water content in the moss and upper organic layers. Correlation analysis among the parameters indicated that the parameters were statistically independent, as all R^2 values were less than 0.094 between pairs of parameters.

2.5. Evaluation of STM-TEM Performance for Different Ecosystem Types

We coupled the STM with version 4.2 of the Terrestrial Ecosystem Model (TEM) [McGuire *et al.*, 2001], which includes hydrology derived from the water balance model of Vorosmarty *et al.* [1989] and provides spatially distributed snow depth estimates based on precipitation inputs. In the coupled model (STM-TEM), the STM operates with an internal 0.5-day time step and monthly inputs of air temperature and snow depth. The

snow depth is calculated by a specified snow density and snow water equivalent, which is provided from the simulation of hydrology by TEM (Figure 1b). We verified soil temperatures simulated by STM-TEM for four sites that represent the structural diversity of ecosystems that occur throughout high latitudes. These sites include a black spruce site in Canada and white spruce (*Picea glauca*), aspen (*Populus tremuloides*), and tussock tundra (*Eriophorum Vaginatum*) sites in Alaska (Table 3).

The black spruce site in Canada is the old black spruce (OBS) site of the northern study area (NSA) of the Boreal Ecosystem-Atmosphere Study [Sellers *et al.*, 1997]. The white spruce ecosystem is a 100-year old forest located on a south-facing slope in the Bonanza Creek Experimental Forest with a silt-loam soil that contains permafrost. The aspen ecosystem is a 100-year old forest located near Fairbanks, Alaska with a silt-loam soil that contains no permafrost. The tussock tundra site is located near the Toolik Lake field station on a site with an organic soil that contains permafrost. We defined the profile of the system and parameters of STM-TEM for each of these sites based on physical properties of soils for each site (Table 1). The presence or absence of permafrost is prescribed through the initial temperature profile at each site. For application of the STM-TEM to these sites, we conducted simulations from 1975 to 1997 and compared the simulated and observed monthly soil temperatures at different depths for a period of time near the end of the simulations. The monthly climate data for driving the STM-TEM were determined from data measured at local weather stations or study sites (Table 3).

2.6. Evaluation of Carbon Fluxes for a Black Spruce Forest

In the STM-TEM, monthly soil temperature of the upper organic layer is used to drive the processes of decomposition and gross nitrogen mineralization in the simulation by the model (Figure 1b). To evaluate the performance of the model in simulating ecosystem carbon fluxes, we parameterized the STM-TEM for a black spruce forest site at the Bonanza Creek Experimental Forest, Alaska similar to the procedures described by *Clein et al.* [in press; see also *Amthor et al.*, in press] and applied the model to simulate carbon dynamics for the black spruce site in Canada. To evaluate how uncertainty in simulated soil temperatures might influence estimates of carbon dynamics by the STM-TEM, we simulated carbon fluxes for two additional soil temperature scenarios. We manipulated the baseline simulated soil temperature of the upper soil organic layer (scenario B) by increasing (scenario I) or decreasing (scenario D) monthly temperatures of the layer by 1°C and compared simulated carbon fluxes among these soil thermal scenarios. The carbon fluxes we evaluated include monthly gross primary production (GPP), which is the amount of carbon taken up by the vegetation through the process of photosynthesis, and monthly ecosystem respiration (RESP), which is the amount of carbon released to the atmosphere through respiration by the vegetation and through decomposition of soil organic matter. Net ecosystem production (NEP), which represents the net exchange of carbon with the atmosphere is calculated as the difference between GPP and RESP. Increases in ecosystem carbon storage are indicated by positive values of NEP, while decreases in carbon storage are indicated by negative values of NEP.

2.7. Application to the Range of Black Spruce Ecosystems across North America

To evaluate the ability of the STM-TEM to operate at large temporal and spatial scales, we applied the black spruce parameterization of the model for the NSA-OBS black spruce site to simulate soil thermal dynamics for the range of black spruce forest ecosystems across North America north of 50°N from 1900 to 2100. The climate data for the historical period (1900 to 1994) were developed at 0.5° spatial resolution by the Max Planck Institute for Meteorology (M. Heimann, unpublished data, 2000) by interpolating the monthly temperature anomalies of *Jones* [1994] and the monthly precipitation anomalies of *Hulme* [1995] to 0.5° resolution and then adding them to the long-term monthly air temperature and precipitation in the Cramer-Leemans CLIMATE database, which is an update of *Leemans and Cramer* [1991] database. The climate data for the projected period (1995 to 2100) were based on monthly temperature and precipitation ramps defined from a transient simulation of the Hadley Center CM2 model. The CM2 simulation we used considered the radiative forcing associated with the combined effects of changes in greenhouse gases and sulphate aerosols [*Mitchell et al.*, 1995]. The methods for creating the projected monthly climate (air temperature and precipitation) are described in *McGuire et al.* [2000a].

3. Results

3.1. Evaluation of STM Performance

3.1.1. Simulated Daily Soil Temperature. For the black spruce site at the Bonanza Creek Experimental Forest, the daily soil temperatures estimated by the four simulations

at various depths (0, 23, 32, 42, and 52 cm and upper organic soil layer) generally fit the observed data well (Table 4 (top)). For linear regression analyses between simulated and observed soil temperatures, the proportion of variance explained (R^2) ranged from 0.61 to 0.91, slopes of the analyses ranged 0.80 to 1.10, and intercepts were less than 0.60°C . In general, simulated soil temperatures near the surface were more accurate than simulated soil temperatures deeper in the profile. For the soil temperature aggregated across the upper organic layer, which is the temperature that is used to drive soil biogeochemical processes in the coupled model, R^2 values (0.77 to 0.79), slopes (0.80 to 0.94), and intercepts (-0.06 to 0.14°C) across the four simulations were similar.

Although these comparisons indicate that the temporal resolution of internal time step and of input data did not substantially influence the overall accuracy of daily soil temperature simulated by the STM for the year of observed soil temperature, there are some seasonal differences among the simulations. For surface temperature (Figure 4a), simulations III and IV tended to underestimate from April to July and tended to overestimate from August to October and in March. Except for March the surface temperature estimated by simulations I and II did not show these biases. For the soil temperature of the upper organic layer (Figure 4b), simulations III and IV tended to underestimate during April, May, December, and January and tended to overestimate from July to September and during March. Simulations I and II also tended to underestimate soil temperature in December and January and overestimate soil temperature in March.

These patterns suggest that differences among the simulations are related more to the temporal resolution of the input data than to resolution of the internal time step. To formally evaluate how differences in daily soil temperature among the simulations were influenced by differences in the temporal resolution of internal time step and input data, we calculated D_{RMS} for various soil depths between pairs of simulations (Table 5 (top)). At each depth in the profile, D_{RMS} was greater for pairs I-III, I-IV, II-III, and II-IV than for pairs I-II and III-IV. This result indicates that the simulations were more influenced by the temporal resolution of input data than by the temporal resolution of internal time step. Because D_{RMS} for pairs I-III, I-IV, II-III, and II-IV were greater for depths nearer the surface of the profile with values near 4°C at the surface, it appears that the temporal resolution of input data primarily influences estimates of soil temperature close to the surface. For the upper organic layer, D_{RMS} between simulations I-IV and II-IV was less than 1°C. Thus the version of the model that uses 0.5-day internal time step and monthly input data may be acceptable if a root-mean-square error of 1°C in daily soil temperature is acceptable for driving soil processes in a daily biogeochemical model.

3.1.2. Simulated Monthly Soil Temperature and Active Layer Depth. The monthly soil temperature at the various depths and the active layer depth estimated by the four simulations generally fit the observed data well (Table 4(bottom)). For linear regression analyses between simulated and observed soil temperatures, the proportion of variance explained (R^2) ranged from 0.65 to 0.95, slopes ranged from 0.80 to 1.12, and the intercepts were less than 0.63°C. In contrast to the analysis for simulated daily soil temperatures, the accuracy of simulated monthly soil temperatures did not deteriorate

with increasing depth, although the simulations were most accurate at the surface. For the soil temperature aggregated across the upper organic soil layer, R^2 values (0.82 to 0.86), slopes (0.80 to 0.95), and intercepts (-0.06 to 0.50°C) across the four simulations were similar. For the regression analysis between observed and simulated active layer depths, R^2 values (0.85 to 0.95), slopes (0.99 to 1.43), and intercepts (-0.01 to 0.06 m) across the four simulations were comparable. The seasonal differences noted in the analysis of simulated daily soil temperatures is reflected in the comparison between observed and simulated monthly soil temperatures (Figure 5). For monthly surface temperature (Figure 5a), simulations I and II matched the observed data from May to September, tended to underestimate from October to December, and tended to overestimate from February to April. Simulations III and IV slightly underestimated monthly soil temperature from May to July and in November, December, and February and slightly overestimated soil temperature from August to October. For monthly temperature of the upper organic soil layer (Figure 5b), simulations I and II performed well from May to September, but underestimated from October to January. Except for August, September, and March, simulations III and IV tended to underestimate monthly temperature in the upper organic soil layer.

These patterns suggest that differences among the simulations were related more to temporal resolution of the input data than to resolution of the internal time step, which is a conclusion from the analysis of daily soil temperatures. Conclusions from the results of the monthly D_{RMS} analyses (Table 5(bottom)) are also similar to those of the daily analyses as they indicate that (1) the simulations were more influenced by the temporal

resolution of input data than by the temporal resolution of internal time step. (2) the temporal resolution of the input data primarily influences estimates of temperature close the soil surface, and (3) D_{RMS} for all pairs of simulations was less than 1°C for the upper organic soil layer. For active layer depth, D_{RMS} was less than 0.06 m for all pairs of simulations. Thus the version of the model that uses 0.5-day internal time step and monthly input data accurately estimates the depth of the active layer and may be acceptable if a root-mean-square error of 1°C in monthly soil temperature is acceptable for driving soil processes in a monthly biogeochemical model.

3.2. Uncertainty Analyses

For the uncertainty analysis under the normal climate scenario, 30 to 80% of the variance in monthly soil temperature of the upper organic soil layer was explained by uncertainty in a subset of the parameters (Table 1, Figure 6), including the moss thickness (V1), moss thermal conductivity (V5 and V6), and snow thermal conductivity (V25). From January to April, uncertainty in moss thickness (Figure 6, V1) explained less variability than from June to October. Soil temperature was sensitive to uncertainty in the parameters describing the thermal conductivity of thawed and frozen moss (Figure 6), but was more sensitive to uncertainty in thermal conductivity of thawed moss (V6) during summer than to the uncertainty of thermal conductivity of frozen moss (V5) during winter (Figure 6). Although uncertainty in snow thermal conductivity (V25) explained almost 30% of the variability in soil temperature from January to April, it only explained 2% and 11% of the variability in November and December, respectively (Figure 6).

The sensitivity of soil temperature in the upper organic layer to uncertainty in each of the parameters varied among the nine climate scenarios. The pattern of sensitivity among climate scenarios to uncertainty in the thermal conductivity of snow (Figure 7) and in moss thickness (Figure 8) illustrates that the pattern varies among parameters. For snow thermal conductivity, the sensitivity of soil temperature of the upper organic layer to uncertainty in this parameter ranged from approximately 10 to 30% from December to April under the normal and low temperature scenarios (Figure 7a and 7b), but soil temperature was insensitive during other months of the year and under the high temperature scenarios (Figure 7c). For moss thickness, the sensitivity of soil temperature to uncertainty in this parameter ranged from approximately 20 to 30% from May to October under all temperature scenarios (Figure 8). From December to April, uncertainty in moss thickness explains less than 10% of the variability in soil temperature across scenarios because snow thermal conductivity is a more important parameter in these months. The uncertainty analyses suggest that the accuracy to which parameters should be determined depends on the parameter and for some parameters depends on the climate space to which the model is applied.

3.3. Applications to Different Ecosystem Types

To evaluate the performance of the coupled model for different ecosystem types, in which the STM receives snow depth data from the hydrology model of TEM, we parameterized the model for a black spruce ecosystem in Canada and for white spruce, aspen, and tussock tundra ecosystems in Alaska (Table 1; see section 2). For the black

spruce ecosystem. soil temperatures simulated by the coupled model reproduced the observed data well at various depths in the profile (Figure 9). For regressions between simulated and observed at different depths, R^2 ranged from 0.96 to 0.98, slopes ranged from 0.88 to 1.04, and intercepts ranged from 0.72 to 1.56°C (Table 6 (top)). These results indicate that the model can be applied to black spruce ecosystems with different structural characteristics and different soil thermal regimes when the model has information on structural characteristics relevant to the dynamics of the soil thermal regime.

For application to other ecosystems in high-latitude regions of North America, soil temperatures simulated by the coupled model reproduced the observed data well at various depths in the profile for white spruce (Figure 10), aspen (Figure 11), and tussock tundra (Figure 12) ecosystems in Alaska. For regressions between simulated and observed temperatures at different depths in these ecosystems, R^2 ranged from 0.72 to 0.96, slopes ranged from 0.71 to 1.04, and intercepts ranged from -0.64 to 0.60°C (Table 6 (middle-bottom)). These results indicate that the model can be applied to different high-latitude ecosystems when the model has information on structural characteristics, physical properties, and boundary conditions relevant to the dynamics of the soil thermal regime.

3.4. Evaluation of Carbon Fluxes Simulated for a Black Spruce Forest

The estimates of monthly GPP and RESP simulated by the STM-TEM for the simulated soil temperature of the upper organic soil layer in the baseline scenario were

highly correlated with tower-based estimates for the black spruce site in Canada (Figure 13: $R^2 = 0.93$ for GPP and 0.94 for RESP). While the slopes of regression between observed and simulated were not significantly different from 1 for both GPP and RESP (slopes = 1.01 for GPP and 1.06 for RESP), the intercepts were significantly different from 0 (intercept = $-7.5 \text{ g C m}^{-2} \text{ month}^{-1}$ for GPP and $-10.6 \text{ g C m}^{-2} \text{ month}^{-1}$ for RESP). Simulated monthly NEP generally fit the seasonal trends of the field-based estimates, although the correlation between field-based and simulated estimates of NEP ($R^2 = 0.60$) was lower than for estimates of GPP and RESP. Similar to the relationships between observed and simulated GPP and RESP, the slope between simulated and observed NEP (0.82) was not significantly different from 1, while the intercept ($-2.21 \text{ g C m}^{-2} \text{ month}^{-1}$) was statistically different from 0. The estimates of GPP, RESP, and NEP of scenario B were highly correlated with estimates simulated for scenarios I and D ($R^2 = 0.99$ for all B-I and B-D comparisons) with slopes that were not significantly different from 1 (slopes ranged from 0.96 to 1.02 for B-I comparisons and from 0.97 to 1.02 for B-D comparisons) and intercepts (less than $0.50 \text{ g C m}^{-2} \text{ month}^{-1}$ for all B-I and B-D comparisons) that were not significantly different from 0. These analyses indicate that differences of less than 1°C in simulated temperatures for the upper organic soil layer do not significantly affect the short-term carbon dynamics simulated by the STM-TEM.

3.5. Application to the Range of Black Spruce Ecosystems across North America

We applied the parameterization of the STM-TEM for the black spruce forest in Canada to simulate soil thermal dynamics for the range of black spruce forest ecosystems

across North America north of 50°N from 1900 to 2100 at a spatial resolution of 0.5° latitude x longitude. This simulation maintained constant structural characteristics of the simulated soil profile, as defined by the black spruce site used to parameterize the model, but was driven by air temperature and snow depth that varied both spatially and temporally. The simulation of mean annual soil temperature within the upper organic soil layer for four different decades (1930s, 1980s, 2030s, and 2080s) responded to the spatial and temporal climatic variability that was used to drive the simulation (Figure 14). For all decades a north-south gradient in soil temperatures for this layer was maintained across the range of black spruce in North America north of 50°N. Across decades, the soil temperature at this depth increased from the 1930s to the 2080s in a fashion consistent with the scenario of climatic warming that was used to drive the simulation. These results indicate that the model has the potential to be used at large spatial scales to simulate the response of the soil thermal regime to climate change and variability.

4. Discussion

In this study we modified an extant model of permafrost dynamics for incorporation into a large-scale biogeochemical model that is driven by monthly climate data. Our incorporation of permafrost dynamics was based on an extant version of the Goodrich model, which uses a numerical approach to simulate soil temperatures throughout the soil profile. Although analytical approaches to heat conduction represent an alternative to the numerical approach we have implemented in this study, they have a number of limitations for applications to ecosystems affected by permafrost [*Goodrich*,

1976; *Romanovsky et al.*, 1997]. *Williams and Smith* [1989] point out that analytical solutions to the heat conduction are only applicable when transient effects of phase change are not important. The numerical solution of the Goodrich model is able to consider how phase changes are influenced by the effects of latent heat, which dominate the thermal dynamics of a freezing and thawing soil. In contrast, analytic approaches are only capable of predicting monotonic thaw penetration and tend to overestimate thaw depth because the approach fails to properly account for heat storage effects [see *Goodrich*, 1976]. Possible disadvantages of the Goodrich approach include computational costs and the number of parameters that need to be specified for implementing the approach. Therefore, we evaluated both temporal and spatial scaling issues to determine suitability of this approach for incorporation into a large-scale ecosystem model.

4.1. Temporal Scaling Issues

Romanovsky et al. [1997] conducted a comprehensive evaluation of three numerical models used in simulations of the active layer and permafrost temperature regimes with respect to internal time step and with respect to the depth step of different layers, and concluded that the choice of optimum time and depth steps appears to be specific to the application. The choices we made for depth steps in this study were based on what we considered to be an acceptable compromise between computational efficiency and simulation accuracy. Our evaluation of model performance indicated that there was little difference between simulations of daily or monthly soil temperature that

used different internal time steps considered in this study (0.5 hours and 0.5 days), and all applications of the model accurately simulated the depth of the active layer. Between simulations that used input climate data at different temporal resolutions (daily versus monthly), we did find some differences in simulated daily and monthly soil temperature. Our evaluation of these differences indicated that monthly resolution climate data could be used to drive simulations if an error of less than 1°C is acceptable for driving soil biogeochemical processes. Results of a sensitivity analysis indicate that an error of less than 1°C in the temperature of the upper organic soil layer does not significantly affect the carbon dynamics simulated by the STM-TEM. Furthermore, simulations with the STM-TEM indicate that annual carbon balance across the boreal region of North America is sensitive to the timing of spring thaw [Zhuang et al., unpublished, 1999], which is a conclusion reached in a site-specific analysis of this issue by *Frolking et al.* [1996]. The ongoing development of data sets that describe the freezing and thawing of the land surface at large spatial scales [e.g., *Running et al.*, 1999; *Frolking et al.*, 1999] represents important information for evaluating the timing of soil thermal dynamics simulated by the STM-TEM at large spatial scales.

4.2. Spatial Scaling Issues

The application of the model to the range of black spruce ecosystems across North America north of 50°N from 1900 to 2100 demonstrated to us that the soil thermal model has the capability to operate over spatial and temporal domains that consider substantial variation in surface climate. It is important to recognize that this application

did not consider spatial variation in vegetation distribution. It also did not consider spatial variation in structural characteristics, physical properties, and lower boundary conditions of the soil thermal regime. The application also did not consider temporal changes in vegetation, structural characteristics, and physical properties associated with disturbance and gradual vegetation dynamics, e.g., changes in tree line. Our evaluation of model performance for different representative ecosystem types of high-latitude regions in North America indicated that the model can be applied to different vegetation types when it has information on structural characteristics, physical properties, and lower boundary conditions relevant to the soil thermal regime. Although a number of vegetation classifications are available at the global scale, classifications that can be linked to structural characteristics, physical properties, and lower-boundary conditions of the soil thermal regime in high latitudes will be most useful in the context of simulating soil thermal dynamics at large spatial scales. The development of spatially resolved data sets that describe structural characteristics, physical properties, and lower-boundary conditions of the soil thermal regime are necessary to facilitate progress in modeling the soil thermal regime at large spatial scales.

Our uncertainty analyses are relevant to the development of spatially resolved data sets in that they provide insight on which structural characteristics and physical properties of the soil thermal regime need to be determined for improving spatial applications of the STM-TEM. These analyses were primarily focused on soil temperature of the upper organic layer, which is the temperature used to drive soil biogeochemical processes in the coupled model. The uncertainty analyses identified that

soil temperature estimates of the model for the organic layer were sensitive to variability in moss thickness and thermal conductivity under "normal" conditions of air temperature and snow depth, which is consistent with the field studies of *Dyrness* [1982]. Other modeling studies, for example, *Frolking and Crill* [1994] who adopted the method of *Clymo* [1984], highlight the need to consider how the physical properties of moss influence soil thermal dynamics. In addition, soil temperature was sensitive to uncertainty in snow thermal conductivity, a result that has been highlighted in other modeling studies [*Zhang et al.*, 1996, 1997]. The uncertainty analyses of the study also revealed that the accuracy to which these parameters should be determined depends on the climate, a result that has been reported for other parameters in land surface schemes [*Pitman*, 1994]. With respect to the development of spatial data sets that describe the structural and physical properties of the soil thermal regime, our study indicates that effort should be prioritized on developing data sets that describe spatial variability of snow and moss thickness and of snow and moss thermal conductivity. Besides the development of data sets for "best" estimates of the parameters, it is also important to develop data sets for uncertainty in the parameter estimates.

4.3. Additional Issues and Future Directions

The dynamics of snow influence the soil thermal regime in cold regions because the low thermal conductivity of snow makes it a good insulator [*Goodrich*, 1976, 1978a, 1978b; *Zhang et al.*, 1996; *Sturm et al.*, 2001]. Data sets for the timing, spatial distribution, and properties of snow represent a major uncertainty because the density of

weather stations in high-latitude regions is low, and the reliability of precipitation data from these stations is low [McGuire *et al.*, 2000a]. The thermal properties of snow may also need to be considered in more detail than in the version of the STM in this study, in which snow cover is homogeneous with respect to thermal conductivity. Some studies have shown that separation of snow cover into wind slab and depth hoar fractions influences permafrost dynamics [Zhang *et al.*, 1996; Loth and Graf, 1998]. Microrelief and vegetation may interact with wind and snow seasonal cover to influence the physical and thermal properties of snow to affect the soil thermal regime in permafrost dominated regions [Sturm *et al.*, 2001]. As it is not clear whether data sets that describe the spatial and temporal variability of thermal properties for multiple layers of snow can be developed, the current version of the STM does not consider this variability.

Several studies have demonstrated that soil drainage in high-latitude ecosystems influences carbon dynamics and storage by affecting decomposition [Oechel *et al.*, 1995; Harden *et al.*, 2000; Christensen *et al.*, 1998]. The current version of the STM-TEM primarily uses the hydrology of a freely draining large-scale hydrological model [Vorosmarty *et al.*, 1989] to provide the STM with snow water equivalent, but the STM-TEM does consider how the active layer affects hydrology to influence soil thermal dynamics. As the STM-TEM accurately simulates active layer depth, it should be able to better consider spatial variability in carbon dynamics if it is modified so that active layer dynamics influence the hydrology of the moss, organic, and mineral layers in the soil and so that the hydrology of these layers influence both the soil thermal regime and the carbon dynamics. This is especially important in ecosystems recovering from

disturbance events, which may substantially affect active layer depth and alter the thickness and properties of the moss and organic layers in the soil. We are currently developing a version of the STM-TEM that has been modified to consider these issues. Data sets that describe the spatial and temporal variability in the moisture of soil layers and ecosystem carbon dynamics with respect to soil drainage and disturbance history are needed to evaluate the performance of coupled models of soil thermal and ecosystem dynamics.

Acknowledgments. We thank two anonymous reviewers, whose constructive comments were very helpful in revising a previous draft of this paper. This research was supported by the NASA Land Cover and Land Use Change Program (NAG5-6275), the NSF Taiga Long Term Ecological Research Program (DEB-9810217), the NSF Arctic System Science and Arctic Natural Science Programs (OPP-9614253, OPP-9732126, OPP-9870635), and the Alaska Cooperative Fish and Wildlife Research Unit.

References

- Amthor, J. S., et al., Boreal forest CO₂ exchange and evapotranspiration predicted by nine ecosystem process models: Intermodel comparisons and relationships to field measurements. *J. Geophys. Res.*, in press.
- Bartell, S. M., A. L. Brenkert, R. V. O'Neill, and R. H. Gardener. Temporal variation in regulation of production in a pelagic food web model. in *Complex interactions in lake communities*, edited by S. R. Carpenter, pp. 101-118. Springer-Verlag, New York, New York, USA, 1988.
- Beltrami, H., and J. C. Mareschal. Recent warming in eastern Canada inferred from geothermal measurements. *Geophys. Res. Lett.*, 18, 605-608, 1991.
- Brown, R. J. E., The distribution of permafrost and its reaction to air temperature in Canada and the U.S.S.R. *Arctic*, 13, 163-177, 1960.
- Chapin, F. S., III, et al., Feedbacks from arctic and boreal ecosystems to climate. *Global Change Biol.*, 6, S211-S223, 2000.
- Chapman, W. L., and J. E. Walsh. Recent variations of sea ice and air temperatures in high latitudes. *Bull. Am. Meteorol. Soc.*, 74, 33-47, 1993.
- Christensen, T. R., S. Jonasson, A. Michelsen, T. V. Callaghan, and M. Hastrom. Environmental controls on soil respiration in Eurasian and Greenlandic Arctic. *J. Geophys. Res.*, 103, 29,015-29,021, 1998.
- Clein, J. S., B. L. Kwiatkowski, A. D. McGuire, J. E. Hobbie, E. B. Rastetter, J. M. Melillo, and D. W. Kicklighter. Modeling carbon responses of tundra ecosystems to historical and projected climate: A comparison of a fine- and coarse-scale

- ecosystem model for identification of process-based uncertainties, *Global Change Biol.*, 6, S127-S140, 2000.
- Clein, J. S., A. D. McGuire, X. Zhang, D. W. Kicklighter, J. M. Melillo, S. C. Wofsy, and P. G. Jarvis. The role of nitrogen dynamics in modeling historical and projected carbon balance of mature black spruce ecosystems across North America: Comparisons with CO₂ fluxes measured in the Boreal Ecosystem Atmosphere Study (BOREAS), *Plant and Soil*. In press.
- Clymo, R.. The limits of peat bog growth. *Philos. Trans. R. Soc. London, Ser. B*, 303, 605-654, 1984.
- Cramer, W., D. W. Kicklighter, A. Bondeau, B. Moore III, G. Churkina, B. Nemry, A. Ruimy, A. L. Schloss, and the participants of the postdam NPP model intercomparison. Comparing global models of terrestrial net primary productivity (NPP) overview and key results. *Global Change Biol.*, 5 (Suppl. 1), 1-15, 1999.
- Dyrness, C. T.. Control of depth to permafrost and soil temperatures by the forest floor in black spruce/feathermoss communities. *U.S. For. Serv. Res. Note PNW-396*, Dept. of Agric., Washington, D.C., 1982.
- Epstein, H. E., M. D. Walker, F. S. Chapin III, and A. M. Starfield. A transient, nutrient-based model of arctic plant community response to climate warming. *Ecol. Appl.*, 10 (3), 2000, 824-841, 2000.
- Everett, J. T., and B. B. Fitzharris. The Arctic and the Antarctic, in *The Regional Impacts of Climate Change: An Assessment of Vulnerability*, edited by R. T. Watson, M.

- C. Zinyowera, R. H. Moss, and D. J. Dokken, pp. 85-103. Cambridge Univ. Press, New York, 1998.
- Frolking, S., and P. Crill, Climate controls on temporal variability of methane flux from a poor fen in southeastern New Hampshire: Measurement and modeling, *Global Biogeochem. Cycles*, 8(4), 385-397, 1994.
- Frolking, S., et al., Modelling temporal variability in the carbon balance of a spruce/moss boreal forest, *Global Change Biol.*, 2, 343-366, 1996.
- Frolking, S., K. C. McDonald, J. S. Kimball, J. B. Way, R. Zimmermann, and S. W. Running, Using the space-borne NASA scatterometer (NSCAT) to determine the frozen and thawed seasons, *J. Geophys. Res.*, 104, 27,895-27,907, 1999.
- Garagulya, L. S., V. E. Romanovsky, and N. V. Seregina, Modeling temperature fields during nonhomogeneous rock freezing and thawing, *Russian Geocryological Research*, vol.1, pp. 34-42, Russ. Acad. of Science, Moscow, Russia, 1995.
- Goulden, M. L., et al., Sensitivity of boreal forest carbon balance to soil thaw, *Science* 279, 214-217, 1998.
- Goodrich, L. E., A numerical model for assessing the influence of snow cover on the ground thermal regime, Ph.D. thesis, 410 pp., McGill Univ., Montreal, Quebec, 1976.
- Goodrich, L. E., Some results of a numerical study of ground thermal regimes, in *Proceedings of 3rd international Conf. On Permafrost*, vol.1, pp. 29-34, Nat. Res. Counc. of Canada, Ottawa, 1978a.

- Goodrich, L. E.. Efficient numerical technique for one-dimensional thermal problems with phase change. *Int. J. Heat Mass Transfer*, 21, 615-621, 1978b.
- Guymon, G. L., and T. V. Hromadka II. Finite element model of transient heat conduction with isothermal phase change (two and three dimensional). *CRREL Spec. Rep. 77-38*. 163 pp., Corps of Eng., U.S. Army, Hanover, N. H., 1977.
- Guymon, G. L., T. V. Hromadka II. and R. L. Berg. Two-dimensional model of coupled heat and moisture transport in frost-heaving soils. *J. of Energy Resour. Technol.*, 106, 336-343, 1984.
- Halsey, L.A., D. H. Vitt, and S. C. Zoltai. Disequilibrium response of permafrost in boreal continental western Canada to climatic change. *Clim. Change*, 30, 57-73, 1995.
- Harden, J. W., S. E. Trumbore, B. J. Stocks, A. Hirsch, S. T. Gower, K. P. O'Neill, and E. S. Kasischke. The role of fire in the boreal carbon budget. *Global Change Biol.*, 6 (Suppl. 1), 174-184, 2000.
- Heimann, M., et al., Evaluation of terrestrial carbon cycle models through simulations of the seasonal cycle of atmospheric CO₂: First results of a model intercomparison study. *Global Biogeochem. Cycles*, 12, 1-24, 1998.
- Hillman, G. R., Some hydrological effects of peatland drainage in Alberta's boreal forest. *Can. J. For. Res.*, 22, 1588-1596, 1992.
- Hulme, M., A historical monthly precipitation data for global land areas from 1900 to 1994, gridded at 3.75 x 2.5 resolution. Clim. Res. Unit, Univ. of East Anglia, Norwich, United Kingdom, 1995.

- Jones, P. D.. Hemispheric surface air temperature variations: a reanalysis and update to 1993. *J. Clim.*, 7, 1794-1802. 1994.
- Kicklighter, D. W., et al.. A first-order analysis of the potential role of CO₂ fertilization to affect the global carbon budget: A comparison of four terrestrial biosphere models. *Tellus, Ser. B*, 343-366. 1999.
- Lachenbruch, A. H., J. H. Sass, B. V. Marshall, and T. H. Moses Jr.. Permafrost, heat flow, and the geothermal regime at Prudoe Bay, Alaska. *J. Geophys. Res.*, 87, 9301-9316. 1982.
- Lachenbruch, A. H., and B. V. Marshall. Changing climate: Geothermal evidence from permafrost in the Alaskan Arctic. *Science*, 234, 689-697. 1986.
- Leemans, R., and W. P. Cramer. The IIASA database for mean monthly values of temperature, precipitation, and cloudiness on an terrestrial grid. *IIASA RR-91-18*, International Institute for Applied Systems Analysis, Laxenburg, Austria, 1991.
- Loth, B., and H. Graf. Modeling the snow cover in climate studies. 1. Long-term integrations under different climatic conditions using a multilayered snow-cover model. *J. Geophys. Res.*, 103, 11,313-11,327. 1998.
- McGuire, A. D., and J. Hobbie. Global climate change and the equilibrium responses of carbon storage in arctic and subarctic regions, pp. 53-54, in *Modeling the arctic system: A workshop report of the Arctic System Science Program*. Arct. Res. Consort. of the U. S., Fairbanks, Alaska, 1997.
- McGuire, A. D., J. M. Melillo, L. A. Joyce, D. W. Kicklighter, A. L. Grace, B. Moore III, and C. J. Vorosmarty. Interactions between carbon and nitrogen dynamics in

- estimating net primary productivity for potential vegetation in North America. *Global Biogeochem. Cycles*, 6, 101-124, 1992.
- McGuire, A. D., J. M. Melillo, D. W. Kicklighter, and L. A. Joyce. Equilibrium responses of soil carbon to climate change: Empirical and process-based estimates. *J. of Biogeogr.*, 22, 785-796, 1995.
- McGuire, A. D., J. Clein, J. M. Melillo, D. W. Kicklighter, R. A. Meier, C. J. Vorosmarty, and M. C. Serreze. Modeling carbon responses of tundra ecosystems to historical and projected climate: The sensitivity of pan-arctic carbon storage to temporal and spatial variation in climate. *Global Change Biol.*, 6, 141-159, 2000a.
- McGuire, A. D., J. M. Melillo, J. T. Randerson, W. J. Parton, M. Heimann, R. A. Meier, J. S. Clein, D. W. Kicklighter, and W. Sauf. Modeling the effects of snowpack on heterotrophic respiration across northern temperate and high latitude regions: Comparison with measurements of atmospheric carbon dioxide in high latitudes. *Biogeochemistry*, 48, 91-114, 2000b.
- McGuire, A. D., et al., CO₂, climate and land-use effects on the terrestrial carbon balance, 1920-1992: An analysis with four process-based ecosystem models. *Global Biogeochem. Cycles*, 15, 1,183-206, 2001.
- Mitchell, J. F. B., T. C. Johns, J. M. Gregory, and S. F. B. Tett. Climate response to increasing levels of greenhouse gases and sulphate aerosols. *Nature*, 376, 501-504, 1995.

- Oechel, W. C., S. J. Hastings, G. L. Vourlitis, M. Jenkins, G. Reichers, and N. Grulke. Recent change of arctic tundra ecosystems from a net carbon dioxide sink to a source. *Nature*, 361, 520-523, 1993.
- Oechel, W. C., G. L. Vourlitis, S. J. Hastings, and S. A. Bocharov. Change in arctic CO₂ flux over two decades: Effects of climate change at Barrow, Alaska. *Ecol. Appl.*, 5, 846-855, 1995.
- Oechel, W. C., G. L. Vourlitis, S. J. Hastings, R. C. Zulueta, L. Hinzman, and D. Kane. Acclimation of ecosystem CO₂ exchange in the Alaskan Arctic in response to decadal climate warming. *Nature*, 406, 978-981, 2000.
- Osterkamp, T. E., and J. P. Gosink. Variations in permafrost thickness in response to changes in paleoclimate. *J. Geophys. Res.*, 94, 4423-4434, 1991.
- Osterkamp, T. E., and V. E. Romanovsky. Evidence for warming and thawing of discontinuous permafrost in Alaska. *Permafrost Periglacial process.*, 10, 17-37, 1999.
- Overpeck, J., et al.. Arctic environmental change of the last four centuries. *Science*, 278, 1251-1256, 1997.
- Pitman, A. J., Assessing the sensitivity of a Land-Surface Scheme to the parameter values using a single column model. *J. of Clim.*, 7, 1856-1869, 1994.
- Romanovsky, V. E., L. N. Maximova, and N. V. Seregina. Paleotemperature reconstruction for freeze-thaw processes during the Late Pleistocene through the Holocene, in *Proceedings International Conference. Role of Polar Regions in*

- Global Change*, vol. 2, pp. 537-542. Geophys. Inst., Univ. of Alaska, Fairbanks, 1991a.
- Romanovsky, V. E., L. S. Garagula, and N. V. Seregina. Freezing and thawing of soils under the influence of 300- and 90-year periods of temperature fluctuation, in *Proceedings of International Conference. Role of Polar Regions in Global Change*, vol. 2, pp. 543-548. Univ. of Alaska, Fairbanks, 1991b.
- Romanovsky, V. E., T. E. Osterkamp, and N. S. Duxbury. An evaluation of three numerical models used in simulation of the active layer and permafrost temperature regimes. *Cold Reg. Sci. Technol.*, 26, 195-203, 1997.
- Rose, K. A., E. P. Smith, R. H. Gardner, A. L. Brenkert, and S. M. Bartell. Parameter sensitivities, Monte Carlo filtering, and model forecasting under uncertainty. *J. of Forecasting*, 10, 117-133, 1991.
- Running S. W., J. B. Way, K. C. McDonald, J. S. Kimball, S. Froking, A. R. Keyser, and R. Zimmermann. Radar remote sensing proposed for monitoring freeze-thaw transitions in boreal regions. *Eos Trans. AGU*, 80(19), 213, 220-221, 1999.
- Schimel, D., et al., Carbon storage by the natural and agricultural ecosystems of the US (1980-1993). *Science*, 287, 2004-2006, 2000.
- Sellers, P. J., et al., BOREAS in 1997: Experiment overview, scientific results, and future directions. *J. Geophys. Res.*, 102, 28,731-28,769, 1997.
- Serreze, M. C., J. E. Walsh, F. S. Chapin III, T. Osterkamp, M. Dyurgerov, V. Romanovsky, W. C. Oechel, J. Morison, T. Zhang, and R. G. Barry,

- Observational evidence of recent change in the northern high-latitude environment. *Clim. Change*, 46, 159-207, 2000.
- Shaver, G. R., W. D. Billings, F. S. Chapin III, A. E. Giblin, K. J. Nadelhoffer, W. C. Oechel, and E. B. Rastetter. Global change and the carbon balance of arctic ecosystems. *BioScience*, 42, 433-441, 1992.
- Sturm, M. J. P. McFadden, G. E. Liston, F. S. Chapin III, C. H. Racine, and J. Holmgren. Snow-shrub interactions in Arctic tundra: a hypothesis with climate implications. *J. of Clim.*, 14, 336-344, 2001.
- Tian, H. J. M. Melillo, D. W. Kicklighter, A. D. McGuire, J. Helfrich, B. Moore III, and C. J. Vörösmarty. Effect of interannual climate variability on carbon storage in Amazonian ecosystems. *Nature*, 396, 664-667, 1998.
- Tian, H., J. M. Melillo, D. W. Kicklighter, A. D. McGuire, and J. Helfrich. The sensitivity of terrestrial carbon storage to historical climate variability and atmospheric CO₂ in the United States. *Tellus, Ser. B*, 414-452, 1999.
- Tian, H., J. M. Melillo, D. W. Kicklighter, A. D. McGuire, B. Moore III, and C. J. Vörösmarty. Climatic and biotic controls on interannual variations of carbon storage in undisturbed ecosystems of the Amazon Basin. *Global Ecol. and Biogeogr.*, 9, 315-335, 2000.
- Turner, M. G., Y. Wu, L. L. Wallace, W. H. Romme, and A. Brenkert. Simulation winter interactions among ungulates, vegetation, and fire in northern Yellowstone park. *Ecol. Appl.*, 4(3), 472-496, 1994.

- Vitt, H. D., L. A. Halsey, and S. C. Zoltai. The changing landscape of Canada's western boreal forest: The current dynamics of permafrost. *Can. J. For. Res.*, 30, 283-287. 2000.
- Vorosmarty, C. J., B. J. Peterson, E. B. Rastetter, and P. A. Steudler. Continental scale models of water balance and fluvial transport: An application to south America. *Global Biogeochem. Cycles*, 3, 241-265, 1989.
- Waelbroeck C., P. Monfray, W. C. Oechel, S. Hastings, and G. Vourlitis. The impact of permafrost thawing on the carbon dynamics of tundra. *Geophys. Res. Lett.*, 24(3), 229-232, 1997.
- Williams, P. J. and M. W. Smith. *The frozen Earth, fundamentals of geocryology*. 306pp. Cambridge University Press. 1989.
- Xiao, X., J. M. Melillo, D. W. Kicklighter, A. D. McGuire, R. G. Prinn, C. Wang, P. H. Stone, and A. P. Sokolov. Transient climate change and net ecosystem production of the terrestrial biosphere. *Global Biogeochem. Cycles*, 12, 345-360, 1998.
- Zhang, T., T. E. Osterkamp, and K. Stamnes. Influence of the depth hoar layer of the seasonal snow cover on the ground thermal regime. *Water Resour. Res.*, 32(7), 2075-2086, 1996.
- Zhang, T., T. E. Osterkamp, and K. Stamnes. Effects of climate on the active layer and permafrost on the North Slope of Alaska, U.S.A., *Permafrost Periglacial Process.*, 8, 45-67, 1997.

Table 2.1. Parameters Used for Simulations of the Soil Thermal Model (STM) for a Black Spruce Stand at the Bonanza Creek Experimental Forest (BNZ) Near Fairbanks, Alaska and the Coupling of the STM with the Terrestrial Ecosystem Model (STM-TEM) for a Black Spruce Stand in Canada (NSA-OBS), and White Spruce (WS), Aspen (AS), and Tussock Tundra (TT) sites in Alaska^a

Parameter Code	Description	Normal Value					Minimum	Maximum	Unit
		BNZ	NSA-OBS	WS	AS	TT			
V1	Moss thickness	0.12 (0.035) ^b	0.10 (0.05)	0.15 (0.15)	0.15 (0.15)	0.20 (0.10)	0.05	0.35	Meter (m)
V2	Upper organic soil thickness	0.28 (0.025)	0.20 (0.05)	0.15 (0.15)	0.15 (0.15)	0.20 (0.15)	0.15	0.50	Meter (m)
V3	Lower organic soil thickness	0.64 (0.020)	0.15 (0.10)	0.30 (0.30)	0.30 (0.30)	0.40 (0.15)	0.15	0.65	Meter (m)
V4	Upper mineral soil thickness	0.40 (0.100)	0.85 (0.10)	0.60 (0.30)	0.30 (0.30)	0.90 (0.30)	0.30	2.00	Meter (m)
V5	Moss thawed thermal conductivity	0.10	0.20	0.45	0.50	0.15	0.10	0.50	W m ⁻¹ K ⁻¹
V6	Moss frozen thermal conductivity	0.12	0.31	0.56	1.20	0.26	0.12	1.20	W m ⁻¹ K ⁻¹
V7	Upper organic soil thawed thermal conductivity	0.30	0.20	1.20	1.00	0.70	0.20	1.20	W m ⁻¹ K ⁻¹
V8	Upper organic soil frozen thermal conductivity	0.68	0.31	1.50	1.50	1.50	0.30	1.50	W m ⁻¹ K ⁻¹

V9	Lower organic soil thawed thermal conductivity	0.50	0.50
V10	Lower organic soil frozen thermal conductivity	1.60	1.0
V11	Upper mineral soil thawed thermal conductivity	0.75	0.50
V12	Upper mineral soil frozen thermal conductivity	1.60	1.00
V13	Moss water content	0.04	0.08
V14	Upper organic soil water content	0.65	0.20
V15	Lower organic soil water content	0.65	0.08
V16	Upper mineral soil water content	0.45	0.20
V17	Moss thawed volumetric heat capacity	1.70	1.70
V18	Moss frozen volumetric heat capacity	1.50	1.50

1.40	1.20	0.70	0.40	1.40	$\text{W m}^{-1} \text{K}^{-1}$
2.10	2.10	1.50	0.60	2.20	$\text{W m}^{-1} \text{K}^{-1}$
1.40	1.20	1.20	0.50	1.60	$\text{W m}^{-1} \text{K}^{-1}$
2.10	2.10	2.10	1.00	2.50	$\text{W m}^{-1} \text{K}^{-1}$
0.44	0.10	0.65	0.03	0.60	Volumetric %
0.10	0.10	0.10	0.10	0.70	Volumetric %
0.33	0.19	0.10	0.08	0.65	Volumetric %
0.33	0.23	0.43	0.10	0.45	Volumetric %
1.20	1.50	1.50	1.20	3.50	$\text{MJ m}^{-1} \text{K}^{-1}$
1.00	1.20	1.20	1.00	3.50	$\text{MJ m}^{-1} \text{K}^{-1}$

V19	Upper organic soil thawed heat capacity	1.70	1.70	2.40	2.30	1.30	1.30	2.50	MJ m ⁻¹ K ⁻¹
V20	Upper organic soil frozen heat capacity	1.60	1.50	2.20	2.20	1.20	1.20	3.50	MJ m ⁻¹ K ⁻¹
V21	Lower organic soil thawed heat capacity	2.60	1.70	2.80	2.10	1.30	1.50	3.50	MJ m ⁻¹ K ⁻¹
V22	Lower organic soil frozen heat capacity	1.60	1.50	1.70	1.70	1.20	1.50	3.50	MJ m ⁻¹ K ⁻¹
V23	Upper mineral soil thawed heat capacity	2.60	2.60	2.80	3.10	3.10	1.50	3.50	MJ m ⁻¹ K ⁻¹
V24	Upper mineral soil frozen heat capacity	1.60	2.40	1.70	1.70	1.70	1.50	3.50	MJ m ⁻¹ K ⁻¹
V25	Snow thermal conductivity	0.20	0.20	0.15	0.17	0.20	0.10	0.30	MJ m ⁻¹ K ⁻¹

^aThe uncertainty analyses were conducted for the BNZ black spruce site. In uncertainty analyses, parameters were varied within the minimum and maximum values shown here under the assumption of a uniform random distribution.

^bThe numerical value following the thickness of each layer was the depth step of the simulation.

Table 2.2. Combinations of Different Air Temperature and Snow Depth Scenarios for the Study of the Uncertainty Analyses for Simulations of Soil Temperature by the Soil Thermal Model (STM) for the Black Spruce Ecosystem at Bonanza Creek Experimental Forest near Fairbanks, Alaska

Code	Description
LT-SS	Lower temperature and shallower snow depth
LT-NS	Lower temperature and normal snow depth
LT-DS	Lower temperature and deeper snow depth
NT-SS	Normal temperature and shallower snow depth
NT-NS	Normal temperature and normal snow depth
NT-DS	Normal temperature and deeper snow depth
HT-SS	Higher temperature and shallower snow depth
HT-NS	Higher temperature and normal snow depth
HT-DS	Higher temperature and deeper snow depth

Table 2.3. Applications of the Coupled Model (STM-TEM) in Which the Soil Thermal Model (STM) Was Coupled to the Terrestrial Ecosystem Model (TEM), to Simulate Soil Temperature for Four Different Representative Ecosystem Types in High-Latitude Regions of North America

Vegetation Type	Stand Location	Driving Data	Depths of Soil Temperatures Simulated and Observed	Reference
Black spruce	Northern study area (NSA) near Manitoba, Canada	Thompson airport weather station, data from 1975 to 1997	5, 20, 20, 50, and 100 cm, depths relative to the surface of moss	<i>Sellers et al.</i> , [1997]
White spruce	333 mile Parks Highway, Fairbanks, Alaska	Field-based air temperature from 1994 to 1997, precipitation data from the Fairbanks International Airport weather station in period 1994 to 1997	Soil surface, 15, and 30 cm, depths are relative to the surface of moss and lichen	R. E. Erickson, personal communication, 1999
Aspen	20 mile Chena Hot Springs Rd., Fairbanks, Alaska	Field-based air temperature from 1994 to 1997, precipitation data from the Fairbanks International Airport weather station in period 1974 to 1997	Same as white spruce site	R. E. Erickson, personal communication, 1999
Tussock tundra	Toolik Lake tussock tundra site of Arctic Long-Term Ecological Research (LTER), Alaska	For period of 1995 to 1997, measured air temperature at the site, measured precipitation at Betties FAA Airport	10, 20, 35, and 40 cm, depths are relative to the surface of moss layer	G. Shaver, personal communication, 1999

Table 2.4. Slope, Intercept, and Proportion of Variation (R^2) Explained by Linear Regressions Between Field-Based and Simulated Daily and Monthly Soil Temperatures at Various Depths and Active Layer Depths for Simulations I, II, III, and IV of the Black Spruce Stand at Bonanza Creek Experimental Forest from May 1996 to April 1997^a

	Daily Soil Temperature ^b					
	0 cm	23 cm	32 cm	42 cm	52 cm	Upper Organic
Simulation I						
R^2	0.91	0.85	0.74	0.61	0.66	0.77
Slope	0.97*	0.95	0.87	0.88	1.09	0.94
Intercept	-0.03	0.43	0.19	0.05 ^{&}	-0.12	0.11
Simulation II						
R^2	0.91	0.85	0.74	0.61	0.66	0.77
Slope	0.97*	0.93	0.83	0.84	1.10	0.92
Intercept	-0.08 ^{&}	0.35	0.07 ^{&}	-0.06 ^{&}	-0.13	0.03 ^{&}
Simulation III						
R^2	0.85	0.82	0.76	0.68	0.67	0.78
Slope	0.98*	0.94	0.88	0.91	0.99*	0.89
Intercept	0.35	0.59	0.33	0.19	-0.18	0.14
Simulation VI						
R^2	0.85	0.82	0.76	0.68	0.66	0.79
Slope	0.98*	0.93	0.84	0.88	1.08	0.80
Intercept	0.32	0.52	0.22	0.09 ^{&}	-0.05 ^{&}	-0.06 ^{&}

Monthly Soil Temperature ^c							
	0 cm	23 cm	32 cm	42 cm	52 cm	Upper Organic	Active Layer Depth
Simulation I							
R^2	0.95	0.88	0.77	0.65	0.82	0.82	0.95
Slope	0.99	0.96	0.89	0.89	1.10	0.95	1.08
Intercept	-0.08 ^{&}	0.43	0.21	0.07 ^{&}	-0.10 ^{&}	0.11	0.03 ^{&}
Simulation II							
R^2	0.95	0.87	0.77	0.66	0.82	0.82	0.90
Slope	0.99	0.94	0.84	0.86	1.12	0.93	1.43 [*]
Intercept	-0.12 ^{&}	0.35	0.08 ^{&}	-0.05 ^{&}	-0.11 ^{&}	0.03 ^{&}	0.06 ^{&}
Simulation III							
R^2	0.92	0.85	0.79	0.74	0.84	0.86	0.85
Slope	0.98	0.94	0.89	0.94	1.03	0.90	0.99
Intercept	0.44	0.62	0.37	0.26	-0.11 ^{&}	0.50	0.02 ^{&}
Simulation VI							
R^2	0.92	0.85	0.80	0.74	0.84	0.86	0.94
Slope	0.99	0.93	0.85	0.91	1.12	0.80	1.00
Intercept	0.42	0.56	0.25	0.15 ^{&}	0.04 ^{&}	-0.06 ^{&}	-0.01 ^{&}

^aField-based estimates are the dependent variables, and the simulated estimates are the independent variables. Tests for significance were performed with a two sided t-test at $\alpha=0.05$ level. The four simulations that varied with respect to the temporal resolutions of internal time step and of climate data used to drive simulations. (See Figure 2 and section 2 for more information).

^bAll linear regressions were significant at $\alpha=0.05$ level with $p < 0.001$. An asterisk indicates slopes that were not significantly different from 1.0 and an ampersand indicates intercepts that were not significantly different from 0.0.

^cAll linear regressions were significant at $\alpha=0.05$ level with $p < 0.001$. None of the slopes were significantly different from 1.0 except for the slope indicated with asterisk. An ampersand indicates intercepts that were not significantly different from 0.0.

Table 2.5. Root Mean Square (RMS) Deviations of Simulated Daily and Monthly Soil Temperature Between Pairwise Combinations of Simulations I, II, III, and IV of Soil Temperature and Active Layer Depths for the Black Spruce Stand at Bonanza Creek Experimental Forest from May 1996

Daily Soil Temperature							
	0 cm	23 cm	32 cm	42 cm	52 cm	Upper Organic	
I. II	0.43	0.17	0.71	0.18	0.09	0.14	
I. III	3.85	1.16	0.85	0.67	0.62	1.52	
I. IV	3.85	1.14	0.84	0.67	0.63	0.88	
II. III	3.90	1.25	0.98	0.75	0.65	1.49	
II. IV	3.90	1.23	0.93	0.72	0.64	0.90	
III. IV	0.05	0.11	0.20	0.15	0.22	0.86	

Monthly Soil Temperature							
	0 cm	23 cm	32 cm	42 cm	52 cm	Upper Organic	Active Layer Depth (m)
I. II	0.13	0.14	0.21	0.17	0.08	0.13	0.03
I. III	3.11	1.07	0.78	0.60	0.56	0.67	0.01
I. IV	3.10	1.05	0.78	0.60	0.57	0.79	0.01
II. III	3.13	1.16	0.92	0.70	0.60	0.74	0.04
II. IV	3.13	1.14	0.87	0.67	0.59	0.81	0.06
III. IV	0.05	0.10	0.19	0.14	0.21	0.40	0.02

^aFour simulations that varied with respect to the temporal resolutions of internal time step and of climate data used to drive the simulations (see Figure 2 and section 2 for more information). The daily RMS deviation values were calculated on the basis of 365 daily estimates of soil temperature, and the monthly RMS deviations were calculated on the basis of 12 monthly estimates of soil temperature.

Table 2.6. Slope, Intercept, and Proportion of variation Explained by Regression Analyses Between Observed and Simulated Soil Temperature at Various Depths in the Soil Profile for an Old Black Spruce Forest in Canada, a White Spruce Forest in Alaska, an Aspen Forest in Alaska, and a Tussock Tundra Site in Alaska^{a,b}

Old Black Spruce			
	5 cm	10 cm	20 cm
R ²	0.96	0.98	0.96
Slope	1.04 [*]	0.88	0.98 [*]
Intercept	0.72	1.40	1.56

White Spruce			
	0 cm	15 cm	30 cm
R ²	0.96	0.81	0.78
Slope	0.95 [*]	0.93 [*]	0.94 [*]
Intercept	-0.54	-0.17 ^{&}	-0.18 ^{&}

Aspen			
	0 cm	15 cm	30 cm
R ²	0.95	0.84	0.72
Slope	0.99 [*]	0.85	0.71
Intercept	-0.64	0.46	0.60

Tussock Tundra				
	10 cm	20 cm	35 cm	40 cm
R ²	0.96	0.82	0.82	0.74
Slope	1.02 [*]	1.04 [*]	1.04 [*]	0.95 [*]
Intercept	-0.28	-0.51	-0.22	-0.50

^aField-based soil temperatures are the dependent variables, and the simulated soil temperatures are the independent variables. Tests for significance were performed with a two-sided t-test at $\alpha=0.05$ level. Simulations were conducted with the coupled version of the model (STM-TEM), in which the soil Thermal model (STM) was coupled to the terrestrial ecosystem model (TEM). For more information see Table 3 and section 2.

^bAll linear regressions were significant at $\alpha=0.05$ level with $p < 0.001$. An asterisk indicates slopes that were not significantly different from 1.0 and an ampersand indicates intercepts that were not significantly different from 0.0.

Figure 2.1. (a) Structure of the soil thermal model (STM) in the study. Heat conduction, $H(t)$, is modeled as a function of time (t) within the snow, moss, organic soil, and mineral soil layers. The frozen and thawed phase boundaries move up and down during the simulation. Input data for driving the model include temporal variability in temperature or heat fluxes for upper and lower boundaries and in the depth of snow. The model simulates soil temperature at each depth with daily resolution. (b) Flow of data in the coupled model (STM-TEM), in which the STM receives information on vegetation and the depth of snowpack from the water balance model (WBM) of the terrestrial ecosystem model (TEM), and TEM receives information on soil temperature for driving soil biogeochemical processes.

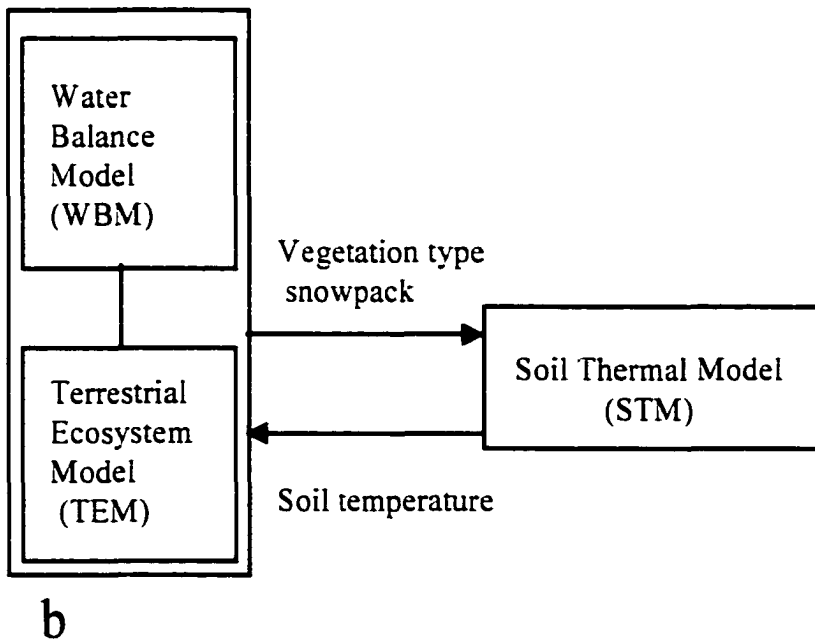
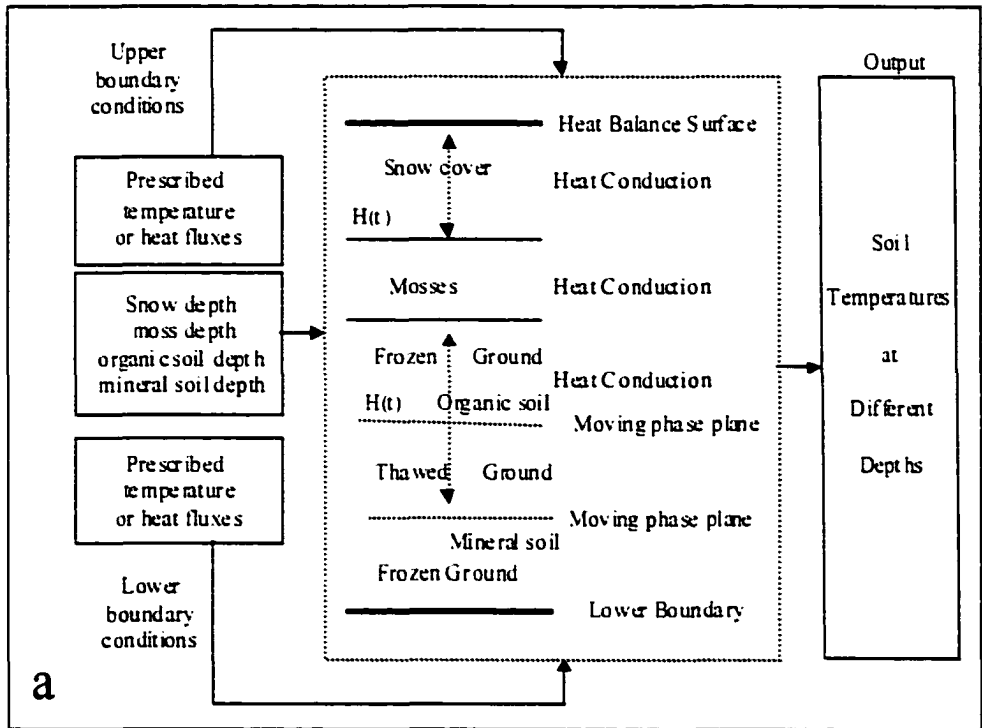


Figure 2.2. Research design for evaluating performance of the STM with respect to the temporal resolutions of internal time step and climate inputs. The performance was evaluated for a black spruce ecosystem in Bonanza Creek site (BNZ) of Long-Term Ecological Research (LTER). Monthly input climate data for simulations III and IV were temporally aggregated from daily air temperature and snow depth. For comparisons between observed and simulated monthly soil temperatures, daily observed and simulated soil temperatures were aggregated. All simulations use the same parameters and initialization protocol.

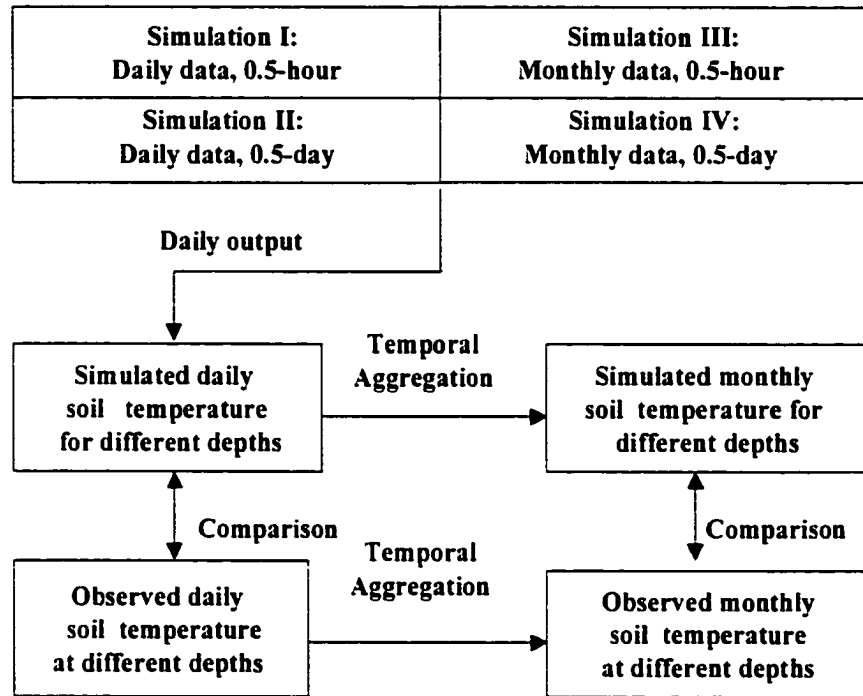


Figure 2.3. (a) Air temperature and (b) snow depth for the black spruce ecosystem at Bonanza Creek Experimental Forest from May 1996 to April 1997.

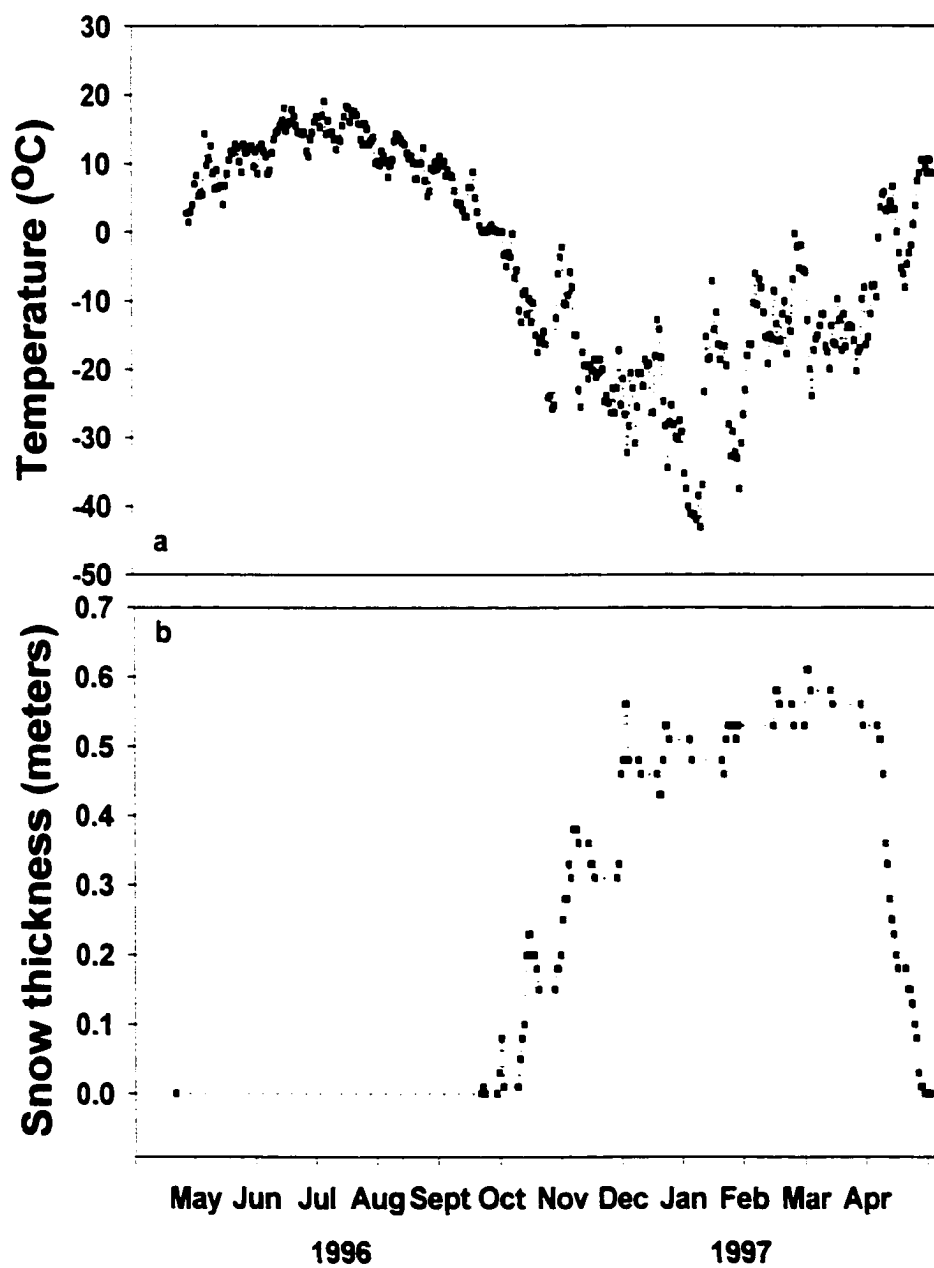


Figure 2.4. Observed and simulated daily soil temperatures for (a) the surface of the soil and (b) the upper organic soil layer.

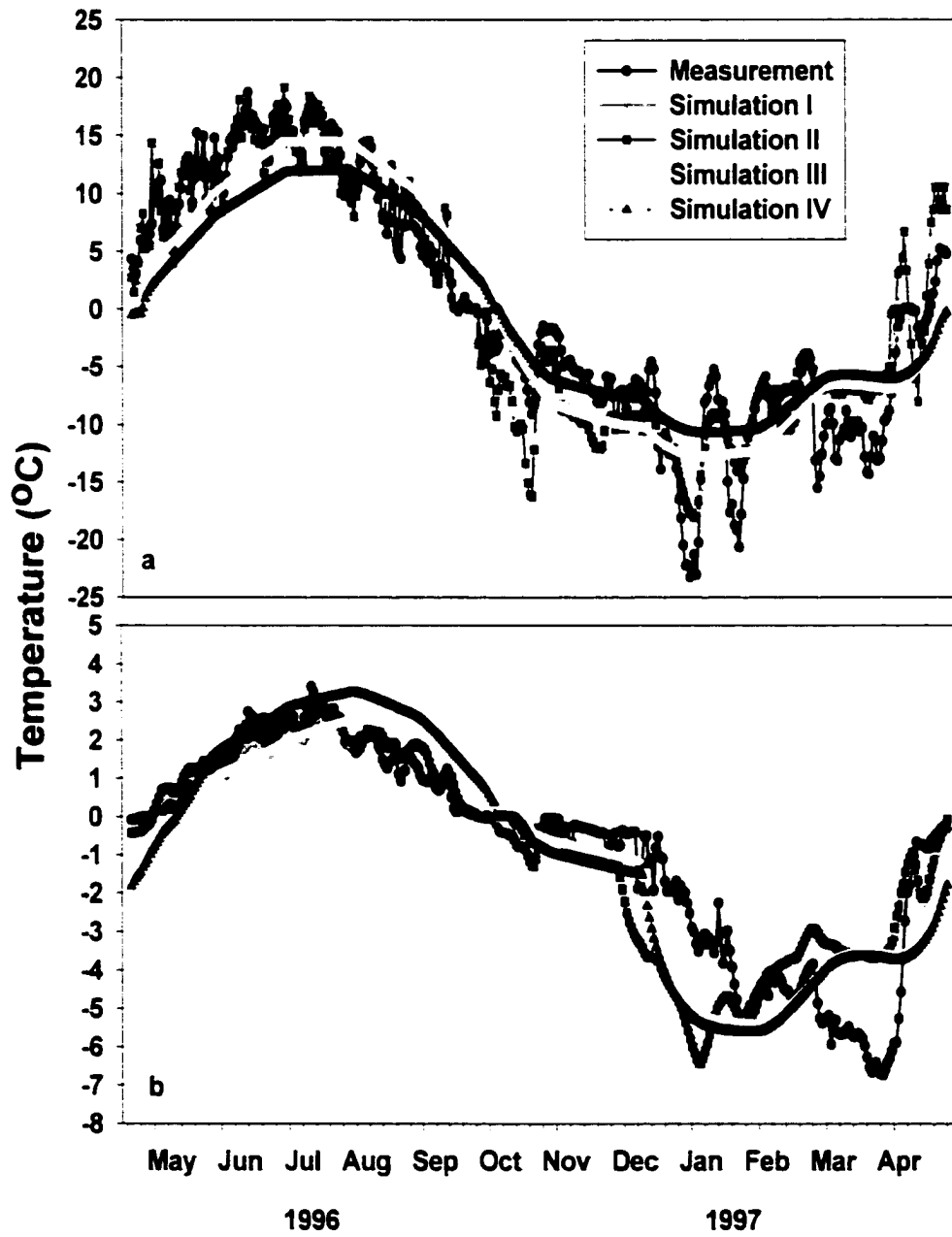


Figure 2.5. Observed and simulated monthly soil temperatures for (a) the surface of the soil and (b) the upper organic soil layer.

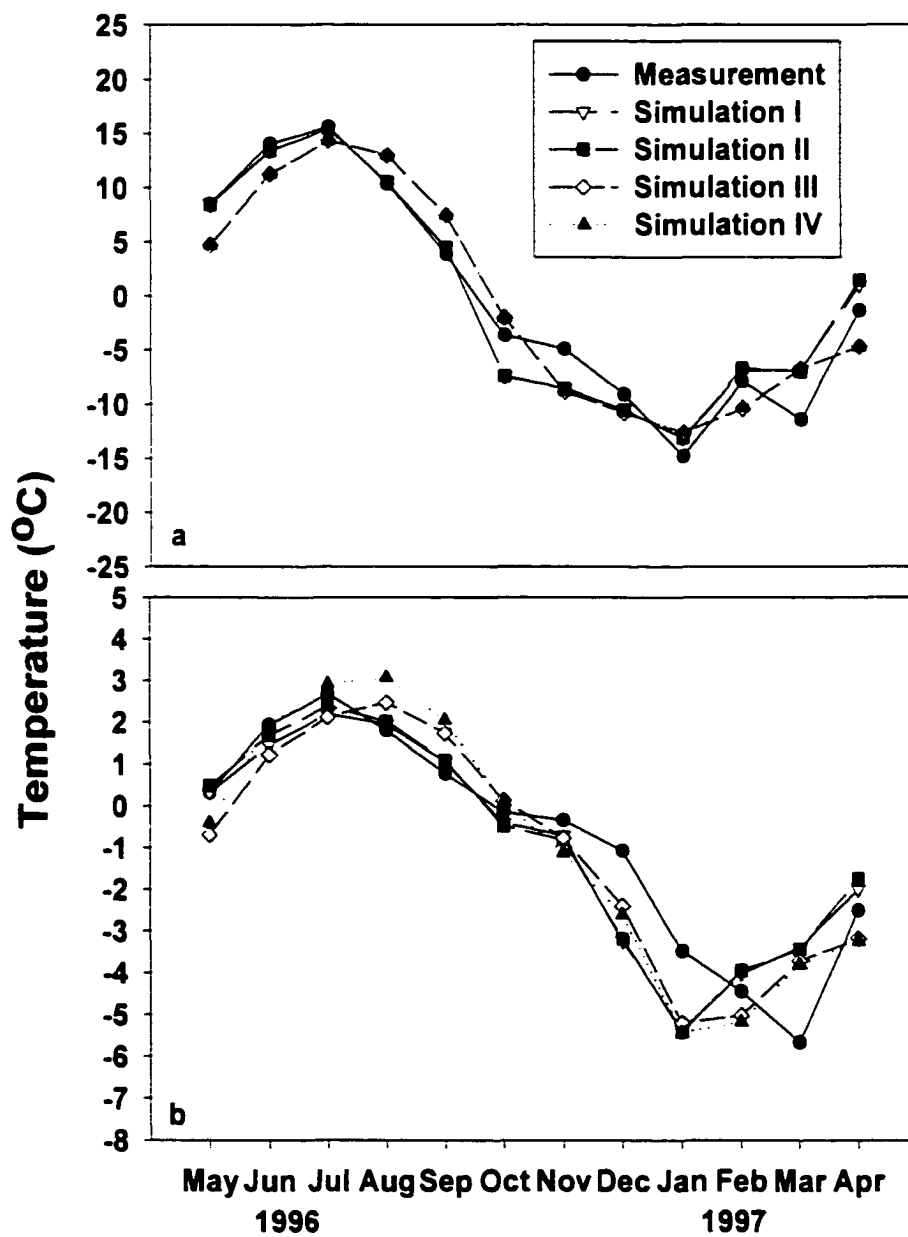


Figure 2.6. Proportion of variation in simulated soil temperature of the upper organic layer explained by variability in parameters in the uncertainty analyses conducted in this study. See Table 1 for additional information on parameters in these analyses.

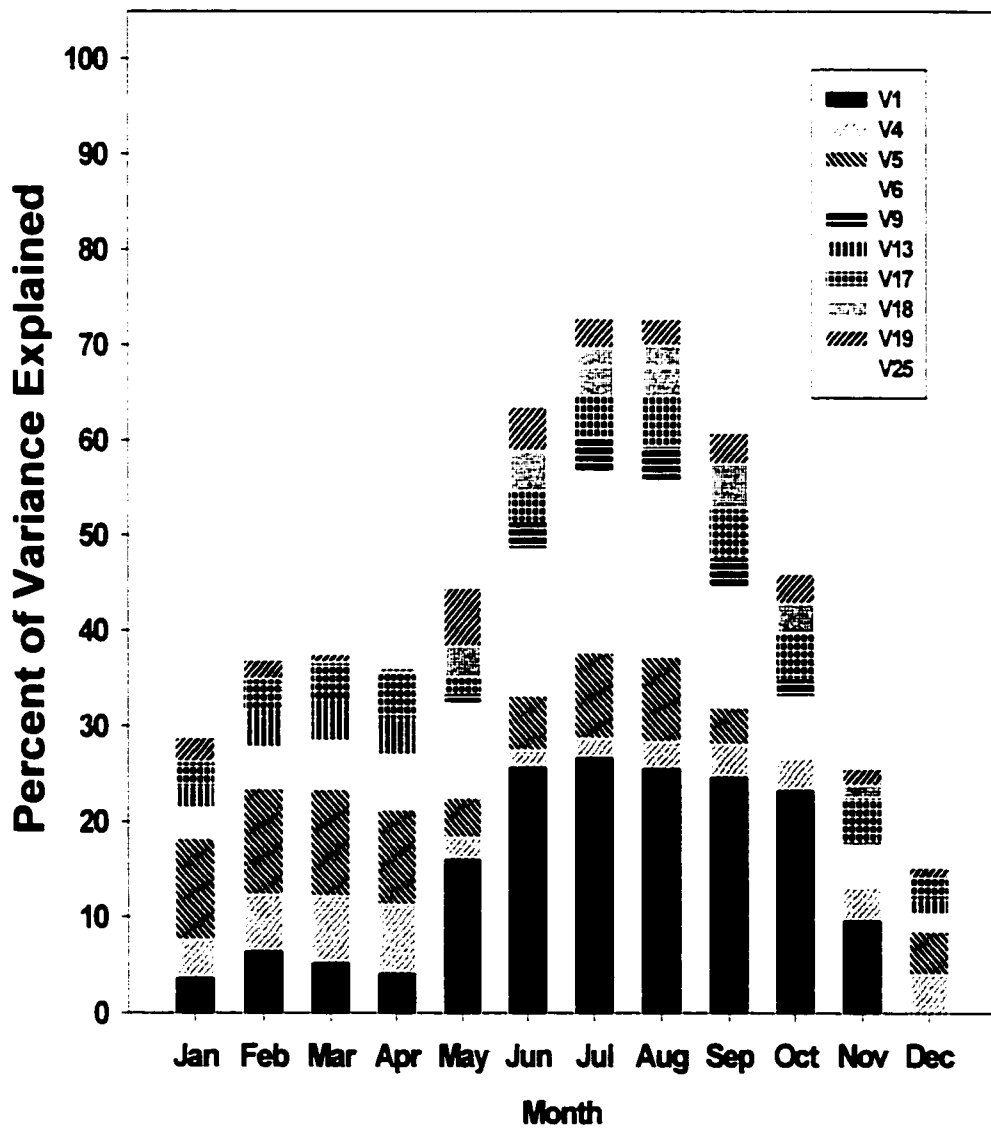


Figure 2.7. Proportion of variation in simulated soil temperature of the upper organic layer to variation in snow thermal conductivity in uncertainty analyses conducted for nine different climate scenarios: (a) low-temperature scenarios, (b) normal temperature scenarios, and (c) high-temperature scenarios. See Table 2 for additional information on the climate scenarios.

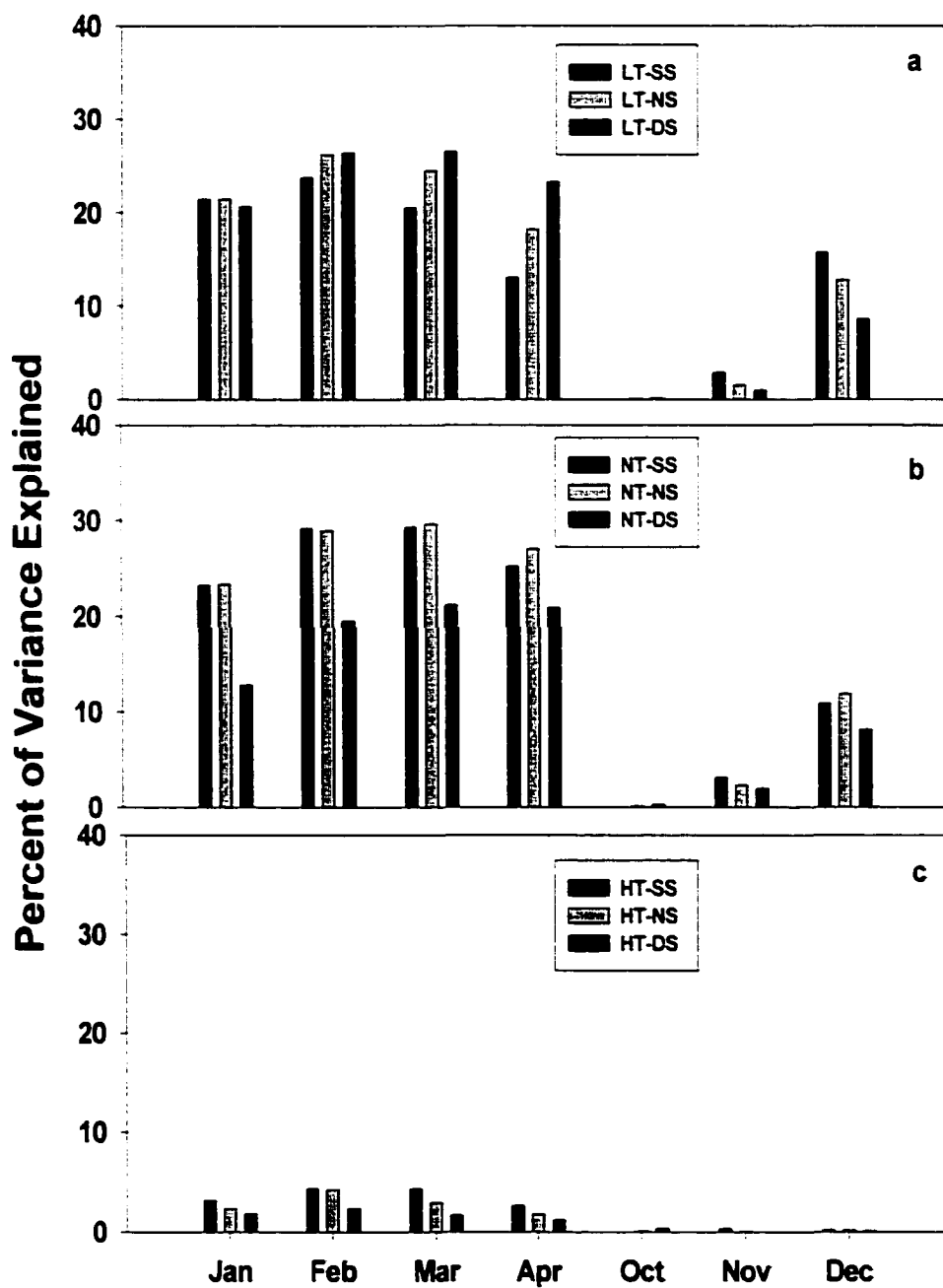


Figure 2.8. Proportion of variation in simulated soil temperature of the upper organic layer to variation in moss thickness in uncertainty analyses conducted for nine different climate scenarios: (a) low-temperature scenarios, (b) normal temperature scenarios, and (c) high-temperature scenarios. See Table 2 for additional information on the climate scenarios.

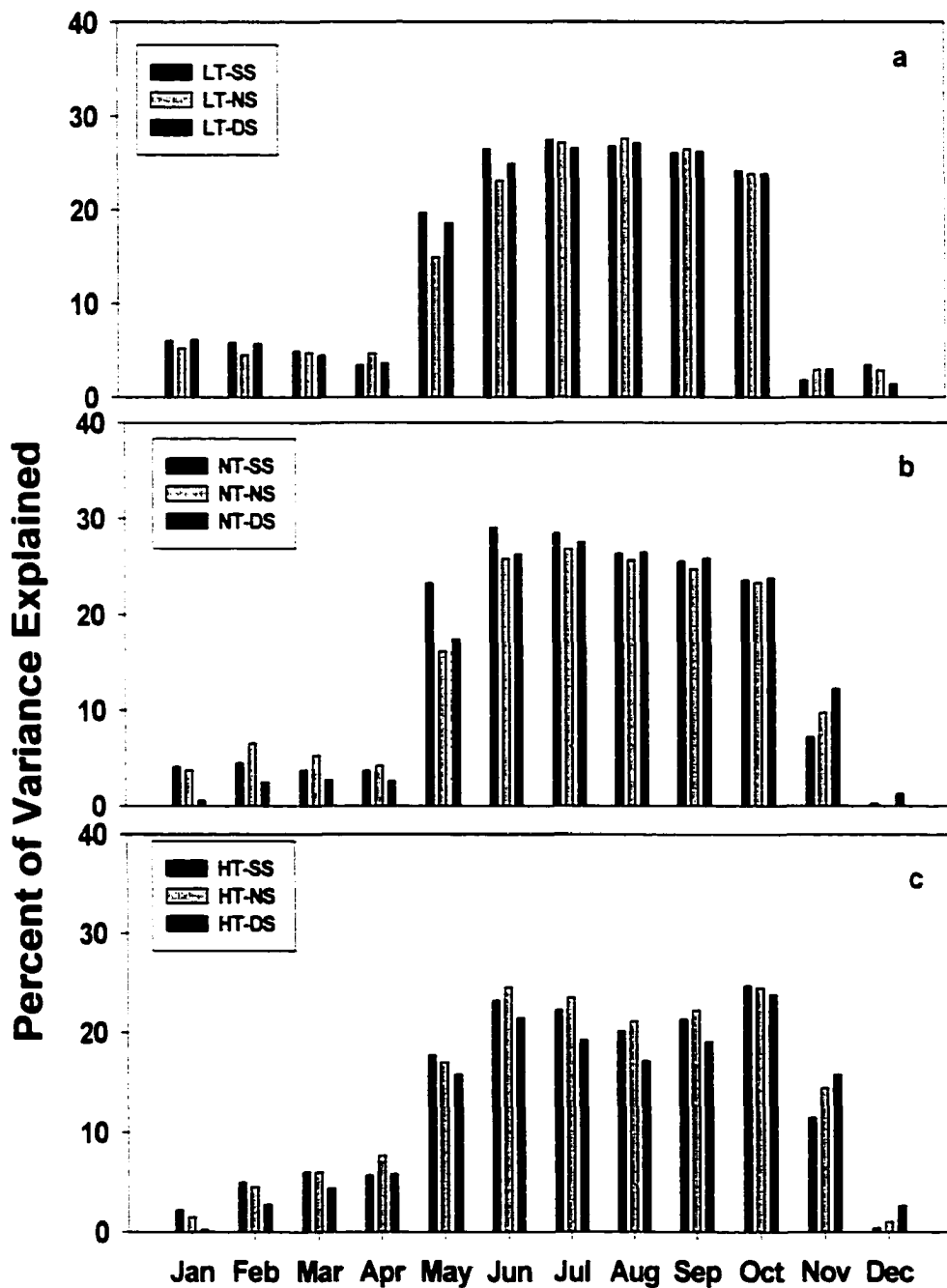


Figure 2.9. Monthly observed and simulated soil temperatures for an old black spruce ecosystem in northern Manitoba, Canada, from 1994 to 1996.

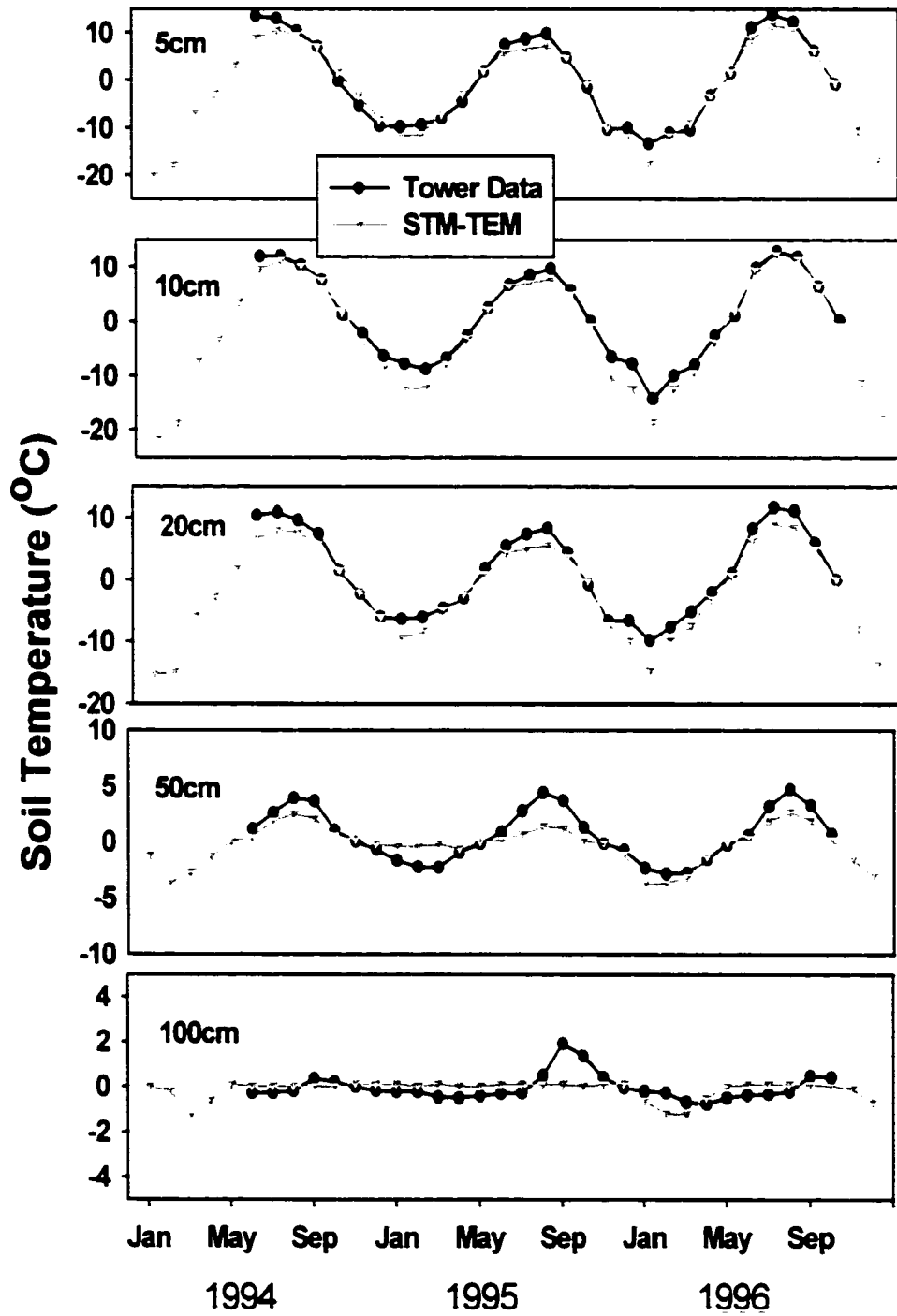


Figure 2.10. Monthly observed and simulated soil temperatures for a white spruce ecosystem in Alaska from 1994 to 1997.

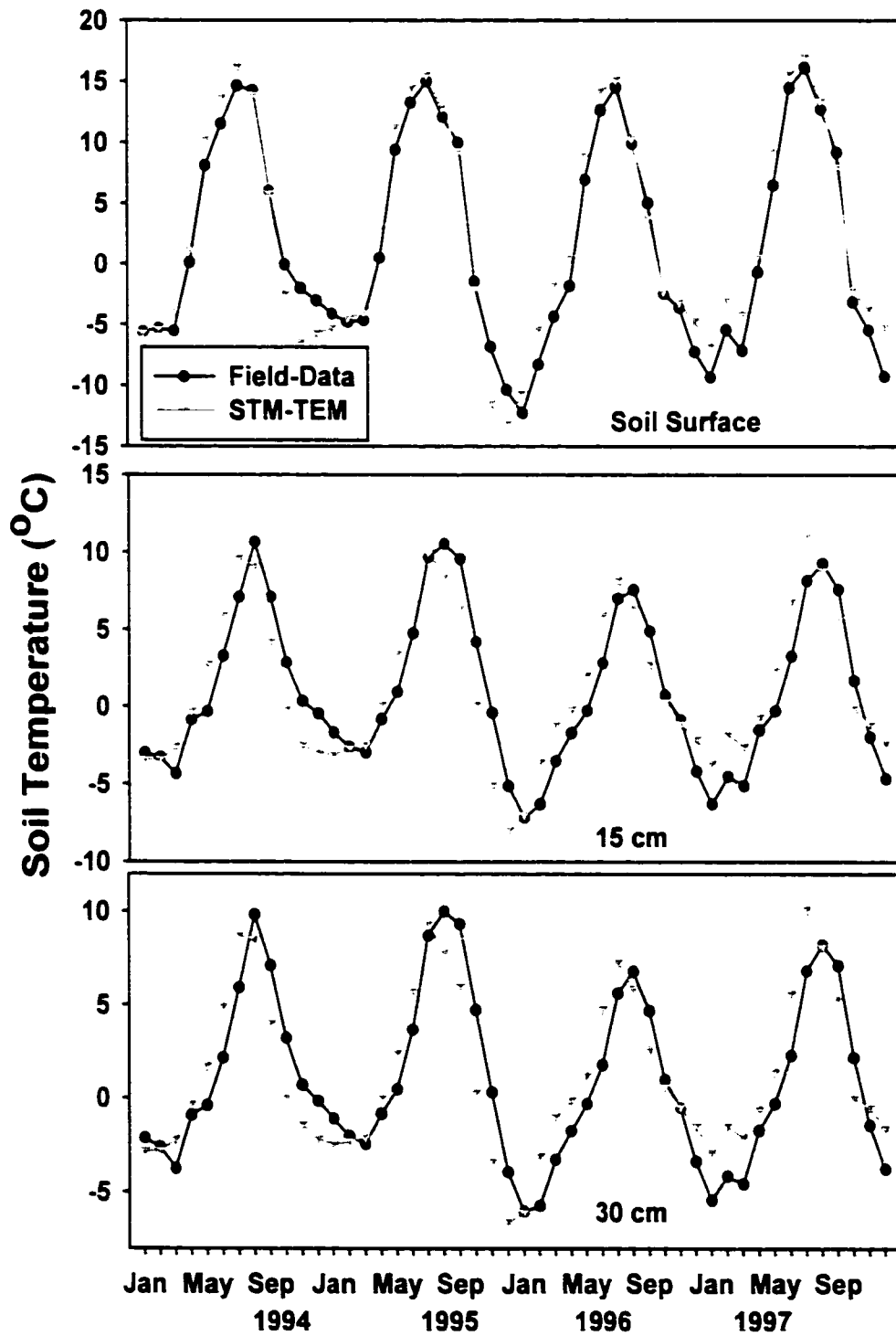


Figure 2.11. Monthly observed and simulated soil temperatures for an aspen ecosystem in Alaska from 1994 to 1997.

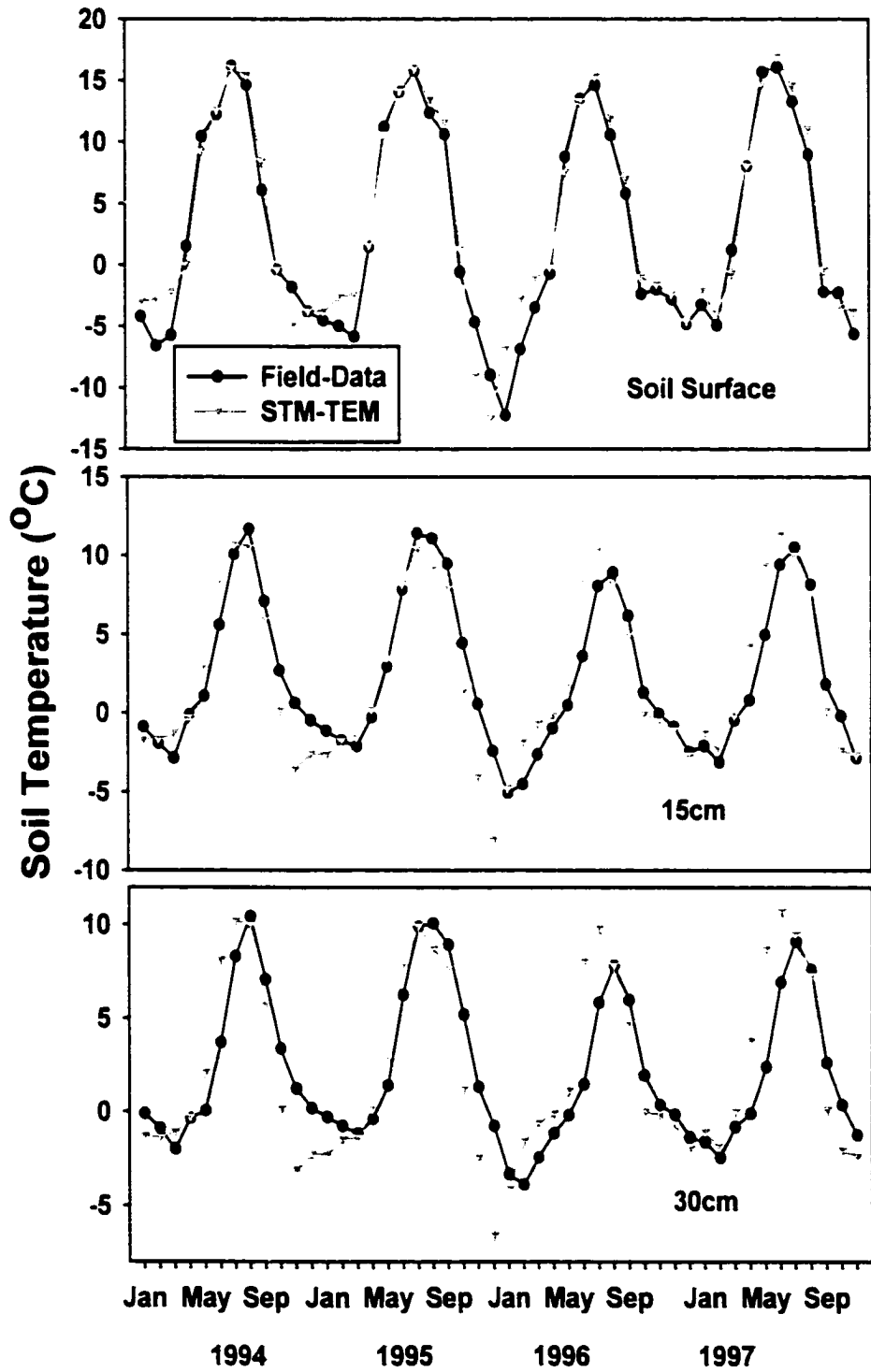


Figure 2.12. Monthly observed and simulated soil temperatures for a tundra ecosystem in Alaska from 1995 to 1997.

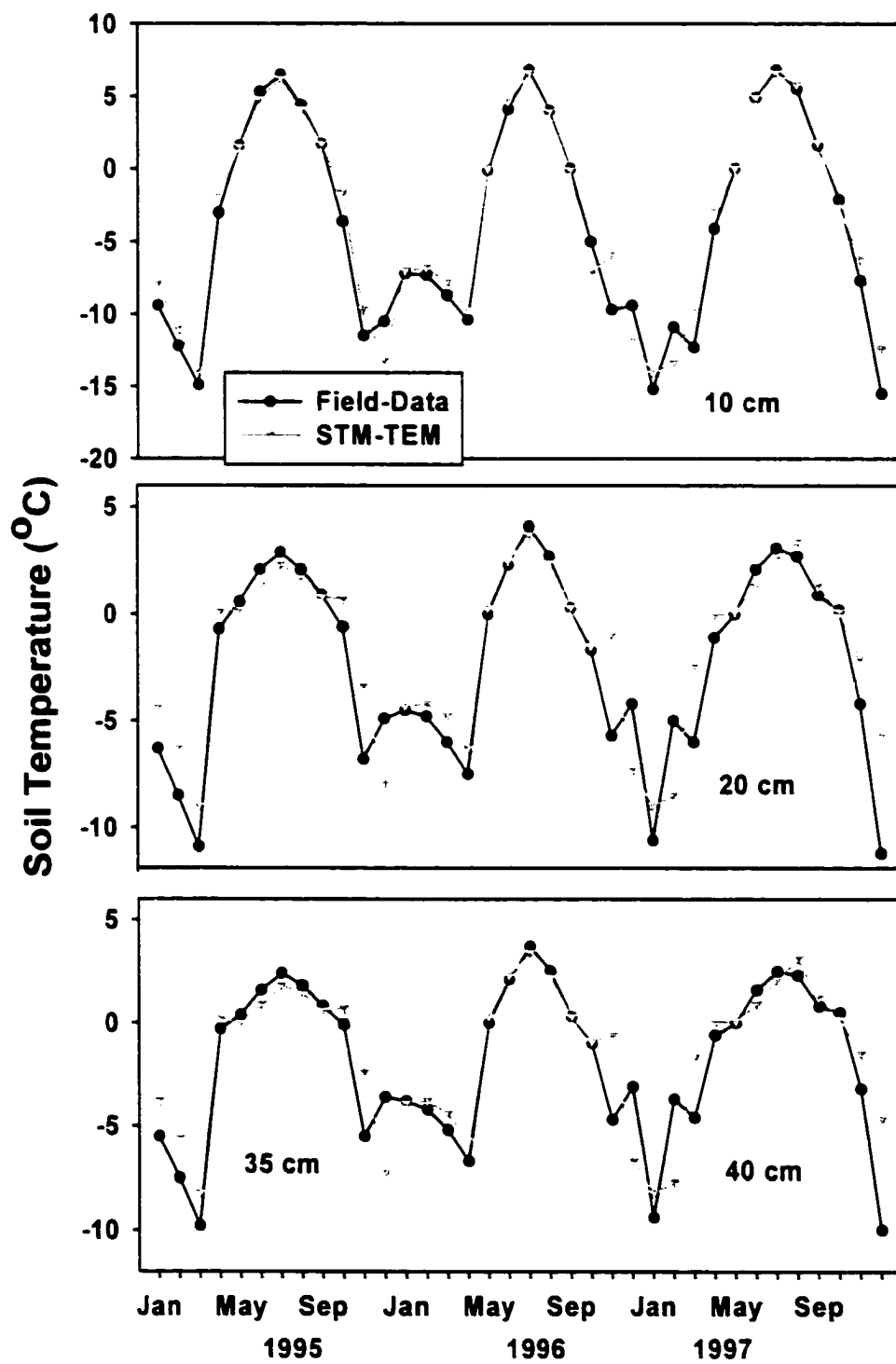


Figure 2.13. Field-based and simulated estimates of (a) monthly gross primary production (GPP) and (b) ecosystem respiration (RESP) for an old black spruce ecosystem in northern Manitoba, Canada from 1994 to 1997. Simulated soil temperatures were used to drive some of the biogeochemical processes in the coupled STM-TEM. Field-based estimates are from *Clein et al.* [in press].

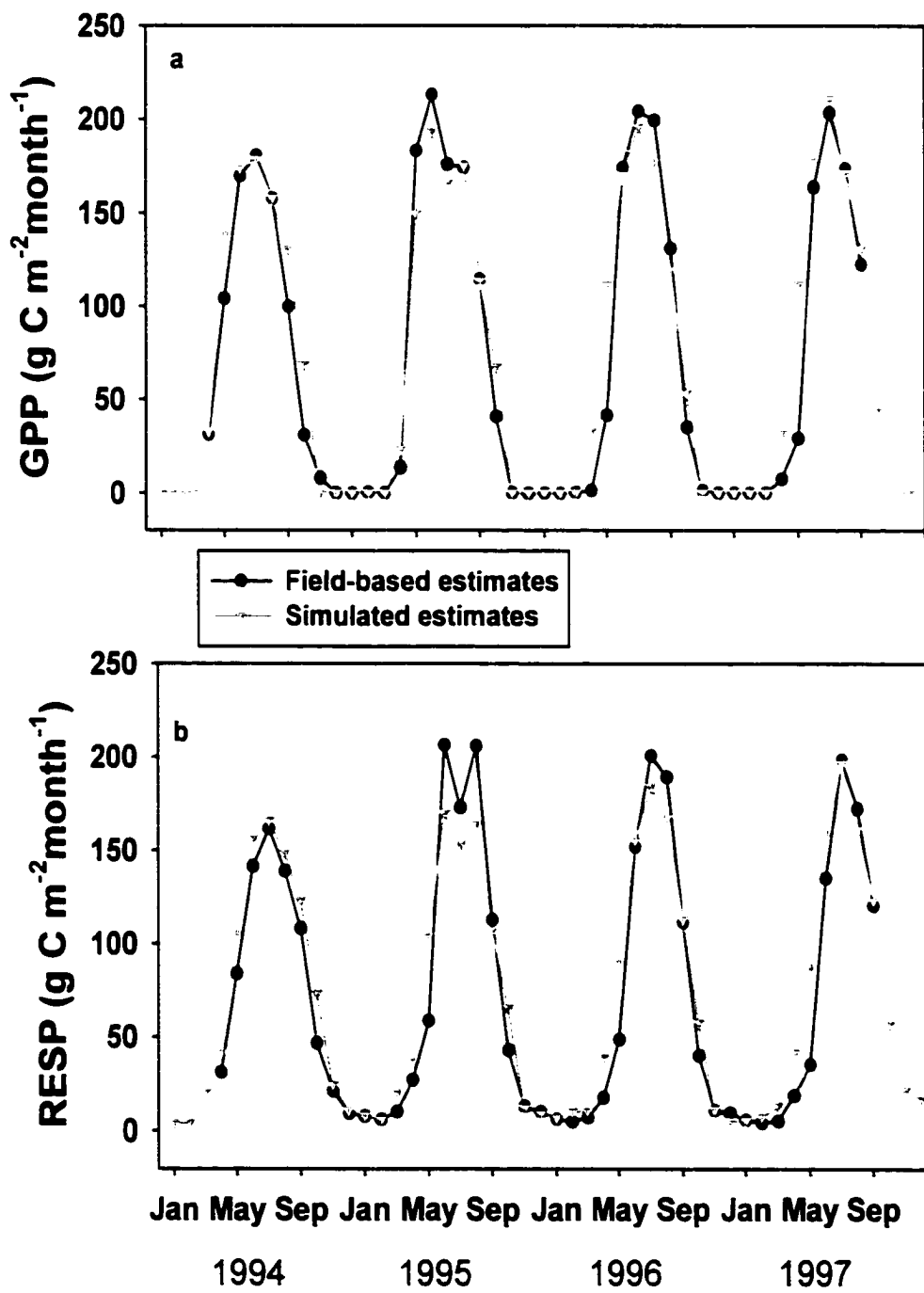
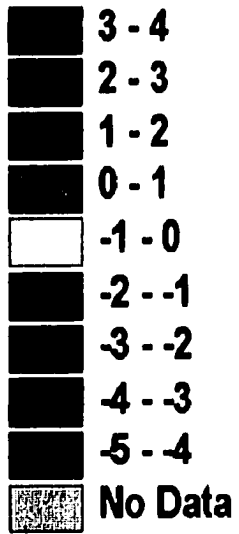
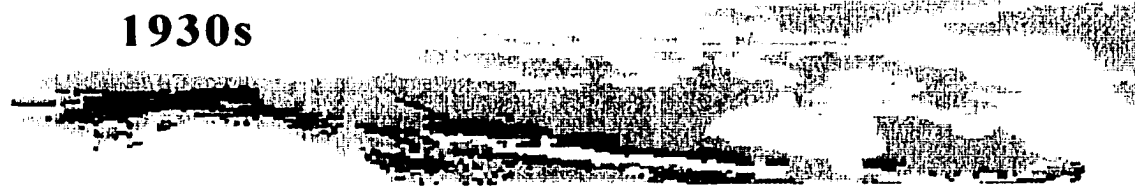


Figure 2.14. Spatial distribution of mean annual soil temperature for the upper soil organic layer simulated by the application of the STM-TEM across the range of black spruce ecosystems in North America north of 50°N during four decades separated by 50 years during the simulation period (1900-2100): (a) 1930-1939, (b) 1980-1989, (c) 2030-2039, and (d) 2080-2089.

**Mean annual soil
temperature (°C)
of the upper organic
soil layer**



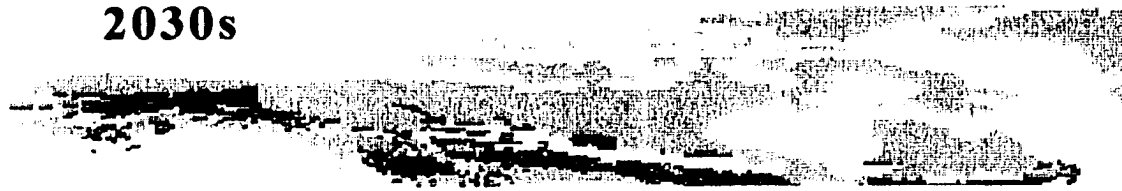
1930s



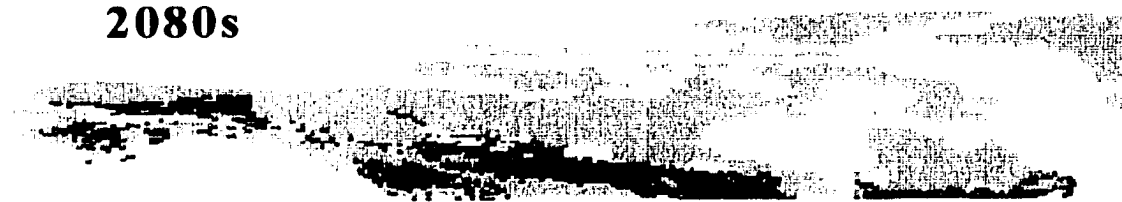
1980s



2030s



2080s



CHAPTER THREE

MODELING SOIL THERMAL AND CARBON DYNAMICS OF A FIRE CHRONOSEQUENCE IN INTERIOR ALASKA¹

Abstract. In this study, the dynamics of soil thermal, hydrologic, and ecosystem processes were coupled to provide the capability to project how the carbon budgets of boreal forests will respond to changes in atmospheric CO₂, climate, and fire, which is a major disturbance in the boreal region. The ability of the model to simulate seasonal patterns of soil temperature, gross primary production, and ecosystem respiration was verified for a mature black spruce ecosystem in Canada, and the age-dependent pattern of vegetation carbon simulated by the model was verified with inventory data on above-ground growth of black spruce in interior Alaska. The model was applied to a post-fire chronosequence in interior Alaska. Simulated soil temperature, soil respiration, and soil carbon storage were compared with measurements of these variables made in 1997. Comparisons between simulated and field-based estimates revealed that the model was able to accurately simulate monthly temperatures at 10 cm ($R > 0.93$) during the growing season for control and burned stands in the chronosequence. Similarly, the simulated and field-based estimates of soil respiration during the growing season for control and burned stands in the chronosequence were correlated ($R = 0.84$ and 0.74 for control and burned

¹In review at *Journal of Geophysical Research – Atmospheres*, Zhuang, Q., A. D. McGuire, K. P. O'Neill, J. W. Harden, V. E. Romanovsky, J. Yarie, Modeling soil thermal and carbon dynamics of a fire chronosequence in interior Alaska.

stands, respectively). The simulated and observed decadal to century-scale dynamics of soil temperature, which are represented by mean monthly temperatures during the growing season (May - September) were correlated among stands of the fire chronosequence ($R = 0.93$ and 0.71 for soil temperature at 20 cm and 10 cm depths, respectively). Similarly, among stands of the chronosequence the simulated and observed decadal to century-scale carbon dynamics were also highly correlated for soil respiration during the growing season ($R = 0.95$) and for soil carbon ($R = 0.91$). Analyses also suggested that, along with differences in fire history, the climate experienced by stands after fire and nitrogen fixation are important factors to consider in simulating the long-term dynamics of soil carbon. Sensitivity analyses were conducted with the model to identify the importance of moss growth after fire, soil moisture levels that might be associated with differences in drainage, and fire severity on soil thermal and carbon dynamics after fire. Taken together, the sensitivity analyses indicate that the growth of moss, changes in the depth of the organic layer, and nitrogen fixation should be represented in models that simulate the effects of fire disturbance in boreal forests. The sensitivity analyses also revealed that soil drainage and fire severity should be considered in spatial application of these models to simulate carbon dynamics at landscape to regional scales.

1. Introduction

High latitude ecosystems occupy a large proportion (22%) of the terrestrial surface and contain approximately 40% of the world's soil carbon inventory that is potentially reactive in near-term climate change [McGuire *et al.*, 1995; Melillo *et al.*, 1995; McGuire and Hobbie, 1997]. Among the world's biomes, boreal forests contain the largest soil carbon pools in the world [Chapin and Mathews, 1993; Post *et al.*, 1982; Gorham, 1991]. Much of the boreal forest is underlain by permafrost, which is susceptible to cycles of degradation (thermokarst) and aggradation [Thie, 1974]. These cycles have in some cases occurred in association with fire [Zoltai, 1993], which is a major disturbance in boreal forests [Kasischke *et al.*, 2000]. The thawing of permafrost after fire has the potential to change the thermal and moisture properties of the soil that have led to substantial soil carbon storage in boreal forest ecosystems.

Fire disturbance in North America's boreal forests was higher in the 1980's than in any previous decade on record [Murphy *et al.*, 1999], and the area of western Canadian boreal forest burned annually has doubled in the last 20 years [Kasischke *et al.*, 2000]. Concurrently, annual surface temperatures in Alaskan boreal and arctic regions have increased 2° to 4° C during the last century [Lachenbruch and Marshall, 1986] and 1° to 2° C in recent decades [Osterkamp and Romanovsky, 1999]. The warming being experienced in Alaska during recent decades is part of a warming trend that is occurring throughout northwestern North America [Beltrami and Mareschal, 1994; Oechel and Vourlitis, 1994; Serreze *et al.*, 2000]. Permafrost throughout Alaska is also currently warming [Osterkamp and Romanovsky, 1999]. Some studies have indicated that wildfire

activity may be related to the warming trend in North America. For example, fire regimes are sensitive to climate in both Alaska [Hess *et al.*, 2001] and Canada [Stocks *et al.*, 2000]. In addition, warming has been identified by Kurz *et al.* [1995] as a possible factor in the increasing fire frequency observed in Canada since 1970 [Kurz and Apps, 1995]. Analyses that have used simulations of changes in climate associated with doubled atmospheric CO₂ suggest that the boreal forest region could experience a 40% increase in the annual amount of area burned [Flannigan and Van Wagner, 1991]. Moreover, the prospect of summer drought, indicated by recent trends in Alaska [Wotton and Flannigan, 1993; Barber *et al.*, 2000] threatens to increase the occurrence of fire.

Changes in the fire regime of boreal forests may have consequences for the global carbon budget because fire disturbance substantially affects carbon storage of boreal forests by influencing both the structure and function of these ecosystems. Fire influences the structure of boreal forest ecosystems through influences on population and vegetation dynamics [Zackrisson, 1977; Schimmel and Granstrom, 1996; De Grandpre *et al.*, 1993; Lynham *et al.*, 1998; Luc and Luc, 1998]. These structural changes have profound influences on the dynamics of permafrost, soil moisture, and soil nutrient cycles in boreal forests [Viereck, 1972, 1973; Dyrness *et al.*, 1989; Wardle *et al.*, 1998; Driscoll *et al.*, 1999; Grogan *et al.*, 2000; Smith *et al.*, 2000; Brais *et al.*, 2000; Yoshikawa *et al.*, in press]. Some studies suggest that disturbance and growth patterns after disturbance at high latitudes may have contributed substantially to the approximately 15% increase in the amplitude of the seasonal cycle measured at some high latitude CO₂ monitoring stations since the 1960s [Zimov *et al.*, 1999; Randerson *et al.*, 1997]. Kurz and Apps

[1999] also indicated that fire disturbance is one of the most important factors affecting the interaction of carbon and permafrost dynamics in North America. Furthermore, some studies have indicated that boreal forests may be a net source of CO₂ if warming greatly increases fire frequency or decomposition [*Kasischke et al.*, 1995; *Kurz and Apps*, 1995].

To evaluate the effects of fire disturbance on carbon source-sink activity in boreal forests, large-scale terrestrial biosphere models need to integrate the processes that influence the soil thermal, hydrological, and biogeochemical dynamics of boreal forest ecosystems. Fire disturbance interacts with all of these processes to influence soil carbon storage [*Harden et al.*, 2000], moss recovery [*Harden et al.*, 1998], and the timing of vegetation recovery [*Waring and Running*, 1998; *Buchmann and Schulze*, 1999; *Schulze et al.*, 2000; *McMurtrie et al.*, 1995; *Ryan et al.*, 1996; *Gower et al.*, 1996]. However, large-scale models have been slow to integrate interactions between fire disturbance and ecosystem dynamics due to long time scales over which these disturbance effects persist and the lack of long-term studies to monitor these changes.

One alternative to long-term studies is to base model development and evaluation on empirical and experimental studies that have used a research design of substituting space for time to gain insight on how ecosystem dynamics change over decades after fire disturbance. Space-for-time substitutions have shown greatest success in illustrating community-wide patterns in systems acknowledged to have strong successional dynamics and where disturbance history is well-documented [*Pickett*, 1989]. In this study we take the important step of integrating interactions between fire disturbance and ecosystem dynamics of boreal forests in interior Alaska into a large-scale ecosystem model, the

STM-TEM [Zhuang *et al.*, in press]. Our objectives in this study were to (1) update the STM-TEM to include the interactions of soil thermal, hydrological, and biogeochemical dynamics; (2) evaluate the performance of the model in simulating the short-term and long-term effects of fire disturbance on soil thermal and carbon dynamics of a fire chronosequence in interior Alaska; and (3) evaluate the effects of different scenarios of moss growth after fire, soil moisture conditions, and fire severity on post-fire carbon dynamics to gain additional insight for the large-scale applications of the model in the boreal region.

2. Methods

2.1. Overview

To achieve our objectives in this study, we followed the steps outlined in the flow diagram of Figure 1. First, we modified the soil thermal model (STM) version of the Terrestrial Ecosystem Model (TEM), the STM-TEM [Zhuang *et al.*, in press], by updating the STM and the hydrological model (HM) to integrate more effectively soil thermal and hydrological dynamics. Modifications of the STM included simulating the effects of recovering moss and fibric organic matter on soil thermal dynamics after fire disturbance. The HM represents a major revision of the Water Balance Model [WBM: *Vorosmarty et al.*, 1989] of TEM, and was structured to simulate the hydrological dynamics of the STM soil profile by representing the soil profile as a three soil-layer system: (1) a moss plus fibric soil organic layer, (2) a humic organic soil layer, and (3) a mineral soil layer. Modifications to TEM included adding formulations to simulate the

thickness of moss, canopy biomass, and leaf area index. The formulation for decomposition in TEM was also modified to consider soil moisture of the humic organic soil layer as calculated by the HM.

The modified STM-TEM was parameterized for black spruce (*Picea mariana* (Mill.) B.S.P.) forests that have been studied at the Bonanza Creek Experimental Forest in interior Alaska as part of the Taiga Long Term Ecological Research (LTER) Program. We then verified the performance of the model by simulating (1) water fluxes, soil moisture, and carbon dynamics of black spruce stands that have been studied as part of the Boreal Ecosystem Atmosphere Study (BOREAS) in northern Manitoba, Canada [see *Sellers et al.*, 1997 for general information on BOREAS] and (2) age-dependent patterns of above-ground vegetation carbon in interior Alaska. Next, we applied the model to a black spruce fire chronosequence in interior Alaska to evaluate its ability to simulate age-dependent patterns of soil thermal and carbon dynamics. Finally, we conducted sensitivity analyses for different scenarios of moss growth after fire, soil moisture conditions, and fire severity to gain insight into factors that might influence the large-scale application of the model.

2.2. Alaska Chronosequence

A black spruce fire chronosequence was established by *O'Neill* [2000] in the eastern Tanana River Valley between the towns of Delta Junction and Tetlin Junction, Alaska (Table 1). The stands of the chronosequence were disturbed by fire in 1996, 1994, 1990, 1987, 1915, and 1855. These stands are similar with respect to slope, drainage, soil

texture, and ground vegetation. In this area, soils in mature black spruce stands typically remain frozen within a meter of the surface, and the upper portion of the soil profiles is composed of relatively undecomposed mosses, moss litter, and roots, or “fibric” organic layer (Agriculture Canada, 1987) that is approximately 25 cm thick in mature stands. This layer is comparable to “Moss plus Upper Duff” layers referred to by foresters [Harden *et al.*, in preparation] and can be considered ground fuel for most boreal fires [Harden *et al.*, 2000]. The lower part of the soil profile consists of highly decomposed and charred (humic) materials that have in many cases accumulated over decades to millennia [as per Trumbore and Harden, 1997] and are 20 to 35 cm thick in mature stands.

Among the stands in the chronosequence, the moss plus fibric soil organic layer varied from 0 to 23 cm, the percentage of ground covered by bryophytes ranged from 0 to 73%, and the humic organic layer varied from 5 to 34 cm (Table 1). The mineral soil was characterized as silt loam or silty clay loam. The thickness of the organic horizons in these stands following fire, which was measured in 1997, varied as a function of fire severity. For example, the stand that burned in 1996 experienced a very light fire severity that left approximately 20 cm of uncombusted organic matter on the soil surface. In contrast, the stands that burned in 1990 and 1994 experienced a more moderate fire severity that resulted in approximately 10 cm of surface organic matter. Among the recently burned stands, the stand that burned in 1987 appears to have experienced the most severe fire with approximately 5 cm of surface organic matter remaining after the fire.

The stands of the black spruce fire chronosequence are subjected to a continental climate characterized by moderate temperatures and precipitation during the summer months (May to August) and exceedingly cold and dry conditions during the winter [O'Neill *et al.*, in review]. Mean monthly air temperature, snow depth, and precipitation have been measured from 1937 to 1999 in Big Delta, which is located near Delta Junction, and from 1954 to 1999 in Tok, which is located near Tetlin Junction (Table 2). Over the periods of measurement, precipitation, snowfall, and air temperature were similar between Big Delta and Tok (Table 2). Soil temperature, soil moisture, soil respiration, and soil carbon storage were measured in 1997 for both recently burned and older control stands of the chronosequence. Details of measurement techniques and procedures are documented in O'Neill [2000].

2.3. Model Development

The first version of the STM-TEM [Zhuang *et al.*, in press] was developed to simulate the soil thermal regime (including permafrost dynamics, soil temperature, and active layer depth) using information on climate, vegetation, soil, and hydrology in boreal forest ecosystems to drive the model. The soil thermal dynamics of the model have been verified and applied to major ecosystem types in high latitudes, and the short-term carbon dynamics have been verified for a black spruce site that was studied as part of BOREAS. In this study, we further developed the STM-TEM so that it was able to simulate how changes in soil thermal dynamics, hydrology, and biogeochemistry interact in the decades following fire in boreal forest ecosystems. This required that we modify the soil thermal

dynamics of the STM to accept input from a hydrology model with a new structure, the HM. We also modified TEM so that the model interacts more effectively with the HM.

We modified the STM so the simulation of soil thermal dynamics depends on simulated variation of moss thickness, soil moisture, and snow pack instead of on prescribed values for these variables (see Figure 2a). The STM receives information on moss thickness from TEM and information on soil moisture and snow pack from the HM. We structured the HM to simulate the hydrological dynamics of the STM soil profile by representing the soil profile as a three soil-layer system (see Figure 2b): (1) a moss plus fibric soil organic layer, (2) a humic organic soil layer, and (3) a mineral soil layer. The HM also considers active layer depth as provided by the STM (Figure 2a) to simulate changes in soil moisture, runoff, and percolation of each of these soil layers (Figure 2b). To consider how canopy development influences hydrology after fire, we implemented Penman and Penman-Monteith formulations [*McNaughton*, 1976; *McNaughton and Jarvis*, 1983] to simulate evaporation and transpiration. This implementation requires leaf area index (LAI), which is provided by a formulation in TEM (see Figure 2a). See the appendix for details of the formulations for simulating water fluxes in the HM.

The TEM was designed to simulate how interactions among carbon and nitrogen dynamics influence carbon dynamics of terrestrial ecosystems at continental to global scales [see *McGuire et al.*, 2001], and has been applied to high latitude regions in a number of studies [*McGuire et al.*, 2000a, 2000b; *Clein et al.*, 2000, in press; *Amthor et al.*, in press; *Potter et al.*, in press; *Zhuang et al.*, in press]. Our modifications to TEM in this study were focused on integrating more effectively the simulation of

biogeochemistry after fire with the soil thermal dynamics simulated by STM and the hydrology simulated by HM. After fire, the STM and HM require information from TEM on how the thickness of moss and leaf area index change (Figure 2a). Therefore, we modified TEM by including formulations to simulate changes in the thickness of moss, canopy biomass, and leaf area index as the stand recovers from disturbance. The TEM requires information from STM on soil temperature of the humic organic layer and from HM on soil moisture of the humic organic layer and on estimated actual evapotranspiration (EET) (Figure 2a). We modified TEM so that soil temperature and soil moisture of the humic organic soil layer influences the simulation of heterotrophic respiration, nitrogen mineralization, and nitrogen uptake by the vegetation. Similar to previous versions of TEM, EET influences the simulation of gross primary production (GPP).

The formulation that we added to TEM for simulating the thickness of moss after fire disturbance is empirical and depends on the number of years after fire:

$$D_{moss} = a \times (1 - e^{-b \cdot t}) \quad (1)$$

where D_{moss} is moss thickness (cm), t is the number of years since fire, and a and b are empirically determined parameters. The fit of the model to measurements of moss thickness in stands of the fire chronosequence is highly significant ($R = 0.97$, $P < 0.01$, $N = 6$) when a is 93.15 and b is 0.002.

The effect of canopy biomass development on monthly carbon uptake from the atmosphere is represented by the function $f(\text{FOLIAGE})$ in the formulation for GPP:

$$\text{GPP} = C_{\max} f(\text{PAR}) f(\text{LEAF}) f(\text{FOLIAGE}) f(\text{T}) f(C_a, G_v) f(\text{NA}) \quad (2)$$

where C_{\max} is the maximum rate of C assimilation. $f(\text{PAR})$ is a scalar that depends on photosynthetically active radiation (PAR). $f(\text{LEAF})$ is leaf area relative to maximum annual leaf area (phenology) and depends on EET. $f(\text{T})$ is a scalar that depends on monthly air temperature. $f(C_a, G_v)$ is a scalar that depends on atmospheric CO_2 concentration (C_a) and relative canopy conductance (G_v), which is influenced by EET. and $f(\text{NA})$ is a scalar function that depends on N availability. The formulation for $f(\text{FOLIAGE})$, which is a scalar function that ranges from 0.0 to 1.0 and represents the ratio of canopy leaf biomass (C_{VL}) relative to maximum leaf biomass ($C_{\text{VL,max}}$), is a logistic function of $f(C_v)$ (Figure 3a):

$$f(\text{FOLIAGE}) = \frac{1.0}{1.0 + m_1 \times e^{m_2 \times v \cdot f(C_v)}} \quad (3)$$

where m_1 and m_2 are parameters, and $f(C_v)$ is a hyperbolic function of the state variable for vegetation carbon (C_v):

$$f(C_v) = \frac{m_3 \times C_v}{1.0 + m_4 \times C_v} \quad (4)$$

where m_3 and m_4 are parameters (see Figure 3b).

The HM uses the LAI calculated by TEM to simulate canopy transpiration. The calculation of LAI by TEM depends on the parameter for specific leaf area (SLA) and on canopy leaf biomass (C_{VL}):

$$LAI = SLA \times C_{VL} \quad (5)$$

in which C_{VL} is estimated as $f(\text{FOLIAGE}) \times C_{VL\text{max}}$, which is a parameter that is determined based on GPP and C_{VL} at the calibration site. The function $f(\text{FOLIAGE})$ has also been incorporated into the formulation for nitrogen uptake in a fashion similar to its effect on GPP to represent the growth of fine root biomass after fire with the assumption that fine root biomass is correlated with canopy biomass.

The flux R_H represents decomposition of all soil organic matter in an ecosystem and is calculated at a monthly time step as follows:

$$R_H = K_d C_S f(M_V) e^{0.069T} \quad (6)$$

where K_d is a rate-limiting parameter that defines the rate of decomposition at 0°C. C_S is the quantity for the state variable that describes carbon in soil organic matter, M_V is mean monthly volumetric soil moisture, and T is mean monthly temperature of the humic organic soil layer simulated by the STM. In this study, M_V is determined by the

simulation of soil moisture for the humic organic soil layer by HM (see appendix for details). Similar to R_H , the fluxes for nitrogen uptake by the vegetation and net nitrogen mineralization have been modified so that they depend on the monthly temperature of humic soil layer simulated by STM and soil moisture of the humic organic soil layer simulated by HM.

2.4. Model Parameterization and Verification

The parameters of STM were based on the existing parameters for the black spruce forest ecosystems in Bonanza Creek Experimental Forest [Zhuang *et al.*, in press]. However, the water content of each soil layer, which was defined as a parameter in the first version of STM, was simulated dynamically in the model version of this study. Similarly, the thickness of the moss plus fibric organic layer, which was defined by a parameter in the first version of STM, also varies dynamically. However, the thickness of the humic organic layer is still specified by a parameter in this version of the STM. For parameters of snow and soil thermal properties, see Zhuang *et al.*, [in press]. The values and sources for parameters in the formulations of vegetation canopy transpiration, canopy evaporation, canopy sublimation, soil surface evaporation, and snow sublimation in the HM are documented in Table 3.

The parameters of TEM for black spruce can be divided into uncalibrated and calibrated parameters. For the uncalibrated parameters, we used the same values as used by Clein *et al.* [in press]. Calibration is primarily used to specify the rate-limiting parameters of the flux equations using the fluxes and pools of a mature stand, i.e., the

calibration site, as constraints. In this study, we calibrated the rate-limiting parameters based primarily on studies by the Taiga LTER Program for black spruce forest ecosystems located at the Bonanza Creek Experimental Forest near Fairbanks in interior Alaska (see Table 4 for information on the fluxes and pools used to calibrate the model). The calibration was similar to the procedures described by *Clein et al.* [in press; see also *Amthor et al.*, in press; *Zhuang et al.*, in press]. In the formulation for $f(\text{FOLIAGE})$, we determined the parameters m_1 , m_2 , m_3 , and m_4 by calibrating the model to the forest inventory data on above-ground vegetation biomass for interior Alaska [*Yarie and Billings*, in press]. The forest inventory data provides estimates of above-ground biomass in metric tons per hectare for 10-year age intervals until age 100 and for 20-year age intervals between age 100 and 200. The values of m_1 , m_2 , m_3 , and m_4 that we used in our simulations were 15.206, -0.3197, 0.0401, and 0.0001, respectively.

To verify the model with respect to carbon fluxes, we conducted the simulation with the parameterization in BNZ site of LTER in Alaska for the old black spruce (OBS) site of the Northern Study Area (NSA) of BOREAS [*Sellers et al.*, 1997]. The simulation was conducted from 1975 to 1997 with the assumption that there is no permafrost in the ecosystem. To drive the model, we used local climate data (air temperature and precipitation) from 1975 to 1997 that were obtained from the Thompson Airport, a Canadian AES station located 40 km east of the NSA-OBS site [See *Clein et al.*, in press; *Zhuang et al.*, in press]. We compared the simulated carbon fluxes to monthly carbon fluxes estimates from 1994 through 1997 based on eddy covariance data [*Goulden et al.*, 1998, as updated by *Dunn et al.* (personal communication, <http://www->

eosdis.ornl.gov/BOREAS/boreas_home_page.html); see also *Clein et al.*, in press]. The carbon fluxes include monthly GPP, the amount of carbon taken up by the vegetation through the process of photosynthesis, and monthly ecosystem respiration (RESP), the amount of carbon released to the atmosphere through respiration by the vegetation and through decomposition of soil organic matter. Net ecosystem production (NEP), which represents the net change in carbon storage of an ecosystem, is calculated as the difference between GPP and RESP assuming negligible loss of organic matter by processes such as leaching. These comparisons indicated that the model was able to reproduce the monthly carbon dynamics at the NSA-OBS site (Figure 4). For GPP and RESP, values of R were larger than 0.97, slopes of a linear regression were not significant from 1.0, and the intercepts were less than $10.0 \text{ g C m}^{-2} \text{ month}^{-1}$. For NEP, the R between simulated and field-based estimates was substantially lower (0.54), the slope (0.46) was substantially different from 1.0, although the intercept was close to 0 ($1.86 \text{ g C m}^{-2} \text{ month}^{-1}$). The contrast among the comparisons for GPP, RESP, and NEP is similar to results obtained in a comparison of fluxes simulated by nine models for the NSA-OBS site [*Amthor et al.*, in press].

To verify the model with respect to the simulation of water fluxes and soil moisture, we conducted the simulations for the NSA-OBS site and for old black spruce forest site at the Southern Study Area of BOREAS (SSA-OBS). For the NSA-OBS simulation, the model was driven as described in the previous paragraph. For the SSA-OBS simulation, we drove the model from 1975 through 1997 with climate data from Nipawin, which is a Canadian AES station not far from the SSA-OBS tower site. Similar

to the simulation for NSA-OBS, the simulation for SSA-OBS was conducted with the assumption that there is no permafrost in the ecosystem. For comparison to simulations for NSA-OBS and SSA-OBS, we aggregated the tower-based estimates of evapotranspiration at half-hour resolution to monthly resolution. The half-hour resolution estimates of evapotranspiration were developed from eddy covariance measurements at the NSA-OBS site [Goulden *et al.*, 1997, 1998, as updated by Dunn *et al.* (personal communication)] and the SSA-OBS site [Jarvis *et al.*, 2000; Newcomer *et al.*, 2000]. Similarly, we aggregated daily or hourly measurements of volumetric soil moisture for the humic organic and mineral soil layers to monthly resolution, for both the NSA-OBS and the SSA-OBS BOREAS sites. The humic organic soil moisture was estimated as the mean of all soil moisture measurements shallower than 45 cm, while the mineral soil moisture was estimated as the mean of all soil moisture measurements deeper than 45 cm and shallower than 105 cm. Comparisons between simulated and field-based estimates indicated that the model reproduced seasonal patterns of evapotranspiration and soil moisture between 1994 and 1997 at both NSA-OBS and SSA-OBS (See Figure 5).

To verify the age-dependent simulation of vegetation carbon, we ran the model to equilibrium, disturbed the stand with fire, and then drove the model for 178 years using mean monthly air temperature and precipitation that was derived by averaging monthly temperature and precipitation data collected at Tok, Alaska between 1954 and 1999. Based on Ryan [1991] and Ryan *et al.* [1997], we estimated above-ground vegetation carbon as 80% of total vegetation carbon simulated by TEM. For the inventory data, we

estimated the above-ground vegetation carbon (g C m^{-2}) by multiplying the inventory survey biomass data by 0.475 [see *Atjay et al.*, 1977]. The simulated and inventory-based above-ground vegetation carbon (Figure 6) were highly correlated ($R = 0.95$, $P < 0.001$, $N = 12$), with a regression slope (0.95) that was not significantly different from 1.0, but an intercept (122.3 g C) that was significantly different from 0.0 ($P < 0.001$, $N = 12$).

2.5. Model Application to the Fire Chronosequence

Our modeling framework considers the effects of atmospheric CO_2 , climate, and fire disturbance on NPP, R_{H} , and fire emissions in simulating changes in carbon pools of terrestrial ecosystems (Figure 7, see also *McGuire et al.*, 2001). Prior to the first scheduled disturbance, the model is run with constant atmospheric CO_2 and constant long-term mean climate until the pools reach equilibrium. The model is then driven with historical CO_2 and climate until a disturbance is scheduled, at which time a proportion of vegetation and soil carbon is consumed and released to the atmosphere. For the soil carbon released to the atmosphere, the entire moss plus fibric organic layer and a proportion of the humic organic layer are considered to be consumed by the fire. Of the vegetation carbon and nitrogen pools prior to disturbance, 1% is retained as live vegetation to start the growth of vegetation after fire. After accounting for vegetation carbon and nitrogen associated with fire emissions and with live vegetation remaining after fire, the remaining vegetation carbon and nitrogen from the pools prior to disturbance is added to the soil organic carbon and nitrogen pools. Subsequent to disturbance, growth of vegetation and associated ecosystem dynamics are driven by

historical CO₂ and climate until the next disturbance is scheduled. The simulations in this study do not consider the fixation of nitrogen during the growth of vegetation after fire, although the nitrogen stocks of vegetation and soil have been adjusted in the initial equilibrium simulations so that target carbon to nitrogen ratios of vegetation and soil are maintained at equilibrium [see *McGuire et al.*, 1997 for more details].

Before applying the model to the fire chronosequence we ran the model to equilibrium using an atmospheric CO₂ level of 284 ppmv and the long-term mean monthly air temperature, precipitation, and cloudiness of the 0.5° grid cell with longitude 143.0° W and latitude 63.5° N, i.e., the Tok grid cell, from the long-term climate data set used in the simulations of *McGuire et al.* [2001]. For the equilibrium simulation, soil texture was extracted for the Tok grid cell from the data sets described in *McGuire et al.* [2001], and we set the initial soil thermal profile and its thermal properties to those of a mature black spruce forest at Bonanza Creek Experimental Forest that is underlain with permafrost similar to that described in *Zhuang et al.* [in press]. For the purposes of this study, we considered the results of the equilibrium solution to be representative of the year 1819. For the simulations over the period from 1820 through 1998, we drove the model with the atmospheric CO₂ data set described by *McGuire et al.* [2001]. From 1820 through 1859 we drove the model with monthly temperature and precipitation corresponding the years 1860 through 1899 in the climate data from *McGuire et al.* [2001]. We used the monthly temperature and precipitation for the period from 1860 through 1953 of the Tok grid cell in the climate data from *McGuire et al.* [2001] to drive the model over the those years. We used the climate data from the Tok weather station to

drive the model from 1954 through 1998. From 1820 through 1998, we used the same monthly cloudiness data set that was used to drive the model to equilibrium in 1819.

To apply the model to the fire chronosequence, we scheduled fires in 1825, 1855, and 1915 for the control stands, and in 1987, 1990, 1994, and 1996 for the recently burned stands (see Figure 8). It is important to recognize the carbon and nitrogen pools of the recently burned stands were derived from the carbon and nitrogen pools of their respective control stands (see Figure 8). Thus, the pools of the stands that burned in 1990 and 1994 were derived from our simulations for the control stands that we estimate to have burned in 1915 and 1855, respectively (see Table 1 and Figure 8). Similarly, the pools of the stands that burned in 1987 and 1996 were derived from our simulation for the control stands that we estimate to have burned in approximately 1825 (Table 1 and Figure 8). It is important to realize that while we represent the control stands for the 1987 and 1996 burns with a single simulation, that measurements were made in control stands that were unique to these burns. At the time of a scheduled disturbance, we assumed a constant severity for all fires in which 23% of vegetation carbon and nitrogen and 36% of soil organic carbon and nitrogen were consumed and released to the atmosphere in fire emissions. These values are typical of above-ground vegetation carbon and ground-layer carbon released from fire in interior Alaska [French *et al.*, 2000]. In the simulations for the control sites that burned in 1855 and 1915, we prescribed the thickness of moss plus fibric organic layer and the humic organic layer by the site conditions in Table 1. In the simulation for the control sites that burned in 1825, we assumed that the soil profile was similar to the profile for the control site that burned

in 1855 . For the recently burned sites, we set the thickness of the moss plus fibric organic layer to 0 immediately after fire because more than 96% of the ground surface is either bare mineral soil or covered with char, and no live mosses are found [O'Neill, 2000]. We set the thickness of the humic organic layer in the recently burned sites to the value measured in 1997 (see Table 1).

We compared soil temperatures at 10 cm and 20 cm depth, soil respiration, and soil carbon storage simulated for stands of the chronosequence in 1997 to field-based estimates of these variables based on field measurements made in 1997. For the burn that occurred in 1994, measurements were made in 1997 for two stands that experienced moderate and severe fires, respectively (see Table 1). Therefore, we averaged measurements for these two stands to develop field-based estimates of soil temperature, soil respiration, and soil carbon storage for the purpose of making comparisons to the simulation for the 1994 burn. We compared soil temperature and soil respiration at monthly resolution to evaluate seasonal dynamics and aggregated these variables over the growing season to evaluate long-term dynamics across the chronosequence. To estimate simulated soil respiration, we added R_H to an estimate of root respiration, which was calculated by multiplying simulated autotrophic respiration by 0.45 based on data for the ratio of root respiration to total autotrophic respiration for black spruce stands in BOREAS [Ryan *et al.*, 1997].

2.6. Sensitivity Analyses

To gain insight into factors that might influence the large-scale application of the model, we conducted sensitivity analyses for different scenarios of (1) moss growth, (2) soil moisture, and (3) fire severity. The sensitivity analyses evaluated the responses of soil thermal, hydrological, nitrogen, and carbon dynamics for the different scenarios. For all simulations conducted for the sensitivity analyses, the model was run to equilibrium using a CO₂ level of 284 ppmv, the monthly cloudiness data for the Tok grid cell from the cloudiness data set used in the model simulations of *McGuire et al.* [2001], and mean monthly temperature and precipitation from the Tok weather station from 1954 to 1999 (see Table 2). After reaching equilibrium, we initiated a fire and then ran the model for 140 years using the same input variables used to drive the model to equilibrium prior to fire disturbance.

The sensitivity analysis to moss growth evaluated how documented moss growth after fire, i.e., the "standard" scenario, influences ecosystem dynamics relative to full moss cover in unburned stands and relative to a scenario in which moss does not grow after fire. In the standard scenario, moss cover is reduced to 0 immediately after fire, 23% of vegetation carbon and nitrogen are released to the atmosphere in fire emissions, 36% of soil carbon and nitrogen are released to the atmosphere in fire emissions, but the depth of the humic organic layer (30 cm) was not reduced by fire in this simulation. As soil drainage has the potential to influence soil moisture of the organic layer in permafrost soils, we were interested in evaluating how differences in soil moisture of the humic organic layer influences ecosystem dynamics. Therefore, we implemented two

soil moisture scenarios in addition to the standard scenario in which volumetric soil moisture of the humic organic layer was prescribed to decrease or increase by 50% during both the equilibrium and post-fire phases of the simulations.

For the sensitivity analysis focused on fire severity, we implemented less severe and more severe scenarios relative to standard scenario, in which 23% of vegetation carbon and nitrogen and 36% of soil carbon and nitrogen were released to the atmosphere in fire emissions. In the less severe scenario, 12% of vegetation carbon and nitrogen and 18% of soil carbon and nitrogen are released as fire emissions. In the more severe scenario, 46% of vegetation carbon and nitrogen and 54% of soil carbon and nitrogen are released as fire. In all scenarios, we assumed that the depth of moss plus fibric organic layer was 0 immediately after fire, and that the depth of the humic organic soil layer (30 cm) was reduced relative to the amount of soil carbon released (18% in the simulation with lower fire severity, 36% in the standard simulation, and 54% in the simulation with higher fire severity).

3. Results

3.1. Soil Thermal Dynamics

Comparisons between simulated and field-based estimates of soil temperature revealed that the model was able to accurately simulate monthly temperatures during the growing season for control and burned stands in the chronosequence (Figure 9 and 10). Most of the simulated monthly soil temperatures at 10 cm depth were within one standard deviation of the mean based on field measurements (Figure 9), and were significantly

correlated to field-based estimates for both control stands (Figure 10a, $R = 0.93$, $P < 0.001$, $N = 14$) and burned stands (Figure 10b, $R = 0.93$, $P < 0.001$, $N = 14$). From May through September, simulated mean monthly temperature at 10 cm depth in burned stands was 2° to 4° C warmer than in control stands (Figure 9). Across all months of the year, simulated mean monthly temperatures at 10 cm depth in burned sites were 3.3° C warmer than in control stands.

Comparisons between simulated and field-based estimates of mean monthly growing season temperature (May - September) in the chronosequence revealed that the model was able to accurately simulate century scale dynamics of soil temperature after fire disturbance (Table 5). Across the chronosequence, the simulation of soil temperature at 20 cm depth ($R = 0.93$, $P < 0.01$, $N = 6$) was more accurate than at 10 cm depth ($R = 0.71$, $P = 0.12$, $N = 6$) because the simulation of soil temperature for the control stand that burned in 1855 was more accurate at 20 cm than at 10 cm (Table 5). With the exception of the 1996 burned site, the simulations indicated that younger stands generally had higher soil temperature than the older stands at both 10 cm and 20 cm depth. Starting with the site that burned in 1994 and ending with the site that burned in 1855, the growing season soil temperatures decline with stand age from 11.8° C to 5.9° C at 10 cm and from 10.5° C to 3.6° C at 20 cm (Table 5). Low temperatures observed in the 1996 burn site in both simulated and field-based estimates are likely associated with the low severity of fire at this stand, which left nearly 20 cm of humic organic material on the soil surface (Table 1). To evaluate this hypothesis, we conducted an additional simulation for the 1996 stand for a burn severity that had a depth of the humic organic layer equal to

that of the 1994 stand that was severely burned. The simulation for a stand that was "severely burned" in 1996 resulted in warmer soil temperatures in comparison to the other stands.

3.2. Soil Respiration Dynamics

Comparisons between simulated and field-based estimates of soil respiration revealed that the model was able to accurately simulate monthly soil respiration during the growing season for control and burned stands in the chronosequence (Figure 11 and 12). Most of the simulated estimates of monthly soil respiration were within one standard deviation of the mean based on field measurements (Figure 11), although the performance of the model for the control stands (Figure 12a: $R = 0.84$, $P < 0.01$, $N = 17$) was generally better than burned stands (Figure 12b: $R = 0.74$, $P < 0.01$, $N = 17$). In general, simulated soil respiration indicated that the burned sites had generally lower rates of soil respiration than control stands, particularly in recently burned sites (Figure 11): for example, fluxes simulated for the 1996 burned stand (Figure 11a) were approximately half those simulated for the control stand. Analysis of the simulated fluxes indicated that the reduction of soil respiration at the burned stand was primarily associated with the reduction of root respiration.

We conducted a set of correlation analyses to evaluate whether the relationship between monthly soil respiration and monthly soil temperature at 10 cm depth were similar between field-based estimates and model estimates during the growing season in 1997 for the months May through September. The 15 unique correlations in this set of

analyses were composed of separate correlations for the field-based estimates and simulated estimates for both the control and recently burned stands associated with the 1996, 1994, 1990, and 1987 burns; there are 15 instead of 16 unique correlations in the set of analyses because the correlations for the simulated estimates were identical for the control sites associated with the 1996 and 1987 burns. Monthly soil respiration was significantly correlated to monthly soil temperature in each of the analyses ($R > 0.68$, $P < 0.01$, $N = 5$ months). Thus, temperature appears to be an important factor controlling field-based and simulated soil respiration of both control and recently burned stands.

Comparisons between simulated and field-based estimates of mean monthly growing season soil respiration (May - September) in the chronosequence revealed that the model was able to accurately simulate century-scale dynamics of soil respiration after fire disturbance (Table 5: $R = 0.95$, $P < 0.01$; $N = 6$ stands). Both simulated and field-based estimates of mean monthly soil respiration over the growing season increased with stand age. Analysis of the simulated fluxes indicated that increases in soil respiration with stand age were primarily associated with increases in root respiration.

3.3. Soil Carbon Dynamics

In the year of fire disturbance, simulated soil carbon stocks of each of the stands in the chronosequence decrease (Figure 13a) because losses associated with the fire emissions are greater than gains associated with the input of dead vegetation carbon after the fire. For all stands in the chronosequence, the model simulates that the stand continues to lose soil carbon for a number of years while decomposition losses are greater

than inputs of carbon to the soil from regrowing vegetation. In 1997, the model simulated that the recently burned stands (1996, 1994, 1990, and 1987) are losing soil carbon (Figure 13a). For the older stands that burned in 1825, 1855 and 1915, the model simulated that soil carbon is accumulating (Figure 13a) because carbon from regrowing vegetation exceeds decomposition losses. Examination of the soil carbon trajectories indicates that it takes approximately 30 to 40 years after fire disturbance before soil carbon starts accumulating (Figure 13a). The simulations also indicate that the stand that burned in 1915 accumulated soil carbon at a faster rate than the stands that burned in 1825 and 1855. To evaluate factors responsible for the pattern, we conducted a set of simulations for the fire chronosequence using climate with no inter-annual variability and the same transient data set of atmospheric CO₂ that was used to drive the simulations represented in Figure 13a. These simulations suggest that along with differences in fire history, that the climate experienced by stands after fire is an important factor responsible for the dynamics of soil carbon.

For five of the stands in the chronosequence, soil carbon of each stand was estimated as the sum of carbon stored in moss, the fibric organic layer, and the humic organic layer from the 1997 measurements of *O'Neill et al.* [in review; see also *O'Neill, 2000*]. The simulated and field-based estimates of soil carbon among the five stands were highly correlated ($R = 0.91$, $P < 0.01$, $N = 5$). The simulated estimates were most similar to field-based estimates of soil carbon for the four youngest stands, but the model underestimated soil carbon of the stand that burned in 1855 by about 30% (Table 5). While it is possible that the control stand that burned in 1855 may represent a biased site

with respect to field-based estimates of soil carbon storage [O'Neill, 2000], additional simulations that we conducted with model suggest that nitrogen dynamics not represented in the model may play a role in the underestimate of soil carbon by the model for the control stand that burned in 1855 (Figure 13b and 13c). In the simulations that were driven by climate with no inter-annual variability, soil carbon stabilizes at approximately 11.000 g C m⁻² instead of the initial steady state value of between 15.000 and 16.000 g C m⁻² (Figure 13b). We hypothesized that the stabilization at approximately 11.000 g C m⁻², and hence the underestimate for the stand that burned in 1855, was associated with the fact that nitrogen was not added to the stand after disturbance. To test this hypothesis, we conducted a set of simulations in which we added nitrogen in equal amounts each year over the course of the simulation to replace the nitrogen lost in fire emissions. We drove these simulations with the same data sets of climate and atmospheric CO₂ concentration that were used to drive the simulations of Figure 13b. In the simulation for the stand that was burned in 1855, soil carbon was estimated to be approximately 16.000 g C m⁻² (Figure 13c), which is similar to the soil carbon measured for that stand (Table 5). In comparison to the simulations with no nitrogen inputs after disturbance, the higher level of soil carbon storage simulated with nitrogen inputs was associated with NPP that was sustained at a higher level after the vegetation had substantially recovered from the fire. Thus, our simulations suggest that nitrogen fixation after fire is an important issue to consider in long-term responses of soil carbon after fire disturbance.

3.4. Sensitivity Analyses

3.4.1. Sensitivity to Moss Growth

The objective of the sensitivity analysis to moss growth was to evaluate how documented moss growth after fire influences ecosystem dynamics relative to full moss cover in unburned stands and relative to a scenario in which moss does not grow after fire. Note that the depth of the humic organic layer was not altered during stand development after fire so that only the effect of changes in moss depth are evaluated in these simulations. The simulations indicated that moss growth clearly affects the long-term dynamics of soil temperature after fire, in which the burned stands are approximately 4° C warmer immediately after fire, and is responsible for a return towards colder soil temperatures of the unburned stand (Figure 14a).

The development of the moss layer also influences the long-term dynamics of soil moisture after fire (Figure 14b), although this effect is much less striking than the effect of moss on soil temperature. For approximately the first 50 years after fire, the mean volumetric soil moisture (VSM) from May to September for the simulations with and without moss growth is much lower than the unburned stand because of both higher evaporation and greater drainage as the moss and fibric organic layers were eliminated by the fire and the active layer became thicker. Soil moisture starts to increase about 50 years after fire in these simulations (Figure 14b) as the canopy closes and causes soil surface evaporation to decrease. After approximately 100 years, soil moisture in the stand with moss growth stabilizes at the same level as the unburned stand as moss

growth, leaf area index, and active layer depth stabilize. The dynamics of soil moisture in the stand without moss growth slightly lags the dynamics of the stand with moss growth (Figure 14b) because the stand without moss growth has higher surface evaporation than the stand with moss growth for the same leaf area.

The effect of moss growth on soil temperature influenced patterns of decomposition and net nitrogen mineralization during stand development. Decomposition gradually decreased after fire because of declines in soil carbon associated with lower inputs of carbon from the vegetation (Figure 14e), but gradually increased through stand development as inputs to soil carbon from vegetation increased along with increases in NPP (Figure 14d). Immediately after fire, our simulations indicated that net nitrogen mineralization drops substantially (Figure 14c) because of immobilization that is enhanced by the high levels of available nitrogen that build up in association with much reduced levels of plant nitrogen uptake. Simulated nitrogen cycling rates gradually increase through stand development after fire (Figure 14c), with higher rates in the simulation with no moss growth after about 60 years that appear to be caused by higher rates of decomposition (R_H ; Figure 14e) that are associated with higher soil temperature.

Differences in net nitrogen mineralization between the simulations with and without moss growth translated into differences in NPP (Figure 14d), with higher NPP in the simulation without moss growth. In comparison to the unburned stand, NPP stabilizes at a lower level in the burned stands because nitrogen lost in fire emissions was not replaced during stand development after fire. While the growth of moss influenced the simulated dynamics of both NPP and decomposition, it had no effect on the long-term dynamics of

NEP (Figure 14f). However the growth of moss does influence the allocation of carbon storage, as the simulation with moss growth has lower levels of vegetation carbon storage (Figure 14g) and slightly higher levels of soil carbon storage (Figure 14h).

3.4.2. Sensitivity to Moisture Conditions

The objective of the sensitivity analysis to moisture conditions was to evaluate how different levels of soil moisture in the humic organic soil layer that could arise because of differences in drainage might influence ecosystem dynamics after fire. In the standard scenario, which was the same as the scenario with moss growth after fire in the previous sensitivity analysis, mean VSM from May to September drops to less than 25% after fire disturbance and returns to approximately 35% after about 100 years of stand development (Figure 15a). In the low soil moisture scenario, May-September VSM drops to approximately 12% after fire and increases to about 18% through stand development, while the high moisture scenario May-September VSM drops to about 36% after stand development and increases to approximately 52% (Figure 15a). It is important to note that the 52% VSM level in the high moisture scenario is approximately the same as the 50% VSM optimum for the function $f(M_V)$ in equation 6 for R_H [see *Tian et al.*, 1999], above which anaerobic conditions start to retard decomposition in the model.

Soil moisture conditions played an important role in controlling soil temperature and in regulating rates of decomposition and net nitrogen mineralization. The simulations indicate that lower levels of soil moisture lead to higher soil temperatures immediately after fire with approximately 1° C difference at 20 cm depth among

scenarios (Figure 15b). Higher soil temperature is maintained throughout stand development for the duration of the simulations in the scenarios with lower soil moisture (Figure 15b). Differences in soil moisture among the scenarios explain differences in decomposition rates (Figure 15e) that were responsible for differences in rates of net nitrogen mineralization (Figure 15c). Thus, in contrast to the sensitivity analysis for moss growth in which differences in soil temperature drove differences in decomposition and net nitrogen mineralization, differences in soil moisture were more important than differences in soil temperature in the responses of decomposition and net nitrogen mineralization in this sensitivity analysis to soil moisture.

Differences in net nitrogen mineralization among the scenarios translated into differences in NPP (Figure 15d), with higher NPP in the simulations with higher soil moisture. While NPP of the standard scenario stabilizes at a lower level than NPP of the unburned stand of Figure 14d because nitrogen lost in fire emissions was not replaced during stand development after fire, differences in soil moisture lead to larger differences in NPP among the moisture scenarios (Figure 15d) with higher NPP in the wetter soils because of higher nitrogen cycling rates (Figure 15c).

For about 60 years after fire, the higher decomposition rates of the wetter scenarios caused lower NEP and higher post-fire losses of carbon from the ecosystem over this period (Figure 15f). It is important to recognize that this response is relevant to soil moisture increases over the range of soil moisture for aerobic decomposition, and not over the range of soil moisture that leads to anaerobic conditions. In contrast, between approximately 60 and 140 years after fire, the higher NPP of the wetter scenarios caused

higher NEP and higher rates of carbon accumulation in the ecosystem over this period (Figure 15f). The different moisture scenarios influenced the allocation of carbon storage, as the wetter simulations led to more vegetation carbon accumulation and less soil carbon accumulation (Figure 15g and 15h).

3.4.3. Sensitivity to Fire Severity

The objective of the sensitivity analysis to fire severity was to evaluate how different changes in the depth and the amount of humic organic matter associated with different fire severities influence ecosystem dynamics after fire. It is important to recognize that while the depth of humic organic matter immediately after fire was influenced by fire severity in the simulations, the depth of this layer was not subsequently altered during the simulation of stand development after fire. The simulations indicated that the effects of fire severity on the depth of the organic layer clearly affects the long-term dynamics of soil temperature after fire. Immediately after fire, a shallower humic organic layer associated with higher levels of fire severity lead to higher soil temperatures with approximately 1.5° C difference at 20 cm depth among scenarios (Figure 16a). Higher soil temperature was maintained throughout stand development for the duration of the simulations in the scenarios with higher fire severity (Figure 16a).

Among the scenarios, there was little effect of fire severity on soil moisture for about 60 years after fire (Figure 16b), after which May-September VSM increased as the canopy closed and eventually stabilized as leaf area stabilized. Although the soil moisture dynamics of the standard scenario slightly lagged the dynamics of the lightly

burned scenario between approximately 60 and 110 years after fire, the two scenarios stabilized at approximately the same level of soil moisture (Figure 16b). In contrast, the effects of fire severity on soil moisture dynamics were most pronounced for the severely burned stand (Figure 16b), which stabilized at soil moisture levels substantially lower than the other two scenarios because of greater drainage associated with a thicker active layer that results from higher soil temperatures.

In contrast to the sensitivity analyses for moss growth and moisture conditions, in which effects of soil temperature and soil moisture explained differences in decomposition among scenarios, higher decomposition rates occurred in the scenarios with lower fire severity (Figure 16e) because the labile pools of soil organic matter were higher in the scenarios with lower fire severity. This pattern occurred even though soil temperatures were higher in the simulations with higher fire severity. Higher decomposition rates in the scenarios with lower fire severity lead to higher rates of net nitrogen mineralization only after about 50 years of stand development (Figure 16c), as it appears that among the scenarios the effects of soil temperature and soil moisture on nitrogen immobilization rates compensated for effects of decomposition on gross nitrogen mineralization rates during the first 50 years after fire. As in the other sensitivity analyses, patterns of net nitrogen mineralization among the scenarios translated into patterns of NPP (Figure 16d). It is important to note that decomposition, nitrogen mineralization, and NPP in the more severely burned scenarios do not recover to pre-fire levels because nitrogen lost in fire emissions was not replaced during stand development in these simulations.

For about 60 years after fire, the higher decomposition rates of the scenarios with lower fire severity caused lower NEP and higher post-fire losses of carbon from the ecosystem over this period (Figure 16f). In contrast, between approximately 60 and 140 years after fire, the higher NPP of the scenarios with lower fire severity caused higher NEP and higher rates of carbon accumulation in the ecosystem over this period (Figure 16f). The different scenarios of fire severity influenced the magnitude of carbon storage, as the scenarios with higher fire severity led to both less vegetation carbon accumulation and less soil carbon accumulation by the end of the simulation (Figure 16g and 16h). Lower carbon accumulation in the more severe fire scenarios occurs because of more nitrogen lost from the ecosystem in fire emissions.

4. Discussion

Wildfire is a major disturbance that influences carbon storage of boreal forests [Kasischke *et al.*, 2000; Schultze *et al.*, 2000; Wirth *et al.*, 1999, in press; Kurz and Apps, 1999; Harden *et al.*, 2000; McGuire *et al.*, in review; McGuire *et al.*, in preparation]. Other factors including increasing atmospheric CO₂, climate change variability, and nitrogen deposition also have the potential to influence ecosystem processes to affect carbon storage in boreal forests [Barber *et al.*, 2000; McGuire *et al.*, 2001]. Traditionally, the role of fire in carbon storage of forests in the boreal region has been estimated with book-keeping models [Kasischke, 1995; Kurz and Apps, 1999; Harden *et al.*, 2000]. As fire disturbance is likely to interact with other factors in complex ways that affect carbon dynamics, it is important to synthesize understanding from field studies into

process-based models that represent the mechanisms responsible for these interactions. In this study, we applied the STM-TEM to a fire chronosequence in interior Alaska to help elucidate how interactions between fire disturbance and other factors influence carbon storage of boreal forests. Specifically, our analysis focused on interactions that are mediated through soil temperature, soil moisture, and nitrogen dynamics. In this discussion, we highlight important findings that resulted from the application of the STM-TEM to the fire chronosequence. We focus first on soil thermal dynamics and then on carbon dynamics. Finally, we discuss future directions for model development and application to evaluate the role of wildfire and other factors on carbon budgets of boreal forests at large spatial scales.

4.1. Evaluation of Soil Thermal Dynamics

While the patterns of soil temperature in 1997 were generally similar between model-based and field-based estimates, it is important to recognize that it was necessary to prescribe the pattern of moss growth through time and the depth of the humic organic layer in 1997 to produce the level of agreement in soil temperature. This was specifically highlighted by the simulation for the stand that burned in 1996, for which soil temperature was colder than in more recently burned stands because a substantial layer of humic organic matter remained after the fire. The sensitivity analyses that were focused on moss growth and fire severity verified that the growth of the moss and organic horizons after fire disturbance are important in the temporal dynamics of simulated soil temperature. It is well known that surface temperature decreases with the increasing

thickness of moss and peat in high latitude ecosystems, and that variations in vegetation canopy per se have a relatively minor influence on the ground thermal regime compared to the surface organic layer [Brown, 1963, 1965, 1983; Riseborough, 1985; William and Smith, 1989]. Fire disturbance affects active layer dynamics of ecosystems underlain by permafrost by altering the insulation provided by moss and organic soil layers [Viereck, 1972, 1973, 1983; Rouse, 1976; Dyrness and Norum, 1983; Van Cleve et al., 1996; Yoshikawa et al., in press]. The simulations that we conducted not only agree with these observations, but also suggest that there are important interactions between soil temperature and soil moisture dynamics. The sensitivity analyses in this study indicate that soil temperature is substantially affected by soil moisture, and that the growth of moss and the humic organic layers play a role in soil moisture dynamics during stand development.

4.2. Evaluation of Carbon Dynamics

Similar to measurements of soil respiration reported for the fire chronosequence [O'Neill et al., in review; see also O'Neill, 2000] and for an experimental burn near Fairbanks, Alaska [Valentine and Boone, unpublished data, 2001], our simulations indicate that soil respiration drops by approximately 50% immediately after fire. This is similar to observations in Canada [Burke et al., 1997; Wang et al., in review]. The loss of root respiration associated with the mortality of vegetation in fire is the mechanism that is clearly responsible for this decline in the simulations that we conducted. While soil respiration declines substantially and immediately after fire, our simulations indicate that

recently burned stands are losing carbon for approximately 30 to 60 years until the ecosystem starts accumulating carbon as NPP becomes greater than decomposition. The 30 to 60 year time period for carbon accumulation in our simulations contrasts with the 7 to 15 year time period from the application of a steady state model based on NPP and decomposition measurements for mature stands in the BOREAS region [*Harden et al.*, 2000; *O'Neill et al.*, unpublished]. The timing of the transition from carbon source to carbon sink activity in the simulations of this study is similar to the findings of *Rapalee et al.* [1998] for stands developing after fire in the BOREAS region of Canada.

Kasischke et al. [1995] hypothesized that decomposition in excess of carbon inputs to the soil lead to cumulative carbon losses after fire (prior to carbon accumulation), which is referred to by some as "post-fire emissions", that are greater than carbon losses in fire emissions. Our sensitivity analysis for fire severity agrees with this hypothesis as decomposition in excess of inputs of carbon to the soil led to mean post-fire carbon losses of 4330 g C m^{-2} prior to carbon accumulation across the three scenarios, while mean losses in fire emissions were 1672 g C m^{-2} across the three scenarios. This result agrees with the observations by *Auclair and Carter* [1993] that post-fire carbon releases were approximately three times the carbon released in fire emissions. Together, the scenarios of the three sensitivity analyses that we conducted in this study indicate that post-fire carbon losses are more sensitive to soil moisture levels and the amount of soil organic matter after fire (including inputs from fire-induced plant mortality) than to differences in soil temperature among scenarios. Preliminary data on the relationship of soil respiration to fire severity for an experimental burn near Fairbanks, Alaska

[*Valentine and Boone*, unpublished data, 2001; see also *Burke et al.*, 1997] agree with the interpretation that the amount of soil organic matter plays a more important role in soil respiration responses after fire than does soil temperature. Thus, our simulations suggest that soil drainage and the effects of fire severity on the initial amount of soil organic matter after fire are more important than post-fire soil temperature dynamics in the magnitude of "post-fire emissions".

After fire, soil carbon declines in our simulations because decomposition is higher than NPP and accumulates once inputs to the soil from NPP become greater than decomposition during stand development. In our sensitivity analyses, NPP drops to very low levels immediately after the fire, increases to a peak between 60 and 100 years after fire, and then declines to stabilize at a lower level in comparison to the peak. The accumulation of vegetation carbon follows the pattern of NPP. The pattern of NPP dynamics with stand age in our simulations is consistent with the pattern identified in other studies [*Buchmann and Schulze*, 1999; *Schulze et al.*, 2000; see also *Bonan and Van Cleve*, 1992; *McMurtrie et al.*, 1995]. In all of our analyses, the pattern of NPP closely followed the pattern of net nitrogen mineralization. Our simulated patterns of net nitrogen mineralization are similar to the patterns documented by *Smith et al.* [2000] for black spruce forests, in which rates in the organic horizons ranged from 0.33 g N m⁻² in a recent burn to 1.71 g N m⁻² from June to October in a mature black spruce forest. Analysis of our simulations indicated that the decline of NPP in older stands is proximately associated with declines in GPP, i.e. declines in photosynthesis. The decline in GPP is tied to lower nitrogen availability as net nitrogen mineralization declines

because of lower organic matter quality with stand age, which is consistent with the nutrient availability hypothesis outlined in *McMurtrie et al.* [1995] and *Gower et al.* [1996]. The decline in NPP with stand age in our simulations is not consistent with the hypothesis that the decline is caused by increases in hydraulic resistance with stand age as the model does not explicitly consider hydraulic resistance. Also, the decline in NPP with stand age in our simulations is not consistent with the hypothesis that the decline is caused by increases in autotrophic respiration with stand age, as autotrophic respiration in our simulations declines in older stands as declines in GPP drive declines in vegetation carbon.

During the carbon accumulation phase of stand development, our sensitivity analyses indicated that carbon accumulation was affected by moss growth, soil moisture, and fire severity. While the effects of moss growth on soil temperature had little influence on the net rate of ecosystem carbon accumulation, moss growth affected the allocation of carbon storage. The lower soil temperature associated with the growth of moss caused lower decomposition and lower net nitrogen mineralization, which led to higher rates of soil carbon accumulation and lower rates of vegetation carbon accumulation, respectively. Soil moisture also affected allocation patterns of carbon storage in which higher soil moisture caused higher decomposition and higher net nitrogen mineralization, which led to lower rates of soil carbon accumulation and higher rates of vegetation carbon accumulation. It is important to recognize that this interpretation of the dynamics is limited to aerobic decomposition as we expect the opposite would occur when decomposition becomes more anaerobic. The results of the

soil moisture sensitivity analysis and the sensitivity of soil carbon storage patterns to transient vs. constant climate (Figure 13a and 13b) indicate that inter-annual and longer term variability in climate has the potential to interact with stand development to influence carbon storage [see also *Lynch and Wu*, 1999].

In our simulations, fire severity also affected carbon accumulation patterns as the higher loss of nitrogen in more severe fires caused lower levels of NPP that led to lower accumulation of vegetation carbon and soil carbon. Similar to our simulations, it has been observed that NPP in larch forests in China is lower in severely burned stands than in lightly burned stands [*Wang et al.*, in press]. Even though decomposition was lower for severely burned stands in our simulations, inputs to the soil from lower NPP were not able to replace higher levels of soil carbon lost in the fire. Furthermore, our sensitivity analysis for fire severity indicated that losses of carbon and nitrogen have the potential to influence carbon storage patterns during stand development more than changes in soil temperature and soil moisture. A number of studies have documented that fire can cause severe nitrogen losses from forests [*Dyrness et al.*, 1989; *Grogan et al.*, 2000; *Driscoll et al.*, 1999; *Smith et al.*, 2000; *Wan et al.*, in press; but see *Brais et al.*, 2000]. The simulations in which we added nitrogen to replace nitrogen losses that occurred in fire emissions indicated that carbon storage was very sensitive to inputs of nitrogen during stand development after fire. Recent syntheses of the carbon costs and benefits of nitrogen fixation indicate that nitrogen fixation rates should change substantially during stand development after disturbance [*Rastetter et al.*, 2001]. We conclude that nitrogen

fixation is an important process to represent in modeling decadal to century scale responses of carbon dynamics during stand development after fire disturbance.

4.3. Additional Issues and Future Directions

Many of our interpretations and conclusions concerning the temporal patterns of soil temperature, moss growth, soil moisture, and carbon dynamics from the application of the STM-TEM to the chronosequence in interior Alaska agree with the interpretations and conclusions from the empirical studies for the chronosequence [see *O'Neill, 2000; O'Neill et al., in review*]. The ability to conduct sensitivity analyses with the model allowed us to use the model as a tool to explore how the complexity of interactions among various factors influence carbon dynamics after fire disturbance in boreal forests. Taken together, the sensitivity analyses indicate that the growth of moss, changes in the depth of the organic layer, and nitrogen fixation should be represented in models that simulate the effects of fire disturbance in boreal forests.

Mosses are a major component of the global boreal forest [*Larsen, 1980; Oechel and Lawrence, 1985*], and both moss and the organic matter underlying moss play important roles in the function of boreal forests [*Richter et al., 2000; Oechel and Van Cleve, 1986; Weber and Van Cleve, 1984; Van Cleve et al., 1983a; Dyrness and Grigal, 1979; Chapin et al., 1987; Viereck et al., 1983; Goulden et al., 1998*]. In the application of the STM-TEM in this study, moss and organic matter were represented by their thermal and hydrologic properties and by their thickness. Emerging information indicates that the thermal conductivity of moss and organic matter increase with

increasing moisture in these layers [*Yoshikawa*, unpublished; *Romanovsky*, unpublished]. As the relationships of thermal conductivity to moisture are more clearly elucidated for moss and organic matter, it will be useful to incorporate those relationships into the model to examine how they influence soil thermal and ecosystem dynamics. Also, changes in moss thickness were represented in our simulations by a simple empirical relationship that may be appropriate only for interior Alaska, and we did not represent changes in the thickness of organic matter. The thermal and hydrologic properties of the moss layer change during stand development as early successional mosses do little to insulate the soil surface while later successional moss species have lower thermal conductivity and higher capacity to hold soil moisture [*Richter et al.*, 2000; see also *Foster*, 1985]. As the humic organic layer also has low thermal conductivity, changes in the thickness of this layer during stand development are important to represent. Thus, future model development should represent how successional dynamics of moss species and changes in the thickness of humic organic matter influence ecosystem processes during stand development after fire.

Besides its role in soil thermal and moisture dynamics, moss respiration accounts for an important portion of field measured soil respiration [*Schlentner and Van Cleve*, 1985; *Frolking et al.*, 1996; *Harden et al.*, 1997; *O'Neill*, 2000]. In comparison to mature stands, mosses may play a greater role in soil respiration of recently burned stands as respiration of early successional mosses can contribute between 20% and 50% of total soil respiration under optimal moisture and light conditions [*O'Neill*, 2000]. Similarly, the dynamics of roots during stand development play an important role in the

contribution of root respiration of black spruce forests [*Valentine and Boone*, unpublished data, 2001; *Ryan et al.*, 1997; *Vogel and Valentine*, unpublished data, 2001]. Also, the turn-over of organic matter in boreal forest soils of mature stands varies with depth [*Trumbore and Harden*, 1997; *Harden et al.*, 2000], and how the quality of soil organic matter changes during stand development of boreal forests after fire is not well understood. Nitrogen fixation is a process that has been documented to play an important role during stand development after disturbance in boreal forests [*Van Cleve et al.*, 1991; *Van Cleve et al.*, 1993; *Klingensmith and Van Cleve*, 1993a, 1993b, *Uliassi*, 1998; *Uliassi et al.*, 2000]. In our applications of the STM-TEM in this study, the biogeochemical function of moss and roots were implicitly considered when calibrating the STM-TEM for a mature black spruce site (see Table 4), and the quality of two fractions of organic matter are represented through the flux equations that influence the dynamics of a single aggregated organic matter compartment [see *McGuire et al.*, 1997]. As the performance of the model in simulating soil respiration was better for the control stands than for the recently burned stands, explicit consideration of moss and root biogeochemistry during stand development as well as the quality of soil organic carbon with depth may improve the simulation of soil respiration during stand development. While our simulations imported and exported nitrogen for initializing the equilibrium simulation [see *McGuire et al.*, 1997], we did not represent the successional dynamics of nitrogen fixation after fire disturbance in our simulations. Thus, future model development should include explicit representation of moss biogeochemistry, the dynamics of different organic matter fractions, and nitrogen fixation during succession.

Our sensitivity analyses with soil moisture and fire severity also revealed that soil drainage should be considered in spatial applications of the model. Soil drainage in boreal forests depends on the spatial and temporal dynamics of permafrost, and influences species composition [Rapalee *et al.*, 1998] and carbon storage [Trumbore and Harden, 1997; see also Lynch and Wu, 1999]. Soil drainage also likely influences aspects of the fire regime at fine spatial scales, such as fire frequency and fire severity [see Harden *et al.*, 2000]. The currently available maps of permafrost and soil drainage for Alaska and other regions are not adequate for accurately representing the role of soil drainage in simulating carbon dynamics at a landscape to regional scales. While substantial advances have been made in developing data sets for the timing and spatial extent of fire in Alaska [Murphy *et al.*, 2000] and Canada [Stocks *et al.*, unpublished], data sets on severity of fires are not yet available for broad regions of the boreal forest. Thus, the ability to apply our modeling framework to simulate carbon dynamics of boreal forests at landscape to regional scales would be enhanced by advances in the development of spatial data sets of soil drainage and fire severity.

Acknowledgments. The senior author thanks Larry Hinzman for insightful discussions about the hydrological aspects of research represented in this paper. We also thank Terry Chapin for valuable comments on previous drafts of this manuscript. This research was supported by the NASA Land Cover and Land Use Change Program (NAG5-6275), the USGS Geologic Division Global Change Research Program, the NSF Taiga Long Term Ecological Research Program (DEB-9810217), the NSF Arctic System Science and Arctic Natural Science Programs (OPP-9614253, OPP-9732126, OPP-9870635), and the Alaska Cooperative Fish and Wildlife Research Unit.

Appendix A: The Hydrological Model (HM)

State Variables and Fluxes Simulated by the HM

The HM considers the dynamics of eight state variables for water (see Figure 2b) including (1) rain intercepted by the canopy (R_I), (2) snow intercepted by the canopy (S_I), (3) snow layer on the ground (G_S), (4) moisture content of the moss plus fibric organic layer (M_{MO}), (5) rainfall detention storage (R_{DS}), (6) snow melt detention storage (S_{DS}), (7) moisture content of the humic organic layer (M_{HU}), and (8) moisture content of the mineral soil layer (M_{MI}). The HM simulates changes in these state variables at monthly temporal resolution from the fluxes of water identified in Figure 2b, which include (1) rainfall (R_F), (2) snowfall (S_F), (3) canopy transpiration ($T_C = T_{C1} + T_{C2}$), (4) canopy evaporation (E_C), (5) through fall of rain (R_{TH}), (6) canopy snow sublimation (S_S), (7) through fall of snow (S_{TH}), (8) ground snow sublimation (GS_S), (9) soil surface evaporation (E_M), (10) snow melt (S_M), (11) percolation from moss plus fibric organic layer to humic organic layer (P_1), (12) percolation from humic organic layer to mineral soil layer (P_2), (13) runoff from the moss plus fibric layer that is derived from rainfall (ROR_{MO}) to the rainfall detention storage pool, (14) runoff from the moss plus fibric layer that is derived from snow melt (ROS_{MO}) to the snow melt detention storage pool, (15) runoff to surface water networks from rainfall detention storage (ROR_{DS}), (16) runoff to surface water networks from snow melt detention storage (ROS_{DS}), and (17) drainage from mineral soil layer to ground water (D_R). The state equations for the HM are:

$$\frac{dR_I}{dt} = R_{Fi} - R_{THi} - E_{Ci} \quad (A1)$$

$$\frac{dS_t}{dt} = S_{Fi} - S_{THt} - S_{St} \quad (\text{A2})$$

$$\frac{dG_S}{dt} = S_{THt} - S_{Mt} - GS_{St} \quad (\text{A3})$$

$$\frac{dM_{\text{NR}}}{dt} = S_{\text{NR}} + R_{\text{THt}} - P_{1t} - E_{\text{NR}} - ROR_{\text{NRt}} - ROS_{\text{NRt}} \quad (\text{A4})$$

$$\frac{dR_{\text{DS}}}{dt} = ROR_{\text{NRt}} - ROR_{\text{DSt}} \quad (\text{A5})$$

$$\frac{dS_{\text{DS}}}{dt} = ROS_{\text{NRt}} - ROS_{\text{DSt}} \quad (\text{A6})$$

$$\frac{dM_{\text{HT}}}{dt} = P_{1t} - P_{2t} - T_{C1t} \quad (\text{A7})$$

$$\frac{dM_{\text{MT}}}{dt} = P_{2t} - T_{C2t} - D_{Rt} \quad (\text{A8})$$

where the subscript t refers to the time step of the calculation (month). Units for all state variables are in mm and for all flux variables are in mm month⁻¹.

Below we describe the details for the calculation of each flux simulated by the HM. See Table 3 for documentation of parameter values used in this study.

Rainfall and Snowfall

Monthly rainfall (R_F) and snowfall (S_F) are calculated from monthly precipitation and mean monthly temperature, which are input data sets used to drive the model.

Following the assumption on the temperature threshold for the split between rainfall and snowfall by *Willmott et al.* [1985], monthly rainfall is equal to monthly precipitation and monthly snowfall is 0 mm when mean monthly temperature is greater than -1° C.

Otherwise monthly snowfall is equal to precipitation and monthly rainfall is 0 mm.

Canopy transpiration

Canopy transpiration (T_C) is calculated similar to the formulation described by *Running and Coughlan* [1988]:

$$T_C = \frac{(RA_C \times \beta) \times (C_p \times \rho_a) \times V_D / \rho_a}{(\beta + \gamma \times (1.0 + R_C / R_A))} \times \frac{D_L \times M_D}{\lambda_w \times 1000} \quad (A9)$$

where T_C is monthly canopy transpiration ($\text{m}^3 \text{month}^{-1}$), β is the derivative of humidity deficit ($\text{mbar } ^\circ\text{C}^{-1}$) at ambient mean monthly air temperature (T). RA_C is mean monthly short wave radiation integrated through the canopy ($\text{MJ m}^{-2} \text{day}^{-1}$). C_p is specific heat of air ($\text{J Kg}^{-1} ^\circ\text{C}^{-1}$), ρ_a is density of air (kgm^{-3}), V_D is vapor pressure deficit (mbar), R_A is canopy aerodynamic resistance (s m^{-1}), R_C is canopy resistance to water vapor, γ is psychometric constant ($\text{mbar } ^\circ\text{C}^{-1}$), λ_w is latent heat of vaporization of water (J kg^{-1}), D_L is day length (s day^{-1}), and M_D is the number of days per month.

The mean radiation integrated through the canopy, RA_C , is calculated as:

$$RA_C = NIRR \times \frac{1.0 - e^{-(1.1 \times 2.2) \times E_R}}{E_R \times LAI / 2.2} \quad (A10)$$

where RA_C is in units of $\text{MJ m}^{-2} \text{day}^{-1}$, $NIRR$ ($\text{MJ m}^{-2} \text{day}^{-1}$) is mean daily short-wave radiation at the top of the canopy as calculated by TEM in the formulation for photosynthetically active radiation. LAI is leaf area index ($\text{m}^2 \text{m}^{-2}$) for the particular month as calculated by TEM (see equation 5), and E_R is a dimensionless extinction coefficient of radiation through the canopy.

The derivative of humidity deficit, β , is calculated as a function of mean monthly temperature (T) and V_D :

$$\beta = V_D \times \frac{4098 + 34.5 \times T}{(237.3 + T)^2} \quad (\text{A11})$$

We calculate mean monthly vapor pressure deficit, V_D , as a function of mean monthly air temperature ($^{\circ}\text{C}$):

$$V_D = 6.1078 \times e^{\frac{17.27 \cdot T}{237.3 - T}} \quad (\text{A12})$$

Canopy resistance to water vapor, R_C , is calculated as the inverse of canopy conductance, G (m s^{-1}):

$$G = G_{\text{MAX}} - DG_w \times (LWP - LWP_{\text{MIN}}) \quad (\text{A13})$$

where G_{MAX} is maximum canopy conductance (m s^{-1}), DG_w is the slope of G vs. LWP , LWP is the mean daily maximum leaf water potential across the month ($-\text{Mpa}$), and LWP_{MIN} is the minimum leaf water potential inducing stomatal closure, defined here as the spring minimum LWP ($-\text{Mpa}$). Mean daily maximum leaf water potential across the month is calculated as:

$$LWP = \frac{0.2}{\text{SOIL}_w / \text{SOIL}_{\text{cap}}} \quad (\text{A14})$$

where SOIL_w is mean monthly soil water content (m^3) integrated across the humic organic and mineral soil layers, and SOIL_{cap} is a parameter for soil water capacity (m^3) of the humic organic and mineral soil layers [see Table 3: also see *Running and Coughlan, 1988; Frohking et al., 1996*].

Canopy interception of rain, canopy evaporation, and through fall of rain

Monthly canopy interception of rain (R_I) is calculated based on monthly rainfall and a parameter for the canopy interception of rainfall per unit rainfall (I_{RMAX}), which is based on *Helvey* [1971, see also *Helvey and Patric, 1965*] (See Table 3). The potential interception of rain (PR_I) is calculated as:

$$PR_I = R_F \times I_{RMAX} \quad (A15)$$

where R_F is monthly rainfall (mm month^{-1}). If R_F is less than PR_I , all rain is intercepted, i.e., R_I is equal to R_F ; otherwise R_I is set up equal to PR_I . Monthly canopy evaporation (E_C) is calculated as equal to monthly canopy interception. Monthly through fall of rain (R_{TH}) is calculated as the difference between monthly rainfall and monthly canopy interception of rain.

Canopy interception of snow, through fall of snow, and canopy snow sublimation

Monthly canopy interception of snow (S_I) is calculated based on monthly snowfall and a parameter that defines the maximum daily interception of snow per unit leaf area (I_{SMAX} , $\text{mm LAI}^{-1}\text{day}^{-1}$; see Table 3), which is based on *Coughlan and Running* [1997]. The potential interception of snow (PS_I) is calculated as:

$$PS_I = M_D \times LAI \times I_{smax} / 2.0 \quad (A16)$$

where M_D is the number of days in the month and LAI is leaf area index ($\text{m}^2 \text{m}^{-2}$) for the particular month as calculated by TEM (see equation 5).

Monthly through fall of snow (S_{TH}) is calculated as the difference between monthly snowfall and monthly canopy interception of snow. Monthly canopy sublimation

of snow (S_S) is calculated based on monthly snow interception and potential sublimation of snow from the canopy (SUB_{CP}). If monthly snow interception is less than SUB_{CP} , then all of the snow is sublimated from the canopy. If monthly snow interception is greater than SUB_{CP} , then the snow sublimated from the canopy is set equal to SUB_{CP} . The calculation of SUB_{CP} in mm month^{-1} is based on a similar calculation in *Coughlan and Running* [1997]:

$$SUB_{CP} = \frac{R_{\lambda} \times 1000}{\lambda_w + K} \times M_D \quad (\text{A17})$$

where λ_w is latent heat of vaporization of water ($\text{MJ mm}^{-1} \text{M}^{-2}$) and K is latent heat fusion ($\text{MJ mm}^{-1} \text{M}^{-2}$).

Soil surface evaporation

The calculation of potential soil surface evaporation (PE_M , mm month^{-1}) of day time is based on the Penman equation [see *Monteith and Unsworth*, 1990; *Waring and Running*, 1998]:

$$PE_M = (E_{rate} + V_D \times 100 \times G_b / \Psi) \times M_D \quad (\text{A18})$$

where E_{rate} is the equilibrium evaporation rate (ms^{-1}) of an extensive, homogeneous wet surface, V_D is the air saturation deficit (mbar), G_b is the soil surface boundary layer conductance for water vapor (ms^{-1}) [*Grace*, 1981, see Table 3], and Ψ is a function that depends on density of air, the gas constant for water vapor, and air temperature.

The equilibrium evaporation rate, E_{rate} , is calculated based on [*McNaughton*, 1976]:

$$E_{\text{rate}} = \frac{\xi \times R_n}{\rho_a \times \lambda_w \times (\xi + 1.0)} \quad (\text{A19})$$

where ξ is the change of latent heat relative to the change of sensible heat of saturated air. R_n is net irradiation (Wm^{-2}) at the soil surface, ρ_a is the density of air, and λ_w is the latent heat of vaporization. The variable ξ is 1.26 at 10°C and is calculated to increase exponentially with mean monthly temperature based on *Dilly* [1968] and *Murray* [1967]:

$$\xi = 0.7185 \times e^{0.0544 \cdot T} \quad (\text{A20})$$

Net radiation at the soil surface, R_n , is calculated based on as [*Coughlan and Running* 1997]:

$$R_n = R_{AC} \times e^{-E_R \cdot L_{AI}/2.2} \quad (\text{A21})$$

where R_{AC} is the mean monthly short-wave radiation integrated through the canopy (see equation A10).

The variable ψ in equation A18 is based on *McNaughton* [1976]:

$$\psi = \rho_a \times (\xi + 1.0) \times G_v \times T \quad (\text{A22})$$

where ρ_a is the density of air (see Table 3), ξ is a the variable described in equation A19, G_v is the gas constant for water vapor ($0.462 \text{ m}^{-3} \text{ kPa kg}^{-1} \text{ K}^{-1}$), and T is mean monthly air temperature in degrees Kelvin.

Similar to *Thornton* [2000], the monthly actual soil evaporation (E_M , mm month^{-1}) is based on the estimated dry and wet days. If the through fall of rain (R_{TH}) is greater than or equal to the potential evaporation (PE_M) within a month, E_M is estimated as:

$$E_M = 0.6 \times PE_M \quad (\text{A23})$$

Otherwise, the E_M is estimated as the proportion of potential evaporation:

$$E_M = E_{VR} \times PE_M \quad (A24)$$

Where E_{VR} is a function of the number of days since rain, and is calculated as:

$$E_{VR} = \frac{0.3}{DSR^{2.0}} \quad (A25)$$

where DSR is days since rain, which is estimated as 10 in this study.

Snow melt and sublimation from ground snow layer

If there is snow on the ground and the surface temperature is above -1°C , maximum monthly snow melt (MS_M) driven by incident radiation on the snow surface (R_n , see calculation of R_n above) is calculated based on *Coughlan* [1991] as:

$$MS_M = M_D \times \alpha \times R_n / K \quad (A26)$$

where MS_M is in units mm month^{-1} , α is snow albedo (see Table 3), and K is the latent heat fusion (see Table 3). If the MS_M is less than the amount of snow on the ground, then snow melt (M_S) is equal to MS_M , otherwise M_S is equal to the amount of snow on the ground. If air temperature is less than -1°C , M_S is 0, and potential sublimation (PGS_S) from snow on the ground is calculated as:

$$PGS_S = M_D \times R_{SUB} / L_S \quad (A27)$$

where PGS_S is the potential sublimation of snow (mm month^{-1}); L_S is latent heat of sublimation (KJ kg^{-1} , see Table 3), and R_{SUB} is a radiation-based variable that drives sublimation. R_{SUB} is calculated as:

$$R_{SUB} = R_n \times S_A \quad (A28)$$

where parameter S_A is radiation absorptivity of snow (KJkg^{-1}). If the amount of snow on the ground is greater than PGS_S , then snow sublimation (GS_S) is equal to PGS_S , otherwise GS_S is equal to the amount of snow on the ground.

Available Water Capacity, Percolation, and Drainage

The available water capacity of each soil layer is an important parameter for calculating percolation and drainage. Available water capacity of each layer depends on field capacity and wilting point:

$$AWC_{MO} = FC_{MO} - WP_{MO} \quad (\text{A29})$$

$$AWC_{HU} = FC_{HU} - WP_{HU} \quad (\text{A30})$$

$$AWC_{MI} = FC_{MI} - WP_{MI} \quad (\text{A31})$$

where AWC_{MO} , AWC_{HU} , and AWC_{MI} are parameters for available water capacity (mm). FC_{MO} , FC_{HU} , and FC_{MI} are parameters for field capacity (mm), and WP_{MO} , WP_{HU} , and WP_{MI} are parameters for wilting point (mm) of the moss plus fibric, humic organic, and mineral soil layers, respectively.

FC_{MO} , FC_{HU} , FC_{MI} , WP_{MO} , WP_{HU} , and WP_{MI} are calculated as:

$$FC_{MO} = D_{moss} \times PFC_{MO} \times 10 \quad (\text{A32})$$

$$FC_{HU} = D_{HU} \times PFC_S \times 10 \quad (\text{A33})$$

$$FC_{MI} = D_{MI} \times PFC_S \times 10 \quad (\text{A34})$$

$$WP_{MO} = D_{moss} \times PWP_{MO} \times 10 \quad (\text{A35})$$

$$WP_{HU} = D_{HU} \times PWP_S \times 10 \quad (\text{A36})$$

$$WP_{Mf} = D_{Mf} \times PWP_S \times 10 \quad (A37)$$

where D_{moss} , D_{HU} , and D_{MI} are depths (m) of the moss plus fibric, humic organic, and mineral soil layers, respectively. PFC_{MO} and PWP_{MO} are field capacity (%) and wilting point (%) for moss plus fibric layer, and PFC_S and PWP_S are parameters for field capacity (%) and wilting point (%) for the soil. D_{moss} is either calculated dynamically (see equation 1) or prescribed, while D_{HU} and D_{MI} are prescribed. The parameters PFC_S and PWP_S are calculated based on soil texture as in version 4.0 and 4.1 of TEM [McGuire *et al.*, 1995, 1997; Tian *et al.*, 1999]:

$$PFC_S = (PF_A \times P_{S-C}) + PF_B \quad (A38)$$

$$PWP_S = (PW_A \times P_{S-C}) + PW_B \quad (A39)$$

where PF_A , PF_B , PW_A , and PW_B are parameters. P_{S-C} is the proportion of silt plus clay in the mineral soil calculated a function of soil texture calculated based on the percent of silt (PCT_{silt}) and percent of clay (PCT_{clay}) from input data sets of soil texture:

$$P_{S-C} = (PCT_{\text{silt}} + PCT_{\text{clay}}) \times 0.01 \quad (A40)$$

where parameters PCT_{silt} and PCT_{clay} are the percentages of silt and clay in the soil, respectively.

Percolation and drainage are calculated, in part, based on an empirical equation described by Neilson [1993, 1995; see also Haxeltine, 1996, Pan *et al.*, in review] that is expressed as:

$$P_L = p_C \times \left(\frac{AW_L}{AWC_L} \right)^4 \times M_D \quad (A41)$$

where P_L is the monthly percolation from the upper (L) to lower soil layer (L-1); P_C is the empirical percolation coefficient that depends on soil texture; AW_L is the available soil water in the upper soil layer (L), AWC_L is the available water holding capacity for the upper layer (L) that depends on the soil texture, and M_D is the number of days in the month. When soil temperature of a soil layer is lower than 0°C , there is no percolation into the layer from the layer above and there is no percolation to the layer below; otherwise there is percolation based on equation A41. While the above formulation is used to calculate percolation from the moss layer to the humic organic layer (P_1), the formulation is used to make an initial estimate of percolation from the humic organic layer to the mineral soil layer (IP_2), and the initial estimate of drainage from the mineral soil layer to ground water (ID_R). Percolation from the humic organic and mineral soil layers is calculated based on the initial estimates of percolation and excess percolation determined after available water is updated (see below).

Available water of the moss plus fibric layer (AW_{MO}) is updated monthly as:

$$AW_{MOt} = AW_{MOt-1} + S_M + R_{TH} - P_1 - E_M \quad (\text{A42})$$

If the available water content of the moss plus fibric layer exceeds available water capacity, then runoff from the moss plus fibric layer is (RO_{MO} , mm month^{-1}) is calculated as:

$$RO_{MO} = AW_{MO} - AWC_{MO} \quad \text{if } AW_{MO} > AWC_{MO} \quad (\text{A43})$$

RO_{MO} is partitioned to runoff derived from rainfall (ROR_{MO} , mm month^{-1}) and from snow melt (ROS_{MO} , mm month^{-1}) as:

$$ROR_{MO} = \frac{S_M \times RO_{MO}}{R_{CH}} \quad (A44)$$

$$ROS_{MO} = \frac{R_{TH} \times RO_{MO}}{R_{CH}} \quad (A45)$$

where R_{CH} is recharge (mm month^{-1}) is calculated as:

$$R_{CH} = S_M + R_{TH} \quad (A46)$$

If the humic organic layer is within the active layer, then available water of the humic organic layer (AW_{MO}) is updated monthly as:

$$AW_{HU_t} = AW_{HU_{t-1}} + P_1 - T_{c1} - IP_2 \quad (A47)$$

otherwise AW_{HU_t} is equal to $AW_{HU_{t-1}}$. If the available water content of the humic organic layer exceeds available water capacity, the excess water is forced to percolate to the mineral soil layer if the mineral soil layer is also within the active layer:

$$EP_{HU_t} = AW_{HU_t} - AWC_{HU_t} \quad \text{if } AW_{HU_t} > AWC_{HU_t} \quad (A48)$$

and percolation from the humic organic layer (P_2) is calculated as the sum of IP_2 and EP_{HU_t} .

If the mineral soil layer is within the active layer, then available water of the mineral soil layer (AW_{MI}) is updated monthly as:

$$AW_{MI_t} = AW_{MI_{t-1}} + P_2 - T_{c2} - ID_R \quad (A49)$$

otherwise AW_{MI_t} is equal to $AW_{MI_{t-1}}$. If the available water content of the mineral soil layer exceeds available water capacity, the excess water is forced to drain to ground water:

$$EP_{MI_t} = AW_{MI_t} - AWC_{MI_t} \quad \text{if } AW_{MI_t} > AWC_{MI_t} \quad (A50)$$

and drainage from the mineral soil layer (D_R) is calculated as the sum of ID_R and EP_{MI} .

Partitioning of transpiration between the humic organic and mineral soil layers

Canopy transpiration (T_C) is split into two components, T_{C1} and T_{C2} , based on the extraction rates of transpired water from the humic organic layer (β_1) and mineral soil (β_2) layer (i.e., $\beta_1 + \beta_2 = 1.0$), respectively:

$$T_{C1} = \beta_1 \times T_C \quad (A51)$$

$$T_{C2} = \beta_2 \times T_C \quad (A52)$$

The extraction rates represent fractions of available water distributed in the two soil layers and are calculated as:

$$\beta_1 = \frac{AW_{HU}}{AW_{HU} + AW_{MI}} \quad (A53)$$

$$\beta_2 = \frac{AW_{MI}}{AW_{HU} + AW_{MI}} \quad (A54)$$

where AW_{HU} and AW_{MI} describe available soil water in the humic organic and mineral soil layers, respectively. Active layer depth influences available soil water in the humic organic and mineral soil layers through the effects of equations A47 and A49.

Runoff

Similar to the water balance model of *Vorosmarty et al.* [1989], whenever field capacity of the moss plus fibric layer is attained, the excess water is transferred to

subsurface runoff pools for rainfall and snow melt derived runoff as described above in equations A43, A44, and A45. Runoff from the rainfall and snowmelt detention pools to surface water networks is also calculated similar to the water balance model of *Vorosmarty et al.* [1989]. Runoff from the rainfall detention storage pool (ROR_{DS} , mm month⁻¹) is calculated as:

$$ROR_{DS} = 0.5 \times (R_{DS} + C_p \times (R_{TH} + S_M - PET)) \text{ when } M_{MO} = FC_{MO} \cdot R_{TH} + S_M \geq PET \quad (A55)$$

$$ROR_{DS} = 0.5 \times R_{DS} \quad \text{when } M_{MO} < FC_{MO} \text{ or } R_{TH} + S_M < PET \quad (A56)$$

where R_{DS} is rainfall-derived retention in mm (see equation A5), C_p is the proportion of surplus water attributable to rain ($R_{TH}/[R_{TH}+S_M]$), M_{MO} is the moisture (mm) of moss plus fibric layer, and FC_{MO} is field capacity (mm) of moss plus fibric layer (see equation A32), and PET is potential evapotranspiration (mm month⁻¹).

PET is calculated based on the Jensen-Haise formulation [*Jensen and Haise*, 1963], which depends on air temperature and radiation:

$$PET = [0.04 \times ((\frac{9.0}{5.0} \times T) + 32.0) - 0.37] \times NIRR \times 0.016742 \times M_D \quad (A57)$$

where T is mean monthly air temperature (°C), $NIRR$ is short-wave radiation at the top of the canopy, and M_D is the number of days in the month. If PET is calculated to be less than 0.0, then PET is set up to equal to 0. Estimated actual evapotranspiration (EET , mm month⁻¹) is calculated based on the estimates of evaporation, sublimation, and transpiration as:

$$EET = S_s + GS_s + E_c + E_M + T_{C1} + T_{C2} \quad (A58)$$

Runoff from the snow melt detention storage pool (ROS_{DS} , mm month^{-1}) depends on elevation. For sites at elevations of 500 m or below, ROS_{DS} is equal to 10% of S_{DS} pool in the first month of snowmelt. In subsequent months, these sites will lose 50% of S_{DS} per month. At higher elevations, sites will lose 10% of S_{DS} in the first month, followed by 25% in the second month and 50% thereafter.

Volumetric soil moisture and water filled-pore space

Some of the formulations in TEM require the use of either percent volumetric soil moisture (VSM) or percent water-filled pore space (WFPS). Estimates of VSM for each of the soil layers are calculated from the state variables M_{MO} , M_{HU} , M_{MI} as:

$$VSM_{MO} = \frac{M_{MO}}{D_{MOSS}} \times 0.1 \quad (\text{A59})$$

$$VSM_{HU} = \frac{M_{HU}}{D_{HU}} \times 0.1 \quad (\text{A60})$$

$$VSM_{MI} = \frac{M_{MI}}{D_{MI}} \times 0.1 \quad (\text{A61})$$

where VSM_{MO} , VSM_{HU} , and VSM_{MI} are volumetric soil moisture (%) for three soil layers, respectively. In equations A59 - A61, the factor 0.1 is used to convert to percent as M_{MO} , M_{HU} , and M_{MI} are in mm and D_{MOSS} , D_{HU} , and D_{MI} are in m.

Estimates of WFPS for each of the soil layers are calculated from the state variables M_{MO} , M_{HU} , M_{MI} as:

$$WFPS_{MO} = \frac{M_{MO}}{POR_{MO}} \quad (\text{A62})$$

$$WFPS_{HU} = \frac{M_{HU}}{POR_{HU}} \quad (A63)$$

$$WFPS_{MI} = \frac{M_{MI}}{POR_{MI}} \quad (A64)$$

where $WFPS_{MO}$, $WFPS_{HU}$, and $WFPS_{MI}$ are percent of pore space, and POR_{MO} , POR_{HU} , and POR_{MI} are pore space (mm) for moss plus fibric organic, humic organic, and mineral soil layers, respectively.

POR_{MO} is estimated as:

$$POR_{MO} = D_{MOSS} \times MO_{PO} \times 10 \quad (A65)$$

where parameter MO_{PO} is the porosity of moss plus fibric layer (%).

POR_{HU} and POR_{MI} are calculated as:

$$POR_{HU} = D_{HU} \times PCT_{PO} \times 10 \quad (A66)$$

$$POR_{MI} = D_{MI} \times PCT_{PO} \times 10 \quad (A67)$$

where PCT_{PO} is a function of the proportion of silt plus clay (P_{S-C}).

PCT_{PO} is calculated as:

$$PCT_{PO} = PCT_{POA} \times P_{S-C} + PCT_{POB} \quad (A68)$$

where PCT_{POA} and PCT_{POB} are parameters.

Reference

- Aguado, E.. Radiation balances of melting snow covers at an open site in the central Sierra Nevada, California. *Water Resour. Res.* 21, 11, 1034-1049, 1985.
- Amthor, J. S., J. M. Chen, J. S. Clein, S. E. Frokling, R. F. Grant, J. S. Kimball, A. W. King, A. D. McGuire, N. T. Nikolov, C. S. Potter, and S. Wang, Comparing hourly, daily, monthly, and annual CO₂ and water vapor exchange of boreal forest predicted by nine ecosystem models: Model results and relationships to measured fluxes. *J. Geophys. Res.* In press.
- Atjay, G. L., P. Ketner, and P. Duvigenaud, Terrestrial primary production and phytomass, in the *Global Carbon Cycle*, edited by B. E. Bolin, T. Degens, S. Kempe, and P. Ketner, scope vol. 13, pp.129-181, John Wiley, New York, 1977.
- Auclair, A. N. D., and T. B. Carter, Forest wildfires as a recent source of CO₂ at northern latitudes. *Canadian Journal of Forest Research* 23:1528-1536.
- Barber, V. A., G. P. Juday, and B. P. Finney, Reduced growth of Alaska white spruce in the twentieth century from temperature-induced drought stress. *Nature* 405: 668-673, 2000.
- Beltrami, H., and J. C. Mareschal, Ground temperature changes in eastern Canada: borehole temperature evidence compared with proxy data. *Terra Nova*, 5, 21-28, 1994.
- Bonan, G. B., and K. Van Cleve, Soil temperature, nitrogen mineralization, and carbon source-sink relationships in boreal forests. *Can. J. For. Res.*, 22, 629-639, 1992.

- Brais, S., P. David, and R. Ouimet, Impacts of wild fire severity and salvage harvesting on the nutrient balance of jack pine and black spruce boreal stands. *Forest Ecology and Management*. 137, 231-243, 2000.
- Brown, R. J. E.. Influence of vegetation on permafrost, *Proceedings, permafrost International Conference*, pp. 20-5. Washington D. C.: NAS/NRC Publication 1287, 1963.
- Brown, R. J. E.. Some observations on the influence of climatic and terrain features on permafrost at Norman Wells, N.W.T. *Canadian Journal of Earth Sciences*, 2, 15-31, 1965.
- Brown, R. J. E.. Effects of fire on the permafrost ground thermal regime. Pages in R. W. Wein, and D. A. MacLean, editors. *The role of fire in northern circumpolar ecosystems*, John Wiley & Sons, Chichester, 1983.
- Buchmann, N., and E. Schulze. Net CO₂ and H₂O fluxes of terrestrial ecosystems. *Global Biogeochemical Cycles*, 13, 3, 751-760, 1999.
- Burke, R. A., R.G. Zepp, M. A. Tarr, W. L. Miller, and B. J. Stocks. Effect of fire on soil-atmosphere exchange of methane and carbon dioxide in Canadian boreal forest sites. *Journal of Geophysical Research* 102, 29289-29300, 1997.
- Chapin, III, F. S., W. C. Oechel, K. Van Cleve, and W. Lawrence. The role of mosses in the phosphorus cycling of an Alaskan black spruce forest. *Oecologia (Berlin)*, 74, 310-315, 1987.
- Chapin, III, F. S., and E. Mathews. Boreal carbon pools: approaches and constraints in global extrapolations In: *Carbon cycling in boreal forests and sub-arctic*

- ecosystems* (eds Vinson, T.S. Kolchugina, TP), pp. 9-20. U.S. Dept. Commerce. Natl Tech. Information Service, Washington DC. 1993.
- Clein, J. S., B. L. Kwiatkowski, A. D. McGuire, J. E. Hobbie, E. B. Rastetter, J. M. Melillo, and D. W. Kicklighter. Modeling carbon responses of tundra ecosystems to historical and projected climate: A comparison of a fine- and coarse-scale ecosystem model for identification of process-based uncertainties. *Global Change Biology*, 6 (Suppl. 1). 127-140. 2000.
- Clein, J. S., A. D. McGuire, X. Zhang, D. W. Kicklighter, J. M. Melillo, S. C. Wofsy, and P. G. Jarvis. The role of nitrogen dynamics in modeling historical and projected carbon balance of mature black spruce ecosystems across North America: Comparisons with CO₂ fluxes measured in the Boreal Ecosystem Atmosphere Study (BOREAS). *Plant and Soil*. *in press*.
- Coughlan, J. C., and S. W. Running. Regional ecosystem simulation: A general model for simulating snow accumulation and melt in mountainous terrain. *Landscape Ecology*, 12. 119-136. 1997.
- Coughlan, J. C., Biophysical aggregation of a forested landscape using a knowledge-based model. Ph.D. thesis. pp. 111. University of Montana. 1991.
- De Grandpre, L., L. Gagnon, and Y. Bergeron. Changes in the understorey of Canadian southern boreal forest after fire. *J. Veg. Sci.*, 4. 803-810. 1993.
- Dilley, A. C., On the computer calculation of vapor pressure and specific humidity gradients from psychrometric data. *J. Appl. Meteorol.*, 7. 717-719. 1968.

- Driscoll, K. G., J. M. Arocena, and H. B. Massicotte. Post-fire soil nitrogen content and vegetation composition in Sub-boreal spruce forests of British Columbia's central interior, Canada. *Forest Ecology and Management*, 121, 227-237, 1999.
- Dyrness, C. T., and D. F. Grigal. Vegetation-soil relationships along a spruce forest transect in interior Alaska. *Can. J. Bot.*, 57, 2644-2656, 1979.
- Dyrness, C. T., and R. A. Norum. The effects of experimental fires on black spruce forest floors in interior Alaska. *Can. J. For. Res.*, 13, 879-893, 1983.
- Dyrness, C. T., K. Van Cleve, and J. D. Levison. The effect of wildfire on soil chemistry in four forest types in interior Alaska. *Can. J. For. Res.*, 19, 1389-1396, 1989.
- Flannigan, M. D. F., and C. E. Van Wagner. Climate change and wildfire in Canada. *Canadian Journal of Forest Research*, 21:66-72, 1991.
- Foster, D. R., Vegetation development following fire in *Picea mariana* (black spruce)-Pleurozium forests of southeastern Labrador. *Canada. J. Ecol.* 73, 517-534, 1985.
- French et al., Controls on patterns of biomass burning in Alaskan boreal forests, in *Fire, Climate Change, and Carbon Cycling in the North American Boreal Forest*, Edited by E.S. Kasischke and B. J. Stocks, page 148-163, Ecological Studies Series, Springer-Verlag, 2000.
- Frolking, S., M. L. Goulden, S. C. Wofsy, S - M. Fan, D. J. Sutton, J. W. Munger, A. M. Bazzaz, B. C. Daube, P. M. Crill, J. D. Aber, L. E. Band, X. Wang, K. Savage, T. Moore, and R. C. Harriss. Modelling temporal variability in the carbon balance of a spruce/moss boreal forest. *Global Change Biology*, 2, 343-366, 1996.

- Goulden, M. L., B. C. Daube, Fan S-M, D. J. Sutton, A. Bazzaz, J. W. Munger, and S. C. Wofsy. Physiological responses of black spruce forest to weather, *J. Geophys. Res.*, 02, 28.987-28,996, 1997.
- Goulden, M. L., S. C. Wofsy, J. W. Harden, S. E. Trumbore, P. M. Crill, S. T. Gower, T. Fries, B. C. Daube, S.-M. Fan, D. J. Sutton, A. Bazzaz, and J. W. Munger. Sensitivity of boreal forest carbon balance to soil thaw. *Science*, 279, 210-217, 1998.
- Gorham, E.. Northern Peatlands, Role in the Carbon Cycle and Probable Responses to Climatic Warming. *Ecological Applications*, 1, 182-195, 1991.
- Gower, S. T., J. G. Vogel, J. M. Norman, C. J. Kucharik, S. J. Steele, and T. K. Stow. Carbon distribution and aboveground net primary production in aspen, jack pine, and black spruce stands in Saskatchewan and Minitoba, Canada. *J. Geophys. Res.*, 102, 29.029-29.041, 1997.
- Gower, S. T., McMurtrie, R. E., and D. Murty. Aboveground net primary productivity decline with stand age: Potential causes. *Tree*, 11, 378-382, 1996.
- Grace, J. C., Some effects of wind on plants. In " *Plants and their Atmospheric environment*". J. Grace, E. D. Ford, and P. G. Jarvis, eds., pp. 31-56. Blackwell, Oxford, 1981.
- Grogan, P., T. D. Bruns, and F. S. Chapin III. Fire effects on ecosystem nitrogen cycling in a California bishop pine forest. *Oecologia*, 122, 537-544, 2000.

- Harden, J. W., K. P. O'Neill, S. E. Trumbore, H. Veldhuis, and B. J. Stocks, Moss and soil contributions to the annual net carbon flux of a maturing boreal forest. *J. Geophys. Res.*, 102, 28805-28816, 1997.
- Harden, J. W., T. Fries, and T. Huntington, Mississippi Basin Carbon Project - Upland Soil Database for Northwestern Mississippi. *U.S. Geological Survey Open-file Report 98-440*, 1998.
- Harden, J. W., S. E. Trumbore, B. J. Stocks, A. Hirsch, S. T. Gower, K. P. O'Neill, and E. S. Kasichke. The role of fire in the boreal carbon budget. *Global Change Biology*, 6 (Suppl. 1), 174-184, 2000.
- Haxeltine, A., modeling the vegetation of the earth. Ph.D. thesis, Lund University, Sweden, 124p, 1996.
- Helvey, J. D., and J. H. Patric. Canopy and litter interception by hardwoods of eastern United States. *Water Resources Research* 1, 193-206, 1965.
- Helvey, J. D., A summary of rainfall interception by certain conifers of North America, in "*proceedings of the Third International Symposium for Hydrology Professors. Biological Effects in the Hydrological Cycle*" (E. J. Monke, ed.), pp. 103-113. Purdue University, West Lafayette, Indiana, 1971.
- Hess, J. C., C. A. Scott, G. L. Hufford, and M. D. Fleming. El Nino and its impact on fire weather conditions in Alaska, *International Journal of Wildland Fire*, 10, 1-13, 2001.

- Jarvis, P. G., The interpretation of the variations in leaf water potential and stomatal conductance found in canopies in the field, *Philosophical Transactions of the Royal Society of London, Series B* 273, 593-610. 1976.
- Jarvis, P.G., and J.B. Moncrieff. "The CO₂ Exchanges of Boreal Black Spruce Forest." In *Collected Data of The Boreal Ecosystem-Atmosphere Study*. Eds. J. Newcomer, D. Landis, S. Conrad, S. Curd, K. Huemmrich, D. Knapp, A. Morrell, J. Nickeson, A. Papagno, D. Rinker, R. Strub, T. Twine, F. Hall, and P. Sellers. CD-ROM. NASA, 2000.
- Jensen, M. E., and H. R. Haise, Estimating evapotranspiration from solar radiation. *J. of the Irrigation and Drainage Division*, 4, 15-41. 1963.
- Kasischke, E. S., N. L. Christensen, and B. J. Stocks, Fire, global warming, and the carbon balance of boreal forests, *Ecological Applications*, 5, 437-451, 1995.
- Kasischke, E. S., K. P. O'Neill, N. H. F. French, and L. L. Borgeau-Chavez, Controls on patterns of biomass burning in Alaskan boreal forests, in *Fire, Climate Change, and Carbon Cycling in the North American Boreal Forest*, edited by E.S. Kasischke and B.J. Stocks, pp.148-163. Ecological Studies Series, Springer-Verlag, 2000.
- Klingensmith, K. M., and K. Van Cleve, Denitrification and nitrogen fixation in floodplain successional soils along the Tanana River, interior Alaska, *Can. J. For. Res.*, 23 (5): 956-963. 1993a.

- Klingensmith, K. M., and K. Van Cleve. Patterns of nitrogen mineralization and nitrification in floodplain successional soils along the Tanana River, interior Alaska. *Can. J. For. Res.*, 23 (5): 964-969, 1993b.
- Kurz, W. A., and M. J. Apps. Retrospective assessment of carbon flows in Canadian boreal forests. *In Forest Ecosystems, Forest Management and the Global Carbon Cycle*. Eds. M J Apps and D T Price. Springer-Verlag, NATO Advanced Science Institute Series, 1995.
- Kurz, W. A., M. J. Apps, B. J. Stocks, and W. J. A. Volney. Global climate change: disturbance regions and tropospheric feedbacks of temperate and boreal forests. *In Biotic Feedbacks in the Global Climate System*. Eds. G. M. Woodwell, and F. T. Makenzie. Oxford University Press, New York, 1995.
- Kurz, W. A., and M. J. Apps. A 70-year retrospective analysis of carbon fluxes in the Canadian forest sector. *Ecological Applications*, 9, 56-547, 1999.
- Lachenbruch, A. H., and B. V. Marshall. Changing climate: Geothermal evidence from permafrost in the Alaskan Arctic. *Science* 234, 689-696, 1986.
- Landsberg, J. J., *Physiological Ecology of Forest Production*. Academic Press, 1986.
- Larsen, J. A., *The boreal ecosystem*. New York, Academic press 500 pp. 1980.
- Luc, L., and S. Luc. Vegetation changes caused by recent fires in the northern boreal forest of eastern Canada. *J. of vegetation Science*, 9, 483-492, 1998.
- Lynch, A. H., and W. Wu. Impacts of fire and warming on ecosystem uptake in the boreal forest. *J. of Climate*, 13, 2334-2338, 1999.

- Lynham, T. J., G. M. Wickware, and J. A. Mason. Soil Chemical changes and plant succession following experimental burning in immature jack pine. *Can. J. Soil Sci.*, 78, 93-104, 1998.
- McGuire, A. D., J. M. Melillo, D.W. Kicklighter, and L. A. Joyce. Equilibrium responses of soil carbon to climate change: Empirical and process-based estimates. *Journal of Biogeography* 22, 785-796, 1995b.
- McGuire, A. D., J. M. Melillo, D. W. Kicklighter, Y. Pan, X. Xiao, J. Helfrich, B. Moore III, C. J. Vorosmarty, and A. L. Schloss. Equilibrium responses of global net primary production and carbon storage to doubled atmospheric carbon dioxide: sensitivity to changes in vegetation nitrogen concentration. *Global Biogeochemical Cycles*, 11, 173-189, 1997.
- McGuire, A. D., S. Sitch, J. S. Clein, R. Dargaville, G. Esser, J. Foley, M. Heimann, F. Joos, J. Kaplan, D. W. Kicklighter, R. A. Meier, J. M. Melillo, B. Moore III, I. C. Prentice, N. Ramankutty, T. Reichenau, A. Schloss, H. Tian, L. J. Williams, and U. Wittenberg. Carbon balance of the terrestrial biosphere in the twentieth century: Analyses of CO₂, climate and land-use effects with four process-based ecosystem models. *Global Biogeochemical Cycles*, 15, 1, 183-206, 2001.
- McGuire, A. D., and J. E. Hobbie. Global climate change and the equilibrium responses of carbon storage in arctic and subarctic regions. *In Modeling the Arctic System: A Workshop Report on the State of Modeling in the Arctic System Science Program*. pp. 53-54. The Arctic Research Consortium of the United States, Fairbanks, Alaska, 1997.

- McGuire, A. D., R. A. Meier, Q. Zhuang, M. Macander, T. S. Rupp, E. Kasischke, D. Verbyla, D. W. Kicklighter, and J. M. Melillo. The role of fire disturbance, climate, and atmospheric CO₂ in the response of historical carbon dynamics in Alaska from 1950 to 1995: The importance of fire history. In preparation.
- McGuire, A. D., M. Apps, J. Beringer, J. Clein, H. Epstein, D.W. Kicklighter, C. Wirth, J. Bhatti, F.S. Chapin III, B. de Groot, D. Efremov, W.Eugster, M Fukuda, T. Gower, L. Hinzman, B. Huntley, G.J. Jia, E. Kasischke, J. Melillo, V. Romanovsky, A. Shvidenko, E. Vaganov, D. Walker. Environmental Variation, Vegetation Distribution, Carbon Dynamics, and Water/Energy Exchange in High Latitudes. *Journal of Vegetation Science*, in review.
- McGuire, A. D., J. M. Melillo, J. T. Randerson, W. J. Parton, M. Heimann, R. A. Meier, J. S. Clein, D. W. Kicklighter, and W. Sauf. Modeling the effects of snowpack on heterotrophic respiration across northern temperate and high latitude regions: Comparison with measurements of atmospheric carbon dioxide in high latitudes. *Biogeochemistry*, 48, 91-114, 2000a.
- McGuire, A. D., J. Clein, J. M. Melillo, D.W. Kicklighter, R. A. Meier, C. J. Vorosmarty, and M. C. Serreze. Modeling carbon responses of tundra ecosystems to historical and projected climate: The sensitivity of pan-arctic carbon storage to temporal and spatial variation in climate. *Global Change Biology*, 6.S141-S159, 2000b.
- McMurtrie, R. E. S. T. Gower, M. G. Ryan, and J. J. Landsberg. Forest productivity: explaining its decline with stand age, *Bull. Ecol. Soc. Am.* 76.152-154, 1995.

- McNaughton, K. G., Evaporation and advection I: evaporation from extensive homogeneous surfaces. *Quarterly Journal of the Royal Meteorology Society*, 102, 81-191, 1976.
- McNaughton, K. G., and P. G. Jarvis. Predicting effects of vegetation changes on transpiration and evaporation. In *"Water Deficit and Plant Growth"* (T. T. Kozlowski, ed.), Vol. 7, pp. 1-47. Academic press, London, 1983.
- Melillo, J. M., D. W. Kicklighter, A. D. McGuire, W. T. Peterjohn, and K. M. Newkirk. Global change and its effects on soil organic carbon stocks. In *Role of Nonliving Organic Matter in the Earth's Carbon Cycle*, ed. R.G. Zepp and C. Sonntag, pp. 175-189. John Wiley & Sons, New York, 1995.
- Monteith, J. L., *Principles of Environmental Physics*, Edward Arnold, 1973.
- Monteith, J. L., and M. H. Unsworth, *Principles of Environmental Physics*, 2nd edition, Arnold, London, 1990.
- Mosteller, F., R. E. K. Rourke, and G. B. Jr. Thomas, *Probability with Statistical Applications*, Reading, MA: Addison-Wesley Publishing Company, Inc., 1961.
- Murphy, P. J., B. J. Stocks, E. S. Kasischke, D. Barry, M. E. Alexander, N. H. F. French, J. P. Mudd, Historical fire records in the North American boreal forest. In: *Fire, Climate Change and Carbon Cycling in North American Boreal Forests* (eds Kasischke, ES Stocks, BJ), pp 274-288, Ecological Studies Series Springer-Verlag, New York, 1999.
- Murray, F. W., On the computation of saturation vapor pressure. *J. Appl. Meteorol.*, 6: 203-204, 1967.

- Neilson, R. P., Vegetation redistribution: A possible biosphere source of CO₂ during climate change. *Water Air Soil Poll.*, 70, 659-673, 1993.
- Neilson, R. P., A model for predicting continental scale vegetation distribution and water balance. *Ecol. Appl.*, 5, 362-386, 1995.
- Newcomer, J., D. Landis, S. Conrad, S. Curd, K. Huemmrich, D. Knapp, A. Morrell, J. Nickeson, A. Papagno, D. Rinker, R. Strub, T. Twine, F. Hall, and P. Sellers, eds. Collected Data of The Boreal Ecosystem-Atmosphere Study. NASA. CD-ROM. NASA, 2000.
- Oechel, W. C., and W. T. Lawrence. Taiga, in *Physiological Ecology of North America Plant Communities*, edited by B. F. Chabot and H. A. Mooney, pp. 66-94. Chapman and Hall, New York, 1985.
- Oechel, W. C., and G. L. Vourlitis. The effects of climate change on land-atmosphere feedbacks in arctic tundra regions. *Trends in Ecology and Evolution*, 9, 324-329, 1994.
- Oechel, W. C., and K. Van Cleve. The role of bryophytes in nutrient cycling in the taiga. In *Forest Ecosystems in the Alaskan Taiga*. Eds. K Van Cleve et al. pp 121-137. Springer-Verlag, New York, 1986.
- O'Neill, K. P., Changes in carbon dynamics following wildfire in soils of interior Alaska. Ph.D. Thesis, Duke University, Durham, 2000.
- O'Neill, K. P., E. S. Kasischke, and D. D. Richter. Seasonal and decadal patterns of soil carbon uptake and emission along an age-sequence of burned black spruce stands in interior Alaska. *J. Geophys. Res.*, in review.

- Osterkamp, T. E., and V. E. Romanovsky. Evidence for warming and thawing of discontinuous permafrost in Alaska. *Permafrost and Periglacial Processes*, 10(1), 17-37. 1999.
- Pan, Y., A. D. McGuire, J. M. Melillo, D.W. Kicklighter, S. Sitch, and I. C. Prentice. A biogeochemistry-based successional model and its application along a moisture gradient in the continental United States. in review
- Pickett, S. T. A., Space-for-time substitution as an alternative to long-term studies. In: *Long-Term Studies in Ecology: Approaches and Alternatives*, ed. G. E. Likens, pp. 110-135. New York: Springer-Verlag, 1989.
- Post, W. M., W. R. Emanuel, P. J. Zinke, and A. G. Stangenberger. Carbon pools and world life zones. *Nature*, 298, 156-159, 1982.
- Potter, C. S., J. S. Amthor, J. M. Chen, J. S. Clein, S. E. Frokling, R. F. Grant, J. S. Kimball, A. W. King, A. D. McGuire, N. T. Nikolov, and S. Wang. Comparison of ecosystem models for interannual carbon and water fluxes in boreal forest. *J. Geophys. Res.* In press.
- Randerson, J. T., M. V. Thompson, T. J. Conway, I. Y., Fung, and C. B. Field. The contribution of terrestrial sources and sinks to trends in the seasonal cycle of atmospheric carbon dioxide. *Global Biogeochemistry and Cycles*, 11, 535-560. 1997.
- Rapalee, G., S. E. Trumbore, E. A. Davidson, J. W. Harden, and H. Veldhuis. Estimating soil carbon stocks and fluxes in a boreal forest landscape. *Global Biogeochemical Cycles*, 12, 687-701. 1998.

- Rastetter, E. B., P. M. Vitousek, C. Field, G. R. Shaver, D. Herbert, and G. I. Agren.
Resource optimization and symbiotic nitrogen fixation. *Ecosystems*, 4, 369-388.
2001.
- Richter, D. D., K. P. O'Neill, and E. S. Kasischke. Stimulation of soil respiration in
burned black spruce (*picea mariana* L.) forest ecosystems: A hypothesis, in *Fir,
Climate Change, and Carbon Cycling in the North American Boreal Forest*,
edited by Kasischke, E. S. and B. J. Stocks, pp. 164-178, Springer-Verlag, new
York, 2000.
- Riseborough, D. W.. Modeling climatic influences on permafrost at a boreal forest site.
Unpublished M. A. thesis, Carleton University, Ottawa, 172pp, 1985.
- Rouse, W. R.. Microclimatic changes accompanying burning in sub-arctic lichen
woodland. *Arctic and Alpine Research*, 8, 4, 357-376, 1976.
- Running, S. W., and J. C. Coughlan. A general model of forest ecosystem processes for
regional applications. I. Hydrologic balance, canopy gas exchange and primary
production processes. *Ecological modelling*, 42, 125-154, 1988.
- Ryan, M. G.. A simple method for estimating gross carbon budgets for vegetation in
forest ecosystems. *Tree Physiology*, 9, 255-266, 1991.
- Ryan, M. G., D. Binkley, and J. H. Fownes. Age-related decline in forest productivity:
Pattern and process. *Advances in Ecological Research*, 7, 213-262, 1996.
- Ryan, M. G., M. B. Lavigne, and S. T. Gower. Annual carbon cost of autotrophic
respiration in boreal forest ecosystems in relation to species and climate. *J.
Geophys. Res.*, 102, No. D24, 28.871-28.883, 1997.

- Schimmel, J., and A. Granstrom. Fire severity and vegetation response in the boreal Swedish forest. *Ecology*, 77, 1436-1450, 1996.
- Schlentner, R. E., and K. Van Cleve. relationships between CO₂ evolution from soil, substrate temperature, and substrate moisture in four mature forest types in interior Alaska. *Can. J. For. Res.*, 15, 97-106, 1985.
- Schulze, E. D., C. Wirth, and M. Heimann. Managing forests after Kyoto. *Science*, 289, 2058-2059, 2000.
- Sellers, P. J., F. G. Hall, R. D. Kelly, A. Black, D. Baldocchi, J. Berry, M. Ryan, K. Jon Ranson, P. M. Crill, D. P. Lettenmaier, H. Margolis, J. Cihlar, J. Newcomer, D. Fitzjarrald, P. G. Jarvis, S. T. Gower, D. Halliwell, D. Williams, B. Goodison, D. E. Wickland, and F. E. Guertin. BOREAS in 1997: Experiment overview, scientific results, and future directions. *J. Geophys. Res.* 102 D24, 28731-28769, 1997.
- Serreze, M.C., J. E. Walsh, F. S. Chapin III, T. Osterkamp, M. Dyurgerov, V. Romanovsky, W. C. Oechel, J. Morison, T. Zhang, and R. G. Barry. Observational evidence of recent change in the northern high-latitude environment. *Clim. Change*, 46, 159-207, 2000.
- Smith, C. K., M. R. Coyea, and A. D. Munson. Soil carbon, nitrogen, and phosphorus stocks and dynamics under disturbed black spruce forests. *Ecological Applications*, 10(3), 775-788, 2000.
- Smith, M. W., Permaforst in the Mackenzie Delta, Northwest Territories. Geological Survey of Canada, Paper 75-28, 34pp, 1976.

- Stocks, B.J., M. A. Fosberg, M. B. Wotton, T. J. Lynham, and K. C. Ryan. Climate change and forest fire activity in North American boreal forests. in *Fire, Climate Change, and Carbon Cycling in the North American Boreal Forest*, edited by E.S. Kasischke and B.J. Stocks, pp. 312-319, Springer-Verlag, New York, 2000.
- Thie, J.. Distribution and thawing of permafrost in the southern part of the discontinuous permafrost zone in Manitoba. *Arctic* 27, p189-200, 1974.
- Thornton, P. E.. *Biome-BGC version 4.1.1*. Numerical Terradynamics Simulation Group (NTSG), School of Forestry, University of Montana Missoula, MT 59812, 2000.
- Tian, H., J. M. Melillo, D. W. Kicklighter, A. D. McGuire, and J. Helfrich. The sensitivity of terrestrial carbon storage to historical climate variability and atmospheric CO₂ in the United States. *Tellus*, 51B, 414-452, 1999.
- Trumbore, S. E., and J. W. Harden. Accumulation and turnover of carbon in organic and mineral soils of the BOREAS northern study area. *J. of Geoph. Res.*, 02, 28.816-8.830, 1997.
- Uliassi, D. D., K. Huss-Danell, R. W. Ruess, and K. Doran. Biomass allocation and nitrogenase activity in *Alnus tenuifolia*: Responses to successional soil type and phosphorus availability. *Ecoscience*, 7 (1), 73-79, 2000.
- Uliassi, D. D., The regulation of symbiotic nitrogen fixation by thinleaf alder in primary succesional forests of the Tanana River floodplian. M.Sc. Thesis. University of Alaska Fairbanks, Fairbanks, Alaska, 1998.

- Van Cleve K., L. Oliver, R. Schlentner, L. A. Viereck, and C. T. Dyrness. Productivity and nutrient cycling in taiga forest ecosystems, *Can. J. For. Res.* 13, 747-766, 1983a.
- Van Cleve, K., C. T. Dyrness, L. A. Viereck, J. Fox, F. S. Chapin III, and W. Oechel. Taiga ecosystems in interior Alaska. *Bioscience*, 33 (1): 39-44, 1983b.
- Van Cleve, K., F. S. Chapin III, C. T. Dyrness, and L. A. Viereck. Element cycling in taiga forests: state-factor control. *Bioscience*. 41 (2): 78-88, 1991.
- Van Cleve, K., J. Yarie, R. Erickson, and C. T. Dyrness. Nitrogen mineralization and nitrification in successional ecosystems on the Tanana River floodplain, interior Alaska. *Can. J. For. Res.*, 23 (5): 970-978, 1993.
- Van Cleve, K., L. A. Viereck, and C. T. Dyrness. State factor control of soil and forest succession along the Tanana river in interior Alaska, U.S.A.. *Arctic and Alpine Research*. 28, 3, 388-400, 1996.
- Viereck, L. A.. Wildfire in the taiga of Alaska. *Quaternary Research*. 3, 465-495, 1973.
- Viereck, L. A.. Ecological effects of river flooding and forest fires on permafrost in the taiga of Alaska. *permafrost: North America Contribution to 2nd International Conference*. 60-67, 1972.
- Viereck, L. A.. The effects of fire in black spruce ecosystems of Alaska and northern Canada. In: *The Role of Fire in Northern Circumpolar Ecosystems (Scope 18)* (eds Wein R. W., MacLean D. A.), pp. 132-145. John Wiley, Chichester, 1983.

- Viereck, L. A., C. T. Dyrness, K. Van Cleve, and M. J. Foote. Vegetation, soils, and forest productivity in selected forest types in interior Alaska. *Can. J. For. Res.*, 13, 703-720, 1983.
- Vorosmarty, C. J., B. J. Peterson, E. B. Rastetter, and P. A. Steudler. Continental scale models of water balance and fluvial transport: An application to south America. *Global Biogeochemical Cycles*, 3, 241-265, 1989.
- Wan, S., D. Hui, and Y. Luo. Fire effects on nitrogen pools and dynamics in terrestrial ecosystems: A meta-analysis. *Ecological Applications*, in press.
- Wang, C., S. T. Gower, Y. Wang, H. Zhao, P. Yan, and B. P. Bond-Lamberty. The influence of fire on carbon distribution and net primary production of boreal *Larix gmelinii* forests in north-eastern China. *Global Change Biology*, in press.
- Wang, C., B. P. Ben-Lamberty, and S. T. Gower. Soil surface CO₂ flux in boreal black spruce fire chronosequence. *Journal of Geophysical Research*, in review.
- Waring, R. H., and S. W. Running, *Forest ecosystems, analysis at multiple scales*, second edition. Academic Press, pp. 370, 1998.
- Wardle, D. A., O. Zackrisson, and M. -C. Nilsson, the charcoal effect in Boreal forests: mechanisms and ecological consequences. *Oecologia*, 115, 419-426, 1998.
- Weber, M. G., and K. Van Cleve. Nitrogen transformations in feather moss and forest floor layers of interior Alaska black spruce ecosystems. *Can. J. For. Res.*, 14, 278-290, 1984.
- Williams, P. J., and M. W. Smith, *The frozen Earth, fundamentals of geocryology*, Cambridge university press, pp306, 1989.

- Willmott, C. J., C. M. Rowe, and Y. Mintz. Climatology of the terrestrial seasonal water cycle. *J. Clim.*, 5, 589-606. 1985.
- Wirth, C., E-D. Schulze, W. Schulze, V. D. Stünzner-Karbe, W. Ziegler, I. M. Miljukowa, A. Sogatchev, A. B. Varlagin, M. Panvyorov, S. Grigorev, W. Kusnetzova, M. Siry, G. Hardes, R. Zimmermann, and N. N. Vygodskaya. Above-ground biomass and structure of pristine Siberian Scots pine forests as controlled by competition and fire. *Oecologia*, 121: 66-80. 1999.
- Wirth, C., E-D. Schulze, B. Lühker, S. Grigoriev, M. Siry, G. Hardes, W. Ziegler, M. Backor, G. Bauer, and N. N. Vygodskaya. Fire and site type effects on the long-term carbon and nitrogen balance in pristine Siberian Scots pine forests. *Plant Soil*. In press.
- Wotton, B. M., and M. D. Flannigan. Length of the fire season in a changing climate. *Forest Chronicle*, 69:187-192. 1993.
- Yarie, J., and S. Billings. Carbon balance of the taiga forest within Alaska. *Ecosystems*. in press.
- Yoshikawa, K., Bolton, W. R., Romanovsky, V. E., Fukuda, M., and L. D. Hinzman. Impacts of wildfire on the permafrost in the boreal forests of interior Alaska. *Journal of Geophysical Research - Atmospheres*. in press.
- Zackrisson, O., Influence of forest fires on the North Swedish boreal forest. *Oikos*, 29, 22-32. 1977.

- Zhuang, Q., V. E. Romanovsky, and A. D. McGuire, Incorporation of a permafrost model into a large-scale ecosystem model: Evaluation of temporal and spatial scaling issues in simulating soil thermal dynamics, *J. Geophys. Res.*, *in press*.
- Zimov, S. A., S. P. Davidov, G. M. Zimova, A. I. Davidova, F. S. Chapin III, M. C. Chapin, and J. F. Reynolds. Contribution of disturbance to increasing seasonal amplitude of atmospheric CO₂, *Science*, 284, 1973-1976, 1999.
- Zoltai, S. C., Cyclic development of permafrost in the peatlands of northwestern Alberta, Canada, *Arctic Alpine Research*, 25, 240-246, 1993.

Table 3.1. Location, Site Characteristics, and History of Burning for Stands of the Fire Chronosequence in Interior Alaska¹.

Year of most recent burn	Stand age (1997 as base year)	Year of previous burn	Location	Soil series	Moss thickness (cm) in 1997 (Feathermoss, fiber, or dead moss)	Percentage of ground covered by bryophytes	Depth of organic soil layer
1996	1	1825 (Approx.)	Tetlin Jct.	Not classified	5.9±1.6	No Measurement	19.8± 2.0
1994 (Severe)	3	1855 (Approx.)	Hajdukovich	Volkmar silt loam	2.1±2.9	65.1±6.7	8.7± 4.2
1994 (Moderate)	3	1855 (Approx.)	Hajdukovich	Volkmar silt loam	2.2±1.9	65.1±6.7	5.7± 3.5
1990	7	1915	Tok Jct.	Not classified	5.8±2.3	27.0±6.3	10.6± 3.0
1987	10	1825 (Approx.)	Delta Jct.	Nenana silt loam	3.7 ±3.2	39.4±5.7	4.7± 2.1
1915	80	Unknown	Tok Jct.	Not classified	14.9±6.6	66.8±9.0	22.3± 4.1
1855	140	Unknown	Gerstle River	Saulich silt loam	23.1	72.5±7.6	33.5

¹Reported values represent the mean ± standard deviation of 20 measurements per plot.

Table 3.2. Comparison of Monthly Climate among Tok Junction from 1954 to 1999, Big Delta from 1937 to 1999, and Tok Junction in 1997. Reported Values Represent the Mean +/- Standard Deviation. Data from National Weather Service, Alaska Region (<http://www.wrcc.dri.edu/summary/climsmak.html>)

	Jan.	Feb.	Mar.	Apr.	May	Jun.
Precipitation (mm)						
Tok Jct.	20.6±1.8	18.8±21.3	10.4±12.2	10.4±12.2	35.6±36.1	129.5±63.5
Big Delta	21.8±19.8	21.3±26.4	17.5±16.8	16.3±23.9	57.4±44.5	151.6±75.4
1997 (Tok Jct.)	44.5	2.5	16.8	6.40	23.90	114.8
Snow fall (mm)						
Tok Jct.	113.5±86.6	89.9±99.6	54.4±57.7	49.0±66.5	16.8±54.6	0.00±0.00
Big Delta	141.7±118.1	132.8±139.1	110.0±107.2	71.4±89.7	16.5±47.0	0.00±0.00
1997 (Tok Jct.)	210.8	111.8	96.5	83.8	0.0	0.0
Air Temperature (°C)						

Tok Jct.	-27.04±6.09	-20.71±5.01	-12.49±3.98	-1.31±2.48	7.07±1.71	12.68±1.51
Elig Delta	-20.04±6.01	-16.27±5.29	-10.74±4.33	-0.82±2.82	8.3±1.87	13.90±1.43
1997 (Tok Jct.)	-29.62	-14.03	-15.60	-0.76	8.07	13.97

=====

=====

Jul.	Aug.	Sept.	Oct.	Nov.	Dec.	Annual
------	------	-------	------	------	------	--------

Precipitation (mm)

Tok Jct.	127.0±69.1	80.0±65.5	42.7±36.1	36.1±37.3	32.3±35.6	20.6±23.1	594.9±191.0
Big Delta	170.9±85.1	126.5±53.6	70.4±38.1	41.9±26.4	31.5±31.0	24.6±25.9	752.1±176.8
1997 (Tok Jct.)	275.6	87.1	39.9	18.8	25.1	34.3	689.6

Snow fall (cm)

Tok Jct.	0.00±0.00	7.4±26.4	34.8±69.9	181.9±158.0	162.1±126.7	116.8±124.2	933.2±309.4
----------	-----------	----------	-----------	-------------	-------------	-------------	-------------

Big Delta	0.00±0.00	0.00±0.00	41.7±69.1	235±147.1	215.6±186.2	148.1±131.1	1129.0±484.1
1997 (Tok Jct)	0.00	0.00	0.00	243.8	149.9	165.1	1061.7

Air Temperature (°C)

Tok Jct.	14.46±1.69	11.90±1.68	5.29±1.59	-5.77±2.49	-18.41±4.14	-25.21±5.19	-4.66±1.43
Big Delta	15.58±1.06	12.89±1.57	6.72±1.68	-3.88±2.98	-14.06±4.49	-19.11±5.64	-2.32±1.34
1997 (Tok Jct.)	17.21	11.92	6.44	-10.58	-13.21	-21.27	-3.96

=====

Table 3.3. Values and Sources of Parameters for the Hydrologic Model Used in This Study

Parameter	Definition	Value	Source and comments
C_p	Specific heat of air, $J\ Kg^{-1}\ ^\circ C^{-1}$	1010.0	See <i>Running and Coughlan</i> [1988]
ρ_A	Density of air, kgm^{-3}	1.292	See <i>Monteith</i> [1973]
R_A	Canopy aerodynamic resistance, sm^{-1}	5	See <i>Landsberg</i> [1986] and <i>Jarvis</i> [1976]
G_{MAX}	Maximum canopy conductance, ms^{-1}	0.0016	See <i>Running and Coughlan</i> [1988]
γ	Psychometric constant, $mbar\ ^\circ C^{-1}$	0.662	See <i>Monteith</i> [1990]
λ_w	Latent heat of vaporization of water, Jkg^{-1}	2.442	The value for $25^\circ C$, see <i>Monteith</i> [1990]
E_R	Dimensionless extinction coefficient of radiation through the canopy	0.5	Values range from 0.3 to 1.5, see <i>Landsberg</i> [1986]
LWP_{MIN}	Minimum leaf water potential inducing stomatal closure, Mpa	0.5	See <i>Running and Coughlan</i> [1988]
I_{RMAX}	The maximum daily canopy interception	0.26	Based on <i>Helvey</i> [1971] and <i>Helvey and Patric</i>

	of rain, mm mm^{-1}	
K	Latent heat fusion, $\text{MJ mm}^{-1} \text{M}^{-2}$	3.5×10^5
I_{SMAX}	Snow interception rate, $\text{mm LAI}^{-1} \text{day}^{-1}$	0.5
G_h	The soil surface boundary layer Conductance, mm s^{-1}	10
G_v	The gas constant for water vapor, $\text{m}^{-3} \text{kPa kg}^{-1} \text{K}^{-1}$	0.462
α	snow albedo, KJ kg^{-1}	0.80
L_S	Latent heat of sublimation, KJ kg^{-1}	2845.0
S_A	Radiation absorptivity of snow, KJ kg^{-1}	0.6
PFC_{MO}	Field capacity of moss plus fibric (%)	51.6
PWP_{MO}	Field wilting point of moss plus fibric layer (%)	32.1
PF_A	Coefficient A for relationship describing dependence of field capacity on mineral soil texture	24.75
PF_B	Coefficient B for relationship describing dependence of field capacity on mineral soil texture	16.025

[1965]

See *Coughlan* [1991]

See *Coughlan and Running* [1997]

Assumed as same as the value of 0.05 m tall

vegetation See *Grace* [1981]

See *Monteith* [1973]

See *Aguado* [1985] and *Running and Coughlan*

[1988]

See *Coughlan* [1991]

See *Coughlan* [1991]

Estimated

Estimated

See *McGuire et al.* [1995, 1997] and *Tian et al.*

[1999]

See *McGuire et al.* [1995, 1997] and *Tian et al.*

[1999]

PW_A	Coefficient A for relationship describing dependence of wilting point on mineral soil texture	24.75	See <i>McGuire et al.</i> [1995, 1997] and <i>Tian et al.</i> [1999]
PW_B	Coefficient B of relationship describing dependence of wilting point on mineral soil texture	3.025	See <i>McGuire et al.</i> [1995, 1997] and <i>Tian et al.</i> [1999]
PCT_{silt}	Percentage of silt in mineral soil (%)	30.0	See <i>McGuire et al.</i> [1995, 1997] and <i>Tian et al.</i> [1999]
PCT_{clay}	Percentage of clay in mineral soil (%)	45.0	See <i>McGuire et al.</i> [1995, 1997] and <i>Tian et al.</i> [1999]
$SOIL_{CAP}$	Soil water capacity (m^3)	2350.0	See <i>Running and Coughlan</i> [1988]
P_C	Percolation coefficients for three layers	5.0 (Moss plus fibric) 4.5 (Humic organic layer) 4.0 (Mineral soil layer)	See <i>Neilson et al.</i> [1993, 1995] and <i>Haxeltine</i> [1996]
MO_{PO}	Porosity of moss plus fibric layer (%)	80.0	Estimated
PCT_{POA}	Coefficient A of relationship describing dependence of porosity on mineral soil texture	28.0	See <i>McGuire et al.</i> [1995, 1997] and <i>Tian et al.</i> [1999]
PCT_{POB}	Coefficient B of relationship describing	33.0	See <i>McGuire et al.</i> [1995, 1997] and <i>Tian et al.</i>

dependence of porosity on mineral soil texture

[1999]

DSR

Days since rain

10

Estimated

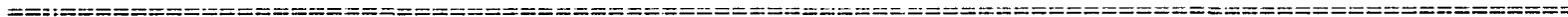


Table 3.4. Values and Sources for Estimated Pools and Fluxes Used to Parameterize the Model for a Black Spruce Forest at Bonanza Creek, Alaska.

Variable	Value ¹	Source and Comments
C_V	3250	Based on Table 2 by <i>Van Cleve et al.</i> [1983b], <i>Oechel and Van Cleve</i> [1986], and <i>Gower et al.</i> [1997] and <i>Ryan et al.</i> [1997]
N_V	15	Based on Table 2 by <i>Van Cleve et al.</i> [1983b]
C_S	15000	Based on <i>O'Neill</i> [2000] and <i>O'Neill et al.</i> [in review]
N_S	505	Based on Tables 10 and 13 in <i>Van Cleve et al.</i> [1983b]
N_{AV}	0.5	Based on <i>Weber and Van Cleve</i> [1984]
GPP	811.9	Based on procedures described in <i>Clein et al.</i> [in press]
NPP	152	Based on Table 3 by <i>Van Cleve et al.</i> [1983b]
NPPSAT	228	Assume a maximum NPP increase of 50% to nitrogen fertilization
NUPTAKE	1.8	Based on <i>Oechel and Van Cleve</i> [1986] and their application of recycling estimates from Tables 3 and 7 by <i>Van Cleve et al.</i> [1983b]

¹Units for annual gross primary production (GPP), net primary production (NPP), and NPPSAT are $\text{g C m}^{-2} \text{yr}^{-1}$. Units for annual N uptake by vegetation are $\text{g N m}^{-2} \text{yr}^{-1}$. Units for vegetation carbon (C_V) and soil carbon (C_S) are g C m^{-2} . Units for vegetation nitrogen (N_V), soil N (N_S), and inorganic N (N_{AV}) are g N m^{-2} .

Table 3.5. Comparison Between Simulated and Field-based Growing Season (May - September) Estimates in 1997 for Soil Temperature at 10 cm, Soil Temperature at 20 cm, Soil Respiration, and Soil Carbon for Stands of the Fire Chronosequence in Interior Alaska. Values for Field-based Estimates Represent Monthly Means \pm Standard Deviation among Sampling Sites [See *O'Neill, 2000; O'Neill et al.*, in review] and Values for Simulated Estimates Represent Monthly Means.

Year of most burn	^a Soil Temperature(°C) at 10 cm		^b Soil Temperature (°C) at 20 cm		^c Soil Respiration (g C m ⁻² month ⁻¹)		^d Soil Carbon (g C m ⁻² yr ⁻¹)	
	Field	Model	Field	Model	Field	Model	Field	Model
	1996	6.81 \pm 2.30	5.55	2.30 \pm 1.86	4.33	59.9 \pm 36.1	48.1	No Measurement
1994	11.30 \pm 2.37	11.80	9.68 \pm 2.53	10.50	80.0 \pm 40.6	77.7	8920.0 \pm 3468.9	9580.2
1990	9.97 \pm 2.95	9.15	9.01 \pm 2.45	8.05	92.3 \pm 54.8	84.9	7789.0 \pm 3635.5	9160.3
1987	9.49 \pm 2.64	9.13	7.36 \pm 2.40	8.38	94.5 \pm 44.6	85.2	8228.0 \pm 3413.2	8288.4
1915	5.57 \pm 2.68	7.20	3.07 \pm 1.77	5.00	108.4 \pm 50.7	99.9	11401.0 \pm 2014.2	11950.6
1855	9.52 \pm 3.18	5.90	3.97 \pm 2.53	3.60	173.4 \pm 75.1	160.4	15772.0 \pm 2710.5	11637.9

^{a, b} Soil temperature at 10 cm and 20 cm are relative to the surface of the soil.

^c Soil respiration includes below-ground autotrophic respiration and decomposition.

^d Field-based estimates represent the sum of carbon in the moss plus fibric and the humic organic layers. Standard deviation of field-based soil carbon estimates were based on the variance of differences equation in *Mosteller et al.* [1961]: $\sigma^2_{X-Y} = \sigma^2_X + \sigma^2_Y$

Figure. 3.1. Flow diagram for the research design in this study.

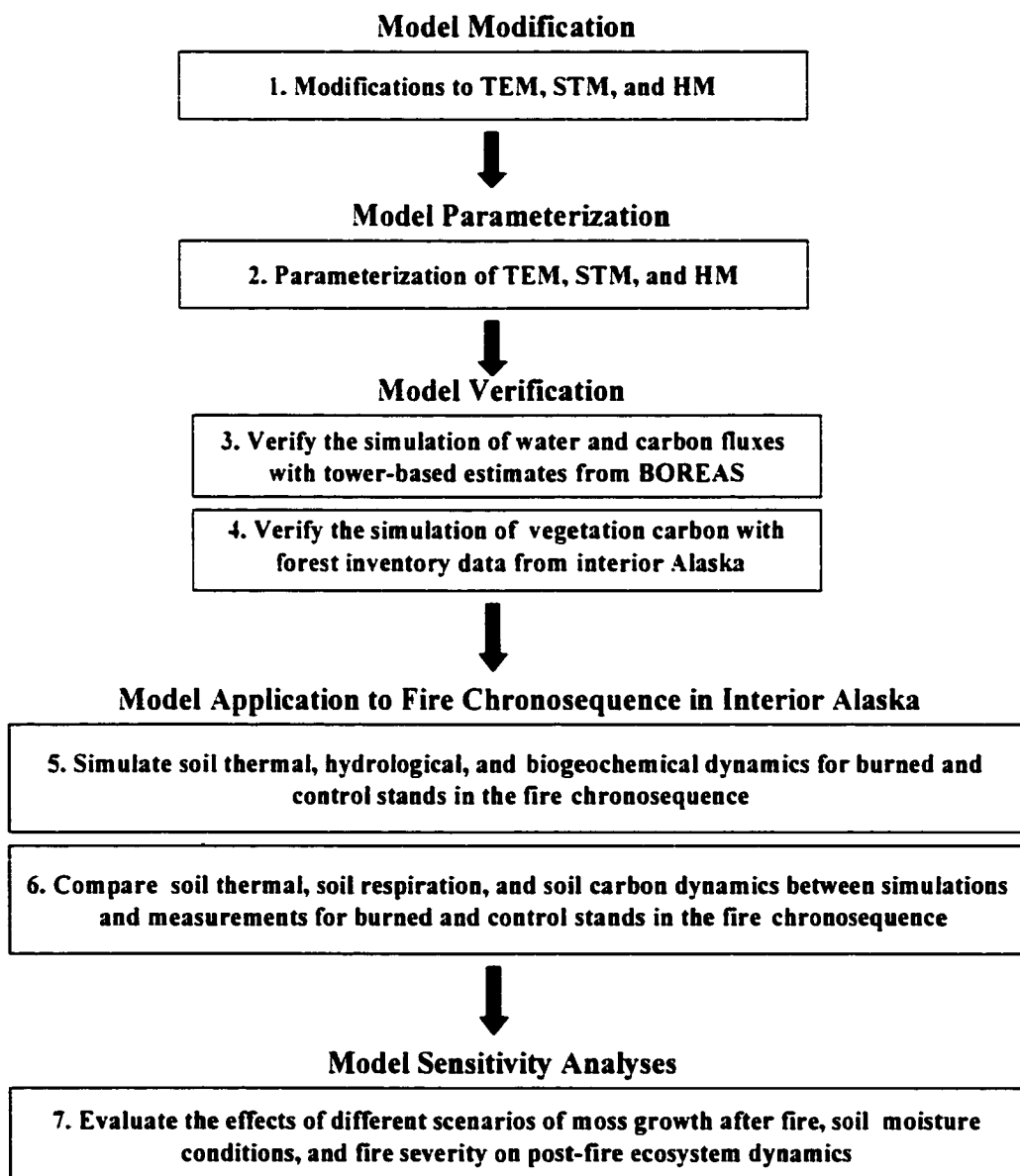


Figure. 3.2. (a) Overview of the model used in this study, which required coupling a hydrological model (HM) with a soil thermal model (STM) and a terrestrial ecosystem model (TEM). The HM receives information on active layer depth from the STM and information on leaf area index from TEM. The STM receives information on moss thickness from TEM and information on soil moisture and snow pack from the HM. The TEM receives information on soil temperature from STM and information on soil moisture and evapotranspiration from HM. (b) The HM considers the dynamics of eight state variables for water including (1) rain intercepted by the canopy (R_i), (2) snow intercepted by the canopy (S_i), (3) snow layer on the ground (G_s), (4) moisture content of the moss plus fibric organic layer (M_{MO}), (5) rainfall detention storage (R_{DS}), (6) snowfall detention storage (S_{DS}), (7) moisture content of the humic organic layer (M_{HU}), and (8) moisture content of the mineral soil layer (M_{MI}). The HM simulates changes in these state variables at monthly temporal resolution from the fluxes of water identified in Figure 2b, which include (1) Rainfall (R_F), (2) Snowfall (S_F), (3) canopy transpiration ($T_C = T_{C1} + T_{C2}$), (4) canopy evaporation (E_C), (5) through fall of rain (R_{TH}), (6) canopy snow sublimation (S_S), (7) through fall of snow (S_{TH}), (8) ground snow sublimation (GS_S), (9) soil surface evaporation (E_M), (10) snow melt (S_M), (11) percolation from moss plus fibric organic layer to humic organic layer (P_1), (12) percolation from humic organic layer to mineral soil layer (P_2), (13) runoff from the moss plus fibric layer to the rainfall detention storage pool (ROR_{MO}), (14) runoff from the moss plus fibric layer to the snow melt detention storage pool (ROS_{MO}), (15) runoff from the rainfall detention storage pool to surface water networks (ROR_{DS}), (16) runoff from the snow melt detention storage pool to surface water networks (ROS_{DS}), and (17) drainage from mineral soil layer to ground water (D_R).

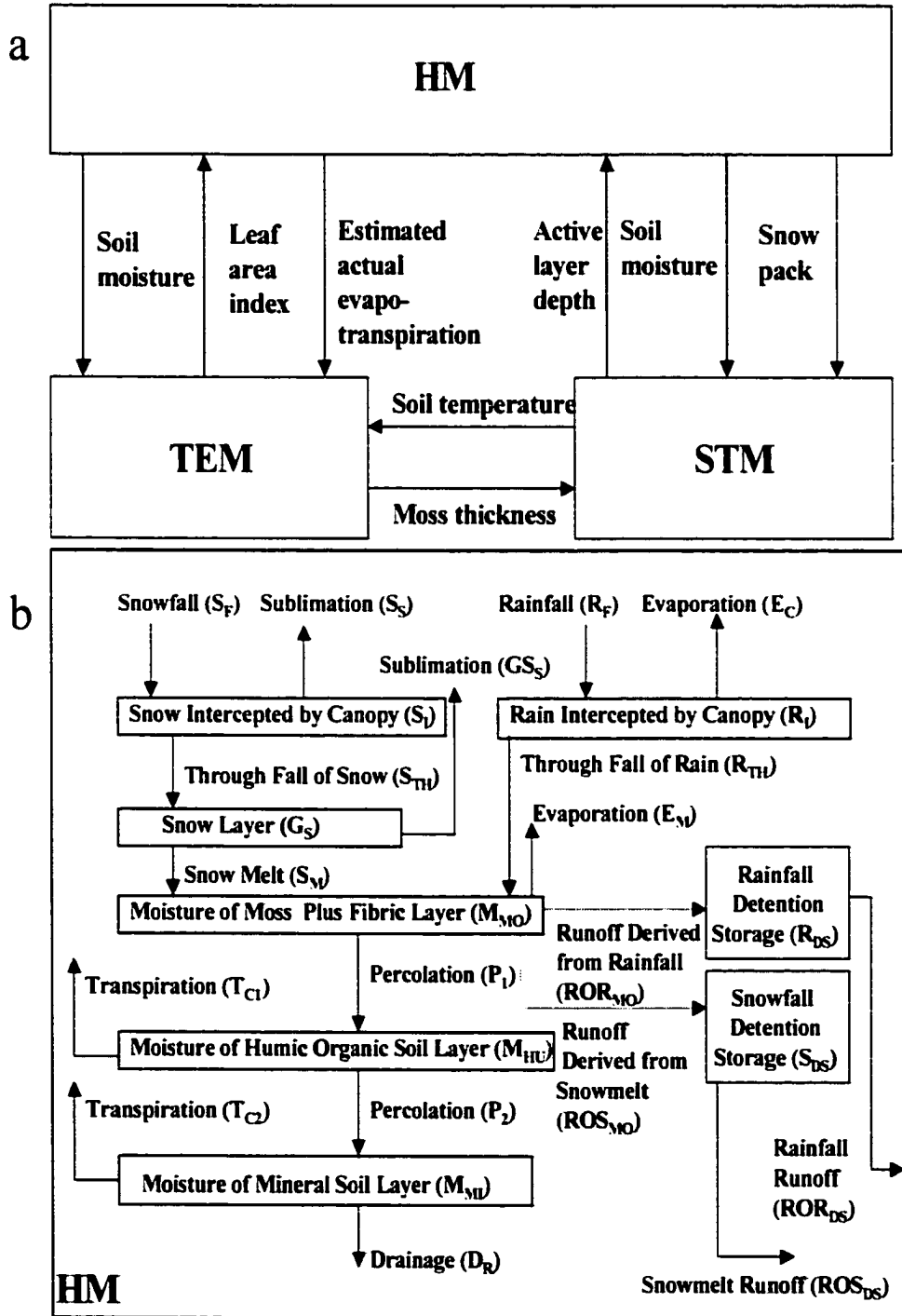


Figure. 3.3. Dependence of the scalar function $f(\text{FOLIAGE})$ in the GPP formulation of TEM on vegetation carbon (C_V) simulated by TEM. (a) $f(\text{FOLIAGE})$ ranges from 0 to 1 following a logistic function of an independent variable defined as the square root of $f(C_V)$, which (b) is represented as a hyperbolic function of C_V . See text for parameterization of these functions.

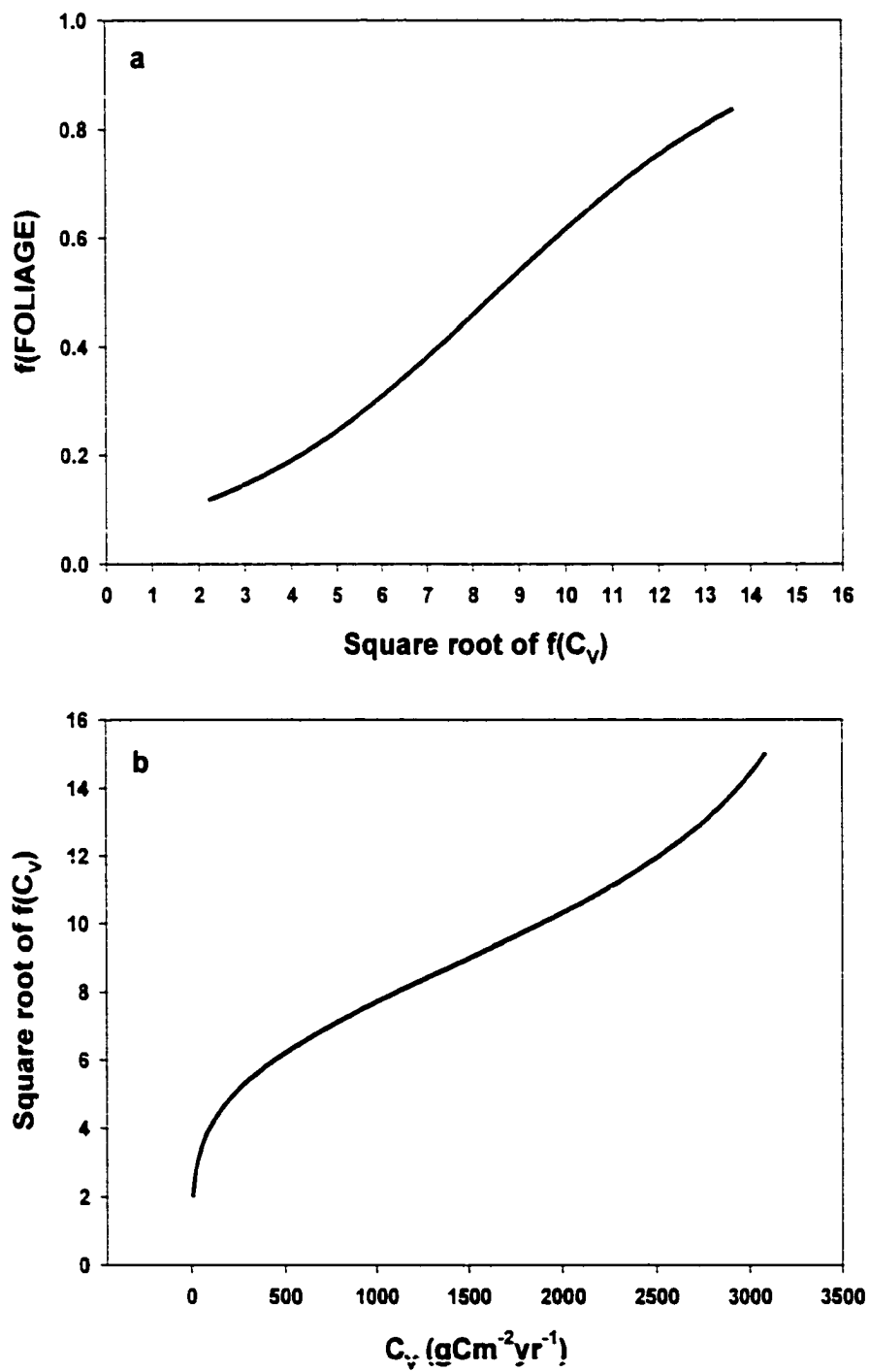


Figure 3.4. Comparison of monthly carbon fluxes between simulated and field-based estimates for an old black spruce forest in the northern study area of the boreal ecosystem atmosphere study (BOREAS). Linear regression between simulated and field-based estimates are compared with the 1:1 line. (a) Monthly estimates of gross primary production from 1994 to 1997; the linear regression was significant ($P < 0.001$, $N = 42$) with $R = 0.97$, slope = 0.98, and intercept = $8.3 \text{ g C m}^{-2} \text{ month}^{-1}$. (b) Monthly estimates of ecosystem respiration from 1994 to 1997; the linear regression was significant ($P < 0.001$, $N = 42$) with $R = 0.98$, slope = 0.96, and intercept = $9.9 \text{ g C m}^{-2} \text{ month}^{-1}$. Monthly field-based estimates were derived from eddy covariance data [Goulden *et al.*, 1998, as updated by Dunn *et al.* (personal communication, http://www-eosdis.ornl.gov/BOREAS/boreas_home_page.html); see also Clein *et al.*, in press].

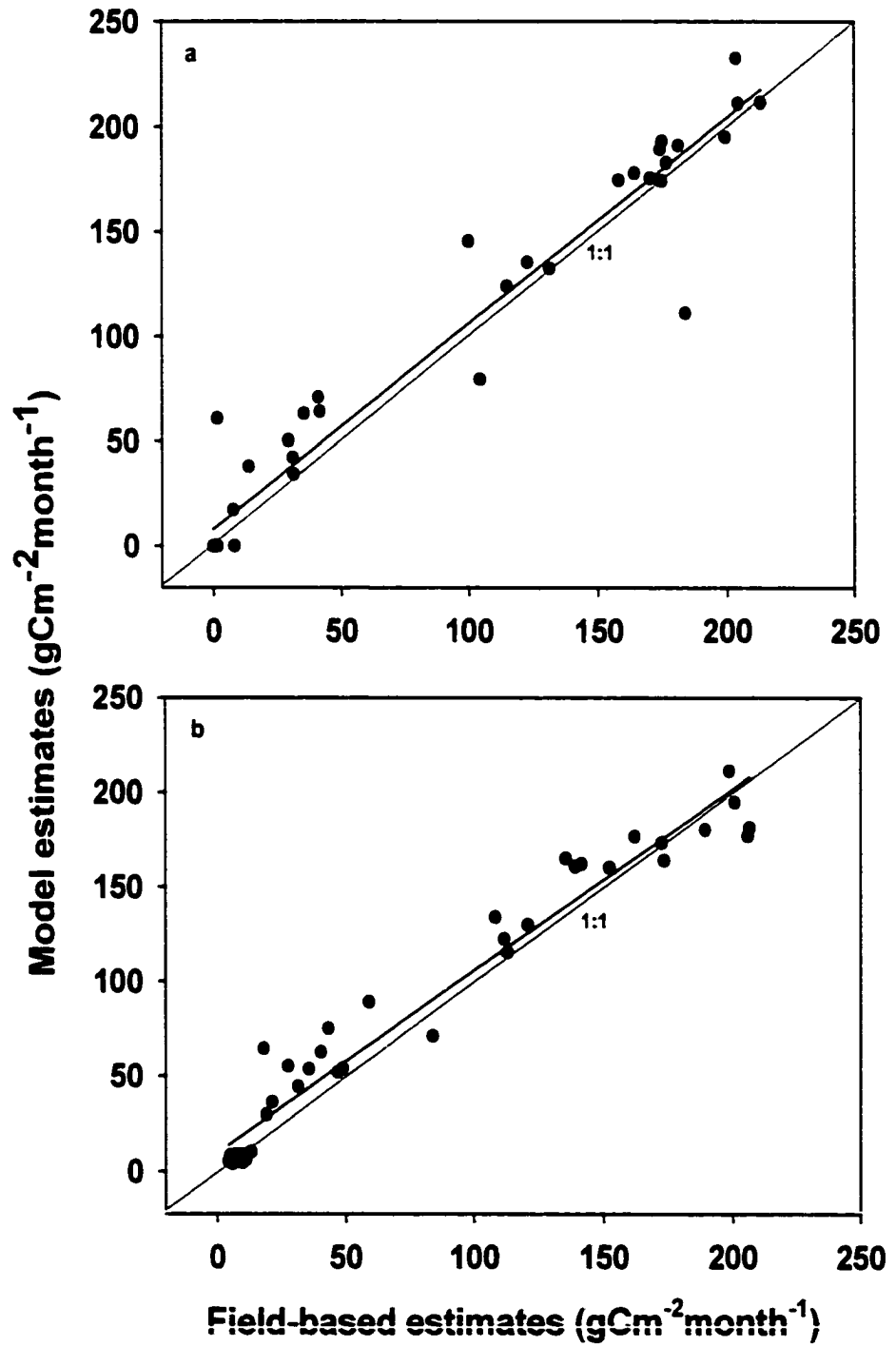


Figure. 3.5. Comparison of monthly evapotranspiration and monthly volumetric soil moisture between simulated and field-based estimates for two old black spruce forests of the boreal ecosystem atmosphere study (BOREAS), one in the northern study area (NSA-OBS) and one in the southern study area (SSA-OBS). (a) and (b) Monthly estimates of evapotranspiration for NSA-OBS and SSA-OBS, respectively. (c) and (d) Monthly estimates of volumetric soil moisture of the humic organic soil layer for NSA-OBS and SSA-OBS, respectively. (e) and (f) Monthly estimates of volumetric soil moisture of the mineral soil layer for NSA-OBS and SSA-OBS, respectively. For comparison to simulations for NSA-OBS and SSA-OBS, we aggregated the tower-based estimates of evapotranspiration at half-hour resolution to monthly resolution. The half-hour resolution estimates of evapotranspiration were developed from eddy covariance measurements at the NSA-OBS site [Goulden *et al.*, 1997, 1998, as updated by Dunn *et al.* (personal communication)] and the SSA-OBS site [Jarvis *et al.*, 2000; Newcomer *et al.*, 2000]. Similarly, we aggregated daily or hourly measurements of volumetric soil moisture for the humic organic and mineral soil layers to monthly resolution for both the NSA-OBS and the SSA-OBS BOREAS sites. The humic organic soil moisture was estimated as the mean of all soil moisture measurements shallower than 45 cm, while the mineral soil moisture was estimated as the mean of all soil moisture measurements deeper than 45 cm and shallower than 105 cm.

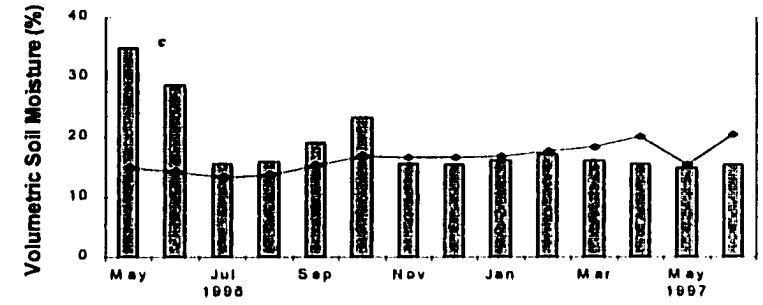
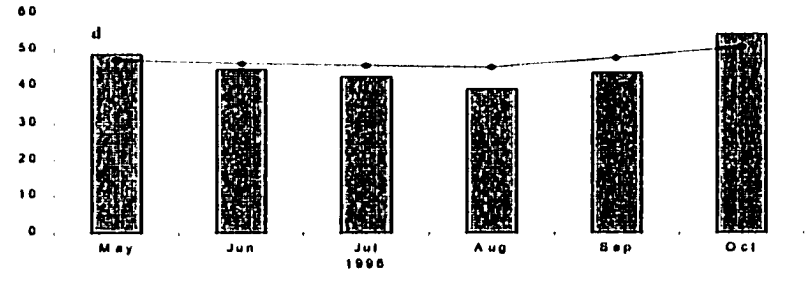
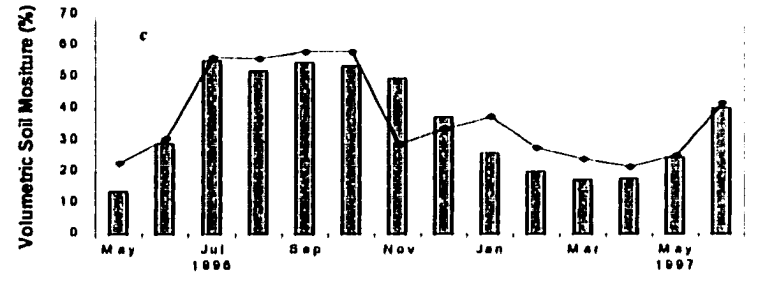
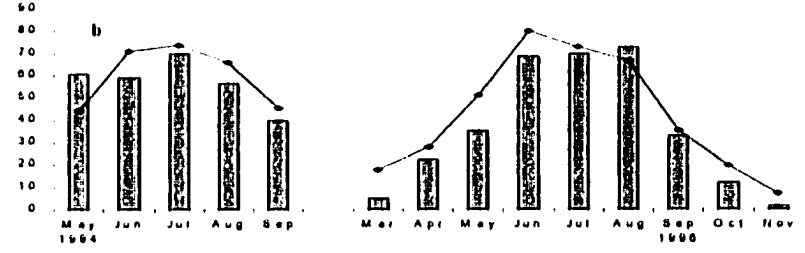
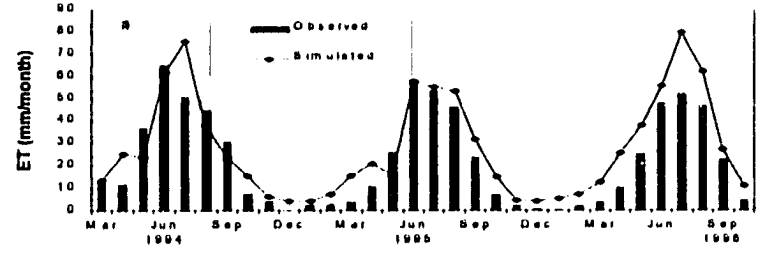


Figure. 3.6. Comparison of simulated above-ground vegetation carbon with forest inventory estimates for black spruce forests in interior Alaska. The forest inventory estimates were derived from estimates of above-ground biomass in metric tons per hectare by *Yarie and Billings* [in press] for 10-year age intervals until age 100 and for 20-year age intervals between age 100 and 200. Linear regression between simulated and inventory-based estimates are compared with the 1:1 line in the inset.

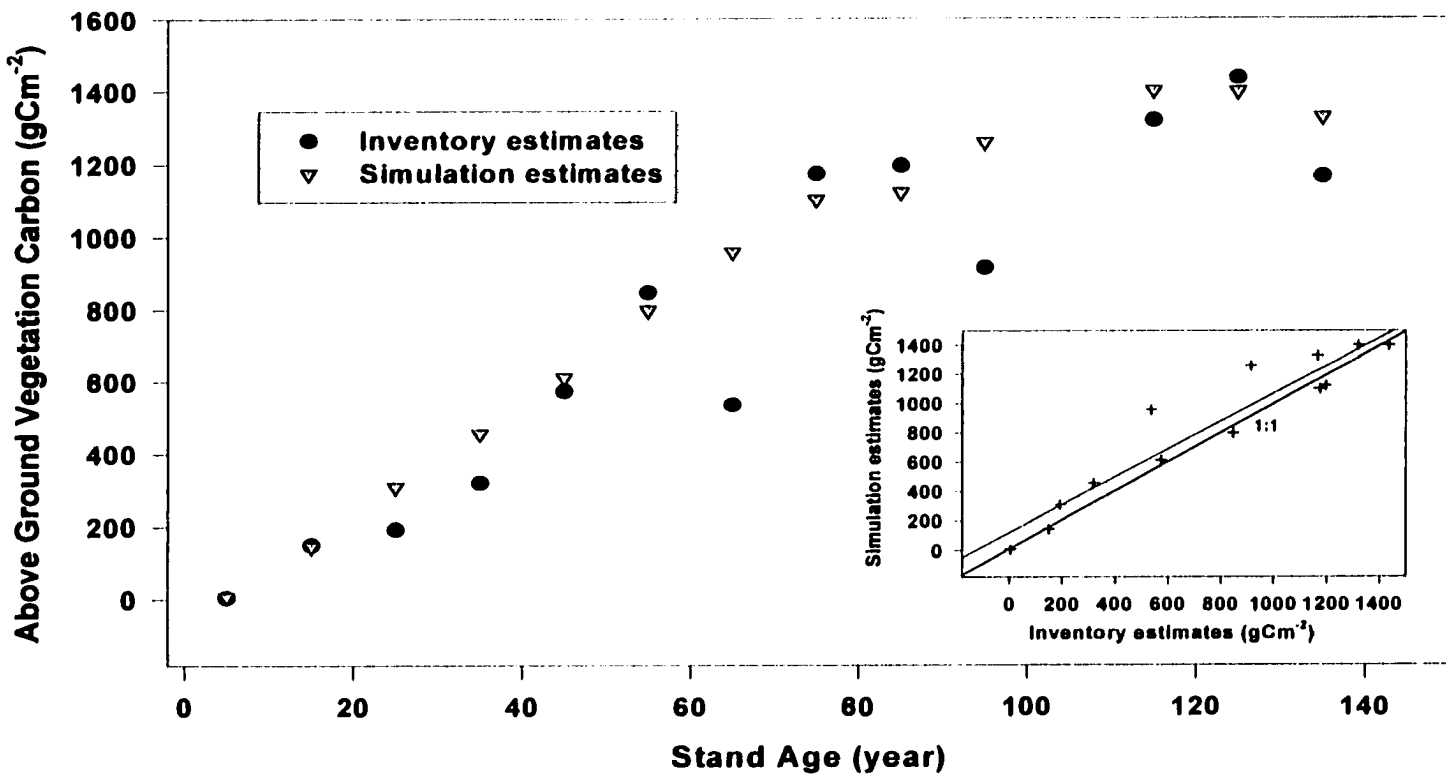
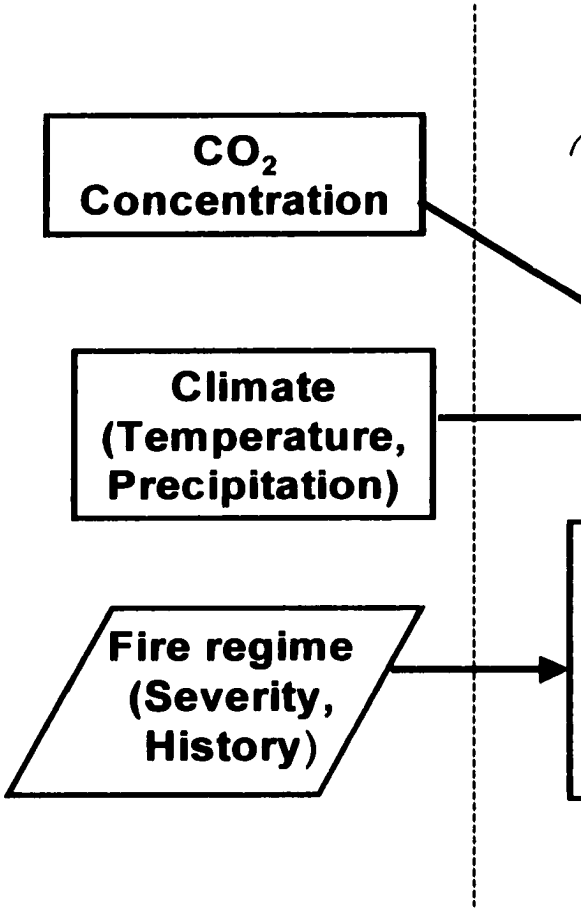


Figure. 3.7. Overview of the simulation of net carbon exchange (NCE) between boreal forest ecosystems and the atmosphere by the Terrestrial Ecosystem Model (TEM) to investigate the effects of fire disturbance on carbon dynamics in boreal forest ecosystems. At any point in time, $NCE = NPP - R_H - \text{fire emissions}$, where NPP is net primary production and R_H is heterotrophic respiration (decomposition). Fire timing and severity affect ecosystem carbon pools to influence fire emissions and post-fire NPP and R_H . Driving data sets of CO_2 concentration and climate also influence NPP and R_H .



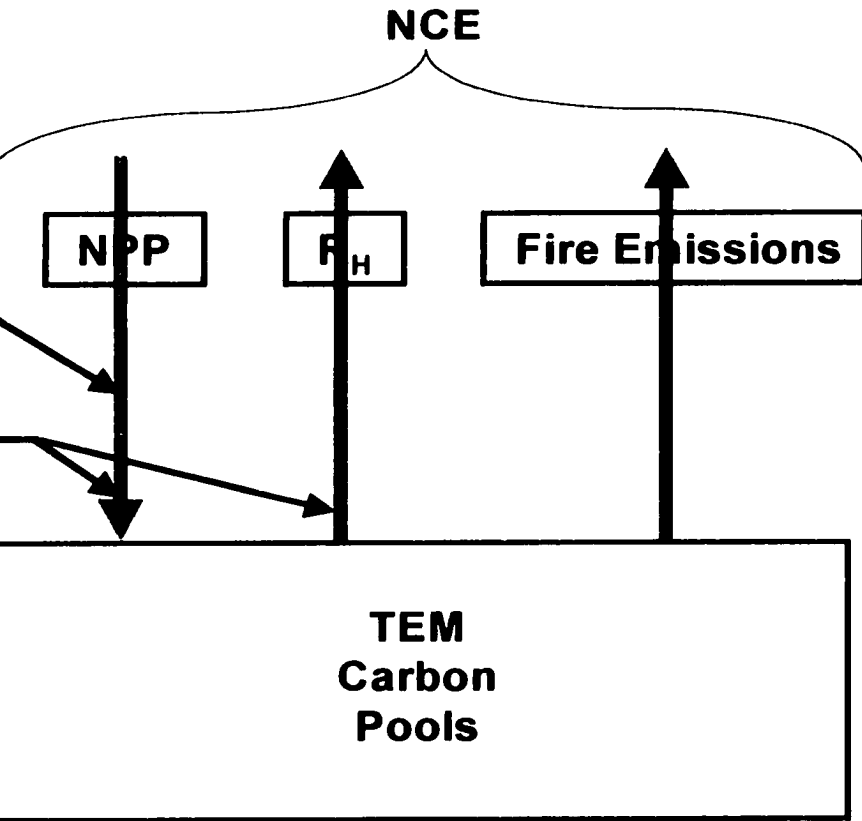


Figure. 3.8. Flow diagram for the derivation of carbon and nitrogen pools in simulating ecosystem dynamics of the control and recently burned stands of the fire chronosequence in interior Alaska. All simulations start from equilibrium conditions in 1819. The control stands for the stands that recently burned in 1996 and 1987 are estimated to have last burned in approximately 1825. The control stands for the stands that recently burned in 1994 and 1990 are estimated to have burned in 1855 and 1915, respectively. Simulated estimates of soil temperature, soil respiration, and soil carbon in 1997 are compared to estimates based on field measurements made in 1997.

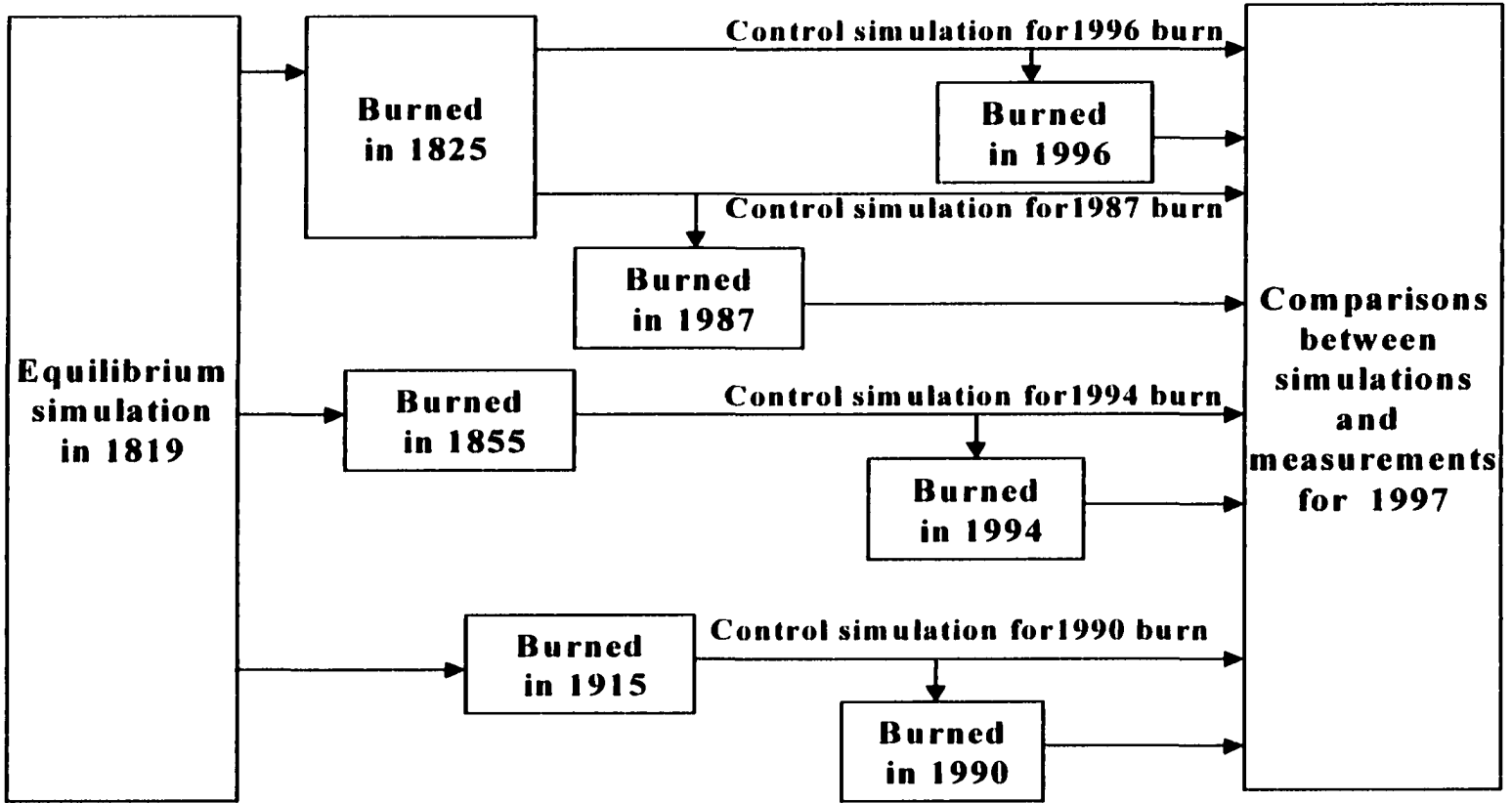


Figure. 3.9. Comparison of monthly soil temperature estimates at 10 cm depth during the growing season in 1997 between simulated and field-based estimates during the growing season for control and burned stands of the fire chronosequence in interior Alaska. Comparison of simulated and field-based estimates for control sites corresponding to recently burned sites in (a) 1996, (c) 1994, (e) 1990, and (g) 1987. Comparison of simulated and field-based estimates for recently burned sites in (b) 1996, (d) 1994, (f) 1990, and (h) 1987. Field-based estimates (mean and standard deviation) were developed from data reported by *O'Neill* [2000] and *O'Neill et al.* [in review].

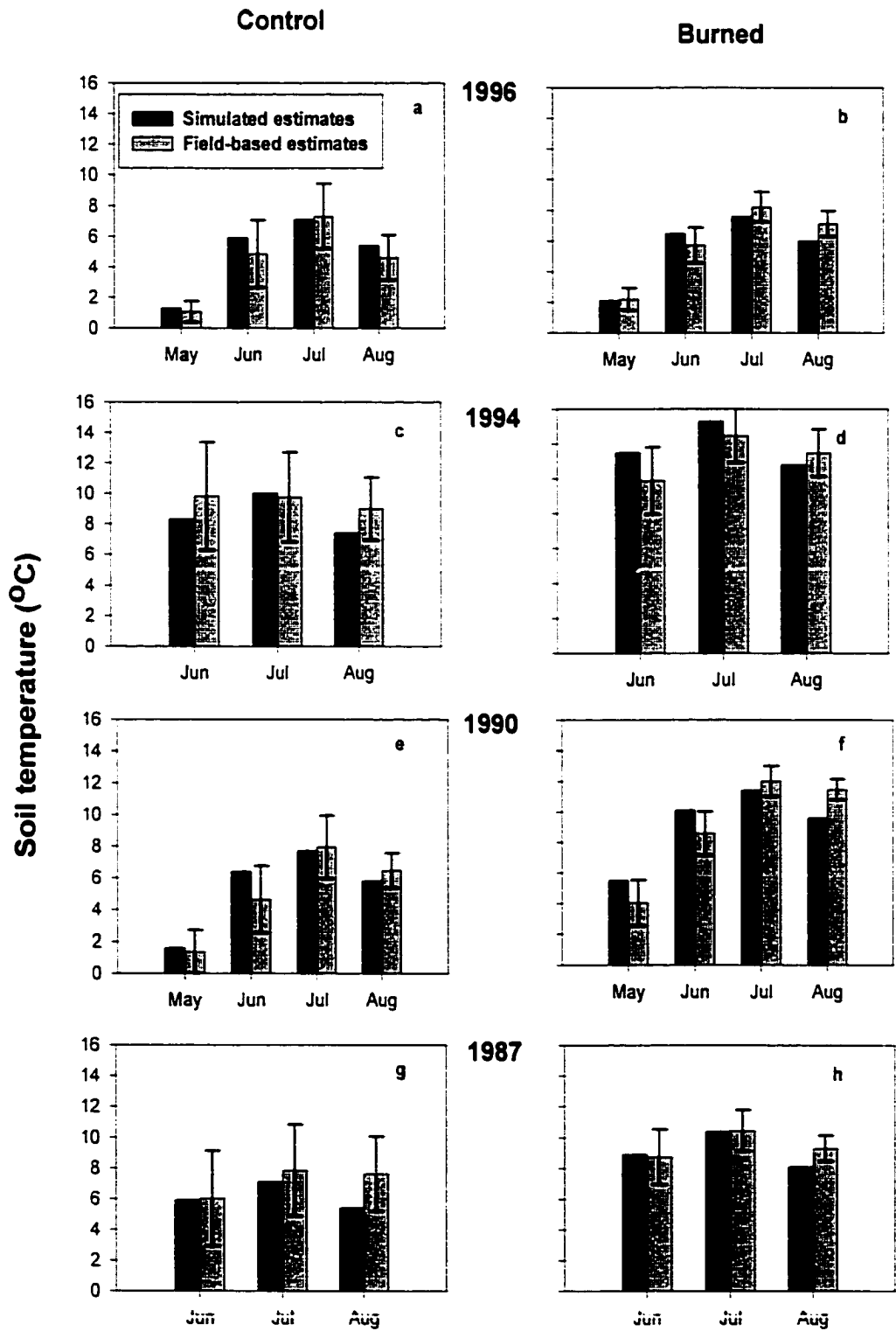


Figure. 3.10. Comparison of regressions of monthly soil temperature estimates at 10 cm depth during the growing season in 1997 between simulated and field-based estimates with the 1:1 lines. The linear regressions were conducted using field-based estimates as the independent variable and simulated estimates as the dependent variable. (a) For control sites, the linear regression was significant ($P < 0.001$, $N = 14$) with $R = 0.93$, slope = 0.82, and intercept = 1.23 °C. (b) For burned sites, the linear regression was significant ($P < 0.001$, $N = 14$) with $R = 0.93$, slope = 0.91, and intercept = 0.83 °C. Field-based estimates (mean and standard deviation) were developed from data reported by *O'Neill* [2000] and *O'Neill et al.* [in review].

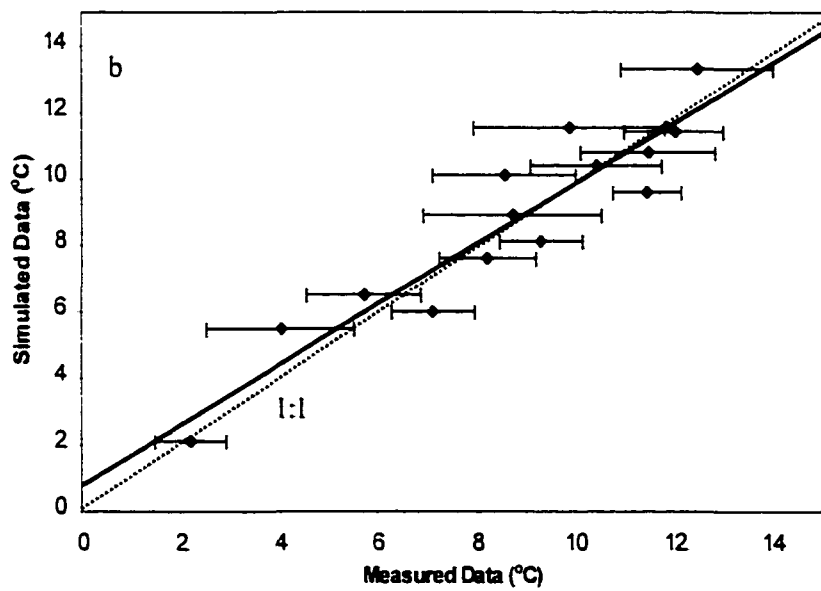
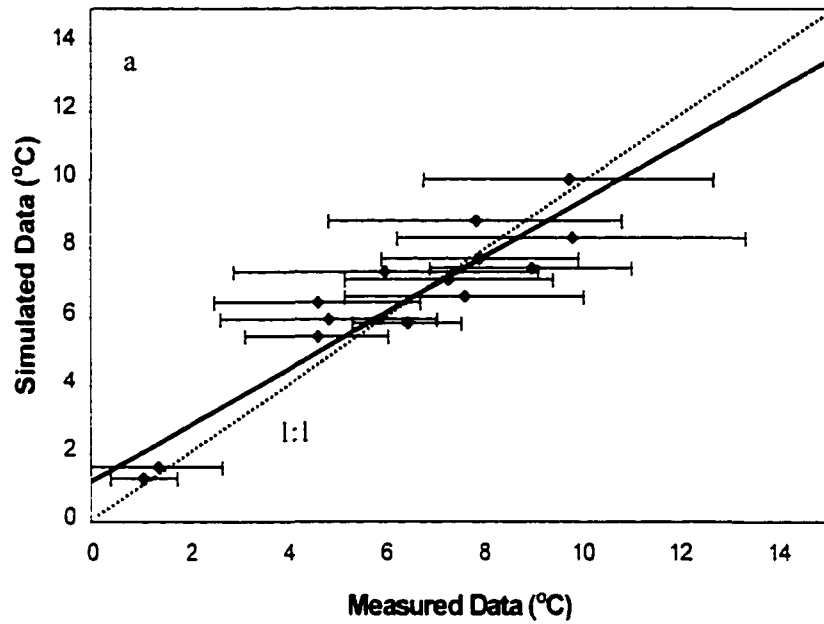


Figure. 3.11. Comparison of monthly soil respiration during the growing season in 1997 between simulated and field-based estimates for control and burned stands of the fire chronosequence in interior Alaska. Comparison of simulated and field-based estimates for control sites corresponding to recently burned sites in (a) 1996, (c) 1994, (e) 1990, and (g) 1987. Comparison of simulated and field-based estimates for recently burned sites in (b) 1996, (d) 1994, (f) 1990, and (h) 1987. Field-based estimates (mean and standard deviation) were developed from data reported by *O'Neill* [2000] and *O'Neill et al.* [in review].

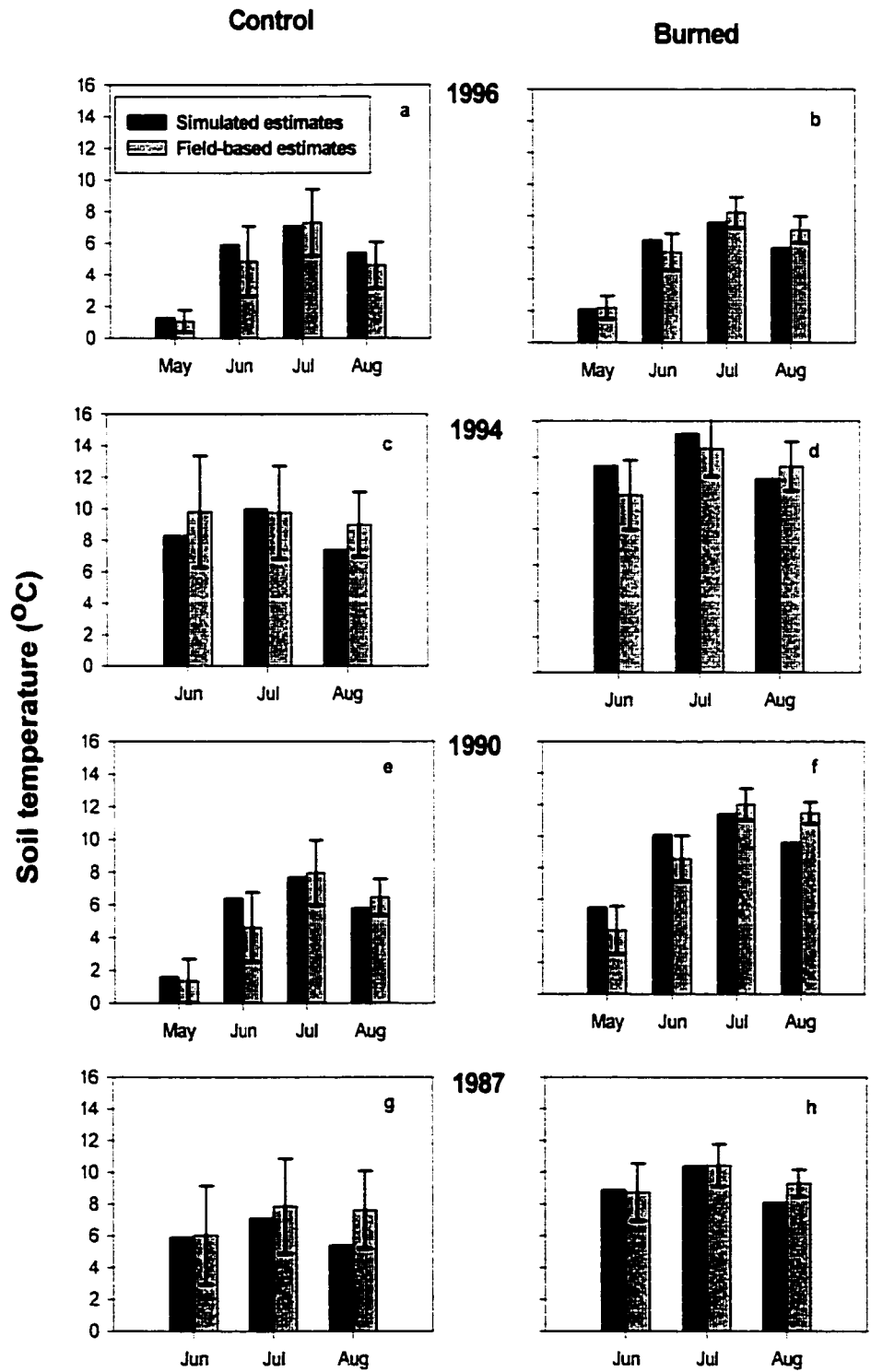


Figure. 3.12. Comparison of regressions of monthly soil respiration estimates during the growing season in 1997 between simulated and field-based estimates with the 1:1 lines.

The linear regressions were conducted using field-based estimates as the independent variable and simulated estimates as the dependent variable. (a) For control sites, the linear regression was significant ($P < 0.001$, $N = 17$) with $R = 0.84$, slope = 0.64, and intercept = $39.6 \text{ g C m}^{-2} \text{ month}^{-1}$. (b) For burned sites, the linear regression was significant ($P < 0.001$, $N = 17$) with $R = 0.75$, slope = 0.78, and intercept = $10.2 \text{ g C m}^{-2} \text{ month}^{-1}$. Field-based estimates (mean and standard deviation) were developed from data reported by *O'Neill* [2000] and *O'Neill et al.* [in review].

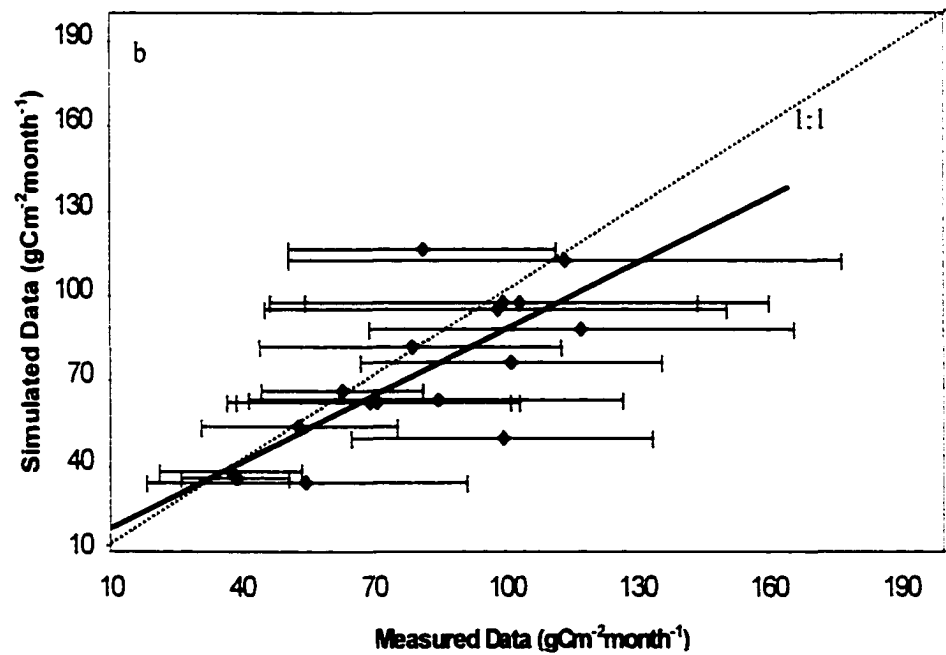
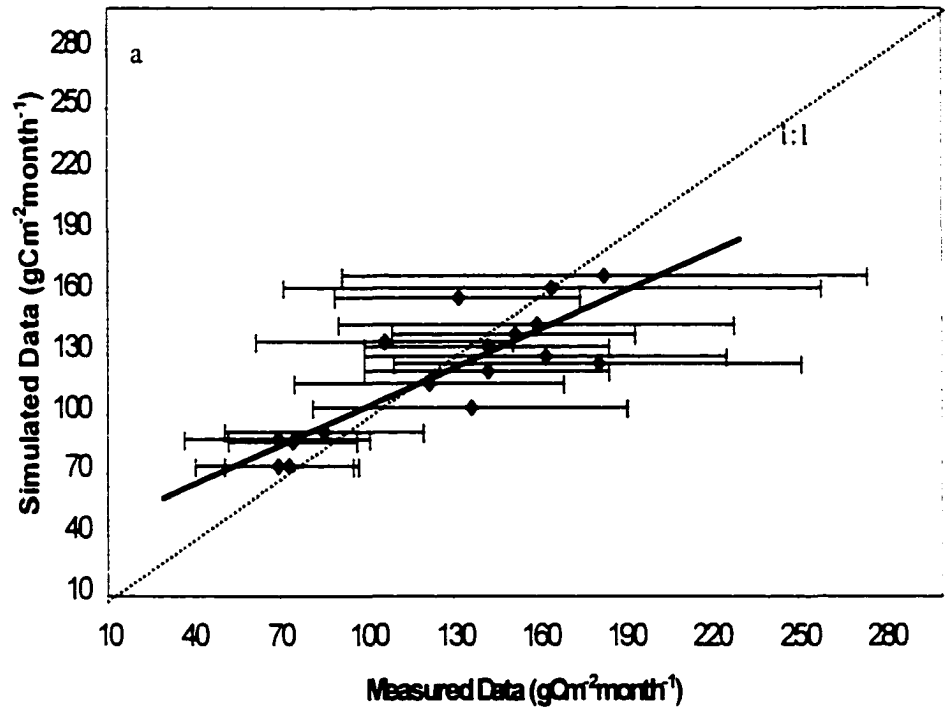


Figure. 3.13. Simulated soil carbon dynamics for control stands (last burned in 1825, 1855, and 1915) and recently burned stands (burned in 1987, 1990, 1994, and 1996) of the fire chronosequence in interior Alaska. (a) Simulations driven with transient climate, transient atmospheric CO₂, and no nitrogen inputs. (b) Simulations driven with constant climate data, transient atmospheric CO₂, and no nitrogen inputs. (c) Simulations driven with constant climate, transient atmospheric CO₂, and the addition during stand development of nitrogen that was lost during fire.

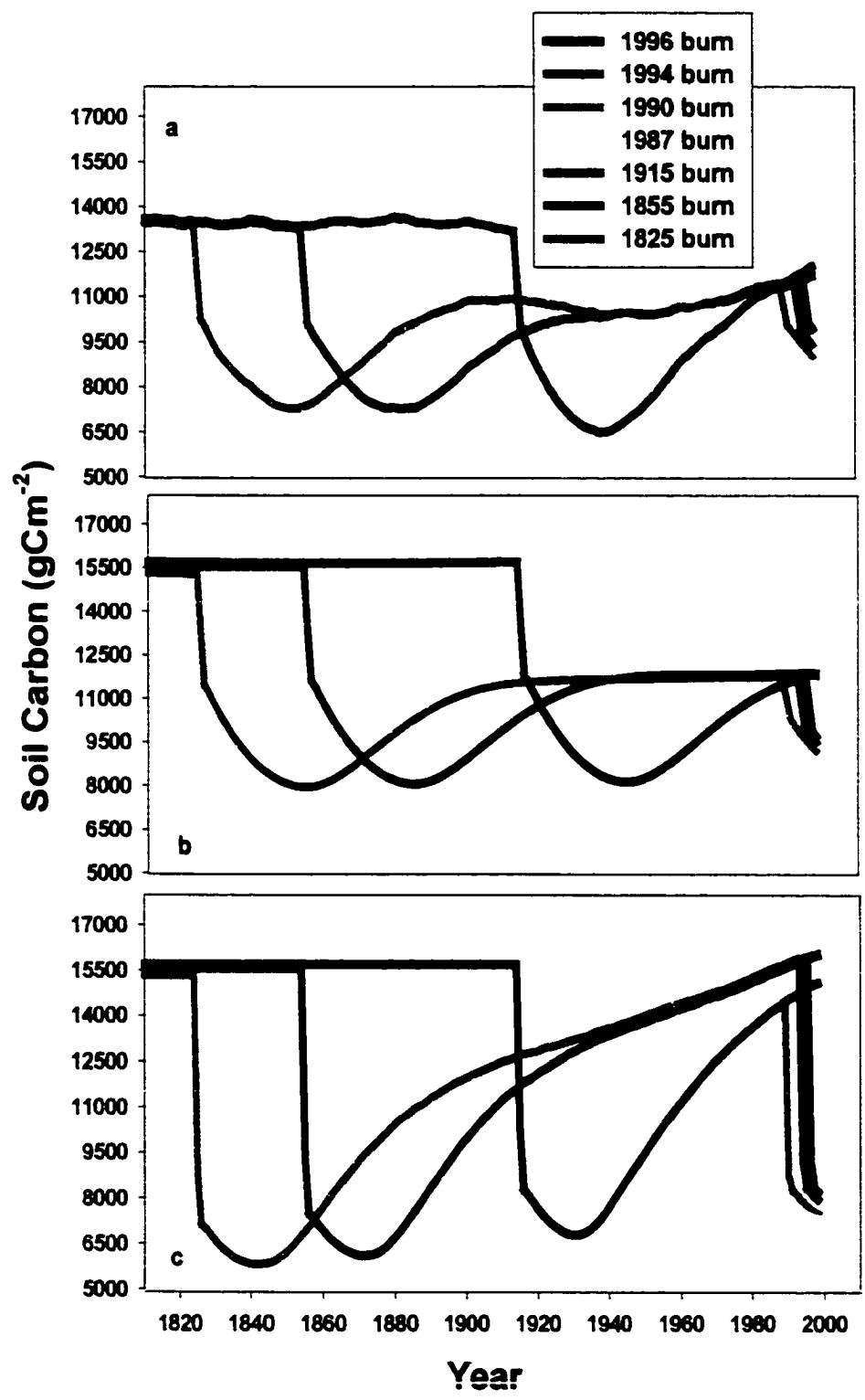


Figure. 3.14. The dynamics of soil temperature, soil moisture, nitrogen cycling, carbon fluxes, and carbon stocks in the sensitivity analysis for moss growth. Scenarios include a stand with moss cover that was not burned (unburned), a stand that was burned and moss was allowed to grow during stand development (burned - moss growth; also known as the "standard" scenario), and a stand that was burned and moss was not allowed to grow during stand development (burned - no moss growth). (a) soil temperature integrated over 20 cm of soil relative to the soil surface, (b) mean volumetric soil moisture of the humic organic layer from May to September, (c) annual net nitrogen mineralization, (d) annual net primary production (NPP), (e) annual heterotrophic respiration/decomposition (R_H), (f) annual net ecosystem production (NEP), (g) vegetation carbon, and (h) soil carbon.

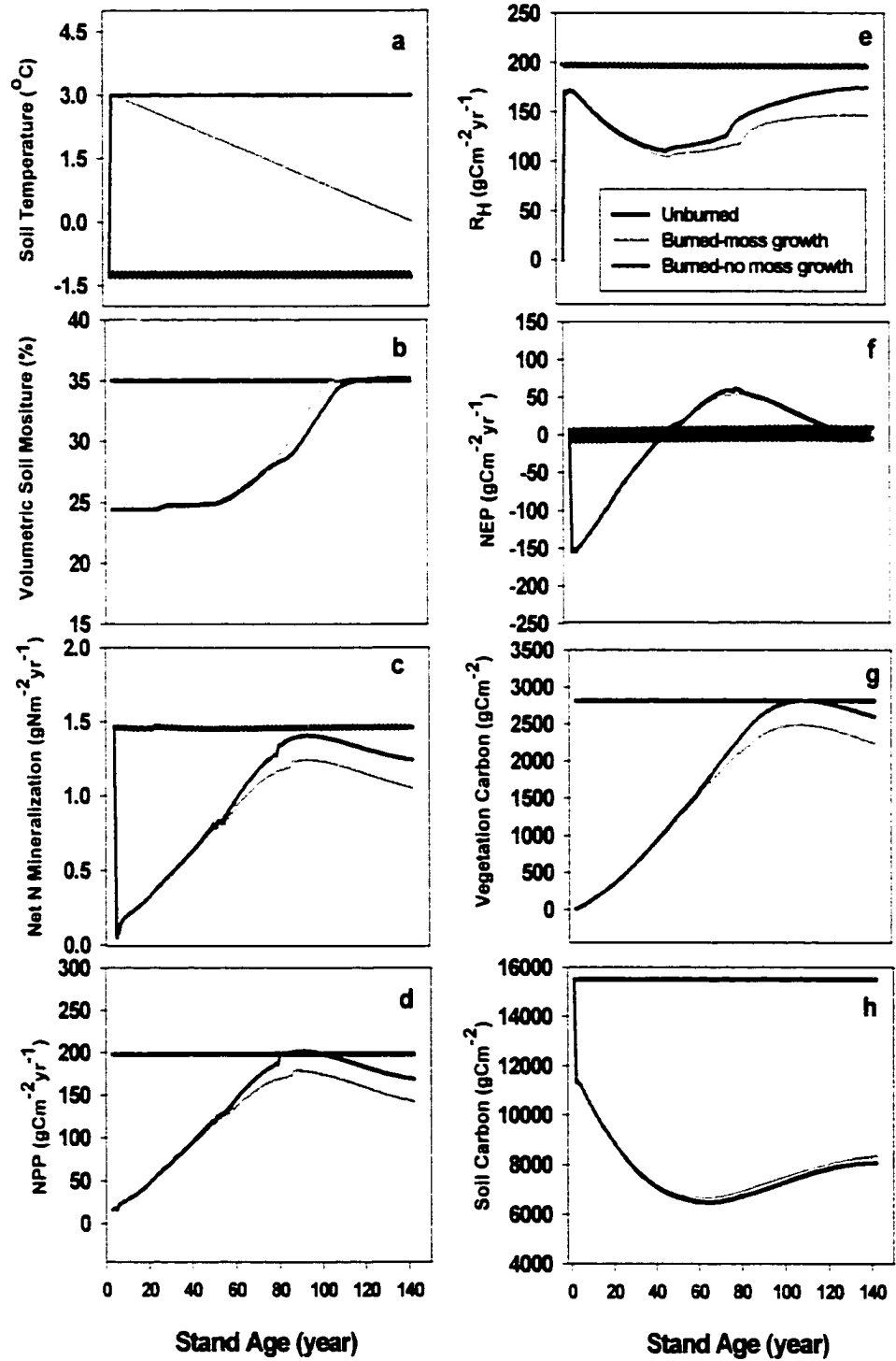


Figure. 3.15. The dynamics of soil moisture, soil temperature, nitrogen cycling, carbon fluxes, and carbon stocks in the sensitivity analysis for soil moisture. Scenarios include the standard scenario, which is the same as the scenario for the burned stand with moss growth in Figure 14, and scenarios in which volumetric soil moisture of the standard scenario was prescribed to be 50% higher (high moisture) and 50% lower (low moisture). (a) mean volumetric soil moisture of the humic organic layer from May to September, (b) soil temperature integrated over 20 cm of soil relative to the soil surface, (c) annual net nitrogen mineralization, (d) annual net primary production (NPP), (e) annual heterotrophic respiration/decomposition (R_H), (f) annual net ecosystem production (NEP), (g) vegetation carbon, and (h) soil carbon.

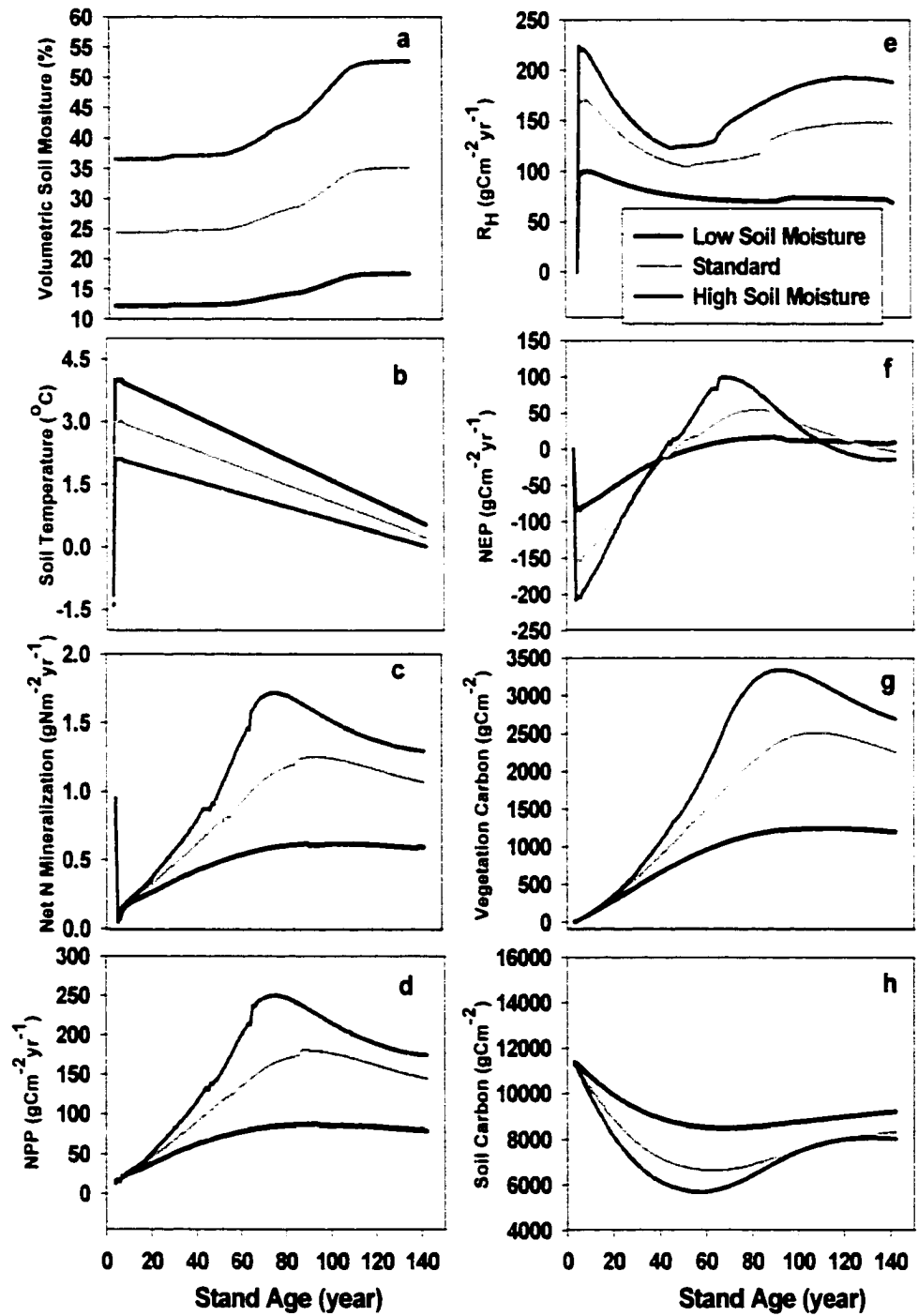
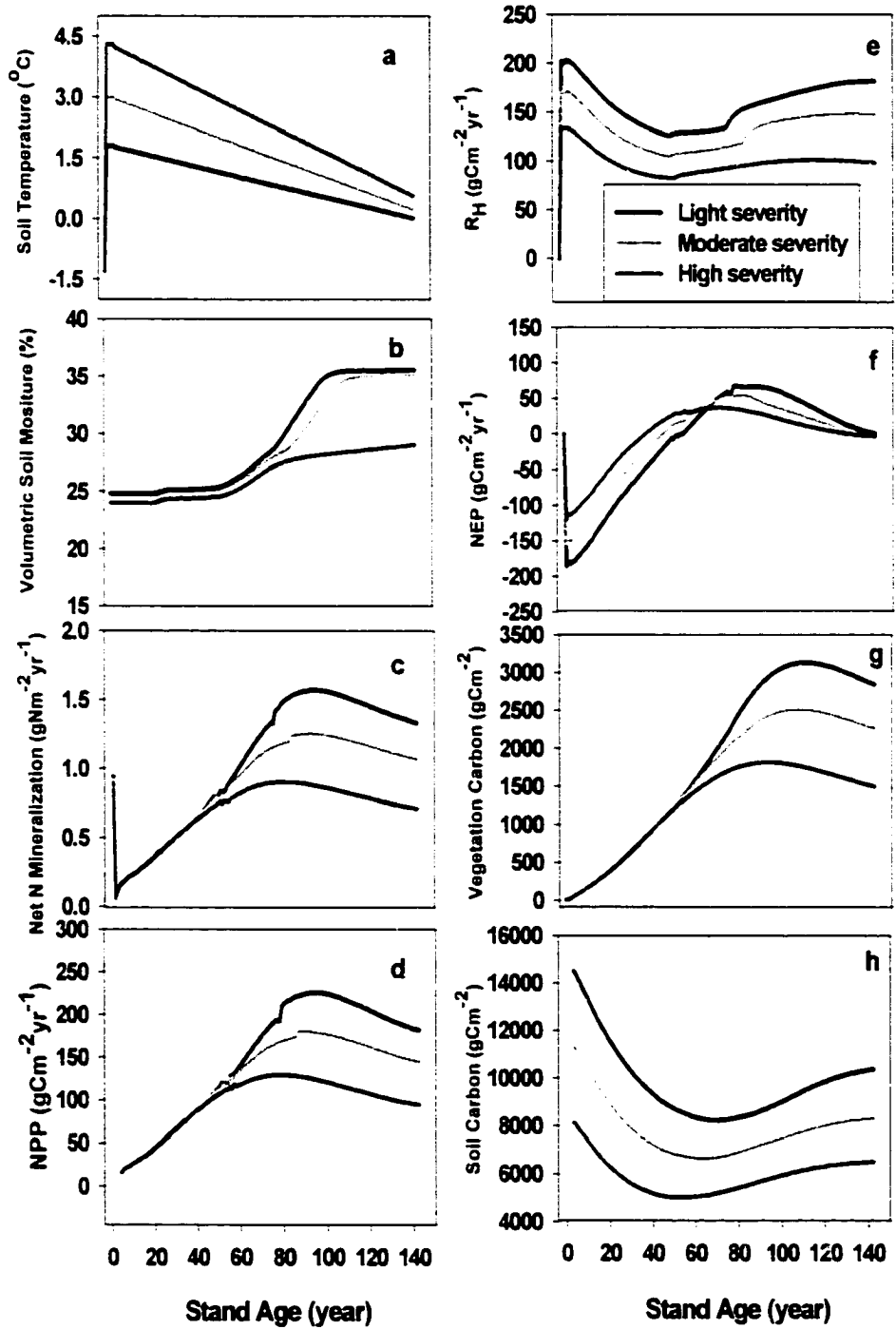


Figure. 3.16. The dynamics of soil temperature, soil moisture, nitrogen cycling, carbon fluxes, and carbon stocks in the sensitivity analysis for fire severity. Scenarios include stands that experienced light burn severity (12% vegetation and 18% soil carbon and nitrogen released in fire emissions), moderate burn severity (23% vegetation and 36% soil carbon and nitrogen released in fire emissions), and severe burn severity (46% vegetation and 54% soil carbon and nitrogen released in fire emissions). The thickness of the organic layer was decreased by 18%, 36%, and 54% of 30 cm for the light burn, moderate burn, and severe burn scenarios, respectively. (a) soil temperature integrated over 20 cm of soil relative to the soil surface, (b) mean volumetric soil moisture of the humic organic layer from May to September, (c) annual net nitrogen mineralization, (d) annual net primary production (NPP), (e) annual heterotrophic respiration/decomposition (R_H), (f) annual net ecosystem production (NEP), (g) vegetation carbon, and (h) soil carbon.



CHAPTER FOUR

FUTURE OPPORTUNITIES

1. Implications of Freeze-Thaw Dynamics for the Global Carbon Cycle

There are two prevailing hypotheses about how climate warming will influence carbon balance in boreal forests. One is that climate warming will significantly release carbon (C) through increases in soil decomposition that are greater than increases in net primary production (NPP), a response that may act as a positive feedback to climate through increasing the growth of atmospheric CO₂ [*Houghton and Woodwell*, 1989; *Oechel et al.*, 1993]. Another hypothesis is the response of C dynamics associated with the response of nitrogen (N) dynamics to warming [*Shaver et al.*, 1992]. This hypothesis is based on the inference that soil organic N would be released as inorganic N in association with increased decomposition rates caused by elevated temperature [e.g., see *Nadelhoffer et al.*, 1991], and predicts that the increased availability of N will lead to increased NPP in high latitude ecosystems, which are generally limited by N availability. This hypothesis predicts that high latitude ecosystems should be a net sink for atmospheric CO₂ as increases in NPP should be larger than releases from decomposition because the vegetation has a much higher C:N ratio than the soil [*Shaver et al.*, 1992]. *Van Cleve et al.* [1990] found that experimentally warming the forest floor of a black spruce stand for three summers increased decomposition, foliar N concentration, and photosynthesis, which suggests that tree production increased in association with greater N availability. *Bonan and Van Cleve* [1992] used a forest dynamics model [*Bonan* 1990a, 1990b] to simulate how soil temperature, N mineralization and tree growth affect C

fluxes in boreal forest stands. Over a 25-year period, the simulations indicated that soil warming increases decomposition, N mineralization, and C uptake by trees, resulting in a net increase in C storage in the vegetation. *Oechel et al.* [2000] argue that although there may be acclimation of ecosystem CO₂ exchange in the Alaskan Arctic in response to decadal climate warming, that further climate change may still exacerbate CO₂ emissions from Arctic ecosystems because winter releases in CO₂ [see *Winston et al.*, 1997; *Oechel et al.*, 1997] may be greater than uptake in summer.

In addition to aforementioned hypotheses of carbon cycle responses to climate warming, some studies have shown that the growing season advances and lengthens in high latitude ecosystems as the climate of the Northern Hemisphere warms. For example, *Keeling et al.* [1996] argued that the 40% increase in the amplitude of the seasonal cycle and the seven day advance in zero-crossing point for the atmospheric CO₂ concentration measured at Mauna Loa since the 1960s have been caused by climate warming in the northern hemisphere. Also *Myneni et al.* [1997] estimated that the growing season of northern hemisphere terrestrial ecosystems may have increased by 12 days during the period of 1981-1991 as inferred from trends of the seasonal normalized difference vegetation index (NDVI) record from the advanced very high resolution radiometer (AVHRR). Similarly, analysis of local weather records across Alaska suggests that the growing season has been extended by over 14 days in the last 50 years by increasing spring temperatures [*Running et al.*, 1999]. It appears that the timing of spring thaw and the duration of the growing season are strongly linked to the carbon balance of boreal and arctic systems [*Running et al.*, 1999; *Frolking et al.*, 1996; *Goulden et al.*, 1998]. In

contrast, *Barber et al.* [2000] showed that the growth of Alaskan white spruce has been reduced in the twentieth century because of temperature-induced drought stress. These studies suggest that climate warming may have nonlinear impacts on plant production and carbon balance of high latitude ecosystems. *Running et al.* [1999] stated that the freeze-thaw transition represents the closest analog to a biospheric and hydrologic on/off switch existing in nature, profoundly affecting surface meteorological conditions, ecological trace gas dynamics, and hydrological activity. This transition period initiates snowmelt, which immediately accelerates runoff and stream discharge. Ecosystem responses are equally rapid, as rates of soil heterotrophic respiration and photosynthetic activity of evergreen trees increase with the new presence of liquid water.

In Chapter 2 of this dissertation, I described the development of the STM-TEM, which represents the integration of a soil thermal model (STM) into a large-scale ecosystem model (TEM). My analyses demonstrated that the STM-TEM is capable of simulating soil thermal dynamics of high latitude ecosystems over substantial spatial and temporal domains. A logical next step is to apply the model to evaluate whether interactions among climate change, freeze-thaw dynamics, and growing season length in the Northern Hemisphere can explain trends that have been observed in the atmospheric concentrations of CO₂ at monitoring stations. Currently, I am parameterizing the STM-TEM with soil thermal measurements from Long Term Ecological Research (LTER) sites in the United States for major biomes of the globe. I will evaluate the performance of these parameterizations with measurements at different sites, and then apply the model to evaluate how changes in freeze-thaw dynamics may be influencing global carbon

dynamics in recent decades. The exchange of carbon with the atmosphere simulated by the STM-TEM will be coupled to the Model of Atmospheric Transport and Chemistry [MATCH; *Rasch et al.*, 1997; *Mahowald et al.*, 1997; *Dargaville et al.*, in review], which can then simulate atmospheric concentrations of CO₂ at monitoring stations. By comparing simulated atmospheric concentrations of CO₂ with observed atmospheric concentrations at monitoring stations, I will be able to evaluate if changes in freeze-thaw dynamics in response to climate, as represented by the STM-TEM, can explain observed patterns of trends in the growth of the seasonal amplitude and zero-crossing point of atmospheric CO₂ that have been observed at some monitoring stations.

2. Issues to Address in Future Model Development and Application

I developed the version of the STM-TEM in Chapter 3 by restructuring the hydrologic model of the STM-TEM described in Chapter 2, and verified the new version with measurements of soil thermal dynamics, water fluxes and soil moisture, carbon fluxes, and age-dependent dynamics of vegetation carbon. I applied the model to a fire chronosequence in Interior Alaska and evaluated model performance in simulating soil temperature, soil respiration, and soil carbon storage. I also conducted sensitivity analyses to gain insights on how moss growth, soil drainage, and fire severity affect ecosystem processes during stand development after fire disturbance. These analyses and consideration of other process studies have revealed a number of issues that should be addressed in future model development and application: (1) moss and organic layer dynamics during succession; (2) soil drainage and other issues associated with soil

moisture; (3) allocation of vegetation tissue to leaves, wood, and roots; (4) variability of below-ground carbon dynamics with depth in the soil profile; (5) nitrogen cycle issues; and (6) spatial data set development. Future development of the STM-TEM to address these issues will enhance the ability of the model to be used as a tool for gaining additional insight into how interactions among climate change, permafrost dynamics, and fire disturbance influence processes in high latitude ecosystems. Below, I discuss how these issues might be considered in future development and application of the STM-TEM.

2.1. Moss and Organic Layer Dynamics During Succession

The results of the sensitivity analyses that I conducted in Chapter 3 indicate that the growth of moss and changes in the depth of the organic layer during succession should be represented in models that simulate the effects of fire disturbance in boreal forests. Currently, the dynamics of the thickness of moss is represented by an empirical function and the depth of the organic layer is defined as a static parameter. Future model development should represent how successional dynamics of moss species and changes in the thickness of humic organic matter influence ecosystem processes during stand development after fire through effects on soil thermal and hydrologic conductivity. Also, moss biogeochemistry is currently considered only during parameterization of the model. Future model development should also include explicit representation of moss biogeochemistry so that the seasonal responses of moss biogeochemistry are segregated

from vascular biogeochemistry as moss may be more active at the beginning and end of summer while vascular species may be more active in mid-summer.

2.2. Soil Drainage and Other Issues Associated with Soil Moisture

The sensitivity analyses with soil moisture in Chapter 3 revealed that soil drainage should be considered in spatial applications of the model. Soil drainage in boreal forests depends on the spatial and temporal dynamics of permafrost, and influences species composition [Rapalee *et al.*, 1998] and carbon storage [Trumbore and Harden, 1997; see also Lynch and Wu, 1999]. Soil drainage also likely influences aspects of the fire regime at fine spatial scales, such as fire frequency and fire severity [see Harden *et al.*, 2000]. Thus, future development of the STM-TEM should focus on more fully considering the effects of soil drainage on carbon dynamics of high latitude ecosystems.

While the current version of the STM-TEM considers the interactions between the active layer dynamics and soil moisture, it is not currently equipped to represent the influences of soil drainage as soil water is routed to runoff or drainage so that soil moisture does not exceed field capacity. Thus, model development should be implemented to allow field capacity to be exceeded for soil drainage conditions that impede runoff or drainage. This model development is particularly important for representing anaerobic decomposition of wetland ecosystems in high latitudes. For example, several studies indicate that there is a strong "hysteresis" between anaerobic decomposition (i.e., methane flux) and the rise and fall of the water table associated with active layer dynamics in ecosystems affected by permafrost [see Moore and Roulet,

1993; *Frolking*, 1993; *Frolking et al.*, in review; *Hilbert et al.*, 2000; *Vardy et al.*, 2000].

Therefore, it is important to modify the STM-TEM so that it can consider how interactions among soil drainage and permafrost dynamics influence the water table to affect ecosystem processes.

Two important soil moisture issues that are not currently represented in the STM-TEM include the effect of soil moisture on soil thermal conductivity and the effects of unfrozen water on below-ground physical and biological processes. Soil thermal properties, such as soil thermal conductivity, are currently prescribed in the STM-TEM for each of the soil layers, and these properties are currently not affected by dynamics of soil moisture. While it has been appreciated for some time that soil thermal conductivity strongly depends on soil moisture [*Hinzman et al.*, 1991], evidence is now emerging that is elucidating how soil thermal conductivity depends on soil moisture [*Yoshikawa et al.*, in press; *Abu-Hamdeh and Reeder*, 2000]. These relationships should be implemented into the STM-TEM so that the model can more fully consider how soil thermal dynamics depend on soil moisture.

The representation of unfrozen water in numerical soil thermal models is important because unfrozen water has effects on physical and biological processes in ecosystems of high latitudes. A number of studies have identified that unfrozen water strongly influences heat and mass transport processes [e.g. *Smith and Riseborough*, 1985; *Nixon*, 1986; *Osterkamp*, 1987; *Williams and Smith*, 1989; *Riseborough*, 1990; *Osterkamp and Gosink*, 1991; *Burn*, 1992; *Osterkamp and Fei*, 1993; *Romanovsky and Osterkamp*, 2000]. The physical and chemical properties of frozen ground and permafrost are quite

sensitive to temperature when unfrozen water is present [*William and Smith*, 1989; *Romanovsky and Osterkamp*, 2000; *Kudryavtsev*, 1981]. Also, because frozen soil moisture reduces hydraulic conductivity, hydrological dynamics of permafrost dominated ecosystems depend on the amount of unfrozen water in the frozen layer as well as the presence or absence of a talik layer below the seasonally frozen layer [*Burt and Williams*, 1976]. For example, conditions that lead to decreased infiltration that restricts drainage can cause high soil moisture and more runoff [see also *Waelbroeck et al.*, 1997; *Kane and Stein*, 1983; *Fox*, 1992]. A number of studies have also identified that unfrozen water influences soil biological activity when soil temperatures are less than 0° C [*Coxson and Parkinson*, 1987; *Malhi et al.*, 1990; *Sommerfeld et al.*, 1991, 1993; *Brooks et al.*, 1995, 1996; *Clein and Schimel*, 1995; *Gilichinsky and Wagener*, 1995; *Schimel et al.*, 1996].

While the STM-TEM does not currently represent unfrozen water in the frozen soil, the effects of unfrozen water on soil thermal dynamics has been evaluated with Goodrich model, which was the basis for the development of STM-TEM [see *Romanovsky et al.*, 1997; *Romanovsky and Osterkamp*, 1997; *Osterkamp and Romanovsky*, 1997]. The dependence of gravimetric or volumetric unfrozen water content of a frozen soil on temperature can be represented with a power function [*Lovell*, 1957] or other empirical relationships [see *Osterkamp and Romanovsky*, 1997; *Anderson and Morgenstern*, 1973] so that the effects of unfrozen water can be incorporated into the equations of heat conduction models [see *Romanovsky et al.*, 1997; *Romanovsky and Osterkamp*, 2000]. The incorporation of unfrozen water into the STM-TEM should allow the model to simulate talik formation and dynamics after disturbance, which is important

to consider so that soil drainage can be properly represented during stand development after disturbance. Furthermore, the representation of unfrozen water into the STM-TEM will allow the model to consider the effects of unfrozen water on soil biological processes as those effects become better elucidated.

2.3. Allocation of Vegetation Tissue to Leaves, Wood, and Roots

The STM-TEM currently represents vegetation as one compartment for structural carbon, one compartment for structural nitrogen, and one compartment for labile nitrogen storage. For a given leaf area index, the model allocates additional effort towards either carbon or nitrogen uptake depending on the degree to which nitrogen uptake and nitrogen mobilized from storage can meet the nitrogen requirement of new production. While the model implicitly represents allocation towards carbon and nitrogen uptake, it does not explicitly represent allocation to leaves, wood, and roots as leaf area index is empirically calculated based on the structural carbon pool and effective fine root surface area for uptake of nitrogen is assumed to be correlated to leaf area index. In the study I conducted with the STM-TEM, I therefore made assumptions about the amount of above-ground biomass and below-ground autotrophic respiration for purposes of parameterizing, verifying, and validating the model. Below I provide additional information on these assumptions so that the sensitivity of model dynamics to these assumptions may be assessed in future studies.

Based on *Gower et al.* [1997], I assumed that 80% of total vegetation carbon is allocated to above-ground vegetation carbon. This assumption was made so that the age-

dependent dynamics of vegetation carbon of black spruce forest ecosystems simulated by the STM-TEM could be parameterized based on analyses of inventory survey data by *Yarie and Billings* [in press]. This parameterization influences the age-dependent simulation of leaf area index, gross primary production, the distribution of radiation through the canopy, and evapotranspiration. Based on *Ryan et al.* [1997], I assumed that root respiration was 45% of total autotrophic respiration simulated by the STM-TEM. This assumption was made so that I could develop model-based estimates of soil respiration for comparison with field-based estimates. If allocation to root biomass varies during stand development or across the landscape, then this assumption may produce biased estimates of soil respiration. While there are some data available on partitioning of vegetation carbon and autotrophic respiration in forested ecosystems [e.g., *Flanagan and Van Cleve*, 1977; *Law et al.*, 1999; *Gaudinski et al.*, 2000; *Ruess et al.*, in preparation], it is completely clear how partitioning of vegetation carbon and autotrophic respiration should vary during succession or across the landscape for a single vegetation type, or how this partitioning should vary among different vegetation types. Thus, it is important to ascertain the sensitivity of dynamics simulated by the model to these assumptions with respect to stand development, topographic position, geographic location, and vegetation heterogeneity. In this way the model can be used as a tool to help focus field studies of allocation on issues that will reduce model-based uncertainty. The understanding of model-based uncertainty should also assist in the development of a version of the STM-TEM that explicitly considers the dynamics multiple vegetation pools.

2.4. Variability of Below-Ground Carbon Dynamics with Depth in the Soil Profile

The current version of STM-TEM treats soil organic matter as a compartment for soil organic carbon, a compartment for soil organic nitrogen, and a compartment for available soil nitrogen, and uses soil temperature and soil moisture of the organic soil layer to drive the processes (e.g., decomposition, nitrogen uptake, and nitrogen mineralization) that influence the fluxes into and out of these pools. Several studies have documented that soil carbon quantity and quality vary with depth in the soil profile of ecosystems [see *Trumbore and Harden, 1997; Harden et al., 2000; Rapalee, in press; Rapalee et al., 1998; Billings et al., 1998; Gaudinski et al., 2000; Neff and Asner, 2001*]. As the physical properties of soils also vary with depth, it seems useful to link variability in soil carbon quantity, soil carbon quality, soil temperature, and soil moisture to simulate the depth-based variability in ecosystem processes that occur in the soil. This linkage may be particularly important for high latitude ecosystems, in which the soil physical and chemical environment depends substantially on the presence or absence of permafrost. For example, *Waelbroeck et al. [1997]* indicated that the active layer depth substantially influences the carbon dynamics of tundra ecosystems. *Goulden et al. [1998]* also showed that most of the old CO₂ (i.e., from carbon fixed more than 50 years ago) released in soil respiration from a black spruce forest came from a zone 40 to 80 cm deep, which was well beneath the zone containing moss and tree roots. Development of the STM-TEM to consider this variability will require tracking organic carbon and nitrogen pools by depth and driving the processes affecting these pools with soil temperature and soil moisture by depth. A version of the STM-TEM that considers this variability would be useful as a

tool for examining how the dynamics of these pools are influenced by interactions among soil physics, climate change, and disturbance.

2.5. Nitrogen Cycle Issues

Issues for consideration in future model development of STM-TEM is how the model deals with nitrogen cycling, i.e., nitrogen uptake, allocation to structural tissue, nitrogen returned to the soil in senesced tissue, and the processing of nitrogen in the soil in both organic and inorganic forms. Several studies have suggested that the dynamics of nitrogen in the forest floor and mineral soil of boreal forests should be intimately linked with that of carbon because most nitrogen exists in organic compounds and because heterotrophic microbes, which utilize organic carbon for energy, should play an important role in processing nitrogen to available nitrogen forms in boreal forests [e.g. *Flanagan and Van Cleve*, 1983; *Van Cleve et al.*, 1986; *Paul and Clark*, 1989]. Studies of nitrogen dynamics in ecosystems influenced by permafrost have shown that rates of decomposition and net nitrogen mineralization are very slow, and that the availability of inorganic nitrogen is very low in comparison to temperate and tropical ecosystems [*Chapin and Bledsoe*, 1992; *Van Cleve et al.*, 1983].

Vegetation has the potential to overcome the low availability of inorganic nitrogen in the soil through substantial nitrogen recycling within the vegetation and through the uptake of organic nitrogen in the soil solution. Nitrogen recycling by vegetation in Arctic and subarctic ecosystems is substantial [*Chapin et al.*, 1980; *Chapin and Kedrowski*, 1983; *Jonasson and Chapin*, 1985; *Shaver et al.*, 1990; *Chapin and*

Moilanen, 1991; Shaver and Chapin, 1991], and represents a substantial proportion of nitrogen requirement. The uptake of organic nitrogen as amino acids by the vegetation also represents a substantial proportion of nitrogen requirement in high latitude ecosystems [*McFarland et al.*, in review; *Kielland, 1994, 1997, 2001*].

The current version of the STM-TEM explicitly considers the importance of nitrogen recycled by the vegetation [see *McGuire et al.*, 1992], but only implicitly considers the uptake of organic nitrogen uptake by the vegetation. The uptake of organic nitrogen is represented in the model by parameterizing the rate limiting parameters for uptake of nitrogen from the available nitrogen pool until nitrogen requirement is met through both recycling and uptake. This procedure also influences the parameterization of the rate limiting parameter for nitrogen immobilization. Nitrogen input into the available nitrogen pool is calculated as the difference between gross mineralization, which is highly correlated with decomposition, and nitrogen immobilization. The algorithm in the STM-TEM do not distinguish explicitly among available inorganic and organic nitrogen species in the calculation of gross mineralization or immobilization, and it is not entirely clear if the model accurately represents the dynamics of organic nitrogen uptake in high latitude ecosystems. As processed-based studies further elucidate the dynamics of the nitrogen cycle in high latitude ecosystems, this understanding should be considered for incorporation into the STM-TEM.

The results of the sensitivity analyses that I conducted in Chapter 3 indicate that nitrogen fixation should be represented in models that simulate the effects of fire disturbance in boreal forests. Several studies have identified the importance of the

dynamics of nitrogen fixation, organic nitrogen, and available nitrogen in successional ecosystems [see *Van Cleve et al.*, 1993; *Klingensmith and Van Cleve*, 1993a,b; *Smith et al.*, 2000; *Uliassi et al.*, 2000; *Schimel et al.*, 1998; *Rastetter et al.*, 2001]. After fire disturbance, the initial nitrogen pools in vegetation and soil are dramatically changed [*Dyrness et al.*, 1989, *Levine et al.*, 1991] and the nitrogen dynamics continue to change during stand development [*Pietkainen and Fritze*, 1996; *Lynham et al.*, 1998; *Smith et al.*, 2000; *O'Neill*, 2000]. Thus, future model development with the STM-TEM should explicitly consider nitrogen inputs and losses. Also, as vegetation and moss regenerate, mosses play an important role in the nitrogen economy of the forest floor [*Weber and Van Cleve*, 1983; *Bowden*, 1991], as nitrogen is quickly immobilized and retained by moss, and is subsequently released very slowly in the organic soil layer where the most roots of vascular plants located. Therefore, similar to my earlier recommendation, it is important to explicitly represent the biogeochemistry of moss in future development of the STM-TEM to more fully consider the effects of moss on the nitrogen cycle during stand development.

2.6. Development of Spatial Data Sets

The sensitivity analyses with soil moisture and fire severity in Chapter 3 revealed that soil drainage should be considered in spatial applications of the model. Spatially and temporally explicit data sets on soil drainage and fire severity are also required in modeling the effects of soil drainage on carbon dynamics at landscape to regional scales. The currently available maps of permafrost and soil drainage for Alaska and other high

latitude regions are not adequate for accurately representing the role of soil drainage in simulating carbon dynamics at landscape to regional scales. While substantial advances have been made in developing data sets for the timing and spatial extent of fire in Alaska [Murphy *et al.*, 1999] and Canada [Stocks *et al.*, unpublished], data sets on severity of fires are also not yet available for broad regions of the boreal forest. Thus, the ability to apply future versions of the STM-TEM to simulate carbon dynamics of boreal forests at landscape to regional scales would be enhanced by advances in the development of spatial data sets for soil drainage and fire severity.

References

- Abu-Hamdeh, N. H., and R. C. Reeder, Soil thermal conductivity: Effects of density, moisture, salt concentration, and organic matter, *Soil Sci. Soc. Am. J.*, 64, 1285-1290, 2000.
- Anderson, D. M., and N. R. Morgenstern, Physics, chemistry, and mechanics of frozen ground: A review, *Proc. Int. Conf. Permafrost*, 2nd, 257-288, 1973.
- Barber, V.A., G. P. Juday, and B. P. Finney, Reduced growth of Alaska white spruce in the twentieth century from temperature-induced drought stress, *Nature* 405: 668-673, 2000.
- Billings, S. A., D. D. Richeter, and J. Yarie, Soil carbon dioxide fluxes and profile concentrations in two boreal forests, *Can. J. For. Res.*, 28, 1773-1783, 1998.
- Bonan, G. B., carbon and nitrogen cycling in North American boreal forests. I. Litter quality and soil thermal effects in interior Alaska, *Biogeochemistry*, 10, 1-28, 1990a.
- Bonan, G. B., Carbon and nitrogen cycling in North American boreal forests. II. Biogeographic patterns, *Can. J. For. Res.*, 20, 1077-1088, 1990b.
- Bonan, G. B., and K. Van Cleve, Soil temperature, nitrogen mineralization, and carbon source-sink relationships in boreal forests, *Can. J. For. Res.*, 22, 629-639, 1992.
- Bowden, R. D., Inputs, outputs, and accumulation of nitrogen in an early successional moss (*Polytrichum*) ecosystems, *Ecological Monographs*, 6, 12, 207-223, 1991.
- Brooks, P. D., M. W. Williams, and S. K. Schmidt, Snowpack controls on soil nitrogen dynamics in the Colorado alpine, in *Biogeochemistry of Seasonally Snow-Covered*

- Catchments*. Proceedings of a Boulder Symposium, July 1995. IAHS Publication 228. 283-292. 1995.
- Brooks, P. D., M. W. Williams, and S. K. Schmidt. Microbial activity under alpine snowpack, Niwot Ridge, Colorado. *Biogeochemistry*, 32, 93-113. 1996.
- Burn, C. R.. Recent ground warming inferred from the temperature in permafrost near Mayo, Yukon Territory, in *Periglacial Geomorphology. Proceedings 22nd Binghampton Symposium on Geomorphology*. Dixon J. C., A. D. Abrahams (eds). Wiley: New York. 327-350. 1992.
- Burt, T. P., and P. J. Williams. Hydraulic conductivity in frozen soils. *Earth Surf. Processes*, 1, 349-360. 1976.
- Chapin, F. S. III. and R. A. Kedrowski. Seasonal changes in nitrogen and phosphorous fractions and autumn translocation in evergreen and deciduous taiga trees. *Ecology*, 64, 376-391. 1983.
- Chapin, F. S. III. and L. Moilanen. Nutritional controls over nitrogen and phosphorous resorption from Alaskan birch leaves. *Ecology*, 72, 709-715. 1991.
- Chapin, F. S. III. P. C. Miller, W. D. Nillings, and P. I. Coyne. Carbon and nutrient budgets and their control in coastal tundra. in *An Arctic Ecosystems: The Coastal Tundra at Barrow, Alaska*, edited by J. Brown et al., pp. 458-482, Dowden, Hutchinson, and Ross, Stroudsburg, Pa., 1980.
- Chapin, D. M., and C. S. Bledsoe. Nitrogen fixation in arctic plant communities. In: *Arctic Ecosystems in a Changing Climate, an Ecophysiological Perspective*, ed.

- F. S. Chapin III, R. L. Jefferies, J. F. Reynolds, G. R. Shaver, and J. Svoboda, pp. 301-319. New York: Academic Press, Inc., 1992.
- Clein, J. S., and J. P. Schimel, Microbial activity of tundra and taiga soils at sub-zero temperatures. *Soil Biology and Biochemistry*, 27, 1231-1234, 1995.
- Coxson, D. S., and D. Parkinson, Winter respiratory activity in Aspen woodland forest floor litter and soils. *Soil Biology and Biochemistry*, 19,1, 49-49, 1987.
- Dargaville, R. J., et al., Evaluation of terrestrial carbon cycle models with atmospheric CO₂ measurements: Results from transient simulations considering increasing CO₂, climate and land-use effects. *Global Biogeochemical Cycles*, in review.
- Dyrness, C. T., K. Van Cleve, and J. D. Levison, The effects of wildfire on soil chemistry on four forest types in interior Alaska. *Can. J. For. Res.*, 19, 1389-1396, 1989.
- Flanagan, P. W., and K. Van Cleve, Microbial biomass, respiration, and nutrient cycling in a black spruce taiga ecosystem. in: *Soil organisms as Components of Ecosystems: International Soil Zoology Colloquium*. Uppsala, Sweden, June 21-25. Stockholm: Swedish Natural Science Research Council, ed. U. Lohm and T. Persson. Ecological Bulletin, 25, 261-273, 1977.
- Flanagan, P. W., and K. Van Cleve, Nutrient cycling in relation to decomposition and organic matter quality in taiga ecosystems, *Can J. For. Res.*, 13, 5, 795-817, 1983.
- Fox, J. D., Incorporating freeze-thaw calculations into a water balance model. *Water Resources Research*, 28,9,2229-2244, 1992.

- Frolking, S.. Modeling soil climate controls on the exchange of trace gases between the terrestrial biosphere and the atmosphere. Ph. D. Thesis, University of New Hampshire, Durham, NH, 1993.
- Frolking, S., M. L. Goulden, S. C. Wofsy, S - M. Fan, D. J. Sutton, J. W. Munger, A. M. Bazzaz, B. C. Daube, P. M. Crill, J. D. Aber, L. E. Band, X. Wang, K. Savage, T. Moore and R. C. Harriss. Modelling temporal variability in the carbon balance of a spruce/moss boreal forest. *Global Change Biology*, 2, 343-366. 1996.
- Frolking, S., N. T. Roulet, T. R. Moore, P. J. H. Richard, and M. Lavoie. Modeling northern peatland decomposition and peat accumulation. *Ecosystems*, in review.
- Gaudinski, J. B., S. E. Trumbore, E. Davidson, and S. Zheng. Soil carbon cycling in a temperate forest: radiocarbon-based estimates of residence times, sequestration rates and partitioning of fluxes. *Biogeochemistry*, 51, 33-69. 2000.
- Gilichinsky, D., and S. Wagener. Microbial life in permafrost: a historical review. *Permafrost and Periglacial Processes*, 6, 243-250. 1995.
- Goulden, M. L., S. C. Wofsy, J. W. Harden, S. E. Trumbore, P. M. Crill, and S. T. Gower. Sensitivity of boreal forest carbon balance to soil thaw. *Science*, 279, 210-217. 1998.
- Gower, S. T., J. G. Vogel, J. M. Norman, C. J. Kucharik, S. J. Steele, and T. K. Stow. Carbon distribution and aboveground net primary production in aspen, jack pine, and black spruce stands in Saskatchewan and Manitoba, Canada. *J. Geophys. Res.*, 102, 29,029-29,041. 1997.

- Harden, J. W., S. E. Trumbore, B. J. Stocks, A. Hirsch, S. T. Gower, K. P. O'Neill, and E. S. Kasischke. The role of fire in the boreal carbon budget. Fries, B. C. Daube, S.-M. Fan, D. J. Sutton, A. Bazzaz and J. W. Munger., *Global Change Biology*, 6 (Suppl. 1), 174-184, 2000.
- Hilbert, D., N. T. Roulet, and T. R. Moore. Modeling and analysis of peatlands as dynamic systems. *J. Ecol.*, 88, 1-13.
- Hinzman, L. D., D. L. Kane, R. E. Gieck, and K. R. Everett. Hydrologic and thermal properties of the active layer in the Alaskan Arctic. *Cold Regions Science and Technology*, 19, 95-110, 1991.
- Houghton, R. A., and G. M. Woodwell. Global climate change. *Sci. Am.* 260(4), 36-44, 1989.
- Jonasson, S., and F. S. Chapin, III. Significance of sequential leaf development for nutrient balance of the cotton sedge. *Eriophorum vaginatum L.*, *Oecologia*, 67, 511-518, 1985.
- Kane, D. L., and J. Stein. Water Movement into seasonally frozen soils. *Water Resources Research*, 19, 6, 1547-1557, 1983.
- Keeling, C. D., J. F. S. Chin, and T. P. Whorf. Increased activity of northern vegetation inferred from atmospheric CO₂ measurements. *Nature*, 382, 146-149, 1996.
- Kielland, K., Short-circuiting the nitrogen cycle: Strategies of nitrogen uptake in plants from marginal ecosystems. Pages 70-85. In: *New Concepts in Plant Nutrient Acquisition*, Ae.N., Okada, K., and Arihara, J. (eds.). Springer-Verlag, Berlin, 2001.

- Kielland, K.. Amino acid absorption by arctic plants: implications for plant nutrition and nitrogen cycling, *Ecology*, 75, 2373-2383, 1994.
- Kielland, K.. Role of free amino acids in the nitrogen economy of arctic cryptogams. *Écoscience*, 4, 75-79, 1997.
- Klingensmith, K.M., and Van Cleve, K., Denitrification and nitrogen fixation in floodplain successional soils along the Tanana River, interior Alaska. *Can. J. For. Res.*, 23 (5): 956-963, 1993a.
- Klingensmith, K.M., and K. Van Cleve, Patterns of nitrogen mineralization and nitrification in floodplain successional soils along the Tanana River, interior Alaska. *Can. J. For. Res.*, 23 (5): 964-969, 1993b.
- Kudryavtsev, V. A.. *Permafrost*. short edition. MSU press (in Russian), 1981.
- Law, B. E., M. G. Ryan, and P. M. Anthoni. Seasonal and annual respiration of a ponderosa pine ecosystem. *Global Change Biology*, 5, 169-182, 1999.
- Levine, J. S., W. R. Cofer, E. L. Winstead, S. sebacher, and P. J. Boston. The effects of fire on biogenic soil emissions of nitric oxide and nitrous oxide. *Global Biogeochem. Cycles*, 2, 445-449, 1991.
- Lovell, C. W., Temperature effects on phase composition and strength of partially-frozen soil. *Highway Research Board Bulletin*, 168,74-95, 1957.
- Lynch, A. H., and W. Wu, Impacts of fire and warming on ecosystem uptake in the boreal forest. *J. of Climate*, 13, 2334-2338, 1999.

- Lynham, T. J., G. M. Wickware, and J. A. Mason, Soil chemical changes and plant succession following experimental burning in immature jack pine, *Can. J. Soil. Sci.*, 78, 93-104, 1998.
- Mahowald, N. M., P. J. Rasch, B. E. Eaton, S. Whittlestone, and R. G. Prinn, Transport of ²²²radon to the remote troposphere using the Model of Atmospheric Transport and Chemistry and assimilated winds from ECMWF and the National Center for Environmental Prediction/NCAR, *J. Geophys. Res.*, 102, 28139-28151, 1997.
- Malhi, S. S., W. B. McGill, and M. Nyborg, Nitrate losses in soils: effect of temperature, moisture and substrate concentration, *Soil Biology and Biochemistry*, 22, 6733-737, 1990.
- McFarland, J. W., R. W. Ruess, K. Kielland, and A. P. Doyle, The role of organic nitrogen economy of floodplain balsam poplar stands in interior Alaska, *Ecosystems*, in review.
- McGuire, A. D., J. M. Melillo, L. A. Joyce, D. W. Kicklighter, A. L. Grace, B. Moore III, and J. Vorosmarty, Interactions between carbon and nitrogen dynamics in estimating net primary productivity for potential vegetation in North America, *Global Biogeochemical Cycles*, 6, 2, 101-124, 1992.
- Moore, T. R., and N. T. Roulet, Methane flux: Water table relations in Northern Wetlands, *G. Res. Lett.*, 20, 587-590, 1993.
- Murphy, P. J., B. J. Stocks, E. S. Kasischke, D. Barry, M. E. Alexander, N. H. F. French, and J. P. Mudd, Historical fire records in the North American boreal forest. In: *Fire, Climate Change and Carbon Cycling in North American Boreal Forests*

- (eds Kasischke, ES Stocks, BJ), pp 274-288, Ecological Studies Series Springer-Verlag, New York, 1999.
- Myneni, R. B., C. D. Keeling, C. J. Tucker, G. Asrar, and R. R. Nemani. Increased plant growth in the northern high latitudes from 1981 to 1991. *Nature*, 386, 698-702. 1997.
- Nadelhoffer, K. J., A. E. Giblin, G. R. Shaver, and J. L. Laundre. Effects of temperature and organic matter quality on C, N and P mineralization in soils from arctic ecosystems. *Ecology*, 72, 242-253. 1991.
- Neff, J. C., and G. P. Asner. Dissolved organic carbon in terrestrial ecosystems: synthesis and a model. *Ecosystems*, 4, 29-48. 2001.
- Nixon, J. F.. Thermal simulation of subsea saline permafrost. *Canadian Journal of Earth Science*, 23, 2039-2046. 1986.
- Oechel, W. C., S. J. Hastings, G. L. Vourlitis, M. Jenkins, G. Reichers, and N. Grulke. Recent change of arctic tundra ecosystems from a net carbon dioxide sink to a source. *Nature*, 361, 520-523. 1993.
- Oechel, W. C., G. L. Vourlitis, and S. J. Hastings. Cold-season CO₂ emission from arctic soils. *Global Biogeochemical Cycles*, 11, 163-172. 1997.
- Oechel, W. C., G. L. Vourlitis, S. J. Hastings, R. C. Zulueta, L. Hinzman, and D. Kane. Acclimation of ecosystem CO₂ exchange in the Alaskan Arctic in response to decadal climate warming. *Nature*, 406: 978-981. 2000.
- O'Neill, K. P., Changes in carbon dynamics following wildfire in soils of interior Alaska. Ph.D. Thesis. Duke University, Durham. 2000.

- Osterkamp, T. E.. Freezing and thawing of soils and permafrost containing unfrozen water or brine, *Water Resources Research*, 23, 12, 2279-2285, 1987.
- Osterkamp, T. E., and V. E. Romanovsky, Freezing of the active layer on the coastal plain of the Alaskan Arctic, *Permafrost and Periglacial Processes*, 8, 23-24, 1997.
- Osterkamp, T. E., and J. P. Gosink, Variations in permafrost thickness in response to changes in paleoclimate, *Journal of Geophysical Research*, 94, 4423-4434, 1991.
- Osterkamp, T. E., and T. Fei, Potential occurrence of gas hydrates in the continental shelf near Lonely, Alaska, in *Proceedings of the 6th International Conference on Permafrost*, Beijing, China, 500-505, 1993
- Paul, E. A., and F. E. Clark, *Soil Microbiology and Biochemistry*, New York, Academic Press, 1989.
- Pietikainen, J., and H. Fritze, Soil microbial biomass: Determination and reaction to burning and ash fertilization. In: *Fire in Ecosystems of Boreal Eurasia*, ed. J. D. Goldammer and V. V. Furyaev, pp. 337-349, Netherlands: Kluwer Academic Publisher, 1996.
- Rapalee, G., A simple model to estimate soil carbon dynamics at the BOREAS Northern Study Area, Manitoba, Canada, *Advances in Soil Science*, in press.
- Rapalee, G., S. E. Trumbore, E. A. Davidson, J. W. Harden, and H. Veldhuis, Estimating soil carbon stocks and fluxes in a boreal forest landscape, *Global Biogeochemical Cycles*, 12, 687-701, 1998.

- Rasch, P. J., N. M. Mahowald, and E. B. Eaton, Representations of transport, convection and the hydrologic cycle in chemical transport models: Implications for the modeling of short lived and soluble species, *J. Geophys. Res.*, 102, 28127-28138. 1997.
- Rastetter, E. B., P. M. Vitousek, C. Field, G. R. Shaver, D. Herbert, and G. I. Agren. Resource optimization and symbiotic nitrogen fixation, *Ecosystems*, 4, 369-388. 2001.
- Riseborough, D. W.. Soil latent heat as a filter of the climate signal in permafrost, in *Proceedings 5th Canadian Permafrost Conference*, Quebec, 6-10 June. *Collection Nordicana*, 1, 199-205, 1990.
- Romanovsky, V. E., and T. E. Osterkamp, Thawing of the active layer on the coastal plain of the Alaskan Arctic, *Permafrost and Periglacial Processes*, 8, 1-22, 1997.
- Romanovsky, V. E., T. E. Osterkamp, and N. S. Duxbury. An evaluation of three numerical models used in simulation of the active layer and permafrost temperature regimes. *Cold Reg. Sci. Technol.*, 26, 195-203, 1997.
- Romanovsky, V. E., and T. E. Osterkamp, Effects of unfrozen water on heat and mass transport processes in the active layer and permafrost, *Permafrost and Periglacial Processes*, 11, 219-239, 2000.
- Ruess, R. W., R. L. Hendrick, B. Sveinbjornsson, A. J. Burton, and G. Mauer, Linking fine root dynamics with ecosystem carbon fluxes in Alaskan taiga forests. in prep.
- Running, S. W., J. B. Way, J. McDonald, S. Kimball, S. Frohking, A. R. Keyser, and R. Zimmerman, Radar Remote Sensing Proposed for Monitoring Freeze-Thaw

- Transitions in Boreal Regions, *EOS, Transactions*, American Geophysical Union, 80, 19, 213,220-221,1999.
- Ryan M. G., M. B. Lavigne, and S. T. Gower, Annual carbon cost of autotrophic respiration in boreal forest ecosystems in relation to species and climate. *J. Geophy. Res.*, 102, No. D24, 28,871-28,883, 1997.
- Schimel, J. P., K. Kielland, and F. S. Chapin, III. Nutrient availability and uptake by tundra plants. in *Landscapr Function: Implications for Ecosystem Response to Disturbance; a Case Study in Arctic Tundra*. Reynolds, J. F., and J. D. Tenhunen (eds), Springer: Berlin. 203-221, 1996.
- Schimel, J. P., R. G. Gates, and R. Ruess. The role of balsam poplar secondary chemicals in controlling soil nutrient dynamics through succession in the Alaskan taiga. *Biogeochemistry*, 42, 221-234, 1998.
- Sommerfeld, R. A., R. C. Musselman, J. O. Reuss, and A. R. Mosier. Preliminary measurements of CO₂ in melting snow. *Geophysical Research Letters*, 18,7,1225-1228, 1991.
- Sommerfeld, R. A., A. R. Mosier, and R. C. Musselman. CO₂, CH₄, and N₂O flux through a Wyoming snowpack and implications for global budgets. *Letters to Nature*, 361,140-142, 1993.
- Shaver, G. R., K. J. Nadelhoffer, and A. E. Giblin. Biogeochemical diversity and element transport in a heterogeneous landscape, the North Slope of Alaska, in *Quantitative Methods in Landscape Ecology*, edited by M. Turner and R. Gardener, pp. 105-125, Springer-Verlag, New York, 1990.

- Shaver, G. R., and F. S. Chapin, III, Production: biomass relationships and element cycling in contrasting arctic vegetation types, *Ecol. Monogr.*, 61, 1-31, 1991.
- Shaver, G. R., W. D. Billings, F. S. Chapin, III, A. E. Giblin, K. J. Nadelhoffer, W. C. Oechel, and E. B. Rastetter, Global change and the carbon balance of arctic ecosystems, *BioScience*, 42, 433-441, 1992.
- Smith, M. W., and D. W. Riseborough, The sensitivity of thermal predictions to assumptions in soil properties, in *Proceedings 4th International Symposium on Ground Freezing*, Sapporo, 5-7 August, 17-23, 1985.
- Smith, C. K., M. R. Coyea, and A. D. Munson, Soil carbon, nitrogen, and phosphorus stocks and dynamics under disturbed black spruce forests, *Ecological Applications*, 10, 3, 775-788, 2000.
- Trumbore, S. E., and J. W. Harden, Accumulation and turnover of carbon in organic and mineral soils of the BOREAS northern study area, *J. of Geoph. Res.*, 02, 28, 816-8830, 1997.
- Uliassi, D. D., K. Huss-Danell, R. W. Ruess, and K. Doran, Biomass allocation and nitrogenase activity in *Alnus tenuifolia*: Responses to successional soil type and phosphorus availability, *Ecoscience*, 7, 1, 73-79, 2000.
- Van Cleve, K., O. W. Heal, and D. Robert, Bioassay of forest floor nitrogen supply for plant growth, *Can. J. For. Res.*, 16, 1320-1326, 1986.
- Van Cleve, K., W. C. Oechel, and J. L. Hom, Responses of black spruce (*picea mariana*) ecosystems to soil temperature modification in interior Alaska, *Can. J. For. Res.*, 20, 1530-1535, 1990.

- Van Cleve K., L. Oliver, R. Schlentner, L. A. Viereck, and C. T. Dyrness. Productivity and nutrient cycling in taiga forest ecosystems. *Can. J. For. Res.* 13, 747-766, 1983.
- Van Cleve, K., J. Yarie, R. Erickson, and C. T. Dyrness. Nitrogen mineralization and nitrification in successional ecosystems on the Tanana River floodplain, interior Alaska. *Can. J. For. Res.*, 23, 5, 970-978, 1993.
- Vardy, S. R., B. G. Warner, J. Turunen, and R. Aravena. Carbon accumulation in permafrost peatlands in the Northwest territories and Nunavut, Canada. *The Holocene*. 10, 2, 273-280, 2000.
- Waelbroeck, C., P. Monfray, W. C. Oechel, S. Hastings, and G. Vourlitis. The impact of permafrost thawing on the carbon dynamics of tundra. *Geophysical Research Letters*, 24, 3, 229-232, 1997.
- Weber, M. G., and K. Van Cleve. Nitrogen transformations in feather moss and forest floor layers of interior Alaska black spruce ecosystems. *Can. J. For. Res.*, 14, 278-290, 1984.
- Williams, P. J., and M. W. Smith. *The frozen Earth. fundamentals of geocryology*. 306pp. Cambridge University Press, 1989.
- Winston, G. C., E. T. Sundquist, B. B. Stephens, and S. E. Trumbore. Winter CO₂ fluxes in a boreal forest. *J. Geophys. Res.*, 102, 28,795-28,804, 1997.
- Yarie, J., and S. Billings. Carbon balance of the taiga forest within Alaska. *Ecosystems*. in press.

Yoshikawa, K., Bolton, W. R., Romanovsky, V. E., Fukuda, M., and L. D. Hinzman,

Impacts of wildfire on the permafrost in the boreal forests of interior Alaska.

Journal of Geophysical Research - Atmospheres, in press.